Tertiary treatment of effluents by catalytic ozonation

(Tratamento terciário de efluentes por ozonização catalítica)

Carla Alexandra Orge Fonseca

Dissertation presented for the Ph.D. Degree in

Chemical and Biological Engineering at the

Faculty of Engineering, University of Porto, Portugal

Supervisors: **Prof. Manuel Fernando Ribeiro Pereira**

Prof. José Joaquim de Melo Órfão

LCM – Laboratório de Catálise e Materiais

Laboratório Associado LSRE/LCM

Department of Chemical Engineering

Faculty of Engineering

University of Porto

Portugal

2012

Agradecimentos

Aos meus orientadores, Professor Doutor Fernando Pereira e Professor Doutor José Órfão que me concederam a oportunidade de realizar este projeto. Agradeço toda a sabedoria e conhecimento que me transmitiram durante este anos, bem como a disponibilidade e apoio sempre demostrados, e sem os quais este trabalho era irrealizável.

À Fundação para a Ciência e a Tecnologia (FCT) agradeço a concessão da bolsa de doutoramento (BD/45809/2008). Este trabalho teve também o apoio do FEDER no âmbito do programa COMPETE (projeto PEst-C/EQB/LA0020/2011).

Ao Professor Doutor J. L. Figueiredo, Coordenador Científico do Laboratório de Catálise e Materiais, agradeço todas as facilidades concedidas para a realização deste trabalho.

Ao Doutor Marco Fraga do Laboratório de Catálise do Instituto Nacional de Tecnologia/MCT do Rio de Janeiro, Brasil e ao Professor Doutor Luis Cadús do Instituto de Investigação em Tecnologia Química (INTEQUI), UNSL – CONICET, na Argentina a disponibilização de alguns catalisadores utilizados neste trabalho.

Ao Departamento de Engenharia Química da FEUP pela disponibilização de meios técnicos.

Ao Professor Doutor Carlos Sá e Engenheira Liliana Alves do Centro de Materiais da Universidade do Porto (CEMUP), agradeço a disponibilidade prestada na realização e tratamento dos resultados de XPS.

Ao Professor Doutor Pedro Tavares da UTAD pelo apoio prestado na interpretação dos resultados de XRD.

A todos os colegas e colaboradores do laboratório, tanto aos que ainda cá estão como também aos que já saíram, toda a ajuda experimental disponibilizada e os conhecimentos transmitidos durante a realização deste projeto. Agradeço também os bons momentos passados, bem como a amizade que se criou com alguns destes colegas (eles sabem quem são).

Às minhas amigas de infância que sempre acreditaram em mim e me proporcionam divertidos momentos ao longo da minha vida.

Ao Filipe agradeço todo o amor, juntamente com o apoio, compreensão e alegria demostrados durante estes anos.

À minha avó que está sempre presente na minha vida.

Ao meu Pai e à minha Mãe agradeço o amor, o apoio incondicional, o carinho e a educação que me deram. Sem eles eu não seria a pessoa que sou hoje, e sempre estarei eternamente grata.

Preface

This PhD thesis was carried out at Laboratório de Catálise e Materiais (LCM), Laboratório Associado LSRE/LCM, at the Department of Chemical Engineering, Faculty of Engineering of the University of Porto.

The thesis is divided in 10 chapters. Chapter 1 corresponds to the introduction and Chapter 10 presents the general overview, main conclusions and suggestions for future work. The main core of the text (Chapters 2 to 9) is based on 6 scientific papers already published in refereed journals, whereas the other chapters are in the last phase of preparation to be submitted for publication.

List of publications:

Chapter 2

C. Orge, J. Sousa, F. Gonçalves, C. Freire, J. Órfão, M. Pereira, Development of Novel Mesoporous Carbon Materials for the Catalytic Ozonation of Organic Pollutants, Catal. Lett. 132 (2009) 1-9.

Chapter 3

C. A. Orge, J. J. M. Órfão, M. F. R. Pereira, A. M. Duarte de Farias, R. C. R. Neto, M. A. Fraga, Ozonation of model organic compounds catalysed by nanostructured cerium oxides, Appl. Catal. B: Environ. 103 (2011) 190-199.

Chapter 4

C. A. Orge, J. J. M. Órfão, M. F. R. Pereira, A. M. Duarte de Farias, M. A. Fraga, Ceria and cerium-based mixed oxides as ozonation catalysts, Chem. Eng. J. 200–202 (2012) 499-505.

Chapter 5

C. A. Orge, J. J. M. Órfão, M. F. R. Pereira, Catalytic ozonation of organic pollutants in the presence of cerium oxide-carbon composites, Appl. Catal. B: Environ. 102 (2011) 539-546.

Chapter 6

C. A. Orge, J. J. M. Órfão, M. F. R. Pereira, Composites of manganese oxide with carbon materials as catalysts for the ozonation of oxalic acid, J. Hazard. Mater. 213–214 (2012) 133-139.

Chapter 7

C. A. Orge, J. J. M. Órfão, M. F. R. Pereira, Carbon xerogels and ceria–carbon xerogel materials as catalysts in the ozonation of organic pollutants, Appl. Catal. B: Environ. 126 (2012) 22-28.

Chapter 8

C. A. Orge, J. J. M. Órfão, M. F. R. Pereira, B. P. Barbero, L. E. Cadús, Perovskites as catalysts for the ozonation of selected organic pollutants, to be submitted (2012).

Chapter 9

C. A. Orge, J. J. M. Órfão, M. F. R. Pereira, Benchmarking of selected catalysts in the catalytic ozonation of oxalic acid, dye C. I. Reactive Blue 5 and textile effluents, to be submitted (2012).

Abstract

Heterogeneous catalytic ozonation has been considered as a promising advanced oxidation process (AOP) for removing organic pollutants from industrial and domestic wastewater, as well as from drinking water. Treatment tertiary of effluents by catalytic ozonation has received increased attention due to its extremely high oxidation potential in the degradation and mineralisation of refractory organic pollutants. The main goal of this thesis was to study the ozonation of selected organic pollutants in the presence of suitable catalysts with the aim of improving the mineralisation rates.

The first part of this this work describes the preparation and evaluation of mesoporous carbons, templated via SBA-15 and xerogels, as ozonation catalysts. The mesopouros materials were submitted to different chemical and thermal treatments in order to study the influence of the surface chemistry. Adsorption of the tested dyes on mesoporous carbons was not efficient enough to remove the colour from solutions. Single ozonation allowed a complete colour removal in a few minutes, but the respective mineralisation degree was low. Ozonation catalysed by all mesoporous carbons enhanced the mineralisation rates of dye solutions and the catalytic effect increases with the carbon basicity. Mesoporous materials also had high performances in the ozonation of oxalic acid.

The ozonation of oxalic acid, aniline and the dye C. I. reactive blue 5 in the presence of different nanostructured cerium oxides prepared by different routes and cerium based mixed oxides was studied. In the case of oxalic acid, the catalytic activity increases with the percentage of Ce(III) on the catalyst surface. Both single and catalytic ozonation allowed the total removal of aniline after 30 min of reaction. Samples with the largest amount of oxygen vacancies on their structure presented the best mineralisation degrees in aniline degradation. All cerium containing catalysts tested led to TOC removals close to 100% in the ozonation of the reactive dye. It is believed that the oxidation mechanism with ceria and cerium based mixed oxides occurs predominantly via $HO^{\bullet}$ radicals in the liquid bulk.

Composites with carbon materials and cerium or manganese oxides prepared by precipitation were used as ozonation catalysts. In the case of cerium oxides-carbon composites, most of them had better performances than the parent carbon materials, i.e. a synergic effect clearly occurs. In the range of compositions studied, the catalytic activity increases with the amount of carbon material present in the composites. The reaction mechanism is believed to comprise both surface reactions

and liquid bulk reactions involving $HO^{\bullet}$ radicals. On the contrary, manganese oxide and all manganese oxide-carbon composites presented better performances than carbon materials and synergic effects were not observed. The reaction mechanism is believed to occur mainly by surface reactions, following a direct oxidation of adsorbed molecules by molecular ozone and/or surface oxygenated radicals.

Pore sizes of carbon xerogels were found to play a key role in the degradation of the selected pollutants. Regardless of the preparation method, all the catalysts containing both cerium oxide and carbon xerogel promoted the removal of all oxalic acid in solution after 1 h of reaction, under the conditions tested. Cerium oxide supported on carbon xerogel and a carbon xerogel containing 1% of cerium oxide prepared by one-pot synthesis were the most active catalysts for the ozonation of the dye solution. The carbon xerogel containing 1% of cerium oxide prepared by one-pot synthesis was considered the most promising catalyst, since it presented high activity and its synthesis is easier and less expensive.

Some of the perovskites tested presented high activities in oxalic acid ozonation and the presence of lattice oxygen species on the perovskites surface was found to play an important role. Although the perovskite $LaMnO_3$ was the most active, it suffers lixiviation, and therefore sample $LaCoO_3$ was considered the best catalyst in oxalic acid degradation. Consequently, it was tested in the ozonation of C. I. Reactive Blue 5. This catalyst enhanced the TOC removal of the dye solution, when compared with non-catalytic ozonation, leading to an almost total mineralisation after 3 h, under the conditions used in the experiments.

The composite with 10% of ceria and 90% of activated carbon and the mixed oxide $Ce_{0.75}Zr_{0.25}O_2$ were selected for the study of real textile effluents. The colour was effectively removed by all ozonation systems. An important decrease in organic carbon was observed during ozonation experiments, especially in the catalytic ozonation of the effluent collected after biological treatment.

Sumário

A ozonização catalítica heterogénea tem sido vista como um processo promissor de oxidação avançada na remoção de poluentes das águas residuais industriais e domésticas, bem como das águas para consumo. O tratamento terciário de efluentes através da ozonização catalítica tem recebido constante atenção devido ao seu elevado potencial de oxidação na degradação e mineralização de poluentes orgânicos refratários. Esta tese teve como principal objetivo o estudo da ozonização de poluentes orgânicos selecionados na presença de catalisadores apropriados de forma a atingir níveis de mineralização elevados.

A primeira parte deste trabalho consiste na preparação e avaliação de catalisadores de carbono mesoporosos, réplicas de carbono via SBA-15 e xerogéis de carbono. De forma a avaliar a influência da química superficial dos materiais de carbono, as amostras preparadas foram sujeitas a tratamentos químicos e térmicos adequados. A adsorção dos corantes testados na presença dos materiais de carbono mesoporosos não foi suficiente para remover a cor das soluções. A ozonização simples permitiu remover a cor em poucos minutos, mas a mineralização conseguida foi baixa. A ozonização catalisada pelos carvões mesoporosos aumentou a mineralização das soluções de corante e observou-se que a atividade catalítica aumentava com a basicidade do carvão. Os materiais de carbono mesoporosos também apresentaram elevada atividade catalítica na ozonização do ácido oxálico.

Óxidos de cério nanoestruturados preparados através de diferentes métodos e óxidos mistos com cério foram testados na ozonização do ácido oxálico, da anilina e do corante C. I. Reative Blue 5. Relativamente ao ácido oxálico, verificou-se que a atividade catalítica aumentava com a quantidade de Ce(III) presente na superfície dos catalisadores. Tanto a ozonização simples como a ozonização catalítica removeram completamente a anilina ao fim de 30 min de reação. Durante a degradação da anilina, as amostras com maior quantidade de lacunas à superfície permitiram atingir os níveis de mineralização mais elevados. Na ozonização do corante reativo, todos os catalisadores de cério testados removeram quase 100% do carbono orgânico total (TOC) em solução. Acredita-se que o mecanismo reacional na presença dos óxidos de cério e dos óxidos mistos com cério ocorre principalmente na fase líquida com a participação dos radicais $HO^{\bullet}$.

Os compósitos com carvão e óxidos de cério ou manganês preparados pelo método de precipitação foram avaliados como catalisadores na ozonização.

Relativamente aos compósitos com carvão e óxido de cério, a maior parte deles apresentou atividade superior aos correspondentes materiais de carbono, ou seja, ocorre claramente um efeito sinérgico. Na gama das composições estudadas, verificou-se que a atividade catalítica aumentava com a quantidade de carvão presente nos compósitos. O mecanismo reacional proposto incluiu tanto reações à superfície como reações na fase líquida envolvendo radicais $HO^{\bullet}$. Contrariamente, os compósitos de carvão e óxido de manganês apresentaram atividades catalíticas superiores aos materiais de carbono e concluiu-se que o efeito sinérgico não ocorria. O mecanismo reacional proposto incluiu principalmente reações à superfície através da oxidação direta das moléculas adsorvidas pelo ozono molecular e/ou por radicais oxigenados presentes na superfície.

Verificou-se que o tamanho de poros dos xerogéis de carbono tem um efeito importante na degradação dos poluentes selecionados. Independentemente do método de preparação, todos os catalisadores com óxido de cério e xerogel de carbono removeram todo o ácido oxálico presente em solução após 1 h de reação, nas condições experimentais testadas. O óxido de cério suportado no xerogel de carbono e o xerogel de carbono com 1% de óxido de cério preparado por *one-pot synthesis* foram os catalisadores mais ativos na ozonização do corante. Este último catalisador foi considerado o mais promissor, uma vez que apresenta elevada atividade e a sua preparação é mais rápida e menos dispendiosa.

Na ozonização do ácido oxálico observou-se que algumas das perovskitas testadas apresentavam atividades catalíticas elevadas e que a presença de defeitos de lacuna na superfície dos materiais tinha um efeito positivo. Embora a perovskita $LaMnO_3$ fosse a mais ativa, observou-se alguma lixiviação, e desta forma a amostra $LaCoO_3$ foi considerada a melhor na degradação do ácido oxálico. Consequentemente, o catalisador $LaCoO_3$ foi testado na ozonização do corante C. I. Reative Blue 5. Comparando com a ozonização simples, a amostra selecionada aumentou a remoção do TOC da solução do corante, conseguindo-se uma mineralização praticamente completamente após 3 h de reação, nas condições experimentais consideradas.

Para o estudo com os efluentes têxteis reais, os catalisadores selecionados foram o compósito com 10% de óxido de cério e 90% de carvão ativado e o óxido $Ce_{0.75}Zr_{0.25}O_2$. Todos os sistemas catalíticos testados removeram eficazmente a cor. As reações de ozonização diminuíram a carga orgânica das águas residuais testadas, principalmente a ozonização catalítica no efluente recolhido após o tratamento biológico.

Résumé

L´ozonation catalytique hétérogène a été considérée comme un procédé prometteur d'oxydation avancée pour l'élimination des polluants dans les eaux usées industrielles et domestiques, ainsi que l'eau destinée à la consommation. Le traitement tertiaires des effluents par l'ozonation catalytique a reçu une attention accrue en raison de son potentiel d'oxydation très élevé dans la dégradation et la minéralisation des polluants organiques réfractaires. L'objectif principal de cette thèse était d'étudier l'ozonation de certains polluants organiques en présence de catalyseurs appropriés afin d'améliorer les taux de minéralisation.

La première partie de ce travail décrit la préparation et l'évaluation des carbones mésoporeux, des répliques négatives par SBA-15 et xérogels de carbone dans l'ozonation catalytique. Les matériaux ont été soumis à différents traitements chimiques et thermiques afin d'évaluer l'influence de la chimie de surface. L'adsorption des colorants testés sur les carbones mésoporeux n'était pas suffisamment efficace pour éliminer la couleur des solutions. L'ozonation simple a permis un enlèvement complet des couleurs en quelques minutes, mais le degré de minéralisation respectif était faible. L'ozonation catalysée par tous les carbones mésoporeux a amélioré les taux de minéralisation de solutions de colorant et l'activité catalytique augmente avec la basicité de carbone. Les matériaux mésoporeux ont également eu des performances élevées dans l'ozonation de l'acide oxalique.

L'ozonation de l'acide oxalique, de l'aniline et du colorant C. I. Reactive Blue 5 en présence de différents oxydes de cérium nanostructurés élaborés par voies différentes et oxydes mixtes à base de cérium a été étudiée. Dans le cas de l'acide oxalique, l'activité catalytique augmente avec le pourcentage de Ce (III) sur la surface du catalyseur. Tant l'ozonation simple, comme l'ozonation catalytique ont complètement enlevée l'aniline après 30 minutes de réaction. Les échantillons dont le plus grand nombre de lacunes d'oxygène de leur structure ont présenté les meilleurs degrés de minéralisation dans la dégradation de l'aniline. Tous les catalyseurs à base de cérium testés dans l'ozonation du colorant réactif, ont enlevé près de 100% de TOC. On croit que le mécanisme d'oxydation de l'oxyde de cérium et des oxydes mixtes à base de cérium se produit principalement par l'intermédiaire de radicaux $HO^{\bullet}$ dans la phase liquide.

Les composites avec des matériaux de carbone et les oxydes de cérium ou manganèse, préparés par précipitation ont été utilisé comme catalyseurs

d'ozonation. Dans les cas des composites de carbone et oxyde de cérium, la plupart d'entre eux avaient de meilleures performances que les matériaux carbonés originels, c'est-à-dire qu'un effet synergique se produit clairement. Dans la gamme de compositions étudiées, l'activité catalytique augmente avec la quantité de matériau carboné présent dans les composites. Le mécanisme réactionnel est considéré comprendre les réactions de surface et les réactions dans la phase liquide sur les radicaux $HO^{\bullet}$. Par contre, les composites de carbone et d'oxyde de manganèse ont présenté meilleures performances que les matériaux de carbone et les effets synergiques n'ont pas été observées. Le mécanisme réactionnel est considéré se produire principalement par des réactions de surface, sur l'oxydation directe de molécules adsorbées par l'ozone moléculaire et/ou des radicaux oxygénés dans la surface.

Il a été constaté que la taille des pores du xérogels de carbone a un effet important sur la dégradation de certains polluants. Quelle que soit la méthode de préparation, tous les catalyseurs à base d'oxyde de cérium et de xérogel de carbone favorisé l'enlèvement de tout l'acide oxalique en solution après une heure de réaction, dans les conditions testées. L'oxyde de cérium supporté sur un xérogel de carbone et un xérogel de carbone contenant 1% d'oxyde de cérium préparé par une synthèse *one-pot* ont été les catalyseurs les plus actifs pour l'ozonation de la solution de colorant. Le xérogel de carbone contenant 1% d'oxyde de cérium préparé par synthèse *one-pot* a été considéré comme le catalyseur le plus prometteur, car il présente une activité élevée et sa synthèse est plus facile et moins coûteux.

Dans l'ozonation de l'acide oxalique, certaines pérovskites testées ont présenté activités élevées et la présence d'espèces d'oxygène sur la surface des pérovskites ont eu un rôle positif. Bien que la pérovskite $LaMnO_3$ a été la plus actif, elle souffre de lixiviation, donc le catalyseur $LaCoO_3$ a été considéré comme le meilleur dans la dégradation de l'acide oxalique. Par conséquent, il a été testé dans l'ozonation de C.I. Reactive Blue 5. Ce catalyseur a amélioré l'enlèvement de TOC de la solution de colorant par rapport à l'ozonation simple, conduisant à une minéralisation presque totale après 3 heures, dans les conditions utilisées dans les expériences.

Le composite avec 10% d'oxyde de cérium et 90% de charbon activé et de l'oxyde mixte $Ce_{0.75}Zr_{0.25}O_2$ ont été sélectionnés pour l'étude des effluents textiles réels. La couleur a été éliminée efficacement par tous les systèmes d'ozonation. Une diminution importante de carbone organique a été observée lors d'expériences d'ozonation, en particulier dans l'ozonation catalytique de l'effluent collecté après le traitement biologique.

Contents

List of Figures……xix

List of Tables……xxv

Chapter I 1
1 Introduction 3
1.1 Wastewater treatment 3
1.1.1 Industrial Effluents 5
1.1.2 Organic pollutants 7
1.2 Ozone 10
1.2.1 Catalytic ozonation 13
1.2.1.1 Homogeneous catalytic ozonation 13
1.2.1.2 Heterogeneous catalytic ozonation 14
1.3 Materials selected to be used as catalysts 22
1.3.1 Carbon materials 22
1.3.2 Metal oxides 27
1.4 Objectives and thesis outline 31
References 32
Chapter 2 53
2 Development of novel mesoporous carbon materials for the catalytic ozonation of organic pollutants 55
2.1 Introduction 55
2.2 Experimental 56
2.2.1 Preparation and functionalisation of the mesoporous carbon materials 56
2.2.2 Model organic compounds 57
2.2.3 Characterization of the mesoporous materials 58
2.2.4 Kinetic experiments and analytical methods 59
2.3 Results and discussion 59

2.3.1 Characterization of carbon materials 59
2.3.2 Reactive and acid dyes removal 63
2.3.3 Oxalic acid removal 68
2.4 Conclusions 70
References 71
Chapter 3 75
3 Ozonation of model organic compounds catalysed by nanostructured cerium oxides 77
3.1 Introduction 77
3.2 Experimental 78
3.2.1 Materials 78
3.2.2 Characterization of catalysts 79
3.2.3 Experimental set-up and analytical methods 80
3.3 Results and discussion 81
3.3.1 Samples characterization 81
3.3.2 Kinetic results 91
3.3.2.1 Oxalic acid 91
3.3.2.2 Other organic compounds 94
3.4 Conclusions 99
References 100
Chapter 4 107
4 Ceria and cerium based mixed oxides as ozonation catalysts 109
4.1 Introduction 109
4.2 Materials and methods 111
4.2.1 Materials 111
4.2.2 Experimental set-up and analytical methods 111
4.3 Results and discussion 112
4.3.1 Catalysts characterization 112
4.3.2 Ozonation of selected organic compounds 115
4.3.2.1 Oxalic acid 115
4.3.2.2 Other organic compounds 121

4.4 Conclusions....126
References....126

Chapter 5....131
5 Catalytic ozonation of organic pollutants in the presence of cerium oxide – carbon composites....133

5.1 Introduction....133
5.2 Experimental....134

5.2.1 Materials....134
5.2.2 Kinetic experiments....136

5.3 Results and discussion....137

5.3.1 Characterization of the catalysts....137
5.3.2 Oxalic acid removal....143
5.3.3 Oxamic acid removal....145
5.3.4 C. I. Reactive Blue 5 removal....146
5.3.5 Consideration on reaction mechanism....147

5.4 Conclusions....150
References....151

Chapter 6....155
6 Composites of manganese oxide with carbon materials as catalysts for the ozonation of oxalic acid....157

6.1 Introduction....157
6.2 Experimental....158

6.2.1 Materials and their characterization....158
6.2.2 Kinetic experiments....159

6.3 Results and discussion....160

6.3.1 Catalysts characterization....160

6.4 Ozonation of oxalic acid....166
6.5 Conclusions....172
References....173

Chapter 7....175
7 Carbon xerogels and ceria-carbon xerogel materials as catalysts in the ozonation of organic pollutants....177

7.1 Introduction 177
7.2 Experimental 178
7.2.1 Materials and characterization methods 178
7.2.2 Kinetic experiments 179
7.3 Results and discussion 180
7.3.1 Characterization of the catalysts 180
7.3.2 Kinetic results 184
7.3.2.1 Oxalic acid removal 184
7.3.2.2 Reactive dye removal 186
7.3.3 Considerations on the reaction mechanism 188
7.3.4 Selection of the best catalyst 190
7.4 Conclusions 191
References 192

Chapter 8 195
8 Perovskites as catalysts for the ozonation of selected organic compounds 197

8.1 Introduction 197
8.2 Experimental 198
8.2.1 Catalysts preparation and characterization 198
8.2.2 Kinetics experiments 199
8.3 Results 200
8.3.1 Catalysts characterization 200
8.3.2 Oxalic acid removal 202
8.3.3 Reactive dye ozonation 206
8.4 Conclusions 208

Chapter 9 213
9 Benchmarking of selected catalysts in the catalytic ozonation of oxalic acid, dye C. I. Reactive Blue 5 and textile effluents 215

9.1 Introduction 215
9.2 Experimental 216
9.3 Oxalic acid removal 218

9.4 Reactive dye removal....221
9.5 Treatment of real effluents....222
9.6 Conclusions....233
References....234

Chapter 10....237
10 Conclusions and future work....239

10.1 Motivation....239
10.2 Main conclusions....240
10.3 Suggestions for future work....243

Appendices....245
Appendix A. Schematic representation of the experimental set-up....247
Appendix B. Screening of commercial metal oxides....248
Appendix C. Preparation and evaluation of manganese oxides synthesized by different procedures as ozonation catalysts....251

C.1 Catalysts preparation....251
C.2 Catalysts characterization....253
C.3 Catalytic activity....256

Appendix D. Composites of manganese oxide with activated carbon as catalysts for the ozonation of a reactive dye....259

List of Figures

Figure 1.1: Resonance structures of ozone molecule. 10

Figure 1.2: Schematic representation of the concept of template synthesis [143]... 24

Figure 1.3: Schematic representation of the CMK-1 synthesis using MCM-48 as template [159]. 24

Figure 1.4: Schematic illustration for the synthesis of CMK-3 using SBA-15 as template [166]. 25

Figure 2.1: CO_2 and CO TPD spectra of the templated carbons obtained via SBA-15. 60

Figure 2.2: N_2 adsorption isotherms at 77 K of SBA-15, JC0, XC0 and AC0. 62

Figure 2.3: Micrographs of silica SBA-15 (left) and the templated carbon JCO (right). a) SEM, b) TEM 63

Figure 2.4: Colour and TOC removal for the reactive dye using activated carbon, carbon xerogel and templated carbon as catalysts. 64

Figure 2.5: TOC removal for the reactive dye in the presence of a) templated carbons, b) carbon xerogels. 65

Figure 2.6: TOC removal for the acid dye in the presence of a) templated carbons, b) carbon xerogels. 66

Figure 2.7: Oxalic acid removal by single ozonation, catalysed ozonation and adsorption in the presence of the templated carbon, carbon xerogel and activated carbon. 69

Figure 3.1: X-ray diffractograms of the cerium oxide samples: (a) CeO_2-NP (b) CeO_2-FL, (c) CeO_2-NC, (d) CeO_2. 83

Figure 3.2: FE-SEM images of CeO_2 at 25.000x (a) and 100.000x (b), CeO_2-FL at 12.000x (c) and 100.000x (d), CeO_2-NC at 150.000x (e) and CeO_2-NP at 200.000x (f). 85

Figure 3.3: TEM image of CeO_2-NC (a) and HRTEM images of CeO_2-NC (b), CeO_2-NP (c) and CeO_2-FL (d). 86

Figure 3.4: Raman spectra of the different cerium oxide nanostructures: (a) CeO_2-NP (b) CeO_2-FL, (c) CeO_2-NC, (d) CeO_2. 87

Figure 3.5: TPR profiles of the different cerium oxides: (a) CeO_2-NP (b) CeO_2-FL, (c) CeO_2-NC, (d) CeO_2. 89

Figure 3.6: Experimental and fitted Ce 3d XPS spectra of samples (a) CeO_2, (b) CeO_2-NC, (c) CeO_2-NP, (d) CeO_2-FL. 91

Figure 3.7: Evolution of the dimensionless concentration of oxalic acid during single ozonation and catalytic ozonation with cerium oxide samples. 92

Figure 3.8: Evolution of dimensionless concentration of oxalic acid during catalytic ozonation and effect of *tert*-butanol ($C_{0,\ oxalic\ acid}$ = 1 mM, $m_{catalyst}$ = 350 mg, $C_{tert\text{-}butanol}$ = 10 mM)..... 94

Figure 3.9: Aniline (a) and TOC (b) removal during single ozonation and ozonation catalysed by cerium oxides. 95

Figure 3.10: Evolution of oxalic (a) and oxamic (b) acid concentrations during aniline ozonation. 97

Figure 3.11: Colour (a) and TOC (b) removal for the reactive dye solution during catalytic and non-catalytic ozonation. 99

Figure 4.1: Experimental and fitted Ce 3d spectra of sample CeO_2..... 115

Figure 4.2: Evolution of the dimensionless concentration of oxalic acid during non-catalytic and catalytic ozonation with ceria and mixed oxides with 75 wt% of CeO_2 and 25 wt% of the doped metal oxide (a) and with ceria and cerium-zirconium oxides (b). 116

Figure 4.3: Evolution of the dimensionless concentration of oxalic acid during adsorption, catalytic ozonation and effect of *tert*-butanol ($C_{tert\text{-}butanol}$ = 10 mM)..... 118

Figure 4.4: Evolution of the dimensionless concentration of oxalic acid during Successive catalytic ozonation experiments using a) $Ce_{0.75}Zr_{0.25}O_2$ and b) $Ce_{0.50}Zr_{0.50}O_2$..... 120

Figure 4.5: Evolution of the dimensionless concentration of aniline during adsorption, single ozonation and ozonation catalysed by ceria and some ceria-based mixed oxides. 122

Figure 4.6: Evolution of the dimensionless TOC concentration in the aniline solution during adsorption, non-catalytic and catalytic ozonation in the presence of ceria and ceria-based mixed oxides. 123

Figure 4.7: Evolution of the dimensionless dye concentration during non-catalytic, adsorption and catalytic ozonation in the presence of ceria and ceria-based mixed oxides. 124

Figure 4.8: Evolution of the dimensionless TOC concentration during non-catalytic and catalytic ozonation in the presence of ceria and mixed oxides with 75 wt% of CeO_2 and 25 wt% of the doped metal oxide (a) and during non-catalytic, adsorption and catalytic ozonation in the presence of ceria and cerium-zirconium oxides (b). 125

Figure 5.1: X-ray diffractograms of selected catalysts: (a) AC0, AC0-Ce-O_1, AC0-Ce-O_4 and Ce-O and (b) XC, XC-Ce-O_2 and Ce-O. 139

Figure 5.2: Experimental and fitted Ce 3d XPS spectra of samples (a) CeO_2, (b) AC0-Ce-O_1, (c) AC0-Ce-O_3, (d) AC0-Ce-O_4, (e) ACoxid-Ce-O_2 and (f) XC-Ce-O_2. 140

Figure 5.3: SEM images and EDS analyses of samples (a) AC0, (b) XC, (c) Ce-O, (d) AC0-Ce-O_1, (e) AC0-Ce-O_4, (f) XC-Ce-O_2. 142

Figure 5.4: Oxalic acid removal by single ozonation and catalytic ozonation in the presence of: (a) AC0-Ce-O composites, (b) XC-Ce-O composites and (c) ACoxid-Ce-O composites. 144

Figure 5.5: Oxamic acid removal by single ozonation and catalytic ozonation in the presence of cerium oxide, activated carbon or cerium oxide - activated carbon composites. 145

Figure 5.6: Colour and TOC removal for the reactive dye during single ozonation, and using cerium oxide, activated carbon or cerium oxide - activated carbon composites as catalysts. 147

Figure 5.7: Evolution of the dimensionless concentration of oxalic acid during ozonation catalysed by AC0-Ce-O_3 or XC-Ce-O_2 composites and the corresponding physical mixtures of the same carbon materials with cerium oxide. 148

Figure 5.8: Evolution of the dimensionless concentration of oxalic acid during adsorption, catalytic ozonation and effect of *tert*-butanol ($C_{tert\text{-butanol}}$ = 10 mM). 150

Figure 6.1: SEM micrograph of: (a) AC0, (b) Mn-O, (c) AC0-Mn-O_2 and (d) magnification of zone Z2; EDS analyses of zones Z1 (e) and Z2 (f). 163

Figure 6.2: X-ray diffractograms of selected samples. 164

Figure 6.3: Experimental and fitted Mn 2p XPS spectra of samples (a) Mn-O, (b) AC0-Mn-O_1 and (c) AC0-Mn-O_2. 165

Figure 6.4: Oxalic acid removal by single ozonation and catalytic ozonation in the presence of: (a) AC0-Mn composites, (b) XC-Mn composites and (c) ACoxid-Mn composites (C_0 = 1 mM, m_{cat} = 350 mg, $V_{sol.}$ = 700 mL). 167

Figure 6.5: Evolution of dimensionless concentration of oxalic acid during adsorption on Mn-O, single ozonation and catalytic ozonation with Mn-O and AC0-Mn-O_3, and effect of *tert*-butanol (C_0 = 1 mM, m_{cat} = 350 mg, $V_{sol.}$ = 700 mL, $C_{tert\text{-}butanol}$ = 10 mM). 168

Figure 6.6: Evolution of oxalic acid removal during cyclic experiments (C_0 = 1 mM, m_{cat} = 350 mg, $V_{sol.}$ = 700 mL). 169

Figure 6.7: Evolution of dimensionless concentration of oxalic acid during ozonation catalysed by AC0-Mn-O_4 and the corresponding physical mixture of activated carbon and manganese oxide, and catalytic ozonation with a solution of the manganese precursor with or without *tert*-butanol (C_0 = 1 mM, m_{cat} = 350 mg, $V_{sol.}$ = 700 mL, percentage of Mn = 2.3%, $C_{tert\text{-}butanol}$ = 10 mM). 171

Figure 7.1: X-ray diffractograms of carbon xerogel XC_pH=5.45 and ceria – carbon xerogel materials. 182

Figure 7.2: SEM images of the prepared materials and EDS analysis of the sample 5%Ce/XC_supported. 183

Figure 7.3: Evolution of the dimensionless concentration of oxalic acid during single ozonation and ozonation catalyzed by carbon xerogels prepared at different pH (a) and by cerium oxide and ceria – carbon xerogel materials (b). 185

Figure 7.4: Colour and TOC removal for the reactive dye during single ozonation, and ozonation catalyzed by carbon xerogels prepared at different pH (a) and by cerium oxide and ceria - carbon xerogel materials (b). 187

Figure 7.5: Evolution of the dimensionless concentration of oxalic acid during adsorption, catalytic ozonation and effect of *tert*-butanol ($C_{tert\text{-}butanol}$ = 10 mM). 188

Figure 7.6: Evolution of the dimensionless concentration of oxalic acid in successive experiments with the 5 %Ce_XC_supported sample. 190

Figure 8.1: Temperature programmed reduction profiles of La-containing perovskites. 201

Figure 8.2: X-ray diffractograms of samples. 202

Figure 8.3: Oxalic acid removal by single ozonation and catalytic ozonation in the presence of perovskites (C_0 = 1mM, $m_{catalyst}$ = 100 mg). 203

Figure 8.4: Evolution of dimensionless concentration of oxalic acid during catalytic ozonation, effect of *tert*-butanol, cyclic experiments and reproducibility tests using $LaMnO_3$ (C_0 = 1mM, $m_{catalyst}$ = 100 mg, $C_{tert\text{-butanol}}$ = 10 mM). 206

Figure 8.5: Colour degradation (a) and dimensionless TOC (b) for the reactive dye during single ozonation and using $LaCoO_3$ as catalyst. 208

Figure 9.1: Evolution of the dimensionless concentration of oxalic acid during non-catalytic and catalytic ozonation with carbon materials (a), metal oxides (b), ceria-carbon materials (c) and manganese-carbon materials (d). 220

Figure 9.2: Evolution of the dimensionless concentration of oxalic acid during non-catalytic and catalytic ozonation with carbon materials and ceria-carbon materials. 221

Figure 9.3: Colour (a) and TOC (b) removal for the reactive dye during single and catalytic ozonation in the presence of the best prepared catalysts. 222

Figure 9.4: UV-Vis spectra of effluents A (a) and B (b). 224

Figure 9.5: Evolution of UV-Vis spectrum of real effluent A during non-catalytic ozonation (a), catalytic ozonation in the presence of AC0-Ce-O_4 (b) and $Ce_{0.75}Zr_{0.25}O_2$ (c), and adsorption on AC0-Ce-O_4 (d) and $Ce_{0.75}Zr_{0.25}O_2$ (e). 227

Figure 9.6: Evolution of dimensionless TOC during single ozonation, catalytic ozonation and adsorption experiments of the real textile effluent A. 228

Figure 9.7: Evolution of the UV-Vis spectrum of the real effluent B during non-catalytic ozonation (a), catalytic ozonation in the presence of AC0-Ce-O_4 (b) and $Ce_{0.75}Zr_{0.25}O_2$ (c), and adsorption on AC0-Ce-O_4 (d). 230

Figure 9.8: Evolution of dimensionless TOC during single ozonation, catalytic ozonation and adsorption of the real textile effluent B. 231

Figure A.1: Representation of the experimental set-up for adsorption and ozonation studies. 247

Figure B.1: Evolution of the dimensionless concentration of oxalic acid during catalytic ozonation with commercial samples 250

Figure C.1: N_2 adsorption-desorption isotherms determined at -196 °C. 255

Figure C.2: Evolution of dimensionless concentration of oxalic acid (C_0 = 1 mM) during single ozonation and ozonation catalyzed by manganese oxides synthesized by the reflux method (a), manganese oxides and cobalt oxide prepared by template synthesis (b), and Mn-O/SBA-15 materials and Mn-O/MWCNT (c). 257

Figure D.1: Colour and TOC removal for the reactive dye using activated carbon, manganese oxide and composites. 259

List of Tables

Table 1.1: Characteristics of C.I. Reactive Blue 5 and C.I. Acid Blue 113 dyes. 9

Table 1.2: Properties of the selected compounds. 10

Table 2.1: Characteristics of dyes. 58

Table 2.2: Chemical properties of the materials used. 61

Table 2.3: Textural properties of the materials used. 61

Table 3.1: Surface area (S_{BET}), average crystallite particle size (d), and cubic lattice cell length (a) of all synthesized oxides. 82

Table 3.2: Hydrogen consumption and Ce^{3+} percentage as measured by XPS. 88

Table 3.3: % TOC of non-detected by-products. 97

Table 4.1: BET surface area [17] and relative amount of cerium as Ce(IV) on the surface of the catalysts. 113

Table 5.1: Physical characterization of catalysts. 138

Table 5.2: Relative % of Ce (IV) on surface. 141

Table 6.1: Properties of manganese oxide, carbon materials and composites. 161

Table 7.1: Properties of the prepared samples. 181

Table 8.1: Main characteristics of selected pollutants. 199

Table 8.2: BET surface areas and percentage of lattice oxygen species of La-containing perovskites. 201

Table 9.1: Properties of selected compounds. 216

Table 9.2: Parameters of the industrial effluents selected. 223

Table 9.3: Characterization of the remaining solution after non-catalytic, catalytic and adsorption experiments with effluent A after 3 h. 225

Table 9.4: Characterization of the remaining solution after non-catalytic, catalytic and adsorption experiments with effluent B after 3 h. 232

Table B.1: BET surface areas of commercial metal oxides. 249

Table C.1: Textural properties of the prepared samples. 254

Chapter I

Introduction

The first chapter of this thesis presents an overview about wastewater treatment, especially processes using catalytic ozonation. Initially, a short description of the available technologies for the removal of pollutants in water is reviewed. The main characteristics of some industrial effluents are listed and the use of ozone for wastewater treatment is addressed in more detail. Ozone properties and ozonation reactions are provided. A review of the results reported in the literature about catalytic ozonation is presented. Then, the materials selected in this work to be used as ozonation catalysts are focused: mesoporous carbon materials prepared by diverse procedures and with different properties and metal oxides, with special emphasis to the synthesis and characterization methods. In the last part, the main objectives of this work and the thesis outline are presented.

1 Introduction

1.1 Wastewater treatment

Among the vast range of wastewater treatments available, the selection of the process must consider the initial characteristics of the effluent, the desired final quality, which is dependent on the fate of the treated stream (discharge or reutilization), as well as sludge production and subsequent handling, installation, operation and maintenance costs, and long-term system reliability [1].

Summarizing, industrial effluents may be treated by physicochemical or biological process, or with an integrated treatment. Physicochemical treatment processes include removal of suspended solids, colloidal particles, floating matters, colours and toxic compounds by either sedimentation, flotation, screening, adsorption, coagulation, oxidation, ozonation, electrolysis, reverse osmosis, ultra-filtration, and nano-filtration technologies. Biological processes can be divided in aerobic or anaerobic. Activated sludge process and aerobic biological reactors are examples of aerobic treatments. Anaerobic filter, upflow sludge blanket, fluidized bed, anaerobic lagoon and anaerobic contact reactors are some examples of anaerobic processes. Integrated or hybrid system is designed to take advantage of unique features of two or more processes. Several combinations were reported in the literature, such as coagulation and wet oxidation, ozone and biofilm reactor, air flotation and chemical precipitation, activated sludge and ozonation and anaerobic–aerobic treatment.

Water quality and availability is a challenging problem facing societies all over the world [2, 3]. Then, conventional biological, physical and chemical methods of water and wastewater treatment have limited success when applied to the treatment of industrial effluents, since wastewater contains stable refractory organic compounds. These conventional processes also tend to generate large amounts of sludge, which require treatment before final disposal [4, 5]. Therefore, the introduction of new technologies to degrade these refractory molecules into smaller molecules, which can be further oxidized by biological methods, has become imperative [6].

Advanced oxidation processes (AOPs) have been widely investigated for their potential application, particularly when the source waters contain high concentration of ambiguous, refractory and recalcitrant chemical compounds such as aromatics, pesticides, pharmaceuticals and personal care products, drugs and endocrine

disruptors and others [7]. The principles of AOPs are based on the in situ generation of reactive oxygen species such as hydroxyl radicals, superoxide anions, ozone and hydrogen peroxide for the oxidation of organic compounds that lead to a complete mineralisation [8, 9]. The AOPs include ultrasound, photocatalysis, ozonation, Fenton's chemistry, hydrogen peroxide and others. Operating at ambient temperature and pressure conditions and complete oxidation of organics to inoffensive products such as carbon dioxide and water are the main objectives of AOPs. According to the reported studies, the AOPs are ease to operate, highly efficient in organics oxidation and potentially adaptable to a range of wastewater treatment scales and final treated effluent requirements.

In the Fenton and photo-Fenton processes, that include the UV/Fe^{3+} and oxalate/H_2O_2 operating at ambient temperature and pressure, the basic mechanism strongly depends on the formation of $HO^{\bullet}$ radicals by the reaction with the iron species found in wastewater. The benefits of the Fenton based process are that iron is usually present in abundance in wastewater and the H_2O_2 is easy to handle and environmentally friendly. Contrary to what happens with other AOPs, the formation of reactive hydroxyl radicals in Fenton based processes is preferred at a low acidic pH of 2.6–2.8. Similarly to other AOPs, the disadvantage of the Fenton based processes might be due to competition between the different hydroxyl derivatives, organic and inorganic substrates found in wastewater.

The UV-based photolysis and chemical oxidation processes use similar reactions, but enhance the formation of $HO^{\bullet}$ radicals via the presence of a UV irradiation source. The presence of UV source induces cleavage and formation of $HO^{\bullet}$ radicals from its precursors (i.e. H_2O_2 or O_3). The reactivity for O_3 decomposition under UV irradiation is much higher than H_2O_2. Heterogeneous photocatalytic processes use certain metal oxides that can readily generate hydroxyl radicals on the surface of particles when absorbing UV light. Usually TiO_2 is chosen as photocatalyst.

Ozonation processes operate at ambient temperature and pressure, but require strict pH control at alkaline conditions to avoid the formation of conjugate base HO_2^- which can strongly affect the concentration of reactive radicals formed. Enhancement of ozone reactivity can be interestingly achieved by the introduction of a solid catalyst able to promote ozone decomposition into highly reactive hydroxyl radicals or allow surface reactions to improve treatment efficiency.

1.1.1 Industrial Effluents

Ozone is widely used for treatment of effluents from various industries such as paper, shale oil processing, production and usage of pesticides, dye manufacture, textile dyeing, production of antioxidants for rubber and pharmaceuticals [6]. Ozone is applied in several industrial effluents, such as textile wastewater for remove the colour [10] and reduction of TOC and COD to certain limits beyond which biological oxidation can be used [11, 12], degradation of effluents from production of dyes [13, 14], chlorinated phenols [15, 16], chlorobenzenes [17], pesticides [18, 19] and treatment of wine-distillery wastewaters [20, 21].

Distilleries are one of the most highly polluting industries. Due to stringent requirements being imposed by regulations concerning the discharge of the effluents, there is a growing interest in the development of new technologies and procedures for the treatment of distillery wastewater. Moreover, distillery wastewaters often contain compounds which are not easily decomposed by the microorganisms. The major problem of this industry is the treatment of the highly colored distillery spent wash. In general, distilleries wastewaters are acidic and have a brown colour and a high content of organic substances that differ according to the raw material distilled [22]. Ozonation was demonstrated to be a good technology to improve the biodegradability [23] and ozone dose is the key parameter to treat the effluent effectively with a combined chemical−biological system [20]. Benites et al. verified that ozonation of the aerobically pretreated wastes enhances significantly the organic matter removal in comparison to the ozonation of unpretreated wastes and the increase on the ozone partial pressure leads to an increase in the substrate conversions [21].

Textile industry consumes large volumes of water and chemicals for wet processing of textiles. The chemical reagents used are very diverse in chemical composition, varying from inorganic compounds to polymers and organic products [24]. Then, wastewaters from textile industries contain many types of pollutants such as dyes, detergents, insecticides, fungicides, grease and oils, sulfide compounds, solvents, heavy metals, inorganic salts and fibers. Biological treatment cannot remove many of these recalcitrant and biotoxic pollutants. Therefore, other treatments are necessary to recycle these effluents [25], namely ozonation. The dosage of ozone applied to the dye-containing effluent is dependent on the total colour and residual COD to be removed, with no residue or sludge formation and no toxic metabolites. One major advantage of ozone is that can be applied in its gaseous state and therefore the volume of wastewater and sludge does not increase [24].

Pesticide pollution of water courses is a universal problem with ecological consequences. The major sources of pesticide pollution are wastewaters from agricultural industries and pesticide formulating or manufacturing plants. Ozonation has been recognized as especially efficient for pesticide removal [26] and ozone is currently applied in operational plants either alone or in combination with hydrogen peroxide and/or granular activated carbon filtration [27-30]. Numerous studies have shown that each pesticide has an individual behave during ozonation [19]. Ozonation processes have been effective for the removal from water of several pesticides such as triazine herbicides [31-33]. On the other hand, ozonation appears to be ineffective for lindane and DDT (dichlorodiphenyltrichloroethane) elimination [34].

One of the most important environmental problems related to paper industry is the high consumption of water. High concentrations of some pollutants can be found in pulp and paper wastewaters and the most important products are from the degradation of starch, such as saccharides or carboxylic acids, phenolic compounds derived from lignin and lower amounts of other pollutants that are present in the fresh waters [35]. As wastewaters from recycled papermaking process are biodegradable, they can be treated by biological processes; however, the amount of organic matter is so high that a conventional biological reactor is not functional. A possible way to overcome the problem consists in a combination of two biological stages, first an anaerobic treatment and after an aerobic process. Ozonation can be used as a first stage, followed by treatment in an aerobic biological reactor, achieving a complete degradation of some products and diminishing the organic load.

Over the past few years, pharmaceuticals are considered as an emerging environmental problem due to their continuous input and persistence to the aquatic ecosystem, even at low concentrations [36]. Advanced oxidation processes are promising for an efficient degradation of pharmaceuticals in water and wastewaters, since an increment in the ratio BOD_5/COD and an improvement in the biodegradability of persistent substances are verified. Some pharmaceuticals are extremely reactive towards molecular ozone, such as antibiotics trimethoprim, sulfamethoxazole, clarithromycin, erythromycin and roxithromycin, while others are relatively resistant to ozonation, for example anti-anxiety agent diazepam and the analgesic ibuprofen. However, the degree of degradation of pharmaceutical compounds achieved by ozonation depends on a number of factors, including the

oxidant dose, concentration of pharmaceuticals, wastewater quality parameters and mode of operation [37].

1.1.2 Organic pollutants

Several groups of organic compounds are currently widely used in a vast range of industries, and many of these are strong contaminants when they are released into freshwater ecosystems. Industrial plants generate increasing amounts of wastewater, contaminated with toxic and hazardous organic compounds, which cause severe problems to the environment. Wastewaters produced in many industrial processes often contain organic compounds that are toxic and not removed by direct biological treatment. Summarizing, a wide variety of compounds, such as dyes, detergents, insecticides, pesticides, carboxylic acids, phenolic compounds and pharmaceuticals, are extensively presented in industrial wastewaters.

Intense colour is one of the main characteristics of textile wastewater originated from spent dye baths and dye rinsing operations. Besides the undesirable aaesthetic impact caused by such effluents in receiving natural water courses, the persisting colour and the non-biodegradable nature of most of the textile dyes represent serious problems to the environment [38]. The classification of dyes is based either on the chemical nature of the molecule chromophore, and on the mode of application in the dyeing process. There are about 12 classes of chromophore groups, the most common being the azo, followed by the anthraquinone type. According to the second classification, dyes are named as acid, reactive, disperse, direct, basic, among others. Reactive dyes are one of the most representative classes, since they are used in the dyeing of cotton, which is the mostly used textile substrate. From an ecological point of view, this class of dyes is also the most unfavorable, as they have a low fixation degree compared to other types of dyestuff, since the functional group also bonds to water, becoming hydrolyzed [39, 40]. Then, up to 50% of the dye concentration may remain in the exhausted dyebath. In addition, the effluents produced are frequently heavily coloured and contain high concentrations of salts [39]. One of the most marked features of modern dyes is their high degree of chemical, photolytic and microbiological stability. Thus, dyes are not easily degradable under aerobic conditions, remaining in the conventional biological treatment processes [41-43]. Other conventional treatment technologies, such as chemical coagulation, activated

carbon adsorption, electrochemical treatment and reverse osmosis, are also usually inefficient in removing this type of pollutants. The oxidation of dyes and chemical auxiliaries present in textile effluents lead to the formation of intermediates that are frequently resistant to ozone attack. Such compounds of low reactivity towards ozone may be efficiently removed by oxidation via $HO^{\bullet}$ radicals [44]. Therefore, advanced oxidation processes, as catalytic oxidation, are the main emerging routes for the removal of those persistent compounds [45].

Carboxylic acids are important materials used by chemical industries, such as textile, paper, detergents, plastics and pharmaceutical, and they are often obtained as aqueous solutions. Oxalic acid is a pollutant existing in many effluents especially in metallurgical and textile industrial wastewaters. Furthermore, oxalic acid is a detectable intermediate in the mineralisation of many pesticides and other organic compounds and, at the same time, it is oxidized directly to CO_2 without the formation of any stable intermediate products [46]. Then, oxalic acid has been identified as one of the most common final oxidation products from organic compounds degradation. The low reaction rate constants reported in the literature for the ozonation of oxalic acid and their corresponding anions ($k < 0.04\ M^{-1}\ s^{-1}$ at pH > 5 [44]) explain why this compound always accumulate as final product when organic aqueous solutes are ozonized. The oxidation of organic compounds containing nitrogen functional groups (azo, amine and amide) can also result in the formation of oxamic acid [47, 48], which is more refractory to oxidation than oxalic acid.

Aromatic amines, such as aniline, are important chemicals used as raw material in many industrial processes including the manufacturing of antioxidants, dyes, pigments, rubbers, pharmaceuticals, pesticides, herbicides, explosives, and as a solvent in perfumes, varnish and resins [49]. These compounds are frequently found in industrial effluents and surface water due to their disposal, which cause a series of environmental problems. Their effects on human health have aroused great attention because they have been identified as potential carcinogens and found to possess the ability of preventing oxygen uptake in the blood and damaging the spleen. Generally, these pollutants are not susceptible to anaerobic or aerobic biodegradation, and their elimination cannot be accomplished by conventional biological treatments [50].

Concluding, the wastewaters from chemical industry are generally highly concentrated with organic and inorganic pollutants and may contain many toxic, mutagenic, carcinogenic or nonbiodegradable aromatic compounds that lead to

pollution of the soil and groundwater and cause perturbations in the ecosystem as well as serious health problems.

In this work, dyes, carboxylic acids and aromatic amines are used as model organic compounds. In Table 1.1 and 1.2 are presented, as example, the properties of two dyes and some selected pollutants, respectively.

Table 1.1: Characteristics of C.I. Reactive Blue 5 and C.I. Acid Blue 113 dyes.

Class/ Molecular formula	Commercial name/ 3D representation[a]	Generic name	λ_{max} (nm)
Reactive/ $C_{29}H_{20}ClN_7O_{11}S_3$	Cibacron Blue BR 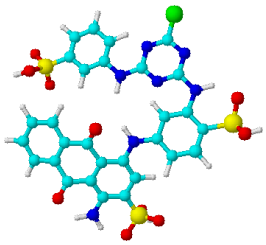	C.I. Reactive Blue 5	597
Acid/ $C_{29}H_{20}ClN_7O_{11}S_3$	Eryonil Navy R 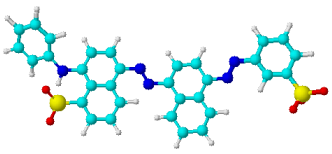	C.I. Acid Blue 113	565

[a] 3D optimization was carried out using the ChemSketch software from ACD.

Table 1.2: Properties of the selected compounds.

Compound		M (g mol^{-1})	pKa
Oxalic acid	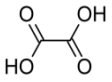	90.04	1.23, 4.19
Oxamic acid	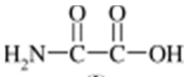	89.05	2.5, 11.8*
Aniline	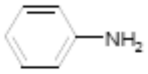	93.1	4.64*

* pKa corresponding to NH_3^+ group.

1.2 Ozone

Ozone is a powerful oxidizing agent and due to its high oxidation and disinfection potential has recently received much attention in water treatment technology. The chemistry of ozone in aqueous solution is complex. Molecular ozone can oxidise water impurities via direct, selective reactions or can undergo decomposition by a chain reaction mechanism resulting in the production of free hydroxyl radicals [51]. The chemical properties of ozone depend on the structure of the molecule. The two extreme forms of resonance structures of ozone molecule are presented in Figure 1.1 [52, 53].

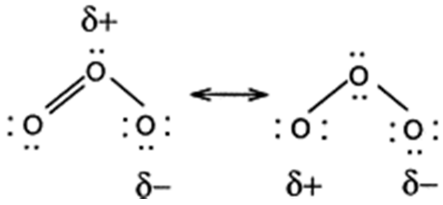

Figure 1.1: Resonance structures of ozone molecule.

Due to its structure, molecular ozone can react as a dipole, an electrophilic or nucleophilic agent. As a result of its high reactivity, ozone is very unstable in water. The half-life time of molecular ozone varies from a few seconds up to few minutes

and depends on pH, water temperature and concentration of organic and inorganic compounds in water [51-53].

Ozone decomposition proceeds through the following five-step chain reaction [54]:

$$O_3 + H_2O \rightarrow 2HO^{\cdot} + O_2 \quad \textbf{1.1}$$

$$O_3 + OH^- \rightarrow O_2^{\cdot -} + HO_2^{\cdot} \quad \textbf{1.2}$$

$$O_3 + HO^{\cdot} \rightarrow O_2 + HO_2^{\cdot} \leftrightarrow O_2^{\cdot -} + H^+ \quad \textbf{1.3}$$

$$O_3 + HO_2^{\cdot} \leftrightarrow 2O_2 + HO^{\cdot} \quad \textbf{1.4}$$

$$2HO_2^{\cdot} \rightarrow O_2 + H_2O_2 \quad \textbf{1.5}$$

The pH value of the solution significantly influences ozone decomposition in water. Basic pH causes an increase of ozone decomposition. At pH < 3 hydroxyl radicals do not influence the decomposition of ozone. For 7 < pH < 10, the typical half-life time of ozone is from 15 up to 25 min [53, 54].

The decomposition of ozone can be significantly lowered in the presence of hydroxyl radicals scavengers due to the following reactions [53, 54]:

$$HO^{\cdot} + O_3 \rightarrow O_2 + HO_2^{\cdot} \quad \textbf{1.6}$$

$$HO^{\cdot} + HCO_3^- \rightarrow OH^- + HCO_3^{\cdot} \quad \textbf{1.7}$$

$$HO^{\cdot} + CO_3^{2-} \rightarrow OH^- + CO_3^{\cdot -} \quad \textbf{1.8}$$

$$HO^{\cdot} + H_2PO_4^- \rightarrow OH^- + H_2PO_4 \qquad 1.9$$

$$HO^{\cdot} + HPO_4^{2-} \rightarrow OH^- + H_2PO_4^- \qquad 1.10$$

In water, there are several compounds that are capable of the initiation, promotion or inhibition of the radical chain reaction process. The initiators, such as OH^-, H_2O_2/HO_2^-, Fe^{2+}, formate and humic substances (HS), are capable of inducing the formation of superoxide ion $O_2^{\cdot -}$ from an ozone molecule. The promoters are responsible for the regeneration of the $O_2^{\cdot -}$ ion from the hydroxyl radicals and they are R_2 - CH - OH, aryl - (R), formate, humic substances and O_3. The inhibitors (CH_3 - COO^-, alkyl - (R), HCO_3^-/CO_3^{2-}, humic substances) are compounds capable of consuming hydroxyl radicals without the regeneration of the superoxide anion [52, 53].

The ability to oxidise organic and inorganic molecules is closely related to the oxidation potential of the oxidant:

$$O_3 + 2H^+ + 2e^- \rightarrow O_2 + H_2O \qquad E^0 = 2.07\,V \qquad 1.11$$

Ozone is used as an effective oxidant in water and wastewater treatment and also air purification. The effective usage of ozone in all the above mentioned fields is vital and therefore extensive research aiming at the utilisation of catalytic ozonation has been undertaken. There are few studies about application of catalytic ozonation in air purification; however, several applications of ozone in water treatment technology are subjects of discussion in many researches.

Ozone is used in disinfection, taste, odour and colour control, oxidation of inorganic pollutants (iron, manganese), oxidation of organic micro and macropollutants, as well as for the improvement of coagulation [52]. There are two main points of oxidant introduction during water treatment: pre-oxidation and intermediate oxidation. Generally, pre-oxidation is applied for the elimination of inorganic compounds, colour, taste, odour, turbidity and suspended solids. During this step, the partial degradation of natural organic matter and inactivation of microorganisms occurs, as well as the coagulation–flocculation–decantation step enhancement takes place. Intermediate oxidation has the aim of the degradation of

micropollutants, the removal of trihalomethanes precursors and increase of biodegradability [55, 56].

1.2.1 Catalytic ozonation

Catalytic ozonation processes can be divided in homogeneous and heterogeneous. In homogeneous catalytic ozonation the ozone decomposition is catalysed by transition metal ions, while in heterogeneous catalytic ozonation ozone decomposition is enhanced by solid catalysts.

1.2.1.1 Homogeneous catalytic ozonation

In the published literature is possible to find two major mechanisms of homogeneous catalytic ozonation. One comprises the decomposition of ozone by metal ions leading to the generation of free radicals. The other involves the formation of complexes between the organic molecule and the catalyst, and subsequent oxidation of the complex. It is necessary to remember that several parameters, such as pH of solution and concentration of the transition metal ion, can influence both the efficiency of the process and its mechanism [57]. Several metal ions were found to be effective as catalysts of the ozonation process. Mn(II), Fe(III), Fe(II), Co(II), Cu(II), Zn(II) and Cr(III) are the most widely used catalysts.

Andreozzi et al. observed a high efficiency of pyruvic acid ozonation in the presence of Mn(IV) and they found that the efficiency increased with a decrease of pH [58]. The effect of *tert*-butanol and sodium bicarbonate on catalytic ozonation indicates that the process proceeds via a radical chain reaction [59]. Additionally, Mn(II) and Mn(IV) were found to have similar activity in another paper reported by Ma and Graham [60].

Pines and Reckhow reported that the catalytic ozonation of oxalic acid in the presence of Co(II) ions proceed via complex formation between an organic molecule and a metal ion [61]. They suggested that the oxidation reaction does not depend on the formation of hydroxyl radicals, since the reaction rate did not change in the presence of *tert*-butanol, a radical scavenger.

In other research by Pli et al. no catalytic activity of Mn(II) ions in the process of oxalic acid removal at pH = 7.5 was observed, while Co(II) revealed high performance [62].

Sánchez-Polo and Rivera-Utrilla confirmed the high catalytic activity of Mn(II), Fe(II) and Zn(II) ions during ozonation of 1,3,6-naphtalenetrisulfonic acid [63].

Furthermore, Xiao et al. reported that Mn (II) had catalytic activity in the removal of dinitrotoluene, while degradation was not observed during the dichlorophenol ozonation. Then, it was concluded that the presence of oxalate plays a vital role in ozonation processes [64, 65]. In ozonation of dinitrotoluene, which does not lead to the formation of oxalic acid as a by-product, Mn (II) had a good performance. On the other hand, during the process of dichlorophenol ozonation, which leads the formation of oxalic acid, no catalytic activity of Mn (II) ions was observed.

In spite of the good results reported in the literature, not all the processes occurring are understood and it is necessary to remove the metal ions from treated water. Therefore, homogeneous catalytic ozonation is not as popular as heterogeneous catalytic ozonation.

1.2.1.2 Heterogeneous catalytic ozonation

Researches on heterogeneous catalytic ozonation began in 1970, however it has now much interest. The major advantage of a heterogeneous over a homogeneous catalytic ozonation is the ease of catalyst recovery from the reaction media. The stability and durability of the catalyst are important factors to determine the quality of the process. Leaching of the catalytic active species, as well as poisoning of the active sites and fouling of the catalyst surface by intermediate reaction products are important parameters, which determine the stability and durability of the catalyst [66].

During the last decade, heterogeneous catalytic ozonation has received much attention in water treatment due to its high oxidation potential [51, 57]. Metal oxides represent one of the most important and widely employed classes of solid catalysts, either as active phases or supports. Minerals are also widely used as catalysts in heterogeneous ozonation. Among the carbon materials, ozonation catalyzed by activated carbon has been reported in several researches. In recent years, heterogeneous catalytic ozonation in the presence of carbon nanotubes has also been studied. There are several factors that affect the heterogeneous catalytic ozonation process. Among the most important are the temperature and pH, which significantly influence ozone stability in water. Ozone decomposition constant is strongly pH dependent and increases with an increase of pH.

MnO_2 is the metal oxide mostly studied in catalytic ozonation. It is reported to be the most efficient in ozone decomposition in gaseous medium [67] and it was verified that the catalytic activity increases with the decrease of pH in removal of pyruvic, oxalic, sulfosalicylic and propionic acids [58, 68, 69]. It has also been reported that commercial MnO_2 is not active, as opposed to MnO_2 formed *in situ* [69, 70]. There is unfortunately a lack of understanding of the reaction mechanisms of MnO_2. Andreozzi et al. proposed that the reaction mechanism involves the adsorption of the substrate on the solid and subsequent attack of ozone on adsorbed organic molecule [68]. Afterwards, Tong et al. proposed the same mechanism [69].

Ma and Graham proved that MnO_2, formed in situ from the ozonation of homogeneous Mn^{2+}, significantly improve the efficiency of the ozonation of atrazine at neutral pH and the presence of humic substances (HS) was found to increase ozonation efficiency [59, 60, 70]. When low concentrations of HS are present in aqueous solution, manganese dioxide and humic substances can initiate ozone decomposition and hydroxyl radicals' formation, producing a greater oxidative effect than would be obtained by MnO_2 or by HS independently. On the other hand, higher concentrations of humic substances are supposed to consume the hydroxyl radicals formed by manganese dioxide and humic substances, decreasing the efficiency of the catalytic process. Adsorption of atrazine on MnO_2 was found to be negligible, removing less than 10% [60].

In another work, catalytic ozonation in the presence of MnO_2 was found to effectively remove TOC and COD of a raw water (containing precursors of trihalomethanes (THMs), humic and fulvic acids) [71].

Furthermore, Dong et al. reported the high activity of β-MnO_2 nanowires during the removal of phenol [72]. Only a very low adsorption of phenol on β-MnO_2 was observed and catalytic ozonation is more efficient than single ozonation in phenol removal. Decomposition of ozone was also more significant, which indicates radical reactions occurring. It was observed that Mn ions dissolved into the solution have a negative impact in the efficiency of the catalytic process and, therefore, it was possible to conclude that the activity verified was mainly from the heterogeneous catalysis on the surface of the catalyst.

Faria et al. [50] reported that manganese, cobalt and cerium oxides catalyse the ozonation of sulfanilic acid and aniline, significantly increasing the mineralisation rate of the corresponding solutions, comparatively to single ozonation. The experimental results showed that intimate mixtures of metal oxides of cerium and

manganese or cerium and cobalt, obtained by coprecipitation, are more efficient ozonation catalysts than the corresponding single metal oxides, which might be related both to their higher surface areas and enhanced redox properties.

The ozonation catalyzed by TiO_2 was found to be efficient for oxalic acid degradation in water at acidic pH [73]. Yang et al. studied ozonation of nitrobenzene on nano-TiO_2 and observed that nano-TiO_2 is catalytically active, if present in the form of rutile and not anatase [74]. Adsorption of nitrobenzene was found to play an important role and its degradation proceeds via radical pathway. Catalytic activity of TiO_2 was also investigated in the process of the removal of pharmaceuticals, such as carbamazepine and naproxen, and an effect on the mineralisation of ozonation by-products and their composition was verified [75]. Rosal et al. studied the degradation of clofibric acid and adsorption and subsequent reaction of organics on catalyst sites are supposed to be the responsible for the enhancement of ozonation rate observed in catalytic runs [76, 77].

Alumina was shown to be an effective catalyst for the ozonation of 2-chlorophenol and the highest efficiency was observed at neutral pH [78].

Cooper and Burch reported that ozone decomposition takes place on the surface of Al_2O_3, which increases the efficiency of oxalic acid, chloroethanol and chlorophenol degradation [79]. On the other hand, Kasprzyk-Hordern and Nawrocki reported no catalytic activity of Al_2O_3 during the removal of aromatic hydrocarbons [80] and ethers [81]. Furthermore, Kasprzyk-Hordern et al. demonstrated the high efficiency of natural organic matter (NOM) removal during its ozonation in the presence of alumina [82]. The difference between catalytic activity of alumina in the removal of aromatic hydrocarbons or ethers and NOM might therefore result from the different adsorption capacity of alumina towards aromatic hydrocarbons and NOM. In opposite, Ernst et al. studied catalytic ozonation of several model compounds (oxalic, acetic and succinic acids) and reported that adsorption of organic molecule is harmful to the activity of γ-Al_2O_3 [82]. Beltrán et al. observed similar results during the process of catalytic ozonation of oxalic acid at pH 2.5 in the presence of alumina [83]. On the other hand, Álvarez et al. reported that adsorption of pyruvic acid on the surface of alumina is a necessary step of the catalytic ozonation process as oxidation reactions take place for the acid molecules already adsorbed on the surface of the catalyst [84]. Concluding, there are several results published in literature about ozonation catalyzed by alumina, but they are very contradictory.

Park et al. reported the use of commercially available goethite (FeOOH) in the removal of natural organic matter [85, 86]. Zhang and Ma also studied the catalytic activity of goethite in the removal of nitrobenzene and they verified that nitrobenzene does not adsorb on the surface of the catalyst and the catalytic ozonation process was found to proceed by a radical pathway [87].

In spite of cerium oxide was found to be particularly effective catalysts in several processes, few studies reported in detail ozonation catalyzed by single cerium oxide. CeO_2 showed high performance in the ozonation of aniline, sulfanilic acid and dyes [50, 88].

Cerium oxides were also found to be effective in the ozonation of simulated wastewater containing phenolic compounds [89]. The combination of ceria and manganese was shown to provide the most active catalyst among the laboratory ceria-based catalysts that were tested. On the other hand, among commercially available catalysts for environmental applications, the best was that containing iron in the presence of manganese (Fe_2O_3−MnO_x).

More recently, TiO_2 deposited on activated carbon was also found to be effective in the removal of methylene blue in the catalytic ozonation process [90].

Beltrán et al. studied catalytic ozonation of oxalic acid on Fe_2O_3/Al_2O_3 and they found out that the removal of oxalate is independent of the presence of *tert*-butanol [91].

The application of ruthenium deposited on several supports as a possible ozonation catalyst was discussed in several papers. Karpel Vel Leitner et al. reported that the method of catalyst preparation plays a vital role in its catalytic activity, since ruthenium deposited on a support via impregnation was found to be much more efficient than ruthenium deposited via ion exchange [92]. The relation between catalytic activity of Ru–CeO_2/TiO_2 and pH of solution was also studied [93]. Carbajo et al. verified high catalytic activity of Rh/CeO_2 during ozonation of pyruvic acid in water [94].

Cobalt supported on SiO_2 [95] or Al_2O_3 [96] have been extensively studied in ozonation process. The high dispersion of Co oxide and the multivalence oxidation states of cobalt were suggested to be responsible for the catalytic activity observed [95]. The use of a Co_3O_4/Al_2O_3 (10 wt% Co) catalysts prepared by the impregnation method has been shown to significantly enhance the ozonation rate of oxalic acid in water at low pH and the presence of *tert*-butanol, a well known $HO^{\bullet}$ radical

scavenger, did not affect the oxalic acid removal rate. However, the occurrence of metal leaching is a major drawback of this catalyst [96]. With the aim of improving the stability of Co/Al_2O_3 catalysts, Álvarez et al. focused on the preparation method and structural characterization [84]. They concluded that the sample containing Co_3O_4 as the main phase provided the most promising results on the ozonation of pyruvic acid [84].

Leitner et. al [92] studied the ozonation of succinic acid in the presence of ruthenium (2%) supported on cerium dioxide and a slightly catalytic activity was verified.

Natural mineral materials, such as brucite (magnesium hydroxide), have been presented as economical and feasible choices for the enhanced ozonation of nitrobenzene, aniline [97] and an azo dye [98]. Natural brucite and magnesia (brucite calcined at 450 °C) were also studied as ozonation catalysts of phenol [99]. Raw bauxite, containing γ-AlOOH as the major component, was reported to be an effective catalyst for the ozonation of 2,4,6-trichloroanisole [100].

Valdés et al. studied ozone decomposition in aqueous solution promoted by zeolite and volcanic sand (composed of: SiO_2, 63.7%; Al_2O_3, 13.9%; Fe_2O_3, 4.7%; Na_2O, 3.8%; K_2O, 3.0%; CaO, 2.9%; MgO, 1.2%) in the ozonation of benzothiazole [101]. Zeolite and volcanic sand increased ozone decay rates and the efficiency of ozone decomposition was found to be dependent on the pH of the solution and pH_{PZC} of the catalyst. Additionally, modification of zeolite and volcanic material with HCl–hydroxylamine treatment resulted in a change in the capacity of the materials to decompose ozone. In the case of modified zeolite, the capacity to decompose ozone increased significantly, probably due to the increase of Lewis acid sites. The catalytic mechanism is supposed to involve both homogeneous (i.e. with the participation of $HO^{\bullet}$ radicals) and surface reactions [102].

Ceramic honeycomb ($2MgO–2Al_2O_3–5SiO_2$) of a low surface area (<0.5 $m^2 g^{-1}$) was reported by Zhao et al. to be an active catalyst for nitrobenzene ozonation [103, 104]. The process was found to proceed via a radical pathway and the highest efficiency of the process was observed at pH of solution close to pH_{PZC} of the catalyst. Therefore, it was suggested that surface bound hydroxyl groups are responsible for the formation of hydroxyl radicals. In other work, Zhao et al. proved again that hydroxyl groups are responsible for the catalytic activity of ceramic honeycomb [105]. Furthermore, the modification of ceramic honeycomb with Mn, Cu and K ions was found to additionally increase catalytic activity of the catalyst in

the ozonation of nitrobenzene [106]. The significant increase of surface area and ability to initiate hydroxyl radicals generation were the responsible for the catalytic behavior verified. Adsorption of nitrobenzene on the surface of the catalysts was negligible.

Perovskite $LaTi_{0.15}Cu_{0.85}O_3$ has been successfully used as catalyst in the ozonation of pyruvic acid at pH = 2.5 and it was concluded that the reaction occurs on the surface of the catalyst [107]. High stability was also observed in the ozonation of gallic acid, substance containing an aromatic ring [108]. The addition of *tert*-butanol had no effect on the catalytic removal of gallic acid, although its presence decreased the mineralisation degree achieved, which indicates the importance of hydroxyl radicals in the decomposition of primary products of gallic acid. The same perovskite was evaluated in the ozonation of different phenolic wastewaters and the catalytic activity and stability were confirmed by consecutive experiments [109]. Recently, copper perovskite was reported as the most appropriate catalyst to improve TOC removal in the ozonation of sulfamethoxazole [110].

In spite of metal oxides being continuously a subject of intense research, metal leaching, low stability and the difficulty of separate the materials from the treated water are sometimes a problem. In order to overcome these troubles, spinel-type ferrite nanoparticles have been extensively studied in several areas, including catalysis. More recently, magnetic Co and Mn-doped γ-Fe_2O_3 prepared by the co-precipitation method was found to be highly effective for the mineralisation of 2,4-dichlorophenoxyacetic acid, the most widely used herbicide in the world, and its derivatives in aqueous solution with ozone. The higher reactivity was attributed to multivalence oxidation states and more Lewis acid sites on the surface of Co, Mn-doped γ-Fe_2O_3 [111]. High efficiency and stability was also verified with magnetic Co-doped Fe_3O_4 suspensions for degradation of toxic pollutants and a hydroxyl reaction mechanism was suggested [112]. More recently, magnetic porous ferrospinel $NiFe_2O_4$ prepared by sol-gel method showed high efficiency in the ozonation of di-n-butyl phthalate [113]. Ren et al. verified that the catalytic process was pH dependent and confirmed that surface hydroxyl groups were the main active sites of $NiFe_2O_4$, suggesting a $HO^{\bullet}$ radicals mechanism.

Concluding, two general mechanisms are proposed for ozonation catalyzed by metal oxides and supported metal oxides. One mechanism suggests the adsorption of ozone and its further decomposition leading to surface bound oxygenated radicals, which are active oxidative species responsible for the oxidation of adsorbed organic molecules. Alternatively, the other mechanism comprises

adsorption of ozone and its further decomposition to hydroxyl radicals that promote oxidation reactions in the liquid phase or in the solid-liquid interface.

Activated carbon was shown to be a good catalysts for ozonation reactions and it is believed that activated carbon enhances the decomposition of dissolved ozone leading to the formation of highly oxidant species such as $HO^{\bullet}$ in solution and surface oxygenated active species.

Firstly, it was observed that activated carbon used together with ozone can provide better removal of colour than when the two techniques are applied individually [114]. After, similar results have been observed for the removal of phenolic compounds from water [115]. Jans and Hoigné showed that a small amount of activated carbon can result in the decomposition of ozone in water leading to the generation of hydroxyl radicals [116]. Furthermore, they reported that ozone decomposition occurs on the surface of activated carbon and hydroxyl radicals formed react with organic molecules in the solution.

Beltrán et al. [117] and Patrícia et al. [118] studied the kinetics of ozone decomposition and revealed that ozone decomposition occurs mainly at basic pH and it is catalysed by hydroxyl ions, which are adsorbed on the surface of the catalyst. Beltrán et al. [117] concluded that hydroxyl radicals are formed mainly in the bulk solution, instead of resulting from surface interactions. In another paper, Beltrán et al. proved that mineralisation of oxalic acid at pH = 2.5 during ozonation proceeds via a radical pathway and occurs in bulk solution [119]. On the other hand, Faria et al. verified that mineralisation of oxalic acid at pH = 3 proceeds via reactions occurring both on the surface of activated carbon and also in the bulk solution [45]. The basicity of activated carbon is responsible for ozone decomposition and adsorption was found to play an important role in the observed catalytic effect of activated carbon during ozonation of carboxylic acids. Sánchez-Polo and Rivera-Utrilla observed similar results in the ozonation of 1,3,6-naftalenesulfonic acid [120].

In other works Beltrán et al. reported that activated carbon is more efficient than single ozonation in the pyruvic acid degradation [119] and the ozonation of gallic acid led to the formation of several by-products, which are mineralised as a result of secondary radical reactions initiated via ozone decomposition on activated carbon [121].

Faria et al. verified that ozonation is an efficient process for the removal of aniline from aqueous solution, though leading to the formation of several by-products [122].

Higher mineralisation rates were obtained at neutral and basic pH and the use of basic activated carbons is advantageous for this process, which might be due both to their enhanced ability to catalyse the decomposition of ozone in aqueous phase and to their adsorption capacity towards organic compounds.

The mineralisation of benzenesulfonic acid and sulfanilic acid was also studied by Faria et al. [123]. The presence of activated carbon during ozonation of these sulfonated aromatic products increases the rate of degradation and mostly enhances the reduction of TOC. The use of a basic activated carbon is again advantageous for this process and the presence of a radical scavenger suggests that the carbon surface plays a role in the reaction mechanism. In another work, they concluded that the combination of activated carbon with ozone enhanced the mineralisation levels of both the dye solutions and the textile effluents [88].

Ma et al. reported that ozonation of nitrobenzene at pH = 6 proceeds through radical reactions and is strongly dependent of *tert*-butanol [124]. Several activated carbons were also effective in the removal of diclofenac from water, with an efficiency close to 100 %, and it was suggested that adsorbed organic compounds (diclofenac and its intermediates) react with adsorbed ozone [125, 126].

Summarizing, the proposed mechanisms of catalytic ozonation on activated carbon are contradictory. Some studies indicate radical processes, others specify that the catalytic activity of activated carbon does not result from the capacity to generate hydroxyl radicals.

Liu et al. presented a mechanism of oxalic acid ozonation on multi-walled carbon nanotubes (MWCNTs) [127]. According to this mechanism, active oxygen species are formed on the surface of the catalyst as a result of ozone decomposition and they react with adsorbed organic molecules, in spite of oxidative reactions also taking place in bulk solution. MWCNTs with different surface chemical properties were used as catalysts for ozone decomposition and for the ozonation of oxalic and oxamic acids [128]. The decomposition of ozone is favoured by MWCNTs with large specific surface areas and low acidic character and the simultaneous use of ozone and MWCNTs produced a significant improvement of oxalic and oxamic acids removal. Successive experimental runs of oxalic acid ozonation showed that the surface chemistry suffers a slight progressive oxidation by exposure to dissolved ozone.

Carbons materials were also used as supports for metals and metal oxides. Ma et al. reported that MnO_2/GAC revealed higher catalytic activity during nitrobenzene

ozonation and the highest efficiency took place at lower pH [124, 129]. They concluded that oxidative reactions do not proceed by radical reactions and adsorption of nitrobenzene on the surface of the catalysts plays an important role.

Metal doped carbon aerogels were studied by Sanchés-Polo et al. as ozonation catalysts of p-cholorobenzoate. *p*-CBA removal rate was increased in presence of Mn aerogel, whereas the presence of Co or Ti doped carbon aerogels had no effect on this rate. The capacity to accelerate this process depends on the dose of aerogel and the concentration of Mn(II) on its surface [130].

Nickel oxide deposited on activated carbon was found to increase the efficiency of *p*-CBA ozonation, leading to almost complete mineralisation [131]. In other work, several metal oxides such as Ni, Fe, Co and Mn were deposited on mesoporous carbon cryogel beds and they were studied in phenol ozonation; however, further researches will be needed to clarify the reaction mechanism [132].

Cerium oxide supported on activated carbon has been shown to be effective ozonation catalyst in the degradation of sulfanilic acid, aniline and an acid dye, nevertheless significant part of the catalytic effect observed was attributed to the support [50]. Faria et al. also reported the use of ceria and a composite of cerium oxide and activated carbon in the ozonation of oxalic and oxamic acids and a strong synergic effect was verified between activated carbon and cerium oxide in the prepared composite [133].

Cerium supported on activated carbon prepared by the dipping method was shown as a promising catalyst for ozonation of dimethyl phthalate (DMP) and its stability was confirmed [134].

Pt deposited on carbon nanotubes showed higher catalytic activity than Pt deposited on activated carbon in oxalic acid degradation. It was concluded that hydrogen peroxide and hydroxyl radicals were generated and participated in the process of oxalic acid ozonation and the redox couple of Pt_{red}/ Pt_{ox} played a key role in the activity improvement of CNT [135].

1.3 Materials selected to be used as catalysts

1.3.1 Carbon materials

Carbon materials have unique properties: high specific surface area and pore volume, good mechanical strength, inertness for most of liquid media and non-

oxidative atmospheres, and the possibility to tailor their textural and chemical properties for a specific application [136-139]. Therefore, they have been applied in several areas, such as gas separation, water and air purification, chromatography and especially in adsorption and catalysis [140-142].

Carbon surface chemistry can be modified by liquid phase treatments with HNO_3 or H_2O_2 using different concentrations and/or contact time, or by thermal treatments at high temperature under different atmospheres (N_2, H_2 or air).

Most of these materials, namely activated carbons, are microporous (porous diameter < 2 nm) and therefore they are used as molecular sieves, in adsorption and in catalytic reactions involving small molecules. However, they cannot be efficiently used in applications involving bulky molecules, such as dyestuffs, electrodes for supercapacitors and fuel cells, and as hosts for enzyme immobilization [143]. Therefore, it is more convenient to use mesoporous carbon materials (2 nm < porous diameter < 50 nm) [144, 145].

The main techniques to obtain mesoporous materials include: a high degree of activation by physical or combined physical/chemical methods, carbonization of carbon precursors composed of one thermosetting component and one thermally unstable component, catalyst-assisted activation of carbon precursors with metal (oxides) or organometallic compounds [146, 147], carbonization of aerogels or xerogels [148-150], replication synthesis with presynthesized hard templates through impregnation, carbonization and template removal and self-assembly using soft templates through co-condensation and carbonization [151]. The synthesis of microporous, mesoporous and macroporous carbons generally use as templates zeolites, mesoporous silicas and synthetic silica opals, respectively.

Significant developments have been achieved in the synthesis of mesoporous carbon materials during the last decade [152]. In order to obtain mesoporous carbons with uniform and interconnected pores, the synthesis via templating has been recently applied [136, 153-155]. The procedure for the synthesis of mesoporous carbons using nanostructured silica as template involves four consecutive steps: preparation of the mesostructured silica; incorporation of a polymeric precursor and respective polymerisation in the interior of the silica pores; carbonization; removal of the silica template. The template must present an appropriate 3D porous structure; on the other hand disordered carbon materials will be formed. Figure 1.2 presents a schematic representation of the template synthesis.

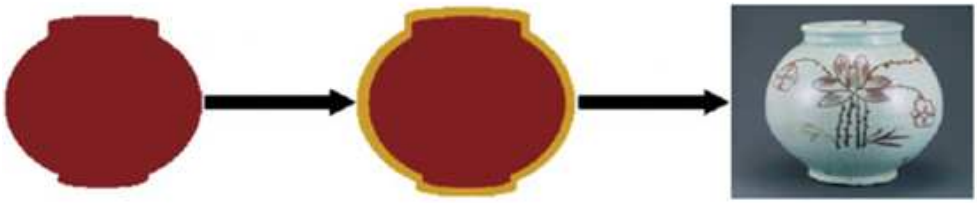

Figure 1.2: Schematic representation of the concept of template synthesis [143].

Beck et al. [156] synthesized the first carbon material with ordered mesopores using MCM-48 silica as template. The synthesized carbon material was designed by CMK-1 and it had a 3D interconnected pore structure with a high BET surface area (1500-1800 m^2 g^{-1}) and large total volume (0.9-1.2 cm^3 g^{-1}) [157, 158]. CMK-1 presented uniform mesopores with diameter of 3 nm, as well as some micropores. Figure 1.3 shows a schematic representation of the CMK-1 synthesis.

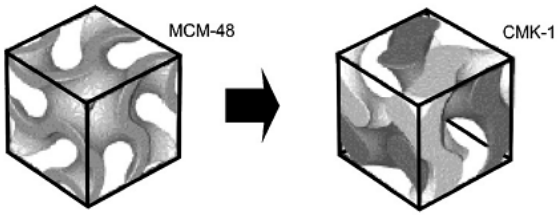

Figure 1.3: Schematic representation of the CMK-1 synthesis using MCM-48 as template [159].

Other group used a different method to obtain a mesoporous carbon (SNU-1) from the same template; however, the resulting carbon was not a real negative replica of the MCM-48, because the replicated carbon underwent a structural transformation during the removal of the silica template [160].

Following the first report on the synthesis of ordered mesoporous carbons using the MCM-48 silica template, various mesoporous carbon materials with different pore structures were synthesized using a variety of different mesoporous silica templates.

Hexagonally ordered mesoporous silica SBA-15 was used as a template for a mesoporous carbon designated as CMK-3 [161]. In the original study by the Stucky group, SBA-15 was reported to have a hexagonal tubular pore structure similar to

that of MCM-41. However, by using SBA-15 silica as the template, Ryoo et al. successfully synthesized an ordered mesoporous carbon in which parallel carbon fibers were interconnected through thin carbon spacers [162-164]. The ordered structure of the CMK-3 carbon was the exact inverse replica of the SBA-15 silica without the structural transformation during the removal of the silica template. CMK-3 type ordered mesoporous carbon was also synthesized by the infiltration of the carbon precursor via adsorption in the vapor phase and using *p*-toluene sulfonic acid impregnated SBA-15 as template [165]. Figure 1.4 presents the schematic illustration of CMK-3 synthesis.

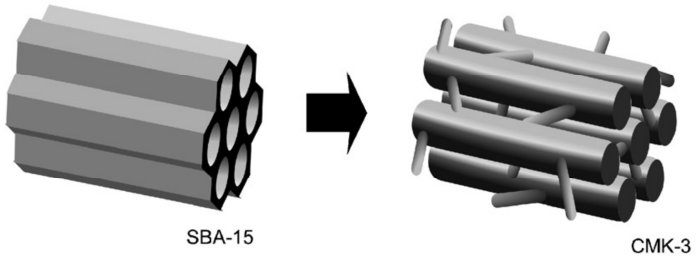

Figure 1.4: Schematic illustration for the synthesis of CMK-3 using SBA-15 as template [166].

CMK-5, a nanopipe-type mesoporous carbon, was also synthesized by Ryoo and co-workers [167]. The hexagonally ordered arrays of carbon nanotubes were obtained from the partial wetting of poly(furfuryl alcohol) onto the SBA-15 silica channels and subsequent carbonization. Several other research groups synthesized similar nanopipe-type ordered mesoporous carbon materials and the catalytic chemical vapor deposition method allowed to obtain ordered mesoporous carbon CMK-3 with a hollow spherical particle shape [168].

Following the first report on MCM-48 silica, much effort has been made to synthesize cubic mesoporous silica with large pores to be used as catalyst for large-sized molecules. Three research groups independently reported the synthesis of mesoporous silica with very large pores using a P123 triblock copolymer ($(EO)_{20}(PO)_{70}(EO)_{20}$) as the template and the successful replication to highly ordered mesoporous carbons [169-171].

Although many mesoporous carbons can be synthesized using different mesoporous silica templates, as described above, the resulting pore sizes are generally less than 10 nm, because the pore size of the replicated mesoporous carbon is generally determined by the wall thickness of the silica template. To synthesize mesoporous carbon materials with uniform pore sizes of > 10 nm, a mesocellular silica foam synthesized by the Stucky group [172-174] was employed as the template [175].

Among the mesoporous silicas, SBA-15 silica has attracted great interest due to their larger pores, thick pore walls and therefore higher hydrothermal stabilities, and significant amounts of microporosity in the walls [176, 177]. In the synthesis of mesoporous SBA-15, nonionic triblock copolymer P123 and strong acidic conditions (pH < 1) are employed in most cases. Later on, extensive works were devoted to tailor the textural and morphological properties of this important kind of mesoporous silica, including mesopore size, microporosity, particle size and morphology [178].

Microporous carbon materials with uniform pores and with ordered regular pore arrays require rigid inorganic templates. Zeolites are aluminosilicate materials having ordered and uniform sub-nanometer sized pores. Since the walls of zeolites have a uniform thickness of < 1 nm, they have been used as inorganic templates for the synthesis of microporous carbons with uniform pore sizes. The Kyotani group [143] adopted the USY zeolite as the template to prepare a microporous carbon. A carbon precursor (poly(acrylonitrile) or poly(furfuryl alcohol)) was incorporated into the pores and channels of the zeolite and carbonization followed by the removal of the zeolite template produced microporous carbon materials.

Spherical silica particles have been used as templates for the synthesis of macroporous carbon materials and the pore size of the resulting materials could be easily controlled by varying the particle size of the silica spheres. Zakhidov et al. used synthetic silica opals as templates to synthetize various macroporous carbon materials [179]. Macroporous carbon materials with glassy carbon, graphitic carbon and diamond were synthesized by the infiltration of a phenol resin, the CVD of propylene gas and plasma-enhanced CVD, respectively, followed by the carbonization. The removal of the silica template by HF etching generated macroporous carbons with inverse opal structures.

Mesoporous carbon xerogels have also attracted a great deal of interest, since they possess excellent characteristics as catalyst supports, such as high surface area, high porosity, open pore network, controllable pore size, and can be prepared in the

desired form (monolith, thin film or powder). Porous carbon materials prepared by polycondensation of hydroxylated aromatics (phenol, catechol, resorcinol, hydroquinone or phloroglucinol) and aldehydes (formaldehyde or furfural) in a solvent followed by drying and pyrolysis have been extensively studied [180]. The nature of the precursors, the gelation conditions and the drying method determine the texture of the carbon material obtained. For the preparation of carbon xerogels, the most common precursors are resorcinol and formaldehyde, and the polymer is usually synthesized using water as solvent and Na_2CO_3 as catalyst, at selected solution pH values. Then, the wet gels are conveniently dried and subsequently carbonized, leading to carbon xerogels. These materials can be conveniently functionalized. The major reactions between resorcinol and formaldehyde include an addition reaction to form hydroxymethyl derivatives (--CH, OH) of resorcinol, and a condensation reaction of the hydroxymethyl derivatives [181]. The catalyst (sodium carbonate) plays an important role in the addition reaction because it promotes the formation of the resorcinol anion by hydrogen abstraction. At the beginning of the reaction, both uncharged resorcinol molecules and a small percentage of charged resorcinol anions exist. Compared to the uncharged resorcinol molecules, the resorcinol anions are more reactive toward the addition of formaldehyde to form the hydroxymethyl derivatives, which are the critical monomers for further polymerization. Upon the formation of these hydroxymethyl derivatives, condensation proceeds via H^+, which acts as a catalyst. In the presence of a proton, the hydroxymethyl derivative of resorcinol loses its -OH group to form a benzyl-type cation (- ph – CH_2^+). The cation then undergoes an electrophilic reaction with the benzene ring of another molecule to connect the two benzene rings with a methylene bridge. Pekala et al. [182] also proved that the cation can react with a hydroxymethyl group of another molecule to form a methylene ether bridge. Such a condensation reaction takes place successively to form a three-dimensional crosslinked polymer. It is verified that both the sodium carbonate as a base catalyst and the proton as an acid catalyst play important roles in the addition and condensation reactions, respectively. If the pH is too low, precipitation occurs. The size of the gel increases, but decreases the number of units. On the other hand, if the pH is too high, condensation is hindered [181].

1.3.2 Metal oxides

Metal oxides represent one of the most important and widely employed classes of solid catalysts, either as active phases or supports [51]. Several reported studies

have shown that metal oxides and supported metal oxides can be efficient for the catalytic ozonation of a vast range of organic contaminants. Supported and unsupported oxides of transition metals are frequently studied ozonation catalysts. Physical properties such as surface area, mechanical strength, density, porous volume and their size distribution are crucial variables to choose a metal oxide. Chemistry stability and surface active sites are essential to make metal oxides efficient catalysts in several catalytic processes.

The most common ozonation catalysts are manganese [68], titanium [83], cobalt [183] and cerium oxide [133]. Some studies have shown that some metals in solution or supported metal oxides such as TiO_2/Al_2O_3, FeO_2/Al_2O_3, Co_3O_4/Al_2O_3 and MnO_2/TiO_2 can be efficient catalysts for ozonation reactions, removing highly refractory compounds [184].

Ceria (cerium oxide, CeO_2) is a cubic fluorite-type oxide, which is considered as the most important of rare-earth oxides [185]. Ceria plays an important role in emerging technologies for environmental and energy-related applications. However, the most important applications of cerium oxide are as catalysts, catalysts promoters and catalysts supports. Ceria-based catalysts have attracted enormous interest because of their various applications in three-way automotive catalysts [186], solid oxide fuel cells [187], water-gas shift [188], CO preferential oxidation [189] and heterogeneous catalytic ozonation [88]. Ceria has an excellent oxygen buffering property due to high tolerance to reversible oxygenation/deoxygenation cycles without disruption of the fluorite lattice-structure. Other important properties of ceria have been demonstrated when synthesized in the form of nanoparticles, such as shifting and broadening of Raman-allowed modes, lattice expansion, ultraviolet blue shifts, an increase in electronic conductivity and enhancing of carbon monoxide oxidation when used as support. The high melting point (2400 °C) is another advantage for high temperature applications such as total oxidation reactions. Obtaining high surface areas via enhancing porosity or decreasing particle size is of prime importance in heterogeneous catalysis. Various routes to obtain nanostructured CeO_2 materials with controlled size and morphology has been also developed using different methodologies, such as precipitation with different precipitating agents, sol-gel, sonochemical, electrochemical, solvothermal, amongst others [190-192]. However, it is difficult to prepare high-surface area nano-CeO_2 using these methods. Several strategies have been used to obtain ceria with high surface area, such as reaction time control and using high pressure water as heat, pressure and mechanical energy carrier. These are known as hydrothermal methods and they

have been used by many researchers to produce high surface area pure and doped cerium oxide [193]. A wide range of well-defined CeO_2 nanostructures (flower, rods, spheres, polyhedrons, tubes, wires, prisms and cubes) have been successfully synthesized via the hydrothermal process. This method shows high efficiency in preparing nanostructured CeO_2 with size/shape controlled by careful adjustment of the hydrothermal conditions without addition of any sort of templates or surfactants and with high catalytic activity for redox-based reactions [185, 194-199].

CeO_2-ZrO_2 is one of the most important commercial catalytic supports due to its high oxygen store capacity [200, 201]. This material has been investigated since the early 1990 and is now known that the incorporation of zirconium into the ceria lattice creates a high concentration of defects improving, thus, the O^{2-} mobility. This property allows the oxidation of hydrocarbons and CO in rich atmospheres. In fact, beyond the treatment of exhaust gas [202-204], these features have also motivated the use of CeO_2-ZrO_2 in a new range of applications, such as CO_2 methane reforming [205] and partial oxidation of methane [206].

Manganese oxide has been widely used as cathodic material, catalyst and magnetic material because of its exceptional structural flexibility, chemical/physical properties, among other excellent characteristics. It is well known that the properties and performances of nanomaterials strongly depend on their phase structures, morphologies and sizes. Thus, several techniques have been developed for the preparation of nanosized manganese dioxides with controlled morphologies and crystalline structures [207]. Because of their unique physicochemical properties and potential applications to various fields, ordered mesoporous transition-metal oxides have received great attention. Unlike the siliceous materials, the transitional metal oxides are more susceptive to hydrolysis, redox reactions, or phase transitions, and possess a number of different coordination numbers and multiple oxidation states. Hence, it is rather difficult to obtain their mesoporous structures. In recent years, the soft and hard templating methods for synthesis of well-ordered mesoporous transition metal oxides have been reported. In terms of the former, soft organic materials, such as block co-polymers, are used to structurally direct transition-metal oxides into organic-inorganic hybrids, often with a hexagonal morphology. After removing the organics by calcination in air, metal oxides with a mesoporous structure can be obtained. However, because the temperature for the thermal treatment without a structural collapse cannot exceed 400 °C, the resulting oxides are not highly crystalline, which may limit their wider application in nanotechnology. Thus, the recently developed nanocasting approach seems to be an attractive

alternative. Typically, ordered mesoporous silica or replicated mesoporous carbon can be employed as a rigid template into which a solution-based precursor of the desired phase is introduced. After generating the desired phase by calcination, the silica template can be dissolved away with a suitable concentration of NaOH or HF solution, finally leaving a replica of mesoporous structure of the target compound. Unfortunately, the inorganic precursors are prone to be adsorbed on the external surface of templates, forming large particles outside the mesopores. Furthermore, the pores cannot be completely filled, even when the vinyl-functionalized silica templates and/or multi-impregnation methods are used, all of which may cause the framework formed inside the pores to be lacking in sufficient internal crosslinkage [208]. MnO_x nanocrystals with various morphologies have been obtained by nanocasting method and due to the easy phase transformation of MnO_x, during preparation, only multivalence mixtures of manganese oxide (MnO_2, Mn_2O_3, Mn_3O_4) are usually obtained [209]. Zhao and coworkers described a microwave digestion technique followed by a thermolysis method to synthetize manganese oxides nanowires, mixture of different valences, in SBA-15 silica [210]. A mesoporous amorphous MnO_2 with a relatively high surface area from SBA-15 via ultrasonic wave treatment, using $KMnO_4$ as a manganese precursor, was report by Zhu et al [211]. Recently, hierarchically porous structural materials at multiple length scales have attracted much attention owing to their large surface areas and regular porosity at the nanometer scale, which can provide many novel properties and have important prospects in many practical applications [207]. Synthesis of supported metal oxides with high dispersion is of great importance. The structure and dispersion depend primarily on the preparation method, the nature of the support, and the type of precursor itself. Generally, catalytic activities over transition metal oxide catalysts are lower than those over noble metal catalysts. However, the inherent advantages of metal oxides, such as low cost, high thermal stability and mechanical strength, make them a promising alternative in several catalytic applications [209].

Perovskite-type oxides display prominent catalytic activities in many fields, such as the total oxidation of methane and of volatile organic compounds [212]. Perovskites are good materials in processes involving high temperatures and oxygen steam-rich atmospheres, due to its highly thermal stability. Perovskite oxides have general formula ABO_3, where A is a large cation and B is a small cation of the d-transition series. The number of potentially interesting perovskites in the oxidation reactions is very large, owing to the number of A and B cations that can enter into this structure.

The great stability of the perovskite framework allows partial substitution at the A sites and/or the B sites modifying the catalytic, redox and structural properties. The substitution at A site with ions having lower valence can allow the formation of structural defects such as anionic or cationic vacancies and/or a change in the oxidation state of the transition metal cation to maintain the electroneutrality of the compound. When the oxidation state of B cation increases, the relative ease of the redox process generates larger quantities of available oxygen at low temperature and the overall oxidation activity enhances. Moreover, the oxygen vacancies favour the catalytic activity in oxidation reactions because they increase the lattice oxygen mobility. Perovskites with lanthanum in A site and transition metals in B site ($LaBO_3$) with B = Mn, Co, Fe, Ni have received much attention.

The preparation method is important both in defining suitable textural characteristics for catalysis and in achieving phases of great purity. The literature describes numerous synthesis methods, most of which involve synthesizing materials for applications other than catalysis and allow incorporation of cations into the functional perovskite structure due to the high calcination temperatures used. Several techniques have been developed to solve the problem of perovskite purity and the most commonly used is the sol–gel citrate method.

1.4 Objectives and thesis outline

I started working on ozonation processes during my Master thesis in 2008. The experimental results obtained and the scientific development previous performed by Faria et al. [1, 213] in our research group was the beginning for carrying out this work. Firstly, mesoporous carbon materials prepared via SBA-15 templating and carbon xerogels with different chemistry properties were tested as ozonation catalysts. Ozonation catalyzed by nanostructured cerium oxides and ceria-based mixed oxides were carried out. Composites of cerium oxide and carbon materials with different compositions were synthesised by the precipitation method and evaluated in catalytic ozonation. Similar work was carried out with manganese oxide-carbon materials composites**.** Carbon xerogels prepared at different pHs and ceria-carbon xerogel materials with different compositions and synthesized by different procedures were tested on ozonation reactions. Catalytic ozonation in the presence of La-containing perovskites prepared by the citrate method was studied. Oxalic acid, oxamic acid, aniline and dyes were selected as model organic. The best catalysts reported in this thesis were also tested with real textile effluents. The

experiments were carried out in a semi-continuous lab-scale reactor (see Appendix A) at room temperature and atmospheric pressure.

This thesis is organized in ten chapters. The main core of this thesis is composed of Chapters 2 to 9.

Chapter 2 is dedicated to the catalytic ozonation in the presence of mesoporous materials prepared via SBA-15 templating and carbon xerogels with different chemistry properties.

Ozonation catalysed by nanostructured cerium oxides and ceria-based mixed oxides are discussed on Chapter 3 and 4.

Chapter 5 and 6 consists in the preparation and evaluation of composites with carbon materials and metal oxides (cerium and manganese oxide, respectively) as ozonation catalyst.

In Chapter 7, carbon xerogels prepared at different initial pH and ceria-carbon xerogels synthesised by diverse procedures and with different compositions are tested.

Chapter 8 explores the catalytic activity of perovkites on ozonation processes.

Chapter 9 compares in the same conditions the performance of the best catalysts reported in previous chapters in the ozonation of oxalic acid and reactive dye. After analysing the results, the two best catalysts are chosen and tested with real textile effluents.

Finally, the main conclusions withdraw from this work and some suggestions for further research are presented in Chapter 10.

References

[1] P. C. C. Faria, Catalytic ozonation of effluents from the textile industry, PhD Thesis in Chemical Engineering, Faculdade de Engenharia da Universidade do Porto, Porto, Portugal (2008).

[2] J. Rivas, O. Gimeno, F. Beltrán, Wastewater recycling: Application of ozone based treatments to secondary effluents, Chemosphere 74 (2009) 854-859.

[3] L. A. Bernal-Martínez, C. Barrera-Díaz, C. Solís-Morelos, R. Natividad, Synergy of electrochemical and ozonation processes in industrial wastewater treatment, Chem. Eng. J. 165 (2010) 71–77.

[4] D.S.S. Raj, Y. Anjaneyulu, Evaluation of biokinetic parameters for pharmaceutical wastewaters using aerobic oxidation integrated with chemical treatment, Process Biochem. 40 (2005) 165-175.

[5] G. Bertanza, C. Collivignarell, I. R. Pedrazzen, The role of chemical oxidation in combined chemical-physical and biological processes: experience of industrial wastewater treatment, Water Sci. Technol. 44 (2001) 109-116.

[6] P. R. Gogate, A. B. Pandit, A review of imperative technologies for wastewater treatment I: oxidation technologies at ambient conditions, Adv. Environ. Res. 8 (2004) 501-551.

[7] M. N. Chong, A. K. Sharma, S. Burn, C. P. Saint, Feasibility study on the application of advanced oxidation technologies for decentralised wastewater treatment, J. Clean. Prod. 35 (2012) 230-238.

[8] M. N. Chong, S. Lei, B. Jin, C. Saint, C. W. K. Chow, Optimisation of an annular photoreactor process for degradation of Congo Red using a newly synthesized titania impregnated kaolinite nano-photocatalyst, Sep. Purif. Technol. 67 (2009) 355-363.

[9] M. N. Chong, B. Jin, C. W. K. Chow, C. Saint, Recent developments in photocatalytic water treatment technology: A review, Water Res. 44 (2010) 2997-3027.

[10] G. Ruppert, R. Bauer, G. Heisler, UV-O_3, UV-H_2O_2, UV-TiO_2 and the photo-Fenton reaction - comparison of advanced oxidation processes for wastewater treatment, Chemosphere 28 (1994) 1447-1454.

[11] J. Perkowski, L. Kos, S. Ledakowicz, Application of ozone in textile wastewater treatment, Ozone Sci. & Eng. 18 (1996) 73-85.

[12] R. J. Rice, Applications of Ozone for Industrial Wastewater Treatment – A Review, Ozone Sci. Eng. 18 (1997) 477–515

[13] S. Liakou, S. Pavlou, G. Lyberatos, Ozonation of azo dyes, Water Sci.Technol. 35 (1997) 279-286.

[14] B.J. Wu, M.A. Eiteman, S. Law, Evaluation of Membrane Filtration and Ozonation Processes for Treatment of Reactive-Dye Wastewater, J. Environ. Eng. Sci. 124 (1998) 272-277.

[15] M. A. Boncz, H. Bruning, W. H. Rulkens, E. J. R. Sudholter, G. H. Harmsen, J. W. Bijsterbosch, Kinetic and mechanistic aspects of the oxidation of chlorophenols by ozone, Water Sci. Technol. 35 (1997) 65-72.

[16] M. Trapido, A. Hirvonen, Y. Veressinina, J. Hentunen, R. Munter, Ozonation, ozone/UV and UV/H_2O_2 degradation of chlorophenols, Ozone: Sci. Eng. 19 (1997) 75-96.

[17] S. J. Masten, M. J. Galbraith, S. H. R. Davies, Oxidation of 1,3,5-trichlorobenzene using advanced oxidation processes, Ozone: Sci. Eng. 18 (1997) 535-547.

[18] R.T. Meijers, E.J Oderwald-Muller, P.A.N.M Nuhn, J. C. Kruithof, Degradation of pesticides by ozonation and advanced oxidation, Ozone Sci. Eng. 17 (1995) 673–686.

[19] G. Reynolds, N. Graham, R. Perry, R. G. Rice, Aqueous ozonation of pesticides: a review, Ozone Sci. Eng. 11 (1989) 339-382.

[20] F. J. Beltrán, J. F. García-Araya, P. M. Álvarez, Wine Distillery Wastewater Degradation. 2. Improvement of Aerobic Biodegradation by Means of an Integrated Chemical (Ozone)−Biological Treatment, J. Agric. Food Chem. 47 (1999) 3919-3924.

[21] F. J. Benitez, J. Beltran-Heredia, F. J. Real, J. L. Acero, Enhancement of the ozonation of wine distillery wastewaters by an aerobic pretreatment, Bioprocess Biosyst. Eng. 21 (1999) 459-464.

[22] X.L. Melamane, P. J. Strong, J. E. Burgess, Treatment of Wine Distillery Wastewater: A Review with Emphasis on Anaerobic Membrane Reactors, S. Afr. J. Enol. Vitic. 28 (2007) 25-36.

[23] F. J. Beltrán, J. F. García-Araya, P. M. Álvarez, Wine Distillery Wastewater Degradation. 1. Oxidative Treatment Using Ozone and Its Effect on the Wastewater Biodegradability, Wine Distillery Wastewater Degradation. 1. Oxidative Treatment Using Ozone and Its Effect on the Wastewater Biodegradability 47 (1999) 3911-3918.

[24] T. Robinson, G. McMullan, R. Marchant, P. Nigam, Remediation of dyes in textile effluent: a critical review on current treatment technologies with a proposed alternative, Biores. Technol. 77 (2001) 247-255.

[25] E. Balanosky, F. Herrera, A. Lopez, J. Kiwi, Oxidative degradation of textile waste water. Modeling reactor performance, Water Res. 34 (2000) 582-596.

[26] S. Chiron, A. Fernandez-Alba, A. Rodriguez, E. Garcia-Calvo, Pesticide chemical oxidation: state-of-the-art, Water Res. 34 (2000) 366-377.

[27] M. Koga, K. Kadokani, R. Shinohara, Laboratory-scale ozonation of water contaminated with trace pesticides, Water Sci. Technol. 26 (1992) 2257–2260.

[28] R.T. Meijeirs, E.J. Oderwald-Muller, P.A. Nuhm, J. C. Kruithof, Degradation of pesticides by ozonation and advanced oxidation, Ozone: Sci. Eng. 17 (1995) 673–686.

[29] P. Roche, M. Prados, Removal of pesticides by use of ozone or hydrogen peroxide/ozone, Ozone: Sci. Eng 17 (1995) 657–672.

[30] E. Orlandini, M.A. Siebel, A. Graveland, J. C. Schippers, Pesticide removal by combined ozonation and granular activated carbon filtration, Water Supply 14 (1996) 99-108.

[31] P. C. Kearney, M. T. Muldoon, C. J. Somich, J. M. Ruth, D. J. Voaden, Biodegradation of ozonated atrazine as a wastewater disposal system, J. Agric. Food Chem. 36 (1988) 1301-1306.

[32] M.-S. Lai, J. N. Jensen, A. S. Weber, Oxidation of simazine: Ozone, ultraviolet, and combined ozone/ultraviolet oxidation, Water Environ. Res. 67 (1995) 340-346.

[33] C. D. Adams, S. J. Randtke, Ozonation byproducts of atrazine in synthetic and natural waters, Environ. Sci. Technol. 26 (1992) 2218-2227.

[34] P. Ormad, A. Puig, J. Sarasa, P. Roche, A. Martin, J. L. Ovelleiro, Ozonation of wastewater resulting from the production of organochlorine plaguicides derived from DDT and trichlorobenzene, Ozone: Sci. Eng. 16 (1994) 487-503.

[35] A. M. Amat, A. Arques, M. A. Miranda, F. López, Use of ozone and/or UV in the treatment of effluents from board paper industry, Chemosphere 60 (2005) 1111-1117.

[36] M. Klavarioti, D. Mantzavinos, D. Kassinos, Removal of residual pharmaceuticals from aqueous systems by advanced oxidation processes, Environ. Int. 35 (2009) 402-417.

[37] P. Verlicchi, A. Galletti, M. Petrovic, D. Barceló, Hospital effluents as a source of emerging pollutants: An overview of micropollutants and sustainable treatment options, J. Hydrol. 389 (2010) 416-428.

[38] N. C. G. Tan, Integrated and sequential anaerobic/aerobic biodegradationof azo dyes, Ph.D. Thesis, Wageningen University, Wageningen, The Netherlands (2001).

[39] C. Allègre, P. Moulin, M. Maisseu, F. Charbit, Treatment and reuse of reactive dyeing effluents, J. Membrane Sci. 269 (2006) 15-34.

[40] C. O'Neill, F. R. Hawkes, D. L. Hawkes, N. D. Lourenço, H. M. Pinheiro, W. Delée, Colour in textile effluents - Sources, measurement, discharge consents and simulation: A review, J. Chem. Technol. Biotechnol. 74 (1999) 1009-1018.

[41] J. R. Easton, The dye maker's view, in Colour in dyehouse effluent. Society of Dyers and Colourists, Bradford, England. (1995).

[42] N. Chahbane, D. L. Popescu, D. A. Mitchell, A. Chanda, D. Lenoir, A. D. Ryabov, K. W. Schramm, T. J. Collins, Fe^{III}-TAML-catalyzed green oxidative degradation of the azo dye Orange II by H_2O_2 and organic peroxides: Products, toxicity, kinetics, and mechanisms, Green Chem. 9 (2007) 49-57.

[43] A. Gottlieb, C. Shaw, A. Smith, A. Wheatley, S. Forsythe, The toxicity of textile reactive azo dyes after hydrolysis and decolourisation, J. Biotechnol. 101 (2003) 49-56.

[44] J. Hoigné, H. Bader, Rate constants of reactions of ozone with organic and inorganic compounds in water--II: Dissociating organic compounds, Water Res. 17 (1983) 185-194.

[45] P. C. C. Faria, J. J. M. Órfão, M. F. R. Pereira, Activated carbon catalytic ozonation of oxamic and oxalic acids, Appl. Catal. B: Environ. 79 (2008) 237-243.

[46] M. Mehrjouei, S. Müller, D. Möller, Degradation of oxalic acid in a photocatalytic ozonation system by means of Pilkington Active™ glass, J. Photochem. Photobiol. A: Chem. 217 (2011) 417-424.

[47] N.K.V. Leitner, P. Berger, B. Legube, Oxidation of amino groups by hydroxyl radicals in relation to the oxidation degree of the α-carbon, Environ. Sci. Technol. 36 (2002) 3083-3089.

[48] M. Skoumal, P.-L. Cabot, F. Centellas, C. Arias, R. M. Rodríguez, J. A. Garrido, E. Brillas, Mineralization of paracetamol by ozonation catalyzed with Fe^{2+}, Cu^{2+} and UVA light, Appl. Catal. B: Environ 66 (2006) 228-240.

[49] J. L. Gómez, G. León, A. M. Hidalgo, M. Gómez, M. D. Murcia, G. Griñán, Application of reverse osmosis to remove aniline from wastewater, Desalination 245 (2009) 687-693.

[50] P. C. C. Faria, D. C. M. Monteiro, J. J. M. Órfão, M. F. R. Pereira, Cerium, manganese and cobalt oxides as catalysts for the ozonation of selected organic compounds, Chemosphere 74 (2009) 818-824.

[51] B. Kasprzyk-Hordern, M. Ziólek, J. Nawrocki, Catalytic ozonation and methods of enhancing molecular ozone reactions in water treatment, Appl. Catal. B: Environ. 46 (2003) 639-669.

[52] B. Langlais, D.A. Reckhow, D. R. Brink, Ozone in Water Treatment: Application and Engineering. Lewis Publishers, Chelsea, Michigan, USA (1991).

[53] J. Nawrocki, S. Biłozor, U. wody, Procesy chemiczne i biologiczne. PWN, Warszawa-Poznań (2000).

[54] W. J. Masschelein, Unit Processes in Drinking Water Treatment. Marcel Dekker, New York (1992).

[55] V. Camel, A. Bermond, The use of ozone and associated oxidation processes in drinking water treatment, Water Res. 32 (1998) 3208-3222.

[56] J. Hoigné, Process Technologies for Water Treatment. Plenum Press, New York (1988).

[57] J. Nawrocki, B. Kasprzyk-Hordern, The efficiency and mechanisms of catalytic ozonation, Appl. Catal. B: Environ. 99 (2010) 27-42.

[58] R. Andreozzi, V. Caprio, A. Insola, R. Marotta, V. Tufano, The ozonation of pyruvic acid in aqueous solutions catalyzed by suspended and dissolved manganese, Water Res. 32 (1998) 1492-1496.

[59] J. Ma, N. J. D. Graham, Degradation of atrazine by manganese-catalysed ozonation—influence of radical scavengers, Water Res. 34 (2000) 3822-3828.

[60] J. Ma, N. J. D. Graham, Degradation of atrazine by manganese-catalysed ozonation: Influence of humic substances, Water Res. 33 (1999) 785-793.

[61] D. S. Pines, D. A. Reckhow, Effect of dissolved cobalt(II) on the ozonation of oxalic acid, Environ. Sci. Technol. 36 (2002) 4046-4051.

[62] Y. PIi, M. Ernst, J.-C. H. Schrotter, Effect of Phosphate Buffer upon CuO/Al_2O_3 and Cu (II) Catalyzed Ozonation of Oxalic Acid Solution, Ozone: Sci. Eng. 25 (2003) 393–397.

[63] M. Sánchez-Polo, J. Rivera-Utrilla, Ozonation of 1,3,6-naphthalenetrisulfonic acid in presence of heavy metals, J. Chem. Technol. Biotechnol. 79 (2004) 902-909.

[64] H. Xiao, R. Liu, X. Zhao, J. Qu, Enhanced degradation of 2,4-dinitrotoluene by ozonation in the presence of manganese(II) and oxalic acid, J. Mol. Catal. A: Chem. 286 (2008) 149-155.

[65] H. Xiao, R. Liu, X. Zhao, J. Qu, Effect of manganese ion on the mineralization of 2,4-dichlorophenol by ozone, Chemosphere 72 (2008) 1006-1012.

[66] L. F. Liotta, M. Gruttadauria, G. Di Carlo, G. Perrini, V. Librando, Heterogeneous catalytic degradation of phenolic substrates: Catalysts activity, J. Hazar. Mater. 162 (2009) 588-606.

[67] S. T. Oyama, Chemical and catalytic properties of ozone, Catal. Rev. - Sci. Eng. 42 (2000) 279-322.

[68] R. Andreozzi, A. Insola, V. Caprio, R. Marotta, V. Tufano, The use of manganese dioxide as a heterogeneous catalyst for oxalic acid ozonation in aqueous solution, Appl. Catal. A: Gen. 138 (1996) 75-81.

[69] S. Tong, W. Liu, W. Leng, Q. Zhang, Characteristics of MnO_2 catalytic ozonation of sulfosalicylic acid and propionic acid in water, Chemosphere 50 (2003) 1359-1364.

[70] J. Ma, N. J. D. Graham, Preliminary Investigation of Manganese-Catalyzed Ozonation for the Destruction of Atrazine, Ozone: Sci. Eng. 19 (1997) 227-240.

[71] M. A. Alsheyab, A. H. Muñoz, Comparative study of ozone and MnO_2/O_3 effects on the elimination of TOC and COD of raw water at the Valmayor station, Desalination 207 (2007) 179-183.

[72] Y. Dong, H. Yang, K. He, S. Song, A. Zhang, β-MnO_2 nanowires: A novel ozonation catalyst for water treatment, Appl. Catal. B: Environ. 85 (2009) 155-161.

[73] F. J. Beltrán, F. J. Rivas, R. Montero-de-Espinosa, Catalytic ozonation of oxalic acid in an aqueous TiO_2 slurry reactor, Appl. Catal. B: Environ. 39 (2002) 221-231.

[74] Y. Yang, J. Ma, Q. Qin, X. Zhai, Degradation of nitrobenzene by nano-TiO_2 catalyzed ozonation, J. Mol. Catal. A: Chem. 267 (2007) 41-48.

[75] R. Rosal, A. Rodríguez, M. S. Gonzalo, E. García-Calvo, Catalytic ozonation of naproxen and carbamazepine on titanium dioxide, Appl. Catal. B: Environ. 84 (2008) 48-57.

[76] R. Rosal, M. S. Gonzalo, A. Rodríguez, E. García-Calvo, Ozonation of clofibric acid catalyzed by titanium dioxide, J. Hazar. Mater. 169 (2009) 411-418.

[77] R. Rosal, M. S. Gonzalo, K. Boltes, P. Letón, J. J. Vaquero, E. García-Calvo, Identification of intermediates and assessment of ecotoxicity in the oxidation products generated during the ozonation of clofibric acid, J. Hazar. Mater. 172 (2009) 1061-1068.

[78] C. H. Ni, J. N. Chen, Heterogeneous catalytic ozonation of 2-chlorophenol aqueous solution with alumina as a catalyst, Water Sci. Technol. 43 (2001) 213-220.

[79] C. Cooper, R. Burch, An investigation of catalytic ozonation for the oxidation of halocarbons in drinking water preparation, Water Res. 33 (1999) 3695-3700.

[80] B. Kasprzyk, J. Nawrocki, Preliminary results on ozonation enhancement by a perfluorinated bonded alumina phase, Ozone: Sci. Eng. 24 (2002) 63-68.

[81] B. Kasprzyk-Hordern, P. Andrzejewski, A. Dąbrowska, K. Czaczyk, J. Nawrocki, MTBE, DIPE, ETBE and TAME degradation in water using perfluorinated phases as catalysts for ozonation process, Appl. Catal. B: Environ. 51 (2004) 51-66.

[82] B. Kasprzyk-Hordern, U. Raczyk-Stanislawiak, J. Swietlik, J. Nawrocki, Catalytic ozonation of natural organic matter on alumina, Appl. Catal. B: Environ 62 (2006) 345-358.

[83] F. J. Beltrán, F. J. Rivas, R. Montero-de-Espinosa, A TiO_2/Al_2O_3 catalyst to improve the ozonation of oxalic acid in water, Appl. Catal. B 47 (2004) 101-109.

[84] P. M. Álvarez, F. J. Beltrán, J. P. Pocostales, F. J. Masa, Preparation and structural characterization of Co/Al_2O_3 catalysts for the ozonation of pyruvic acid, Appl. Catal. B: Environ. 72 (2007) 322-330.

[85] J. S. Park, H. Choi, K. H. Ahn, The reaction mechanism of catalytic oxidation with hydrogen peroxide and ozone in aqueous solution, Water Sci.Technol. 47 (2003) 179-184.

[86] J. S. Park, H. Choi, K. H. Ahn, J. W. Kang, Removal mechanism of natural organic matter and organic acid by ozone in the presence of goethite, Ozone: Sci. Eng. 26 (2004) 141-151.

[87] T. Zhang, J. Ma, Catalytic ozonation of trace nitrobenzene in water with synthetic goethite, J. Mol. Catal. A: Chem. 279 (2008) 82-89.

[88] P. C. C. Faria, J. J. M. Órfão, M. F. R. Pereira, Activated carbon and ceria catalysts applied to the catalytic ozonation of dyes and textile effluents, Appl. Catal. B: Environ. 88 (2009) 341-350.

[89] R. C. Martins, R. M. Quinta-Ferreira, Screening of Ceria-Based and Commercial Ceramic Catalysts for Catalytic Ozonation of Simulated Olive Mill Wastewaters, Ind. Eng. Chem. Res. 48 (2008) 1196-1202.

[90] J. Zhang, K.-H. Lee, L. Cui, T.-s. Jeong, Degradation of methylene blue in aqueous solution by ozone-based processes, J. Ind. Eng. Chem. 15 (2009) 185-189.

[91] F. J. Beltrán, F. J. Rivas, R. Montero-de-Espinosa, Iron type catalysts for the ozonation of oxalic acid in water, Water Res. 39 (2005) 3553-3564.

[92] N. K. V. Leitner, F. Delanoe, B. Acedo, B. Legube, Reactivity of various Ru/CeO_2 catalysts during ozonation of succinic acid aqueous solutions, New J. Chem. 24 (2000) 229-233.

[93] N. Karpel Vel Leitner, H. Fu, pH effects on catalytic ozonation of carboxylic acids with metal on metal oxides catalysts, Topics Catal. 33 (2005) 249–256.

[94] M. Carbajo, F. J. Rivas, F. J. Beltrán, P. Alvarez, F. Medina, Effects of different catalysts on the ozonation of pyruvic acid in water, Ozone: Sci. Eng. 28 (2006) 229-235.

[95] T. L. Rakitskaya, A. A. Ennan, I. V. Granatyuk, A. Y. Bandurko, G. G. A. Balavoine, Y. V. Geletii, V. Y. Paina, Kinetics and mechanism of low-temperature

ozone decomposition by Co-ions adsorbed on silica, Catal. Today 53 (1999) 715-723.

[96] P. Konova, M. Stoyanova, A. Naydenov, S. Christoskova, D. Mehandjiev, Catalytic oxidation of VOCs and CO by ozone over alumina supported cobalt oxide, Appl. Catal. A: Gen. 298 (2006) 109-114.

[97] Y. Dong, K. He, L. Yin, A. Zhang, Catalytic Degradation of Nitrobenzene and Aniline in Presence of Ozone by Magnesia from Natural Mineral, Catal. Letters 119 (2007) 222-227.

[98] Y. Dong, K. He, B. Zhao, Y. Yin, L. Yin, A. Zhang, Catalytic ozonation of azo dye active brilliant red X-3B in water with natural mineral brucite, Catal. Commun. 8 (2007) 1599-1603.

[99] K. He, Y. M. Dong, Z. Li, L. Yin, A. M. Zhang, Y. C. Zheng, Catalytic ozonation of phenol in water with natural brucite and magnesia, J. Hazar. Mater. 159 (2008) 587-592.

[100] F. Qi, B. Xu, Z. Chen, J. Ma, D. Sun, L. Zhang, F. Wu, Ozonation catalyzed by the raw bauxite for the degradation of 2,4,6-trichloroanisole in drinking water, J. Hazar. Mater. 168 (2009) 246-252.

[101] H. Valdés, V. J. Farfán, J. A. Manoli, C. A. Zaror, Catalytic ozone aqueous decomposition promoted by natural zeolite and volcanic sand, J. Hazar. Mater. 165 (2009) 915-922.

[102] H. Valdés, F. A. Murillo, J. A. Manoli, C. A. Zaror, Heterogeneous catalytic ozonation of benzothiazole aqueous solution promoted by volcanic sand, J. Hazar. Mater. 153 (2008) 1036-1042.

[103] L. Zhao, J. Ma, Z. z. Sun, Oxidation products and pathway of ceramic honeycomb-catalyzed ozonation for the degradation of nitrobenzene in aqueous solution, Appl. Catal. B: Environ. 79 (2008) 244-253.

[104] L. Zhao, J. Ma, Z. Sun, Z. Liu, Y. Yang, Experimental study on oxidative decomposition of nitrobenzene in aqueous solution by honeycomb ceramic-catalyzed ozonation, Front. Environ. Sci. Eng. China 2 (2008) 44-50.

[105] L. Zhao, J. Ma, Z. Sun, X. Zhai, Mechanism of influence of initial pH on the degradation of nitrobenzene in aqueous solution by ceramic honeycomb catalytic ozonation, Environ. Sci. Technol. 42 (2008) 4002-4007.

[106] L. Zhao, J. Ma, Z.-z. Sun, X.-d. Zhai, Preliminary kinetic study on the degradation of nitrobenzene by modified ceramic honeycomb-catalytic ozonation in aqueous solution, J. Hazar. Mater. 161 (2009) 988-994.

[107] F. J. Rivas, M. Carbajo, F. J. Beltrán, B. Acedo, O. Gimeno, Perovskite catalytic ozonation of pyruvic acid in water: Operating conditions influence and kinetics, Appl. Catal. B: Environ. 62 (2006) 93-103.

[108] M. Carbajo, F. J. Beltrán, F. Medina, O. Gimeno, F. J. Rivas, Catalytic ozonation of phenolic compounds: The case of gallic acid, Appl. Catal. B: Environ. 67 (2006) 177-186.

[109] M. Carbajo, F. J. Beltrán, O. Gimeno, B. Acedo, F. J. Rivas, Ozonation of phenolic wastewaters in the presence of a perovskite type catalyst, Appl. Catal. B: Environ. 74 (2007) 203-210.

[110] F. J. Beltrán, P. Pocostales, P. M. Álvarez, F. López-Piñeiro, Catalysts to improve the abatement of sulfamethoxazole and the resulting organic carbon in water during ozonation, Appl. Catal. B: Environ. 92 (2009) 262-270.

[111] A. Lv, C. Hu, Y. Nie, J. Qu, Catalytic ozonation of toxic pollutants over magnetic cobalt and manganese co-doped γ-Fe_2O_3, Appl. Catal. B: Environ. 100 (2010) 62-67.

[112] A. Lv, C. Hu, Y. Nie, J. Qu, Catalytic ozonation of toxic pollutants over magnetic cobalt-doped Fe_3O_4 suspensions, Appl. Catal. B: Environ. 117–118 (2012) 246-252.

[113] Y. Ren, Q. Dong, J. Feng, J. Ma, Q. Wen, M. Zhang, Magnetic porous ferrospinel $NiFe_2O_4$: A novel ozonation catalyst with strong catalytic property for degradation of di-n-butyl phthalate and convenient separation from water, J. Coll. Inter. Sci. 382 (2012) 90–96.

[114] G. McKay, G. McAleavey, Ozonation and carbon adsorption in a three-phase fluidised bed for colour removal from peat water, Chem. Eng. Res. Des. 66 (1988) 531-536.

[115] C. A. Zaror, Enhanced oxidation of toxic effluents using simultaneous ozonation and activated carbon treatment, J. Chem.Technol. Biotechnol. 70 (1997) 21-28.

[116] U. Jans, J. Hoigné, Activated carbon and carbon black catalyzed transformation of aqueous ozone into OH-radicals, Ozone: Sci. Eng. 20 (1998) 67-90.

[117] F. J. Beltrán, J. Rivas, P. Álvarez, R. Montero-de-Espinosa, Kinetics of heterogeneous catalytic ozone decomposition in water on an activated carbon, Ozone: Sci. Eng. 24 (2002) 227-237.

[118] P. C. C. Faria, J. J. M. Órfão, M. F. R. Pereira, Ozone Decomposition in Water Catalyzed by Activated Carbon: Influence of Chemical and Textural Properties, Ind. Eng. Chem. Res. 45 (2006) 2715-2721.

[119] F. J. Beltran, F. J. Rivas, L. A. Fernandez, P. M. Alvarez, R. Montero-de-Espinosa, Kinetics of Catalytic Ozonation of Oxalic Acid in Water with Activated Carbon, Ind. Eng. Chem. Res. 41 (2002) 6510-6517.

[120] M. Sánchez-Polo, J. Rivera-Utrilla, Effect of the ozone-carbon reaction on the catalytic activity of activated carbon during the degradation of 1,3,6-naphthalenetrisulphonic acid with ozone, Carbon 41 (2003) 303-307.

[121] F. J. Beltrán, J. F. García-Araya, I. Giráldez, Gallic acid water ozonation using activated carbon, Appl. Catal. B: Environ. 63 (2006) 249-259.

[122] P. C. C. Faria, J. J. M. Órfão, M. F. R. Pereira, Ozonation of aniline promoted by activated carbon, Chemosphere 67 (2007) 809-815.

[123] P. Faria, J. Órfão, M. Pereira, Mineralization of Substituted Aromatic Compounds by Ozonation Catalyzed by Cerium Oxide and a Cerium Oxide-activated Carbon Composite, Catal. Lett. 127 (2009) 195-203.

[124] J. Ma, M. H. Sui, Z. L. Chen, L. N. Wang, Degradation of refractory organic pollutants by catalytic ozonation-activated carbon and Mn-loaded activated carbon as catalysts, Ozone: Sci. Eng. 26 (2004) 3-10.

[125] F. J. Beltrán, P. Pocostales, P. Alvarez, A. Oropesa, Diclofenac removal from water with ozone and activated carbon, J. Hazar. Mat. 163 (2009) 768-776.

[126] F. J. Beltrán, J. P. Pocostales, P. M. Alvarez, J. Jaramillo, Mechanism and kinetic considerations of TOC removal from the powdered activated carbon ozonation of diclofenac aqueous solutions, J. Hazar. Mat. 169 (2009) 532-538.

[127] Z.-Q. Liu, J. Ma, Y.-H. Cui, B.-P. Zhang, Effect of ozonation pretreatment on the surface properties and catalytic activity of multi-walled carbon nanotube, Appl. Catal. B: Environ. 92 (2009) 301-306.

[128] A. G. Gonçalves, J. L. Figueiredo, J. J. M. Órfão, M. F. R. Pereira, Influence of the surface chemistry of multi-walled carbon nanotubes on their activity as ozonation catalysts, Carbon 48 (2010) 4369-4381.

[129] J. Ma, M. Sui, T. Zhang, C. Guan, Effect of pH on MnO_x/GAC catalyzed ozonation for degradation of nitrobenzene, Water Res. 39 (2005) 779-786.

[130] M. Sánchez-Polo, J. Rivera-Utrilla, U. von Gunten, Metal-doped carbon aerogels as catalysts during ozonation processes in aqueous solutions, Water Res. 40 (2006) 3375-3384.

[131] X. Li, Q. Zhang, L. Tang, P. Lu, F. Sun, L. Li, Catalytic ozonation of p-chlorobenzoic acid by activated carbon and nickel supported activated carbon prepared from petroleum coke, J. Hazar. Mater. 163 (2009) 115-120.

[132] T. Yamamoto, S. I. Kim, J. Chaichanawong, E. u. Apiluck, T. Ohmori, Removal of aqueous organic pollutants by adsorption-catalytic process using mesoporous carbon beads loaded with metal oxides, Appl. Catal. B: Environ. 88 (2009) 455-461.

[133] P. C. C. Faria, J. J. M. Órfão, M. F. R. Pereira, A novel ceria-activated carbon composite for the catalytic ozonation of carboxylic acids, Catal. Commun. 9 (2008) 2121-2126.

[134] L. Li, W. Ye, Q. Zhang, F. Sun, P. Lu, X. Li, Catalytic ozonation of dimethyl phthalate over cerium supported on activated carbon, J. Hazar. Mater. 170 (2009) 411-416.

[135] Z. Q. Liu, J. Ma, Y. H. Cui, Carbon nanotube supported platinum catalysts for the ozonation of oxalic acid in aqueous solutions, Carbon 46 (2008) 890-897.

[136] R. Ryoo, S. H. Joo, M. Kruk, M. Jaroniec, Ordered Mesoporous Carbons, Adv. Mater. 13 (2001) 677-681.

[137] A. B. Fuertes, D. M. Nevskaia, Control of mesoporous structure of carbons synthesised using a mesostructured silica as template, Microporous Mesoporous Mater. 62 (2003) 177-190.

[138] W.-H. Zhang, L. Zhang, J. Xiu, Z. Shen, Y. Li, P. Ying, C. Li, Pore size design of ordered mesoporous silicas by controlling micellar properties of triblock copolymer $EO_{20}PO_{70}EO_{20}$, Microporous Mesoporous Mater. 89 (2006) 179-185.

[139] J. L. Figueiredo, M. F. R. Pereira, M. M. A. Freitas, J. J. M. Órfão, Modification of the surface chemistry of activated carbons, Carbon 37 (1999) 1379-1389.

[140] F. Rodriguez-Reinoso, Introdution in Carbon Tecnology. Universidad de Alicante, Secretariado de Publications, Alicante (1997).

[141] J. W. Patrick, Porosity in Carbons: Characterization and Applications. London (1995).

[142] K. Kinoshita, Carbon: Electrochemical and Physicochemical Properties. New York (1987).

[143] J. Lee, J. Kim, T. Hyeon, Recent Progress in the Synthesis of Porous Carbon Materials, Adv. Mater. 18 (2006) 2073-2094.

[144] T. Kyotani, Control of pore structure in carbon, Carbon 38 (2000) 269-286.

[145] F. M. Denlick, M. Tomkiewiez, Proceedings of the Symposium on Electrochemical Capacitors. Pennington, NJ (1996).

[146] H. Marsh, B. Rand, The process of activation of carbons by gasification with CO_2-II. The role of catalytic impurities, Carbon 9 (1971) 63-72.

[147] H. Tamai, T. Kakii, Y. Hirota, T. Kumamoto, H. Yasuda, Synthesis of Extremely Large Mesoporous Activated Carbon and Its Unique Adsorption for Giant Molecules, Chem. Mater. 8 (1996) 454-462.

[148] S. A. Al-Muhtaseb, J. A. Ritter, Preparation and Properties of Resorcinol-Formaldehyde Organic and Carbon Gels, Advan. Mater. 15 (2003) 101-114.

[149] R. W. Pekala, C. T. Alviso, F. M. Kong, S. S. Hulsey, Aerogels derived from multifunctional organic monomers, J. Non-Cryst. Sol. 145 (1992) 90-98.

[150] H. Tamon, H. Ishizata, T. Araki, M. Okazati, Control of mesoporous structure of organic and carbon aerogels, Carbon 36 (1998) 1257-1262.

[151] C. Liang, Z. Li, S. Dai, Mesoporous Carbon Materials: Synthesis and Modification, Ang. Chem. Int. Edit. 47 (2008) 3696-3717.

[152] J. Lee, S. Han, T. Hyeon, Synthesis of new nanoporous carbon materials using nanostructured silica materials as templates, J. Mat. Chem. 14 (2004) 478-486.

[153] F. Schüth, W. Schmidt, Microporous and Mesoporous Materials, Adv. Mat. 14 (2002) 629-638.

[154] F. Schüth, Endo- and Exotemplating to Create High-Surface-Area Inorganic Materials, Angew. Chem. Int. Ed. 42 (2003) 3604-3622.

[155] G. Che, B. B. Lakshmi, E. R. Fisher, C. R. Martin, Carbon nanotubule membranes for electrochemical energy storage and production, Nature 393 (1998) 346-349.

[156] J. S. Beck, J. C. Vartuli, W. J. Roth, M. E. Leonowicz, C. T. Kresge, K. D. Schmitt, C. T. W. Chu, D. H. Olson, E. W. Sheppard, A new family of mesoporous molecular sieves prepared with liquid crystal templates, J. Am. Chem. Soc. 114 (2002) 10834-10843.

[157] R. Ryoo, S. H. Joo, S. Jun, Synthesis of Highly Ordered Carbon Molecular Sieves via Template-Mediated Structural Transformation, J. Phys. Chem. B 103 (1999) 7743-7746.

[158] M. Kruk, M. Jaroniec, R. Ryoo, S. H. Joo, Characterization of Ordered Mesoporous Carbons Synthesized Using MCM-48 Silicas as Templates, J. Phys. Chem. B 104 (2000) 7960-7968.

[159] M. Kruk, M. Jaroniec, S. H. Joo, R. Ryoo, Characterization of Regular and Plugged SBA-15 Silicas by Using Adsorption and Inverse Carbon Replication and Explanation of the Plug Formation Mechanism, J. Phys. Chem. B 107 (2003) 2205-2213.

[160] J. Lee, S. Yoon, T. Hyeon, S. M. Oh, K. B. Kim, Synthesis of a new mesoporous carbon and its application to electrochemical double-layer capacitors, Chem. Commun 21 (1999) 2177-2178.

[161] S. Jun, S. H. Joo, R. Ryoo, M. Kruk, M. Jaroniec, Z. Liu, T. Ohsuna, O. Terasaki, Synthesis of New, Nanoporous Carbon with Hexagonally Ordered Mesostructure, J. Ame. Chem. Soc. 122 (2000) 10712-10713.

[162] M. Kruk, M. Jaroniec, C. H. Ko, R. Ryoo, Characterization of the Porous Structure of SBA-15, Chem. Mater. 12 (2000) 1961-1968.

[163] M. Imperor-Clerc, P. Davidson, A. Davidson, Existence of a microporous corona around the mesopores of silica-based SBA-15 materials templated by triblock copolymers, J. Am. Chem. Soc. 122 (2000) 11925-11933.

[164] S. H. Joo, R. Ryoo, M. Kruk, M. Jaroniec, Evidence for General Nature of Pore Interconnectivity in 2-Dimensional Hexagonal Mesoporous Silicas Prepared Using Block Copolymer Templates, J. Phys. Chem. B 106 (2002) 4640-4646.

[165] A. B. Fuertes, D. M. Nevskaia, Template synthesis of mesoporous carbons from mesostructured silica by vapor deposition polymerisation, J. Mat. Chem. 13 (2003)

[166] A. Vinu, T. Mori, K. Ariga, New families of mesoporous materials, Sci. Technol. Adv. Mater. 7 (2006) 753-771.

[167] S. H. Joo, S. J. Choi, I. Oh, J. Kwak, Z. Liu, O. Terasaki, R. Ryoo, Ordered nanoporous arrays of carbon supporting high dispersions of platinum nanoparticles, Nature 412 (2001) 169-172.

[168] Y. D. Xia, R. Mokaya, Ordered Mesoporous Carbon Hollow Spheres Nanocast Using Mesoporous Silica via Chemical Vapor Deposition, Adv. Mater. 16 (2004) 886-891.

[169] S. Che, A. E. Garcia-Bennett, X. Liu, R. P. Hodgkins, P. A. Wright, D. Zhao, O. Terasaki, T. Tatsumi, Synthesis of Large-Pore Ia (3)d Mesoporous Silica and Its Tubelike Carbon Replica, Angew. Chem. Int. Edit. 42 (2003) 3930-3934.

[170] F. Kleitz, S. H. Choi, R. Ryoo, Cubic Ia3d large mesoporous silica: synthesis and replication to platinum nanowires, carbon nanorods and carbon nanotubes, Chem. Commun. 17 (2003) 2136-2137.

[171] H. Yang, Q. Shi, X. Liu, S. Xie, D. Jiang, F. Zhang, C. Yu, B. Tu, D. Zhao, Synthesis of ordered mesoporous carbon monoliths with bicontinuous cubic pore structure of Ia3d symmetry, Chem. Commun. (2002) 2842-2843.

[172] P. Shmidt-Winkel, J. W. W. Luken, D. Zhao, P. Yang, B. F. Chmelka, G. D. Stucky, Mesocellular siliceous foams with uniformly sized cells and windows J. Am. Chem. Soc. 121 (1999) 254-255.

[173] P. Schmidt-Winkel, C. J. Glinka, G. D. Stucky, Microemulsion templates for mesoporous silica, Langmuir 16 (2000) 356.

[174] P. Schmidt-Winkel, J. W. W. Luken, P. Yang, D. I.Margolese, J. S. Lettow, J. Y.Ying, G. D. Stucky, Microemulsion templating of siliceous mesostructured cellular foams with well-defined ultralarge mesopores, Chem. Mater. 12 (2000) 686.

[175] J. Lee, K. Sohn, T. Hyeon, Fabrication of Novel Mesocellular Carbon Foams with Uniform Ultralarge Mesopores, J. Amer. Chem. Soc. 123 (2001) 5146-5147.

[176] D. Zhao, J. Feng, Q. Huo, N. Melosh, G. H. Fredrickson, B. F. Chmelka, G. D. Stucky, Triblock Copolymer Syntheses of Mesoporous Silica with Periodic 50 to 300 Angstrom Pores, Science 279 (1998) 548-552.

[177] D. Zhao, Q. Huo, J. Feng, B. F. Chmelka, G. D. Stucky, Nonionic Triblock and Star Diblock Copolymer and Oligomeric Surfactant Syntheses of Highly Ordered, Hydrothermally Stable, Mesoporous Silica Structures, J. Am. Chem. Soc. 120 (1998) 6024-6036.

[178] W. Wang, W. Shan, H. Ru, N. Wu, A facile and versatile partitioned cooperative self-assembly process to prepare SBA-15s with larger mesopores, high microporosity and tunable particle sizes, J. Mater. Chem. 21 (2011) 12059-12067.

[179] A. A. Zakhidov, R. H. Baughman, Z. Iqbal, C. Cui, I. Khayrullin, S. O. Dantas, J. Marti, V. G. Ralchenko, Carbon structures with three-dimensional periodicity at optical wavelengths, Science 282 (1998) 897-901.

[180] N. Job, R. Pirard, J. Marien, J. P. Pirard, Porous carbon xerogels with texture tailored by pH control during sol–gel process, Carbon 42 (2004) 619-628.

[181] C. Lin, J. A. Ritter, Effect of synthesis pH on the structure of carbon xerogels, Effect of synthesis pH on the structure of carbon xerogels 35 (1997) 1271-1278.

[182] R. W. Pekala, C. T. Alviso, J. D. Lemay. Chemical Processing of Advanced Materials, New York (1992).

[183] D. S. Pines, D. A. Reckhow, Solid Phase Catalytic Ozonation Process for the Destruction of a Model Pollutant, Ozone: Sci. Eng. 25 (2003) 25-39.

[184] B. Legube, N. K. V. Leitner, Catalytic ozonation: a promising advanced oxidation technology for water treatment, Catal. Today 53 (1999) 61-72.

[185] Y. Guan, E. Hensen, Y. Liu, H. Zhang, Z. Feng, C. Li, Template-Free Synthesis of Sphere, Rod and Prism Morphologies of CeO_2 Oxidation Catalysts, Catal. Lett. 137 (2010) 28-34.

[186] J. Kaspar, P. Fornasiero, M. Graziani, Use of CeO_2-based oxides in the three-way catalysis, Catal. Today 50 (1999) 285-298.

[187] A. M. Silva, A. M. Duarte de Farias, L. O. O. Costa, A. P. M. G. Barandas, L. V. Mattos, M. A. Fraga, F. B. Noronha, Partial oxidation and water–gas shift reaction in an integrated system for hydrogen production from ethanol, Appl. Catal. A: Gen. 334 (2008) 179-186.

[188] A. M. Duarte de Farias, D. Nguyen-Thanh, M. A. Fraga, Discussing the use of modified ceria as support for Pt catalysts on water-gas shift reaction, Appl. Catal. B: Environ. 93 (2010) 250-258.

[189] O. Pozdnyakova-Tellinger, D. Teschner, J. Kröhnert, F. C. Jentoft, A. Knop-Gericke, R. Schlögl, A. Wootsch, Surface Water-Assisted Preferential CO Oxidation on Pt/CeO_2 Catalyst, J. Phys. Chem. C 111 (2007) 5426-5431.

[190] K. Niesz, D. E. Morse, Sonication-accelerated catalytic synthesis of oxide nanoparticles, Nano Today 5 (2010) 99-105.

[191] R. K. Hailstone, A. G. DiFrancesco, J. G. Leong, T. D. Allston, K. J. Reed, A Study of Lattice Expansion in CeO_2 Nanoparticles by Transmission Electron Microscopy, J. Phys. Chem. C 113 (2009) 15155-15159.

[192] X. -H. Lu, X. Huang, S.-l. Xie, D.-Z. Zheng, Z.-Q. Liu, C.-l. Liang, Y.-X. Tong, Facile Electrochemical Synthesis of Single Crystalline CeO_2 Octahedrons and Their Optical Properties, Langmuir 26 (2010) 7569-7573.

[193] A. Bumajdad, J. Eastoe, A. Mathew, Cerium oxide nanoparticles prepared in self-assembled systems, Adv. Colloid Interface Sci. 147-148 (2008) 56-66.

[194] H.-X. Mai, L.-D. Sun, Y.-W. Zhang, R. Si, W. Feng, H.-P. Zhang, H.-C. Liu, C.-H. Yan, Shape-Selective Synthesis and Oxygen Storage Behavior of Ceria Nanopolyhedra, Nanorods, and Nanocubes, J. Phys. Chem. B 109 (2005) 24380-24385.

[195] Tana, M. L. Zhang, J. Li, H. J. Li, Y. Li, W. J. Shen, Morphology-dependent redox and catalytic properties of CeO_2 nanostructures: Nanowires, nanorods and nanoparticles, Catal. Today 148 (2009) 179-183.

[196] B. M. Reddy, G. Thrimurthulu, L. Katta, Y. Yamada, S.-E. Park, Structural Characteristics and Catalytic Activity of Nanocrystalline Ceria−Praseodymia Solid Solutions, J. Phys. Chem. C 113 (2009) 15882-15890.

[197] W. Shan, X. Dong, N. Ma, S. Yao, Z. Feng, The Synthesis of Three-Dimensional CeO_2 and Their Catalytic Activities for CO Oxidation, Catal. Letters 131 (2009) 350-355.

[198] K. Zhou, Z. Yang, S. Yang, Highly Reducible CeO_2 Nanotubes, Chem. Mater. 19 (2007) 1215-1217.

[199] C. Sun, J. Sun, G. Xiao, H. Zhang, X. Qiu, H. Li, L. Chen, Mesoscale Organization of Nearly Monodisperse Flowerlike Ceria Microspheres, J. Phys. Chem. B 110 (2006) 13445-13452.

[200] E. S. Lox, B. H. Engler Handbook of Hetrogeneous Catalysis. G. Ertl, H. Knozinger, J. Weitkamp, Wiley-VCH. **2:** 1559 (1997).

[201] S. Letichevsky, C. A. Tellez, R. R. Avillez, M. I. P. Silva, M. A. Fraga, L. G. Appel, Obtaining CeO_2-ZrO_2 mixed oxides by coprecipitation: role of preparation conditions, Appl. Catal. B: Environ. 58 (2005) 203-210.

[202] H. He, H. X. Dai, L. H. Ng, K. W. Wong, C. T. Au, Pd-, Pt-, and Rh-Loaded $Ce_{0.6}Zr_{0.35}Y_{0.05}O_2$ Three-Way Catalysts: An Investigation on Performance and Redox Properties, J. Catal. 206 (2002) 1-13.

[203] F. Klingstedt, A. K. Neyestanaki, R. Byggningsbacka, L.-E. Lindfors, M. Lundén, M. Petersson, P. Tengström, T. Ollonqvist, J. Väyrynen, Palladium based catalysts for exhaust aftertreatment of natural gas powered vehicles and biofuel combustion, Appl. Catal. A: Gen. 209 (2001) 301-316.

[204] R. J. Farrauto, R. M. Heck, Catalytic converters: state of the art and perspectives, Catal. Today 51 (1999) 351-360.

[205] L. V. Mattos, E. Rodino, D. E. Resasco, F. B. Passos, F. B. Noronha, Partial oxidation and CO_2 reforming of methane on Pt/Al_2O_3, Pt/ZrO_2, and $Pt/Ce–ZrO_2$ catalysts, Fuel Process. Technol. 83 (2003) 147-161.

[206] L. V. Mattos, E. R. de Oliveira, P. D. Resende, F. B. Noronha, F. B. Passos, Partial oxidation of methane on $Pt/Ce–ZrO_2$ catalysts, Catal. Today 77 (2002) 245-256.

[207] H. Chen, X. Dong, J. Shi, J. Zhao, Z. Hua, J. Gao, M. Ruan, D. Yan, Templated synthesis of hierarchically porous manganese oxide with a crystalline nanorod framework and its high electrochemical performance, J. Mat. Chem. 17 (2007) 855-860.

[208] J. Deng, L. Zhang, H. Dai, Y. Xia, H. Jiang, H. Zhang, H. He, Ultrasound-Assisted Nanocasting Fabrication of Ordered Mesoporous MnO_2 and Co_3O_4 with High Surface Areas and Polycrystalline Walls, J. Phys. Chem.C 114 (2010) 2694-2700.

[209] Y. F. Han, F. Chen, Z. Zhong, K. Ramesh, L. Chen, E. Widjaja, Controlled Synthesis, Characterization, and Catalytic Properties of Mn_2O_3 and Mn_3O_4 Nanoparticles Supported on Mesoporous Silica SBA-15, J. Phys. Chem. B 110 (2006) 24450-24456.

[210] B. Tian, X. Liu, H. Yang, S. Xie, C. Yu, B. Tu, D. Zhao, General Synthesis of Ordered Crystallized Metal Oxide Nanoarrays Replicated by Microwave-Digested Mesoporous Silica, Adv. Mater. 15 (2003) 1370-1374.

[211] S. Zhu, Z. Zhou, D. Zhang, H. Wang, Synthesis of mesoporous amorphous MnO_2 from SBA-15 via surface modification and ultrasonic waves, Microporous Mesoporous Mater. 95 (2006) 257–264.

[212] B. P. Barbero, J. A. Gamboa, L. E. Cadús, Synthesis and characterisation of $La_{1-x}Ca_xFeO_3$ perovskite-type oxide catalysts for total oxidation of volatile organic compounds, Appl. Catal. B: Environ. 65 (2006) 21-30.

[213] P. C. C. Faria, Descoloração de efluentes na presença de carvão activado, Master Thesis in Environmental Engineering Faculdade de Engenharia da Universidade do Porto, Porto, Portugal (2003).

Chapter 2

Development of novel mesoporous carbon materials for the catalytic ozonation of organic pollutants[1]

Mesoporous carbon materials prepared via SBA-15 templating and carbon xerogels were tested as catalysts for the ozonation of organic pollutants, and their performances compared to activated carbons. Kinetic results showed that only the combination of the mesoporous carbons with ozone may lead to total mineralisation. The roles of surface chemistry and textural parameters of the catalysts are discussed.

[1] C. Orge, J. Sousa, F. Gonçalves, C. Freire, J. Órfão, M. Pereira, Development of Novel Mesoporous Carbon Materials for the Catalytic Ozonation of Organic Pollutants, Catal. Lett. 132 (2009) 1-9.

2 Development of novel mesoporous carbon materials for the catalytic ozonation of organic pollutants

2.1 Introduction

Carbon materials have been applied in several areas due to their unique properties: high specific surface area and pore volume, good mechanical strength, inertness for most of liquid media and non-oxidative atmospheres, and the possibility to tailor their textural and chemical properties for a specific application [1-4]. Most of these materials, namely activated carbons, are microporous and therefore cannot be efficiently used in applications involving bulky molecules, such as dyestuffs.

Significant developments have been achieved in the synthesis of mesoporous carbon materials during the last decade [5]. In order to obtain mesoporous carbons with uniform and interconnected pores, the synthesis via templating has been recently applied [6-9]. The procedure for the synthesis of mesoporous carbons using nanostructured silica as template involves four consecutive steps: preparation of the mesostructured silica; incorporation of a polymeric precursor and respective polymerisation in the interior of the silica pores; carbonisation; and removal of the silica template. Mesoporous carbon xerogels have also attracted a great deal of interest, since they possess excellent characteristics as catalyst supports, such as high surface area, high porosity, open pore network, controllable pore size, and can be prepared in the desired form (monolith, thin film or powder). They are usually synthesized by the conventional sol-gel approach using formaldehyde and resorcinol, at selected solution pH values. Then, the wet gels are conveniently dried and subsequently carbonized, leading to carbon xerogels [10, 11]. These materials can be conveniently functionalized [12].

With the available technologies, the colour removal from textile effluents is technically possible after a biological treatment, but not yet at affordable costs for the industrials of the sector. In addition, a tertiary treatment is mandatory for a possible water reuse because total decolourisation and organic matter removal must be achieved to meet technical specifications [13]. The utilization of ozone in a tertiary treatment of coloured effluents is a promising technique because high colour and organic matter removals are obtained without generating sludge or secondary effluents, which would require a posterior treatment.

Ozone attacks selectively molecules containing unsaturated bonds, producing saturated compounds such as aldehydes, ketones and carboxylic acids. Due to their low reactivity towards ozone, these compounds have a tendency to accumulate in water. The ozonation processes have been modified to overcome this problem. Catalytic ozonation is an innovative process for the removal of organic pollutants in water, and although its application has been limited to the laboratory scale, the results obtained so far indicate the need for further studies in this area [14, 15]. Therefore, the combination of ozone with homogeneous or heterogeneous catalysts has been studied by several researchers.

The heterogeneous catalytic ozonation aims at increasing the degradation of organic compounds highly refractory to single ozonation, by transforming ozone into more reactive species and/or through adsorption and surface reaction of the pollutants [14]. Activated carbon has been appointed as a very good catalyst in the ozone decomposition [16, 17] and in the mineralisation of dyes [18-21], aromatic compounds [22-27] and carboxylic acids [28-30].

In the present study, the preparation, functionalization and characterization of templated carbons via SBA-15 and carbon xerogels are described. Moreover, kinetic results of the decolourisation and mineralisation of solutions of different classes of dyes by ozonation in the presence of the prepared mesoporous carbons are presented and discussed. In order to evaluate the synergic effect of using ozone and the prepared carbon materials, adsorption and single ozonation, using the same reactor and experimental conditions, were also carried out. Finally, ozonation of oxalic acid in the presence of the above mentioned mesoporous carbons was also studied.

2.2 Experimental

2.2.1 Preparation and functionalisation of the mesoporous carbon materials

The synthesis of the mesostructured SBA-15 silica consisted in the addition of a silicon source, tetraethylortosilicate (TEOS, 99%, Fluka), to an aqueous solution of hydrochloric acid (37%, Riedel-deHaën), containing an adequate surfactant (Pluronic P123, Aldrich), with a molar ratios TEOS/P123/HCl/H_2O = 1.0/0.017/5.7/193. Then, a heat treatment at 125 ºC during one day was carried out. The obtained product was dried and then calcined in air during 4 h at 600 °C using a heating rate of 2 °C min^{-1} [31, 32].

In order to obtain an ordered mesoporous carbon (sample JC0), the SBA-15 silica was impregnated with a solution of para-toluenesulfonic acid (Aldrich) in ethanol (5 M) during 1 h. After drying, a volume of furfuryl alcohol (99%, Aldrich) equal to the silica pore volume was added to the solid. The sample was kept in contact with air during 6h at 80 ºC to form the polymer inside the silica pores, which was subsequently carbonised in nitrogen at 800 ºC during 1 h, using a heating rate of 2 °C/min. Finally, the resultant carbon-silica composite was treated with a solution of hydrofluoric acid (40%, Fluka), at room temperature during 15 h, to remove the silica [6, 32-33]. The sample was washed with distilled water until a neutral pH was reached and dried overnight in an oven at 120 ºC.

The synthesis of the carbon xerogel (sample XC0) consisted in the policondensation of resorcinol (99%, Aldrich) with formaldehyde (37%, Aldrich), at an initially controlled pH (pH = 6), in order to promote the mesoporosity [10]. Polymerisation was carried out at 85 ºC during 3 days. Then, the gel was ground and dried in an oven during 4 days (first day at 60 ºC, second day at 80 ºC, third day at 100 ºC and fourth day at 120 ºC). Finally, the material was carbonised under nitrogen flow at 800 °C using the following temperature programme: from room temperature to 150 ºC (hold 2 h) at 2 ºC min^{-1}, 2 ºC min^{-1} to 400 ºC (hold 1h), 2 ºC min^{-1} to 600 ºC (hold 1 h), 2 ºC min^{-1} to 800 ºC (hold 6 h) and cooling down to room temperature.

The prepared materials were then submitted to different chemical and thermal treatments to obtain materials with different surface chemistries: oxidation with nitric acid 5 M at boiling temperature during 6 h in a Soxhlet (samples JC1 and XC1) and thermal treatment of theses samples in inert atmosphere at 900 °C during 1 h at a heating rate of 10 °C min^{-1} (samples JC2 and XC2). The acid treated samples were used for the heat treatments because we were interested in obtaining a large amount of surface groups in the starting material to produce activated carbons with higher basicity [34]. More details concerning these treatments can be found elsewhere [4].

2.2.2 Model organic compounds

Two dyes with different chemical structures (C.I. Reactive Blue 5 and C.I. Acid Blue 113) and oxalic acid were select as model organic compounds for this study. The characteristics of the selected dyes are presented in Table 2.1 [35]. The dyes were selected as examples of bulky molecules, among those usually used in the textile

industry; oxalic acid was selected because it is one of the most important final products of the oxidation of dyes that is refractory to single ozonation.

Table 2.1: Characteristics of dyes.

Class/ Molecular formula	Commercial name/ 3D representation*	Generic name	Dimensions (Å x Å) $	λ_{max} (nm)
Reactive $C_{29}H_{20}ClN_7O_{11}S_3$	Cibacron Blue BR 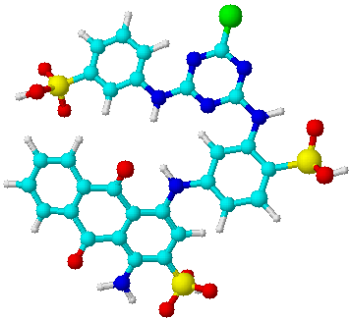	C.I. Reactive Blue 5	15.7x14.4	597
Acid $C_{32}H_{21}N_5Na_2O_6S_2$	Eryonil Navy R 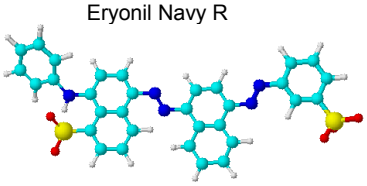	C.I. Acid Blue 113	22.1x9.2	565

*3D optimization was carried out using the ChemSketch software from ACD.
$Considering the largest distances of the two farthest atoms in an axis, in perpendicular directions in the molecule, after 3D optimization.

2.2.3 Characterization of the mesoporous materials

The surface chemistry was characterized by temperature programmed desorption (TPD), total acidity and basicity and pH_{pzc} [36]. The textural characterization was based on the analysis of the nitrogen adsorption isotherms at 77 K. Details about these characterization techniques are described in a previous publication [16]. The structural characterization was obtained from the results of scanning electron microscopy (SEM) on a JEOL JSM 35C / Noran Voyager system, transmission electron microscopy (TEM) on a LEO 906E microscope operating with an accelerating voltage of 120 kV and X-ray diffraction on a Philips X'Pert MPD diffractometer (Cu Kα = 0.15406 nm).

2.2.4 Kinetic experiments and analytical methods

Kinetic experiments were carried out in a lab scale reactor, with cylindrical shape, recirculation jacket and mechanical stirring. The outlet of the reactor was connected to two washing flasks with a KI solution to eliminate the unreacted ozone in the gas phase discharged to the atmosphere. The ozone was produced from oxygen in an Ozone Generator BMT 802X. The experiments were performed at constant gas flow rate (150 cm^3 min^{-1}, measured at room T and P) and constant inlet ozone concentration (50 g Nm^{-3}). The experiments were carried out at room temperature and at the natural pH of the solutions, with a stirring rate of 300 rpm. Three types of experiments were carried out in this experimental set-up, keeping the same operation conditions: adsorption, single ozonation and catalytic ozonation. In each case, 700 cm^3 of dye solution (100 mg L^{-1}) or oxalic acid solution (1 mM) were added into the reactor. In the adsorption and catalytic ozonation experiments, 350 mg of carbon materials (0.1 < particle diameter < 0.3 mm) were also introduced into the reactor. In the adsorption experiments, the ozone-containing stream was replaced by an oxygen stream.

The concentrations of each dye in the solutions were followed by UV-Vis spectrophotometry with a JASCO V-560 UV/Vis spectrophotometer. The UV-Vis spectra were measured at given time intervals. The degree of mineralisation was followed by TOC analysis in a Shimadzu TOC-5000A Analyzer. For the oxalic acid solutions, HPLC analyses were performed, using a Hitachi Elite Lachrom HPLC equipped with a diode array detector. The stationary phase was an YMC Hydrosphere C18 column (250 mm x 4.6 mm) working at room temperature under isocratic elution with a mixture of water, acetonitrile and o-phosphoric acid at pH 2.0.

2.3 Results and discussion

2.3.1 Characterization of carbon materials

Chemical and thermal treatments were carried out on the prepared carbon materials in order to assess the influence of the surface chemistry. The oxidation treatment with HNO_3 increases the acidity and the thermal treatment at high temperature in inert atmosphere increases the basicity of the materials. Figure 2.1 shows the CO_2 and CO TPD spectra of the templated carbons obtained via SBA-15.

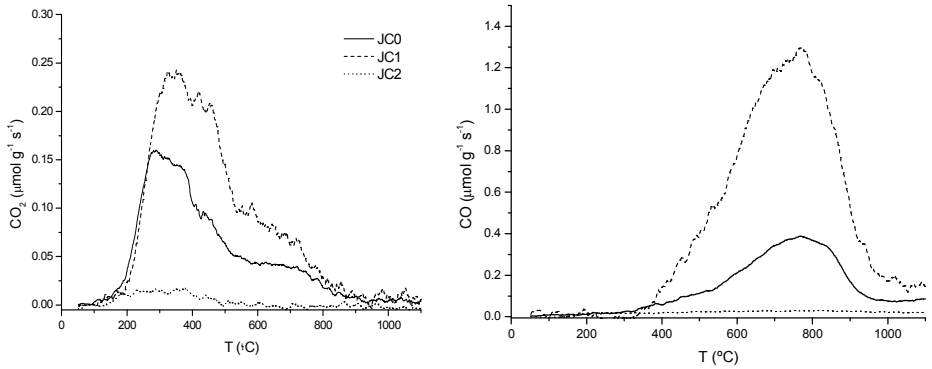

Figure 2.1: CO_2 and CO TPD spectra of the templated carbons obtained via SBA-15.

In the case of templated carbons, the prepared starting material (JCO) already presents an important amount of oxygen-containing surface groups. The oxidation treatment with HNO_3 (sample JC1) originates an increase in both CO and CO_2 peaks. A significant increase of the CO_2 peak at low temperatures, due to the decomposition of carboxylic acids, and a slight increase at high temperatures, due to the decomposition of carboxylic anhydrides and lactones, is observed. In addition, its CO spectrum presents a significant enlargement at all temperatures, which indicates an increase of the carboxylic anhydrides, phenols and carbonyl/quinones surface groups [4]. The TPD spectra of the thermal treated material (sample JC2) show that almost all oxygen-containing surface groups were removed, accordingly to the high temperature used on that treatment. The main features of the corresponding TPD spectra obtained with the xerogel samples (not shown) are similar, being the most important difference the fact that the original sample (XC0) presents lower amounts of CO and CO_2 releasing groups.

Table 2.2 and 2.3 present the chemical and textural properties of the materials prepared, respectively. A commercial activated carbon (NORIT GAC 1240 plus) was used for comparison purposes (sample AC0) and its chemical and textural properties are also included in Table 2.2 and 2.3 [22].

Table 2.2: Chemical properties of the materials used.

Sample	Treatment	CO[a] (μmol g^{-1})	CO_2[a] (μmol g^{-1})	Acidity (μmol g^{-1})	Basicity (μmol g^{-1})	pH_{pzc}
SBA-15	-	-	-	-	-	-
JC0	-	951	501	459	1563	3.5
JC1	HNO_3	5361	928	709	816	3.0
JC2	thermal	46	50	334	1699	6.5
XC0	-	330	149	584	408	7.8
XC1	HNO_3	3189	1340	1584	136	3.1
XC2	thermal	289	166	476	476	8.7
AC0	-	579	63	211	352	8.5

[a] calculated by TPD spectra integration

Table 2.3: Textural properties of the materials used.

Sample	S_{BET} (m^2 g^{-1})	S_{meso}[a] (m^2 g^{-1})	V_{micro}[a] (cm^3 g^{-1})	d_p[b] (nm)
SBA-15	682	552	0.050	6.6
JC0	1120	819	0.134	3.5
JC1	1022	747	0.120	3.2
JC2	740	446	0.128	3.7
XC0	809	329	0.201	37
XC1	1007	440	0.236	37
XC2	790	252	0.221	36
AC0	909	100	0.332	-

[a] Micropore volume (V_{micro}) and mesopore surface area (S_{meso}) calculated by the t-method.

[b] Average mesopore diameter (d_p) obtained from the desorption isotherm using the Barrett, Joyner and Halenda (BJH) method [37].

Compared to the untreated materials, an increase in the acidity and a decrease in the basicity are observed for the samples oxidized with nitric acid, which is in agreement with the lower pH_{pzc} of these samples and higher amount of CO_2

releasing groups in the TPD experiments. In contrast, the heat treated samples show a decrease in the acidity and an increase in the basicity, leading to an increase in their pH_{pzc} and a lower amount of CO_2 releasing groups observed in the respective TPD spectrum.

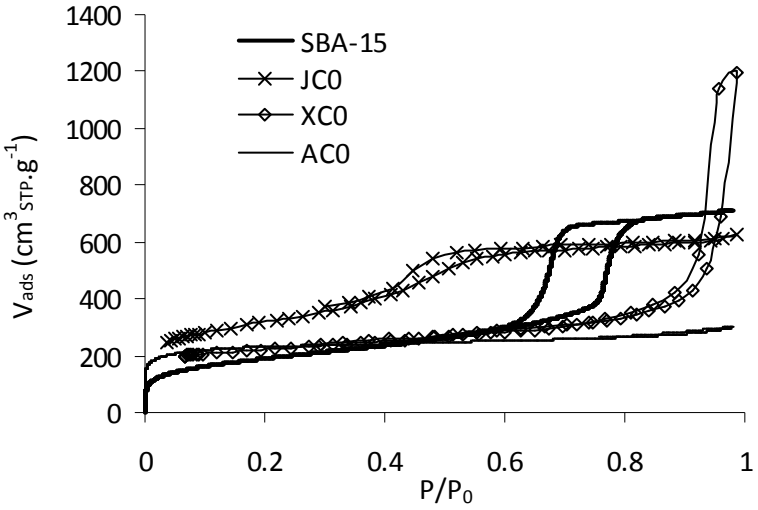

Figure 2.2: N_2 adsorption isotherms at 77 K of SBA-15, JC0, XC0 and AC0.

From Figure 2.2, it can be observed that the prepared nanostructured silica presents an isotherm of type IV with a H1 hysteresis, which is typical of materials with open-ended cylindrical mesopores. In addition, the XRD spectra of this sample (not shown) presented the three peaks at low angles characteristic of ordered hexagonal structures, indicating that this silica has the characteristics of SBA-15 [31]. The SEM and TEM micrographs (see Figure 2.3) corroborate this conclusion. An extended and ordered mesoporosity of the prepared templated carbons was revealed by the analysis of the respective nitrogen adsorption isotherms and SEM and TEM micrographs (see Figures 2.2 and 2.3). With the exception of the thermal treated sample, the templated carbons present a BET surface area higher than 1000 $m^2\ g^{-1}$. Comparing the templated (JC) and the xerogel (XC) carbon materials, although their BET surface areas are similar, the templated samples present mesopore surface areas 1.5 to 2.5 times higher, approximately half of the micropore volume and one tenth of the mesopore size diameter.

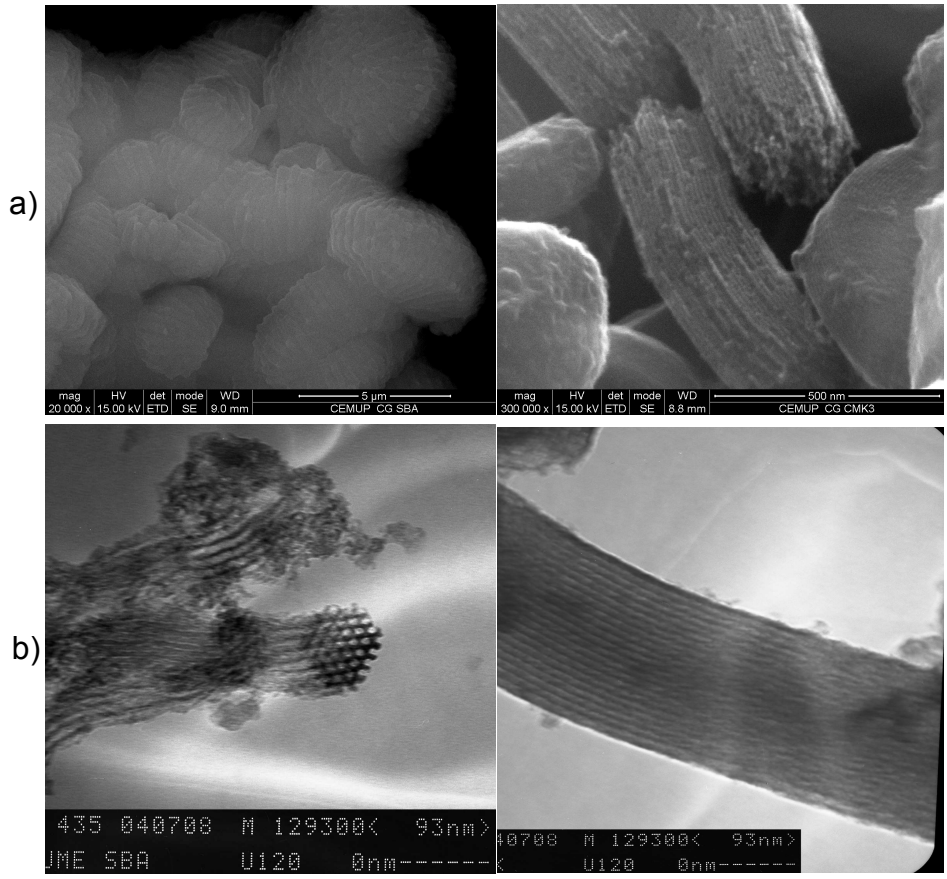

Figure 2.3: Micrographs of silica SBA-15 (left) and the templated carbon JCO (right). a) SEM, b) TEM

2.3.2 Reactive and acid dyes removal

Figures 2.4 to 2.6 present the kinetic results of single ozonation, adsorption and ozonation in the presence of the mesostructured carbon materials for the reactive and acid dyes. In order to compare the performance of the catalytic ozonation using mesoporous carbon materials with that using a typical activated carbon, an additional experiment was carried out in the presence of a commercial activated carbon (sample AC0). Figure 2.4 includes the results obtained with this sample.

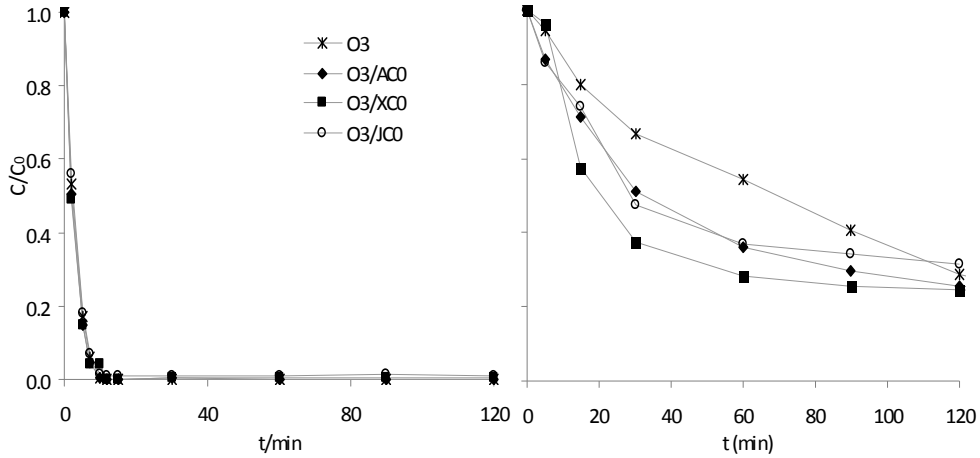

Figure 2.4: Colour and TOC removal for the reactive dye using activated carbon, carbon xerogel and templated carbon as catalysts.

Figure 2.4 shows that a total decolourisation is observed in less than 15 minutes when ozone is applied, and this time is practically independent of the presence of the carbon material. Single ozonation also originates a decrease in the amount of TOC in solution. Nevertheless, this mineralisation is much lower than colour removal, which is an indication that part of the dyes degradation products (colourless) still remains in solution. The advantage of using carbon materials as catalyst is clearly seen in the TOC removal, which is much faster than that obtained by single ozonation.

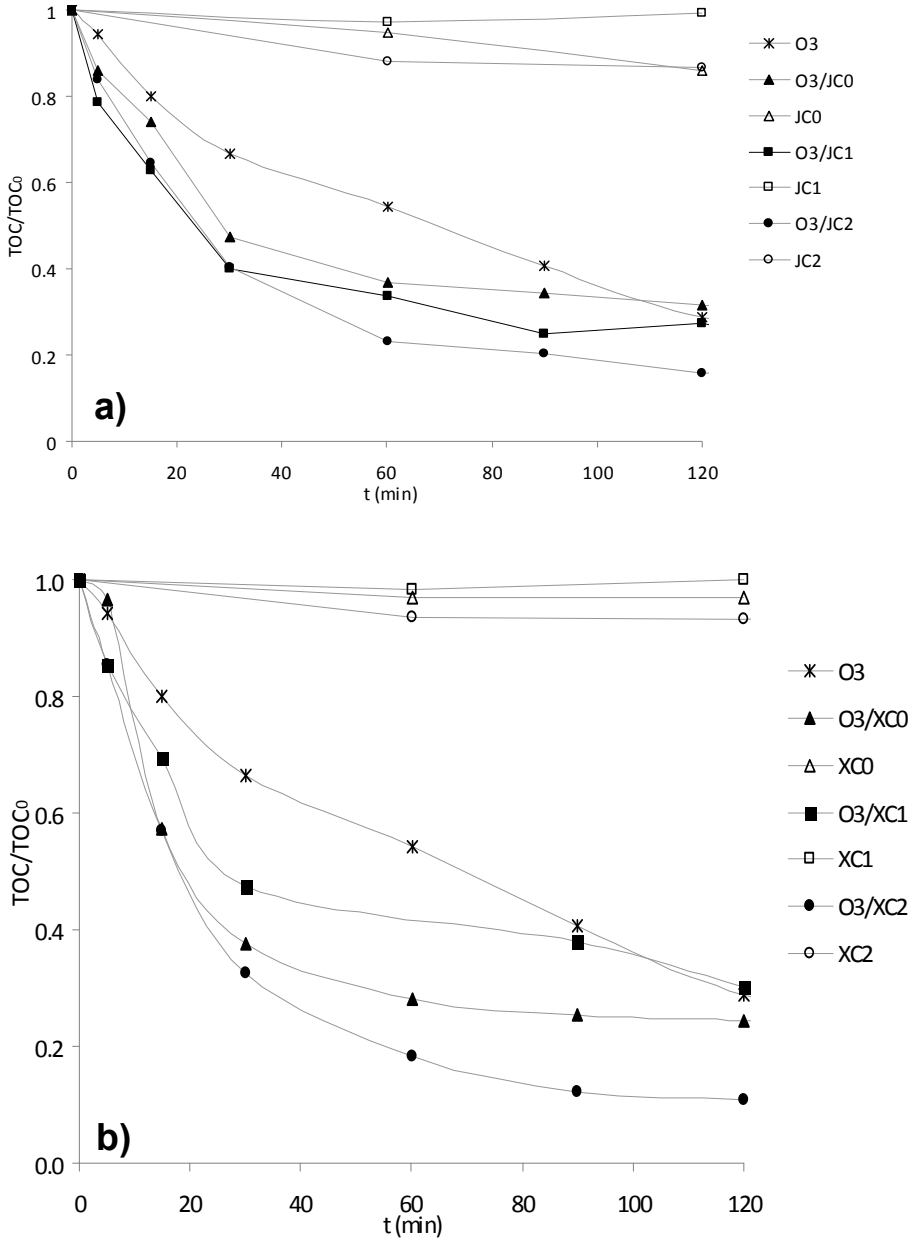

Figure 2.5: TOC removal for the reactive dye in the presence of a) templated carbons, b) carbon xerogels.

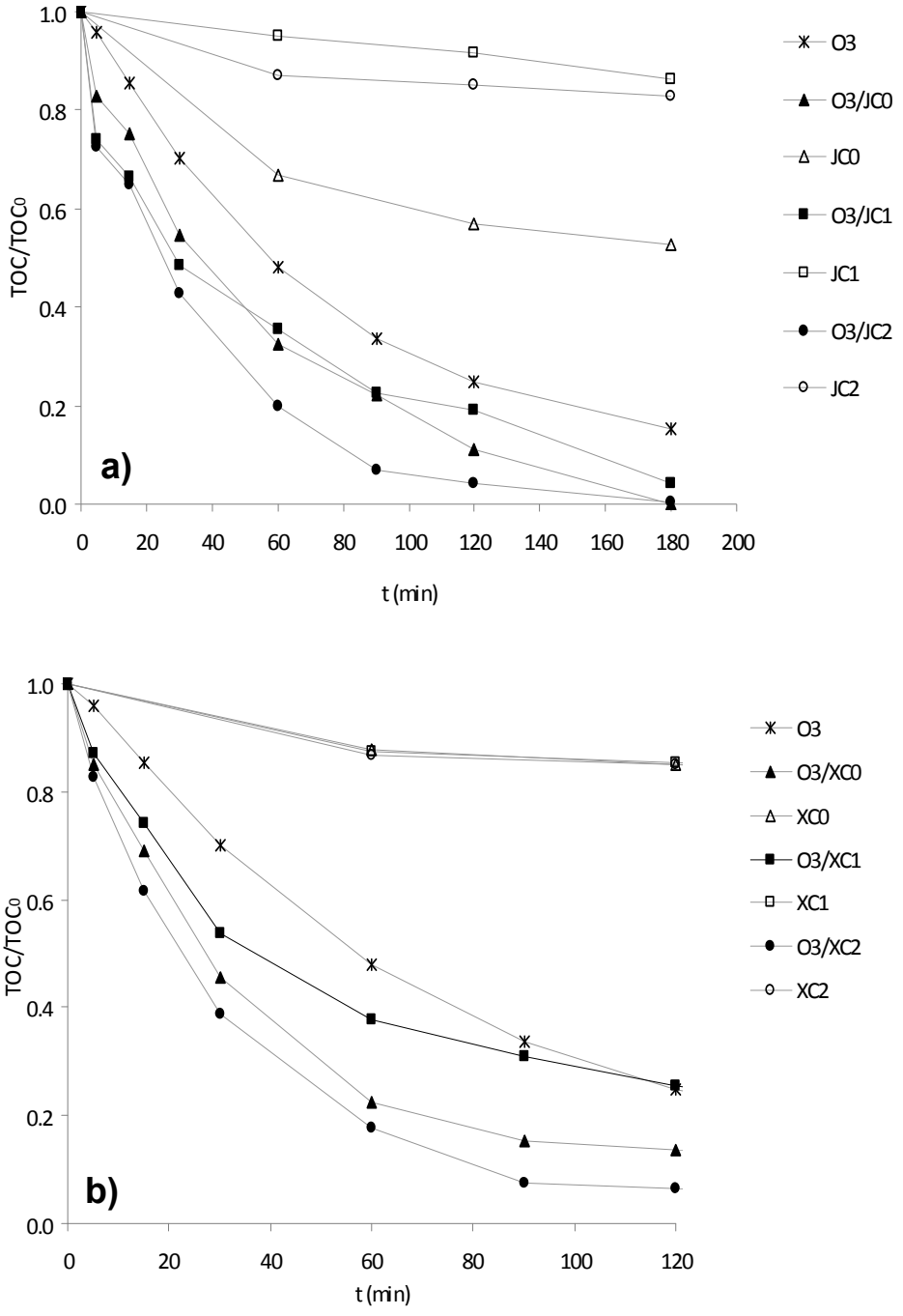

Figure 2.6: TOC removal for the acid dye in the presence of a) templated carbons, b) carbon xerogels.

Independently of the carbon material used and the dye studied, adsorption is not sufficient to remove the colour from the solutions. As expected, the same is observed for TOC removal (see Figures 2.5 and 2.6), because this parameter is directly related to the colour removal when only adsorption is occurring. Generally, adsorption can be responsible for the removal of no more than 10% of TOC after 120min. The only exception is the JC0 sample for the acid dye (see Figure 2.6. a), which was able to remove about 40% in the same period. This difference may be due to the high mesopore surface area of this sample combined with the fact that the acid dye molecule could easily enter into their mesopores when compared to the reactive dye molecule, as explained below.

Mineralisation degrees close to 100% were obtained in several cases when mesoporous carbon materials were used as catalysts in the ozonation of the acid dye tested (see Figure 2.6). In a similar way to the activated carbons, this effect is expected to be associated to their capacity to decompose ozone in highly reactive oxygenated species, such as hydroxyl radicals, able to attack with high efficiency the organic compounds molecules, which justify the significant enhancement of the TOC removal rate when compared to single ozonation. An additional effect may be obtained due to adsorption of the degradation products of the dyes ozonation, which being smaller molecules may be easily adsorbed in the pores of the carbon materials [18]. Adsorption of these intermediates on the carbon surfaces may also contribute to their degradation by surface reactions with the radicals produced by the ozone decomposition [23, 28].

Generally, from the TOC results of the acid dye, it can be observed that ozonation catalysed by templated carbons (samples JC) presents a faster mineralisation rate comparing to the xerogel carbons (samples XC), the opposite being observed for the reactive dye, particularly in the case of the thermal treated samples. This performance can be explained by the effect of the mesopore surface area and size of mesopores of the materials. The molecules of the acid and reactive dyes (see Table 2.1) approximately have cylindrical and spherical shapes, respectively, being the diameter of the cylinder smaller than that of the sphere (9.2 vs 14.4 Å). Therefore, during the first minutes of reaction, some constrains can be envisaged for the access of the reactive dye to the interior of the JC samples, which have smaller pores, and explain the best performance of XC samples in this case, due to their larger mesopores diameter. These constrains are not so effective for the acid dye, which probably explains the best performance of JC samples for its

degradation because of their higher mesopore surface areas. Nevertheless, this effect may be attenuated for longer reaction times, because the ozonation of the dyes originates successively smaller molecules.

The similarity of the TOC removal rate obtained for the templated carbon and the activated carbon in ozonation of the reactive dye (see Figure 2.4), despite the difference in the mesoporous surface areas, may be justified by their surface chemical properties, because the former presents a stronger acid character than the latter, which is known to be unfavourable in the process [18, 27, 38, 39]. An additional explanation for the relatively good performance of the AC sample may relay on its slit-shaped pores, which, comparing to the cylindrical shape pores of XC and JC samples, may allow an easier access of large molecules.

Figures 2.5 and 2.6 show that the less acidic samples (JC2 and XC2) present a faster TOC removal. There is a relationship between the efficiency of ozonation and the basicity of the catalysts (JC1≈JC0<JC2 and XC1<XC0<XC2), which is similar to that previously observed for activated carbons [18]. The ozone decomposition into radicals on the surface of the activated carbon is preceded by an adsorption step where ozone is adsorbed on the carbon surface. The ozone molecules have a higher affinity for basic carbons, which are known to have a high density of delocalized π electrons on the basal planes [16,18, 27, 38]. This phenomenon may explain the order of reactivity observed for these carbon materials. The similar results obtained for samples JC0 and JC1 may be explained by their close pH_{pzc} values (3.5 and 3.0, respectively). It must be stressed that the surface chemistry plays a preponderant role in the catalytic ozonation, because for both materials the thermal treated samples (JC2 and XC2) are clearly the most active, although presenting the lowest surface areas.

2.3.3 Oxalic acid removal

Oxalic acid was also selected for this study because it is one of the most important final products of the oxidation processes, with a high refractory character relatively to single ozonation. Figure 2.7 presents the results obtained for its degradation by catalytic ozonation in the presence of the prepared mesoporous carbons. Data obtained with the activated carbon AC0 are also included, as well as those corresponding to adsorption and single ozonation.

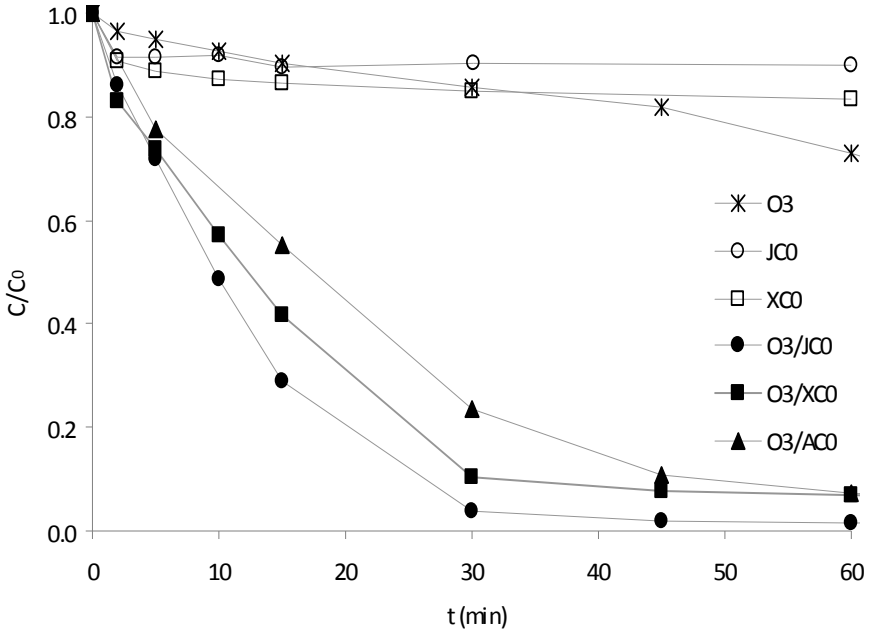

Figure 2.7: Oxalic acid removal by single ozonation, catalysed ozonation and adsorption in the presence of the templated carbon, carbon xerogel and activated carbon.

It can be observed, both for the templated carbon and the carbon xerogel, that single adsorption is not sufficient to remove oxalic acid. The same occurs for single ozonation, although a higher removal than that obtained by adsorption is observed after 60 min. On the contrary, an extended removal of oxalic acid is observed by catalysed ozonation. A higher catalytic effect is observed for the templated carbon samples compared to the xerogel carbons, which is an indication of the importance of the mesoporous surface area of the carbon catalysts (819 m^2 g^{-1} for JC0 vs. 329 m^2 g^{-1} for XC0), because the restrictive role of the mesopores size seems to be negligible in this case, due to the small dimensions of the oxalic acid molecule. For comparative purposes, the results obtained with the commercial activated carbon selected were also included in Figure 2.7, a worst performance being observed in this case, which is an indication of the positive effect of using mesoporous carbons as ozonation catalysts. It is important to notice that JC0 presents the best performance, even being more acid than XC0 and AC0 (see the respective pH_{PZC}

values in Table 2.2), which is known to play a negative role in the catalytic ozonation [28].

The explanation of the synergic effect where using ozone and an activated carbon in the oxidation of oxalic acid was presented recently [28]. This explanation considers the capacity of the activated carbon to promote the ozone decomposition into oxygenated radicals, highly reactive both on the carbon surface and in the solution, which will then react with oxalic acid, respectively adsorbed and non-adsorbed. It is assumed that the catalytic activity of the prepared mesoporous carbons results from similar reaction pathways.

2.4 Conclusions

In this study the use of mesoporous carbons (templated via SBA-15 and xerogels) as ozonation catalyst was reported for the first time. The main conclusions are:

1. Adsorption of reactive and acid dyes on templated carbons and carbon xerogels is not efficient enough to remove the colour from solutions. Single ozonation allows a complete colour removal in a few minutes, but the respective TOC removal efficiency is low.

2. The association of ozone and all the mentioned carbon materials leads to an improved TOC removal from the dye solutions. The catalytic effect increases with the carbon basicity. The most important textural parameters are the mesopore size diameter for the reactive dye and the mesopore surface area for the acid dye.

3. The use of the mesoporous carbons as catalyst for ozonation was also validated in the removal of oxalic acid from solutions, showing an enhanced performance compared to single ozonation or adsorption. The catalytic effect increases with the mesopore surface area.

4. Generally, mesoporous carbons present better performances as ozonation catalysts than the activated carbon tested, which is justified by the higher mesoporosity of the former.

Acknowledgments

Universidade do Porto and Caixa Geral de Depósitos (Projecto de Investigação Científica na Pré-Graduação 2007: IPG58). CAO thanks Fundação para a Ciência e a Tecnologia (FCT) for the research fellowship BD/45809/2008.

References

[1] R. Ryoo, S. H. Joo, M. Kruk, M. Jaroniec, Ordered Mesoporous Carbons, Adv. Mater. 13 (2001) 677-681.

[2] A. B. Fuertes, D. M. Nevskaia, Control of mesoporous structure of carbons synthesised using a mesostructured silica as template, Microporous Mesoporous Mater. 62 (2003) 177-190.

[3] W. H. Zhang, J. Xiu, Z. Shen, Y. Li, P. Ying , C. Li, Pore size design of ordered mesoporous silicas by controlling micellar properties of triblock copolymer $EO_{20}PO_{70}EO_{20}$, Microporous Mesoporous Mater. 89 (2006) 179-185.

[4] J. L. Figueiredo, M. F. R. Pereira, M. M. A. Freitas, J. J. M. Órfão, Modification of the surface chemistry of activated carbons, Carbon 37 (1999) 1379-1389.

[5] J. Lee, S. Han, T. Hyeon, Synthesis of new nanoporous carbon materials using nanostructured silica materials as templates, J. Mater. Chem. 14 (2004) 478-486.

[6] S. Jun, S. H. Joo, R. Ryoo, M. Kruk, M. Jaroniec, Z. Liu, T. Ohsuna, O. Terasaki, Synthesis of New, Nanoporous Carbon with Hexagonally Ordered Mesostructure, J. Am. Chem. Soc. 122 (2000) 10712-10713.

[7] F. Schüth, W. Schmdt, Microporous and Mesoporous Materials, Adv. Mater. 14 (2002) 629-638.

[8] F. Schüth, Endo- and Exotemplating to Create High-Surface-Area Inorganic Materials, Angew. Chem. Int. Ed. 42 (2003) 3604-3622.

[9] G. Che, B. B. Lakshmi, E. R. Fisher, C. R. Martin, Carbon nanotubule membranes for electrochemical energy storage and production, Nature 393 (1998) 346-349.

[10] N. Job, R. Pirard, J. Marien, J.P. Pirard, Porous carbon xerogels with texture tailored by pH control during sol–gel process, Carbon 42 (2004) 619-628.

[11] R. W. Pekala, Organic aerogels from the polycondensation of resorcinol with formaldehyde, J. Mater. Sci. 24 (1989) 3221-3227.

[12] P.V. Samant, F. Gonçalves, M.M.A. Freitas, M.F.R. Pereira, J.L. Figueiredo, Surface activation of a polymer based carbon, Carbon 42 (2004) 1321-1325.

[13] U. Rott, R. Minke, Overview of wastewater treatment and recycling in the textile processing industry, Water Sci. Technol. 40 (1999) 137-144.

[14] B. Kasprzyk-Hordern, M. Ziólek, J. Nawrocki, Catalytic ozonation and methods of enhancing molecular ozone reactions in water treatment, App. Catal. B: Environ. 46 (2003) 639-669.

[15] B. Legube, N. K. V. Leitner, Catalytic ozonation: a promising advanced oxidation technology for water treatment, Catal. Today 53 (1999) 61-72.

[16] P.C.C. Faria, J.J.M. Órfão, M.F.R. Pereira, Ozone Decomposition in Water Catalyzed by Activated Carbon: Influence of Chemical and Textural Properties, Ind. Eng. Chem. Res. 45 (2006) 2715-2721.

[17] P.M. Alvarez, J.F. Garcia-Araya, F.J. Beltran, I. Giraldez, J. Jaramillo, V. Gomez-Serrano, The influence of various factors on aqueous ozone decomposition by granular activated carbons and the development of a mechanistic approach, Carbon 44 (2006) 3102-3112.

[18] P.C.C. Faria, J.J.M. Órfão, M.F.R. Pereira, Mineralisation of coloured aqueous solutions by ozonation in the presence of activated carbon, Water Res. 39 (2005) 1461-1470.

[19] S.H. Lin, C.L. Lai, Kinetic characteristics of textile wastewater ozonation in fluidized and fixed activated carbon beds, Water Res. 34 (2000) 763-772.

[20] S. Gul, O. Ozcan, O. Erbatur, Ozonation of C.I. Reactive Red 194 and C.I. Reactive Yellow 145 in aqueous solution in the presence of granular activated carbon, Dyes Pigm. 75 (2007) 426-431.

[21] P.C.C. Faria, J.J.M. Órfão, M.F.R. Pereira, Activated carbon and ceria catalysts applied to the catalytic ozonation of dyes and textile effluents, Appl. Catal. B: Environ. 88 (2009) 341-350.

[22] P.C.C. Faria, J.J.M. Órfão, M.F.R. Pereira, Ozonation of aniline promoted by activated carbon, Chemosphere 67 (2007) 809-815.

[23] P.C.C. Faria, J.J.M. Órfão, M.F.R. Pereira, Catalytic ozonation of sulfonated aromatic compounds in the presence of activated carbon, Appl. Catal. B: Environ. 83 (2008) 150-159.

[24] C.A. Zaror, Enhanced oxidation of toxic effluents using simultaneous ozonation and activated carbon treatment, J. Chem. Technol. Biotechnol. 70 (1997) 21-28.

[25] F.J. Beltran, F.J. Rivas, R. Monte-de-Espinosa, J. Chem. Technol. Biotechnol. Mineralization improvement of phenol aqueous solutions through heterogeneous catalytic ozonation, 78 (2003) 1225-1233.

[26] J. Ma, M.H. Sui, Z.L. Chen, L.N. Wang, Degradation of refractory organic pollutants by catalytic ozonation-activated carbon and Mn-loaded activated carbon as catalysts, Ozone: Sci. Eng. 26 (2004) 3-10.

[27] J. Rivera-Utrilla, M. Sánchez-Polo, Ozonation of 1,3,6-naphthalenetrisulphonic acid catalysed by activated carbon in aqueous phase, Appl. Catal. B: Environ. 39 (2002) 319-329.

[28] P.C.C. Faria, J.J.M. Órfão, M.F.R. Pereira, Activated carbon catalytic ozonation of oxamic and oxalic acids, Appl. Catal. B: Environ. 79 (2008) 237-243.

[29] F.J. Beltran, F.J. Rivas, L.A. Fernandez, P.M. Alvarez, R. Montero-de-Espinosa, Kinetics of Catalytic Ozonation of Oxalic Acid in Water with Activated Carbon, Ind. Eng. Chem. Res. 41 (2002) 6510-6517.

[30] F.J. Beltran, J.F. Garcia-Araya, I. Giraldez, Gallic acid water ozonation using activated carbon, Appl. Catal. B-Environ. 63 (2006) 249-259.

[31] D. Zhao, Q. Huo, J. Feng, B. F. Chmelka, G. D. Stucky, Nonionic Triblock and Star Diblock Copolymer and Oligomeric Surfactant Syntheses of Highly Ordered, Hydrothermally Stable, Mesoporous Silica Structures, J. Am. Chem. Soc. 120 (1998) 6024-6036.

[32] A. B. Fuertes, Synthesis of ordered nanoporous carbons of tunable mesopore size by templating SBA-15 silica materials, Micropor. Mesopor. Mater. 67 (2004) 273-281.

[33] R. Ryoo, S. H. Joo, M. Kruk, M. Jaroniec, Ordered Mesoporous Carbons, Adv. Mater. 13 (2001) 677-681.

[34] E. Papirer, S. Li, J. B. Donnet, Contribution to the study of basic surface groups on carbons, Carbon 25 (1987) 243-247.

[35] Society of Dyers and Colourists, Colour Index. 3rd revision, Bradford 1998.

[36] P.C.C. Faria, J.J.M. Órfão, M.F.R. Pereira, Adsorption of anionic and cationic dyes on activated carbons with different surface chemistries, Water Res. 38 (2004) 2043-2052.

[37] S.J. Gregg and K.S.W. Sing, Adsorption, Surface Area and Porosity. Academic Press, San Diego 1982.

[38] M. Sánchez-Polo, U. von Gunten, J. Rivera-Utrilla, Efficiency of activated carbon to transform ozone into OH radicals: Influence of operational parameters, Water Res. 39 (2005) 3189-3198.

[39] M. Sánchez-Polo, J. Rivera-Utrilla, Effect of the ozone-carbon reaction on the catalytic activity of activated carbon during the degradation of 1,3,6-naphthalenetrisulphonic acid with ozone, Carbon 41 (2003) 303-307.

Chapter 3

Ozonation of model organic compounds catalysed by nanostructured cerium oxides[1]

Cerium oxides prepared by the precipitation method and hydrothermal synthesis, with distinct morphologies and particle size, were tested as catalysts in the ozonation of selected organic compounds. Oxalic acid, aniline and a reactive dye were used as representative of organic pollutants. In the case of oxalic acid, an increase in the catalytic activity with the increase of the percentage of Ce(III) on the surface was observed. Both single and catalytic ozonation allowed the total removal of aniline after 30 min of reaction; the cerium oxide prepared by the precipitation method was the best catalyst for promoting the mineralisation of aniline solutions. TOC removals close to 100% were obtained in all cases when cerium oxides were used as catalysts in the ozonation of the reactive dye tested.

[1] C. A. Orge, J. J. M. Órfão, M. F. R. Pereira, A. M. Duarte de Farias, R. C. R. Neto, M. A. Fraga, Ozonation of model organic compounds catalysed by nanostructured cerium oxides, Appl. Catal. B: Environ. 103 (2011) 190-199.

3 Ozonation of model organic compounds catalysed by nanostructured cerium oxides

3.1 Introduction

In order to enhance the efficiency of ozonation processes, methods combining ozone with hydrogen peroxide, UV radiation, metallic ions or heterogeneous catalysts have been object of intense research [1]. Heterogeneous catalytic ozonation, which is one of the most attractive alternatives, aims to enhance the removal of more refractory compounds by the transformation of ozone into more reactive species and/or by adsorption and reaction of the pollutants on the surface of the catalyst [1]. The efficiency of the catalytic ozonation depends on the surface properties of the catalyst as well as on the solution pH and the chemical nature of the reactants. Oxides of transition metals, such as manganese [2], titanium [3] or cobalt [4], are amongst the most frequently studied ozonation catalysts. The development of highly effective catalysts for the application in ozonation processes, and the understanding of the inherent mechanisms are of great relevance.

Ceria (cerium oxide, CeO_2) is a cubic fluorite-type oxide, which is considered as the most important of rare-earth oxides [5]. Ceria-based catalysts have attracted enormous interest because of their various applications in three-way automotive catalysts [6], solid oxide fuel cells [7], water-gas shift [8], CO preferential oxidation [9], and heterogeneous catalytic ozonation [10]. Indeed, Faria et al. [11] showed that cerium oxide is an effective ozonation catalyst for the removal of carboxylic acids. It is suggested that the oxide promotes the decomposition of ozone into $HO^{\bullet}$ radicals, which are the main oxidant species responsible for the oxidation of the compounds in the liquid phase. The same authors verified that catalytic ozonation in the presence of cerium oxide significantly increased the extent of mineralisation of sulfanilic acid and aniline, compared to single ozonation [12], and cerium oxide was shown to be active in the mineralisation of several dyes [10].

This avalanche of successful application in catalysis is due to their redox properties (Ce^{4+}/Ce^{3+}), which gives it the ability to store oxygen and release oxygen through the formation of oxygen vacancies due to the reduction of cerium [13]. It is now known that the stability and energy of formation of these oxygen vacancies differ between the surface and the bulk of ceria and also depend on the exposed surface planes [14, 15]. This remarkable oxygen storage/release capability may thus be predicted to be strongly associated with the size, the morphology and the exposed

crystalline planes of ceria particles [16, 17]. Therefore, nanostructured CeO_2 is expected to significantly enhance redox properties because of the easy creation and diffusion of oxygen vacancies at the surface. By controlling the morphology upon synthesis of a specific nanostructure, it is possible to promote the exposition of crystallographic planes containing most active sites for some catalytic reactions [16-19].

In recent years, various routes to obtain nanostructured CeO_2 materials with controlled size and morphology has been developed using different methodologies, such as precipitation with different precipitating agents, sol-gel, sonochemical, electrochemical, solvothermal, amongst others [20-22]. However, a wide range of well-defined CeO_2 nanostructures (flower, rods, spheres, polyhedrons, tubes, wires, prisms and cubes) have been successfully synthesized via the hydrothermal process. This method shows high efficiency in preparing nanostructured CeO_2 with size/shape controlled by careful adjustment of the hydrothermal conditions without addition of any sort of templates or surfactants and with high catalytic activity for redox-based reactions [5, 16-19, 23, 24].

The aim of this work is to study the ozonation of some selected organic pollutants (oxalic acid, aniline and the dye C. I. reactive blue 5) in the presence of different nanostructured cerium oxides, prepared with controlled morphology by precipitation and nontemplate hydrothermal synthesis.

3.2 Experimental

3.2.1 Materials

In this work, four samples of cerium oxide were synthesised by different procedures based on the precipitation method and hydrothermal synthesis; in all syntheses the metal salt solution used was prepared with cerium (III) nitrate, $Ce(NO_3)_3.6H_2O$.

Sample CeO_2 was prepared by precipitation from the corresponding salt aqueous solution using NH_4OH as precipitation agent [25]. The precipitate was filtered and washed with deionized water until the pH of the filtrate remained neutral. Afterwards, the precipitate was calcined at 500 °C in air for 4 h.

In the case of hydrothermal synthesis, three different methods were used to prepare shape-controlled nanostructured cerium oxide samples. In the first procedure [24], 0.033 mol of D-glucose and 0.045 mol of acrylamide were dissolved in water under continuous stirring at room temperature and 0.028 mol of $Ce(NO_3)_3.6H_2O$ were

added. Then, 0.097 mol of NH_4OH (7.5 mol L^{-1}) were added dropwise, and the suspension was shaken for 5 h at room temperature. The suspension was transferred into a 300 mL teflon-lined stainless steel autoclave and thermally treated at 180 °C for 72 h in an electric oven. After the hydrothermal treatment, the brown precipitate was separated by centrifugation, washed with deionized water and ethanol several times and dried at 80 °C for 12 h and then calcined in two steps. First, the solid was heat treated for 5 h at 600 °C (1 °C min^{-1}) under a flow of N_2 (50 cm^3 min^{-1}). In the next step, calcination was carried out under a flow of air (50 cm^3 min^{-1}) for 5 h at 600 °C (1 °C min^{-1}). This sample was denominated as CeO_2-FL.

Nanocubes and nanoparticles were prepared by the hydrothermal method according to the literature [21, 22]. First, 60 mL of NaOH solution (9.3 mol L^{-1}) was added to the $Ce(NO_3)_3.6H_2O$ solution (0.12 mol L^{-1}) dropwise under continuous stirring for 30 min with the formation of a milky slurry. Subsequently, the obtained slurry was transferred into a Teflon-lined steel autoclave. Then, the autoclave was transferred into an electric oven and was submitted to a hydrothermal treatment for 14 h at 100 °C (nanoparticles, CeO_2-NP) or 16 h at 180 °C (nanocubes, CeO_2-NC). After that, the autoclave was naturally cooled down to room temperature, the precipitates were filtered and washed in hot water until constant pH, dried overnight at 110 °C and finally calcined at 500 °C (2 °C min^{-1}) under an air flow (50 cm^3 min^{-1}) for 5 h.

3.2.2 Characterization of catalysts

N_2 equilibrium adsorption isotherms at -196 °C were obtained in an ASAP 2020 apparatus from Micromeritics. Prior to analyses, the materials were outgassed at 5 μm Hg and 150 °C for 24 h.

Powder XRD patterns were recorded on a Rigaku Miniflex diffractometer that uses Cu Kα radiation (30 kV, 15 mA). The samples were spread as thin layers on a glass slide and diffraction patterns were obtained by increasing 2θ from 10° to 90° with 0.02° increments.

Field Emission Scanning Electron Microscopy (FE-SEM) images were obtained on a Quanta 200 FEG microscope operating with an accelerating voltage of 30 kV. Before the analysis, the samples were dispersed in acetone with the aid of ultrasound and deposited on a silicon substrate.

Oxides were also examined by TEM using a Tecnai 20 FEI microscope operating at 200 kV. The samples were ultrasonically suspended in acetone and deposited on a carbon-coated copper grid. All size measurements were processed using ES Vision software version 4.1.

Raman spectra were collected at ambient conditions from a Horiba (Jobin Yvon) spectrometer model HR800 UV, equipped with a CCD detector (-70 °C) and using a He-Ne laser with a 633 nm wavelength (sample power 10 mW). All samples were analyzed with 5 scans and an exposition of 100 s.

The TPR analyses were performed using a 5% H_2/N_2 (vol.%) stream as the reducing gas (30 cm^3 min^{-1}). The mixed oxides were heated up to 1000 °C following a 10 °C min^{-1} linear temperature ramp and the hydrogen uptake was monitored by an on-line Baltzer QMS200 quadrupole mass spectrometer. Before the analyses, the samples were pretreated at 500 °C using a heating rate of 10 °C min^{-1} under a flow of 8% O_2/He (vol.%) at 30 cm^3 min^{-1} in order to eliminate the carbonated species generated by air exposure during handling and storage.

XPS analyses were performed with a VG Scientific ESCALAB 200A spectrometer operating at 15 keV and 300 W. XPS data corresponding to Ce 3d spectra were fitted using the software XPSpeak. To minimize the number of degrees of freedom of the curve fitting procedure, constraints on the binding energy (BE), full width at half maximum (FWHM) and peak areas were applied to each doublet pair.

3.2.3 Experimental set-up and analytical methods

The removal of pollutants was investigated in a slurry lab-scale reactor equipped with agitation. In each experiment the reactor was filled with 700 cm^3 of pollutant solution ($C_{0,oxalic\ acid} = C_{0,aniline}$ = 1 mM, $C_{0,\ dye}$ = 50 mg L^{-1}) at the natural pH ($pH_{0,\ oxalic\ acid}$ = 3.0, $pH_{0,\ aniline}$ = 6.0, $pH_{0,\ dye}$ = 5.5). In the catalytic ozonation experiments, 100 mg of catalyst were introduced in the reactor. Ozone was produced from pure oxygen in a BMT 802X ozone generator. The experiments were performed at constant gas flow rate (150 cm^3 min^{-1}) and constant inlet ozone concentration (50 g m^{-3}). The concentration of ozone in the gas phase was monitored with a BMT 964 ozone analyzer. Ozone in the gas phase leaving the reactor was removed in a series of gas washing bottles filled with iodide potassium solution. The agitation was maintained constant in order to keep the reactor content perfectly mixed and the temperature was set to 25 °C.

The concentration of pollutants and the intermediates formed were followed by HPLC using a Hitachi Elite Lachrom HPLC equipped with a diode array detector. The stationary phases were an Aminex HPX-87H column (300 mm x 7.8 mm), working at room temperature under isocratic elution with H_2SO_4 4 mM, to determine the concentration of oxalic acid and oxamic acid, and a LiChroCART Purospher Star column (250 mm x 4.6 mm), working at room temperature under gradient elution with water and acetonitrile, to follow the concentration of aniline in the solution. The concentration of dye in the solution was followed by UV-Vis spectrophotometry with a JASCO V-560 UV/Vis spectrophotometer. The degree of mineralisation was determined by total organic carbon (TOC) analysis in a Shimadzu TOC-5000A Analyzer.

3.3 Results and discussion

3.3.1 Samples characterization

Textural properties of all nontemplate synthesized cerium oxides were estimated based on the corresponding nitrogen adsorption isotherms and the data collected in Table 3.1 show that all samples present moderate or high specific surface areas. It is also noted that, as a general pattern, those samples obtained via hydrothermal treatment provided the lower values; apart from CeO_2-FL, the surface areas are below 100 $m^2\ g^{-1}$.

Figure 3.1 shows the XRD spectra of the prepared oxides. All catalysts present characteristic peaks associated with the face-centered cubic (fcc) fluorite structure of CeO_2. The peaks are located at 28.7°, 33.1°, 47.5°, 56.2°, 59.2°, 69.7°, 76.7°, 79.3°, and 88.3°, and correspond to the (1 1 1), (2 0 0), (2 2 0), (3 1 1), (2 2 2), (4 0 0), (3 3 1), (4 2 0), and (4 2 2) planes, respectively.

The mean diameter of ceria crystallites was determined by the peak broadening of the (111) reflection in the XRD patterns, following the Scherrer equation (Table 3.1). CeO_2-FL has an average diameter similar to CeO_2, while the other cerium oxides prepared by hydrothermal synthesis have larger crystallite diameters. It is worth noting that even though both samples are obtained through a similar procedure, a difference in the crystallite sizes is accomplished. Such trend is in fact consistent with the distinct time and temperature applied upon synthesis as previously observed by other authors [26]. It is also important to observe that the textural differences observed in the nitrogen adsorption isotherms are in good qualitative

agreement with this enlargement of crystallite size. On the other hand, the unit-cell lengths (*a*) of the hydrothermally treated samples have the same value.

Table 3.1: Surface area (S_{BET}), average crystallite particle size (d), and cubic lattice cell length (a) of all synthesized oxides.

Sample	S_{BET} ($m^2 g^{-1}$)	d (nm)[a]	a (nm)[b]
CeO_2	98	7.7	0.539
CeO_2-NC	54	14.8	0.541
CeO_2-NP	71	10.0	0.541
CeO_2-FL	140	7.9	0.541

[a] average crystallite size obtained from the (111) reflection of diffractograms using Scherrer equation;

[b] lattice parameter determined from the (111) reflection of diffractograms.

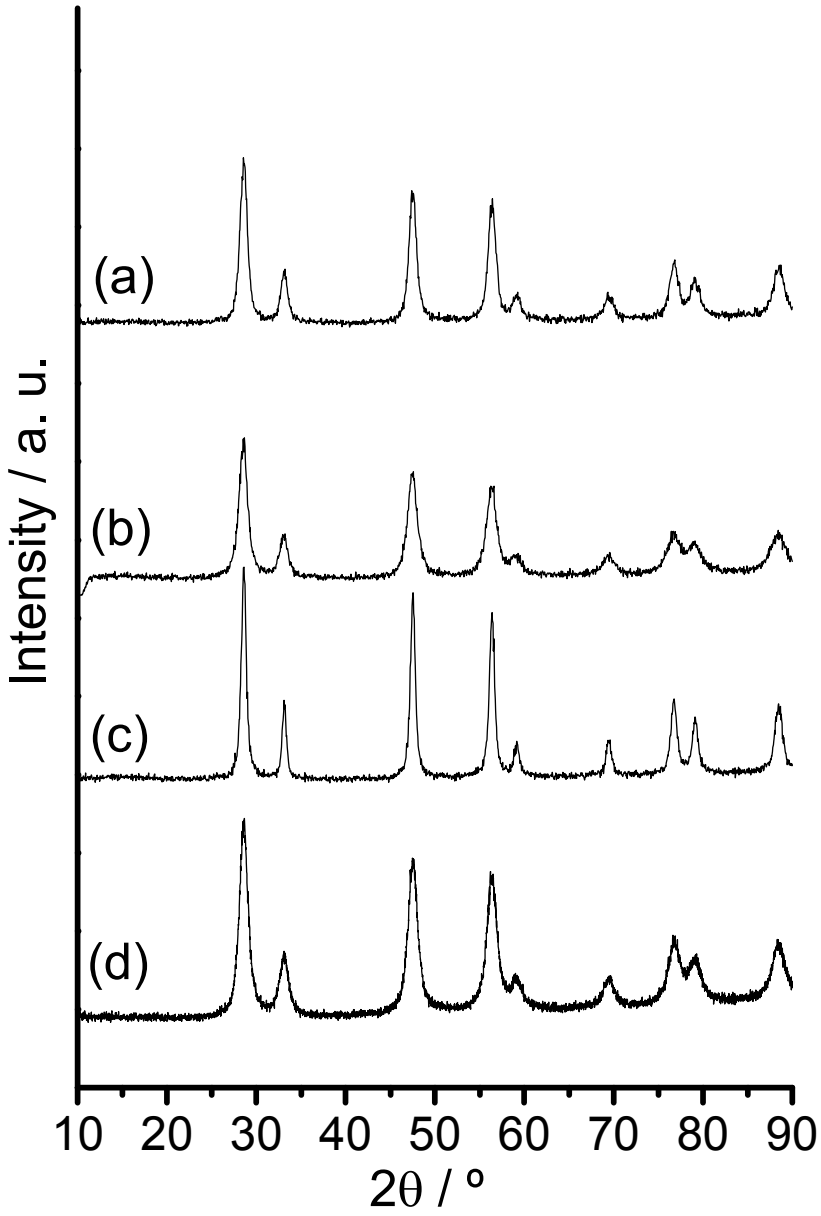

Figure 3.1: X-ray diffractograms of the cerium oxide samples: (a) CeO_2-NP (b) CeO_2-FL, (c) CeO_2-NC, (d) CeO_2.

The morphology of the synthesized oxides was firstly examined by FE-SEM and some representative images are depicted in Figure 3.2. Some remarkable differences in the morphology of cerium oxide samples could already be seen at low magnification. While a non-defined morphology may be seen in the precipitated

oxide (Figure 3.2a and b), a flower-like structure was obtained by one of the hydrothermal treatment applied (Figure 3.2c). In this case, a higher magnification examination of a selected area as indicated in Figure 3.2c revealed that the sample consists of several nanopetals (Figure 3.2d) forming an open porous structure with tri-dimensional architecture. As for both CeO_2-NC and CeO_2-NP samples, the particles could not be described by any ordinary shape and even at high magnification (above 150.000x) no distinguishable morphological features could be envisaged (Figure 3.2e and f).

A more detailed structural analysis was performed by TEM/HRTEM. A global view of the CeO_2-NC at low-magnification is depicted in Figure 3.3a, and indeed evidence the existence of small cube-shaped particles within ~10 – 30 nm. A closer inspection based on the high-resolution images (Figure 3.3b) allows to identify different crystal planes of ceria in cubic fluorite structure, namely (200) and (111), which correspond to interplanar distance of 0.28 and 0.31 nm, respectively. CeO_2-NP and CeO_2-FL, on the other hand, revealed to be formed by aggregates of round-shaped nanoparticles, which could only be clearly examined at high-magnification. The CeO_2-NP sample (Figure 3.3c) presented nanoparticles with size within ~8 – 10 nm and only (111) planes could be identified in the collected images. As for the CeO_2-FL (Figure 3.3d), it was seen that each petal is composed by a large aggregate of nanoparticles with particle size below 5 nm. The existence of such agglomerates is confirmed by the several sets of fringes in the HRTEM image, and their respective spots in the FFT pattern exhibited as inset in Figure 3.3d.

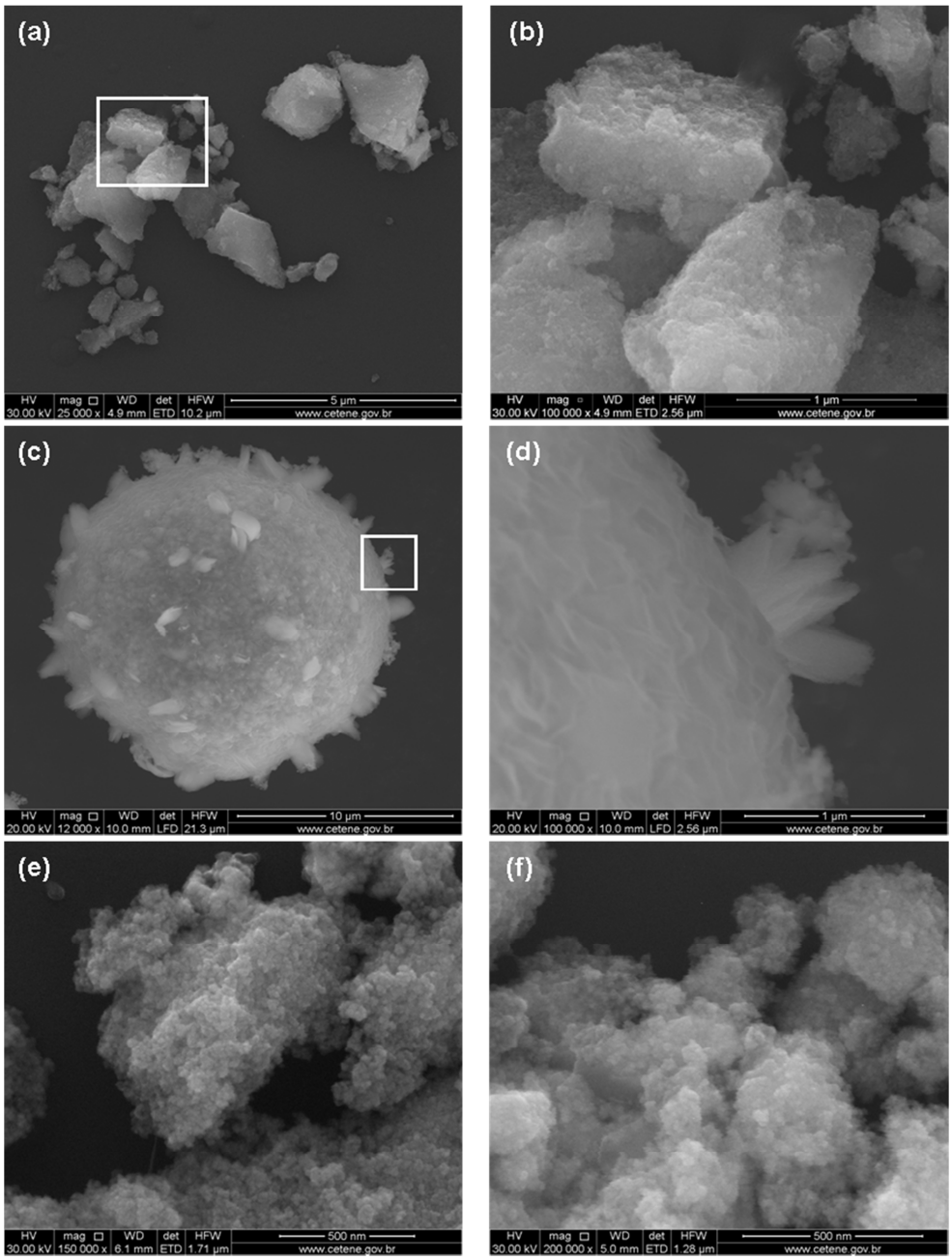

Figure 3.2: FE-SEM images of CeO_2 at 25.000x (a) and 100.000x (b), CeO_2-FL at 12.000x (c) and 100.000x (d), CeO_2-NC at 150.000x (e) and CeO_2-NP at 200.000x (f).

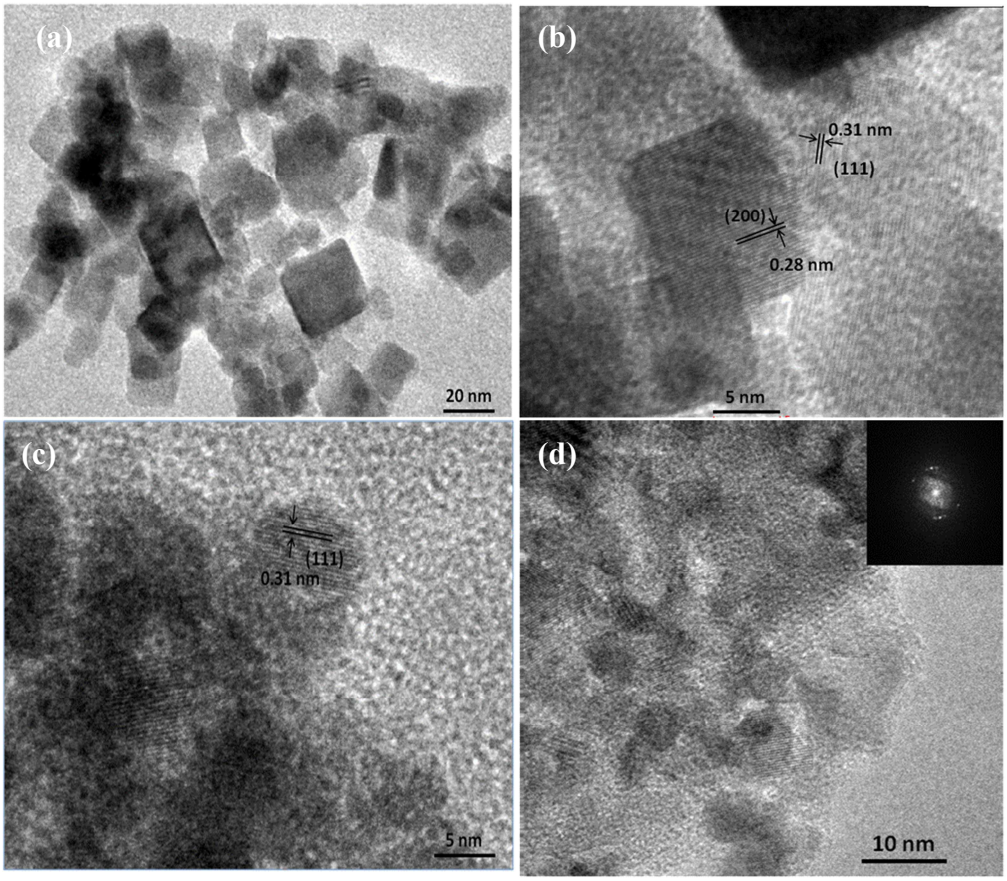

Figure 3.3: TEM image of CeO_2-NC (a) and HRTEM images of CeO_2-NC (b), CeO_2-NP (c) and CeO_2-FL (d).

The Raman spectra of the prepared materials are shown in Figure 3.4. All samples exhibit an intense band between 463 and 466 cm^{-1}, which corresponds to the symmetric stretching of two O around Ce [27]. Weak bands appearing below 300 cm^{-1} and at around 595 cm^{-1}, displayed in the inset of Figure 3.4, are mainly attributed to defect-induced modes [28]. It is thus generally associated with the presence of oxygen vacancies, which affords a qualitative indication of the occurrence of Ce^{3+} in all samples irrespective of the morphology and nanostructure retained.

The reducibility of all oxides was examined by H_2-TPR analyses and the reduction patterns are depicted in Figure 3.5. A typical profile was registered for all cerium oxides, featuring two asymmetrical and broad peaks at around [400-600] °C and [900-1050] °C, which are assigned to the surface and bulk reductions, respectively

[25, 29]. The quantitative data summarized in Table 3.2 were calculated from the first peak.

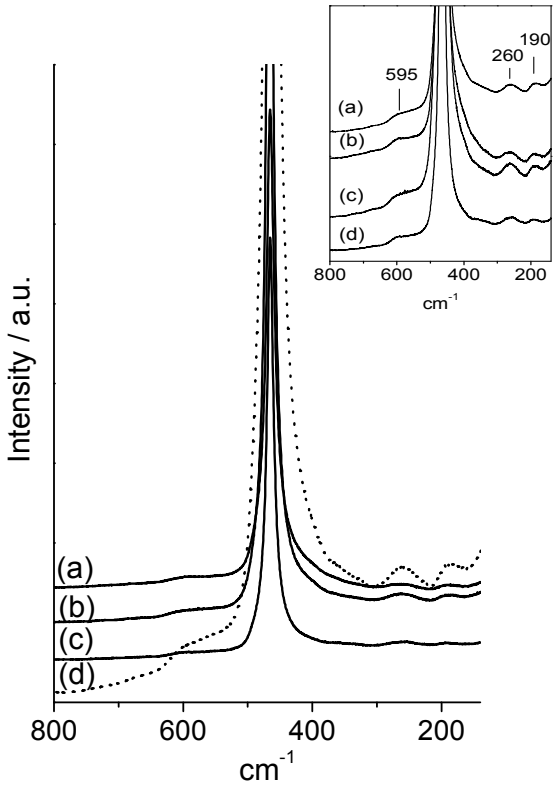

Figure 3.4: Raman spectra of the different cerium oxide nanostructures: (a) CeO_2-NP (b) CeO_2-FL, (c) CeO_2-NC, (d) CeO_2.

Table 3.2: Hydrogen consumption and Ce^{3+} percentage as measured by XPS.

Sample	H_2 consumption ($\mu mol\ g^{-1}$)[a]	H_2 consumption ($\mu mol\ m^{-2}$)[b]	% Ce(III)[c]
CeO_2	539	5.5	44.5
CeO_2-NC	317	5.9	47.5
CeO_2-NP	429	6.0	49.1
CeO_2-FL	605	4.3	44.6

[a] total amount of hydrogen determined by the first peak of TPR profiles;

[b] total amount of hydrogen normalized by surface area (S_{BET});

[c] obtained by XPS analysis.

In a first evaluation, a decrease in total hydrogen consumption was observed for the nanostructured oxides as compared to the ordinary precipitated powder (CeO_2). As for the flowerlike sample, however, a noticeable increase is registered. Such trend in the total hydrogen consumption is consistent with their distinct specific surface areas. As a consequence, a better examination of the surface reducibility, and thus, of the redox surface properties, should rely on the normalized hydrogen uptake, whose values are also collected in Table 3.2. It can be seen that the hydrogen consumption obtained in this work for the surface reduction for sample CeO_2-FL is close to the theoretical coefficient of 4.2 $\mu mol\ m^{-2}$ proposed in the literature [29]. Nevertheless, hydrogen amounts higher than those predicted were recorded for the nanostructured samples, particularly CeO_2-NP and CeO_2-NC, indicating that those nanoxides possess a higher surface reducibility and, therefore, a better catalytic performance in redox-based reactions may be foreseen.

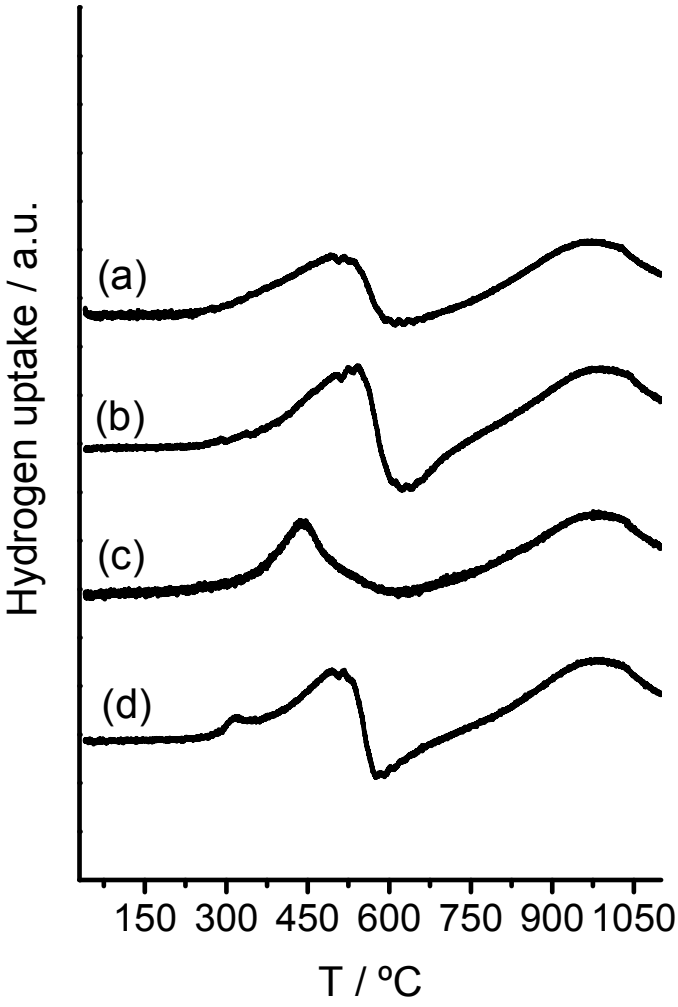

Figure 3.5: TPR profiles of the different cerium oxides: (a) CeO_2-NP (b) CeO_2-FL, (c) CeO_2-NC, (d) CeO_2.

The oxidation states of cerium on the surface of sample CeO_2 and the other nanocatalysts prepared by hydrothermal synthesis were characterized by XPS analyses. According to the literature [30], the Ce 3d XPS spectra of Ce (IV) can be resolved into six features. If some Ce (III) species are present, then two additional peaks and the corresponding satellites are necessary to describe the spectra. Furthermore, Ce (IV) and Ce (III) always show peaks at ~882.5 and ~916.5 eV as well as ~885.0 and ~903.7eV, which are considered fingerprints characterising +4 and +3 oxidation states, respectively [31]. Although Ce 3d spectra of all samples present the characteristic features of cerium (IV) oxide, the coexistence of both Ce

(III) and Ce (IV) species must be considered in order to obtain a good fitting of the experimental data. The curves were fitted with ten peaks [32, 33] (see Figure 3.6). In the Ce $3d_{5/2}$ spin-orbit split doublet for Ce (IV), v_0 and v_2 components represent the intense peaks and v_1 a weak satellite. Correspondingly, v'_0 and v'_2 components represent the Ce $3d_{3/2}$ doublet intense peaks, and v'_1 the associated weak satellite [32, 34-37]. For the oxidation state +3, the main components u_0 and u_1 characterize the Ce $3d_{5/2}$, and u'_0 and u'_1 the Ce $3d_{3/2}$ contribution [32, 38, 39]. Two different approaches have been followed to evaluate the degree of ceria reduction from the XPS spectra. On one hand, some authors have used the relative area of the Ce $3d_{3/2}$ peak at ca. 917 eV (v'_2), characteristic of CeO_2 (it is absent in pure Ce_2O_3) to describe the total amount of cerium present as Ce (IV) [40-42]. However, it has been shown that this procedure may lead to incorrect quantitative results [43]. The second approach takes into consideration the relative intensity of the u_0, u'_0, u_1 and u'_1 peaks, as representative of Ce (III), in the total Ce 3d region [33, 43-45]. The percentages of Ce (III) determined by this last method are reported in Table 6.2. Sample CeO_2-NP has the highest percentage of Ce (III) on the surface (49.1%). On the other hand, for samples CeO_2 and CeO_2-FL, the relative amount of Ce (III) was the smallest. In summary, according to the XPS results it is possible to conclude that the Ce(IV)/Ce(III) redox couple exists on the surface of the ceria catalysts prepared.

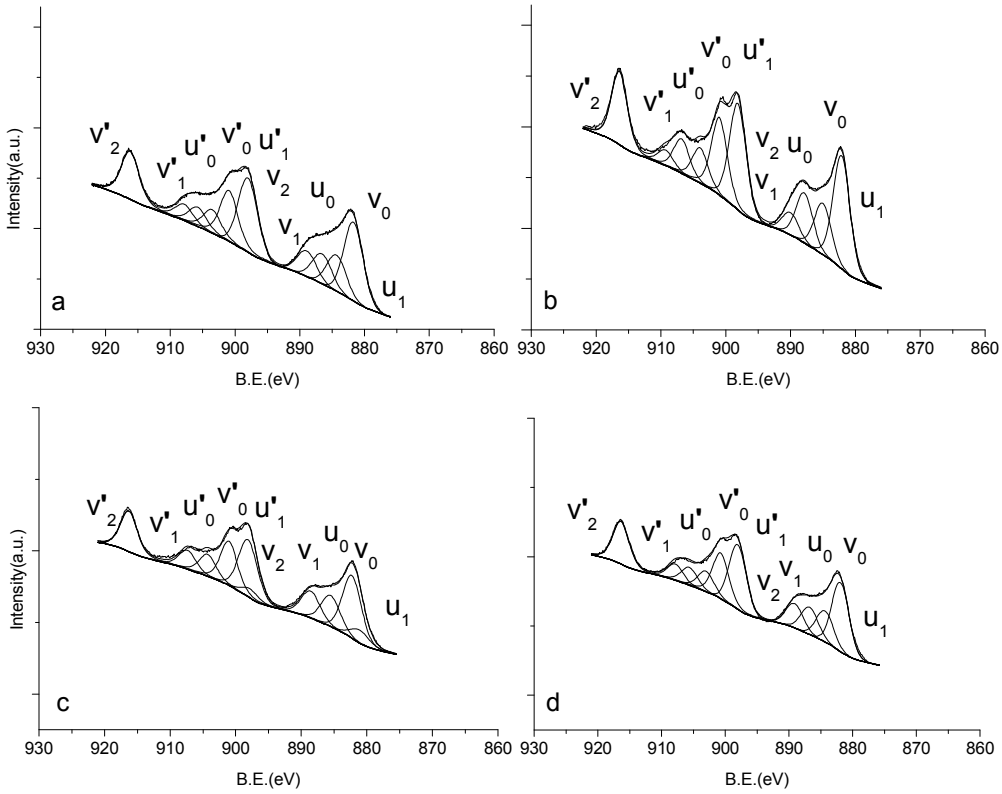

Figure 3.6: Experimental and fitted Ce 3d XPS spectra of samples (a) CeO_2, (b) CeO_2-NC, (c) CeO_2-NP, (d) CeO_2-FL.

3.3.2 Kinetic results

3.3.2.1 Oxalic acid

Oxalic acid was selected for this study because it is one of the most important final products of the oxidation processes, with a high refractory character relatively to single ozonation [11]. Figure 3.7 shows the results obtained with ozone alone and in the presence of nanostructured cerium oxides.

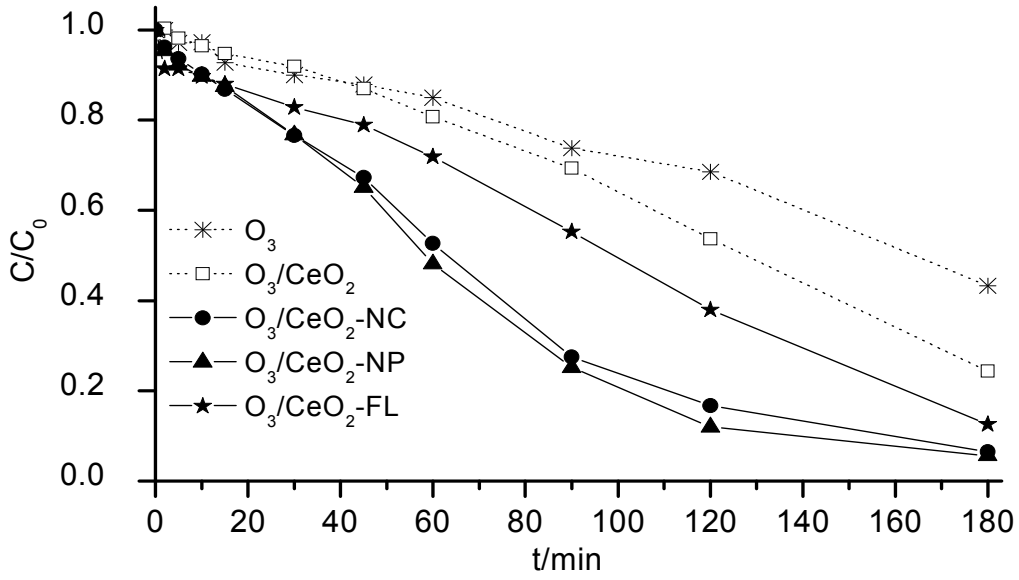

Figure 3.7: Evolution of the dimensionless concentration of oxalic acid during single ozonation and catalytic ozonation with cerium oxide samples.

The presence of the cerium oxides clearly enhanced the mineralisation of the oxalic acid. CeO_2-NC and CeO_2-NP have better performance than the other catalysts, allowing a nearly total mineralisation after 3 h of reaction. The results clearly reveal that the catalytic performance is not simply associated with the surface area since the CeO_2-FL sample, with the highest value, presents the worst performance. On the other hand, it is verified that the catalytic activity increases with the percentage of Ce(III) present on the surface of the prepared nanocatalysts, as measured by XPS and inferred by TPR profiles. In accordance with the literature, Ce(III) species are effective in the decomposition of ozone in $HO^{\bullet}$ radicals, which are the main oxidant species responsible for the oxidation of the compounds in the liquid phase [11].

The ozonation of organic compounds involves a number of complex reactions and many mechanistic approaches have been presented in the literature. It is widely accepted that ozone reacts in aqueous solution with various organic and inorganic compounds, either by direct reaction of molecular ozone or through a radical type reaction involving $HO^{\bullet}$ radicals resultant from the decomposition of ozone in water. In heterogeneous catalytic ozonation, it is generally assumed that both surface and liquid bulk reactions can occur, involving molecular ozone, $HO^{\bullet}$ radicals and surface oxygenated radical species [1]. In general, the proposed mechanisms of ozonation

catalysed by metal oxides assume that the adsorption of organic molecules and ozone takes place on the surface of the catalyst [46]. Ozone interaction with the metal oxide surface results in the formation of free radicals that can initiate a radical chain type reaction both on the surface of the catalyst and in the liquid phase, leading to the production of $HO^{\bullet}$ radicals [47, 48].

In order to verify that the ozonation of oxalic acid in the presence of ceria nanostructured catalysts involves $HO^{\bullet}$ radicals in solution, some experiments were carried out in the presence of *tert*-butanol, a well known $HO^{\bullet}$ radical scavenger. The results obtained are presented in Figure 3.8. These experiments show that the ozonation catalysed by cerium oxides is strongly inhibited in the presence of *tert*-butanol. This experimental observation indicates that, in these conditions, the oxidation mechanism of oxalic acid occurs predominantly by via $HO^{\bullet}$ radicals in the liquid bulk.

The presence of the Ce(IV)/Ce(III) redox couple on the surface of cerium oxides was suggested by Raman spectra and evidenced by XPS analysis. Thus, it is believed that the presence of the Ce(IV)/Ce(III) redox pair on the surface of cerium oxides enhances the decomposition of ozone into highly reactive species in solution, such as $HO^{\bullet}$, which participate in the oxidation reaction mechanism.

Summarizing, it is assumed that in the ozonation catalysed by cerium oxide the oxidation of pollutants occurs mainly in the liquid phase where the main oxidant species are predominantly $HO^{\bullet}$ radicals formed by the interaction between ozone and Ce(III) species.

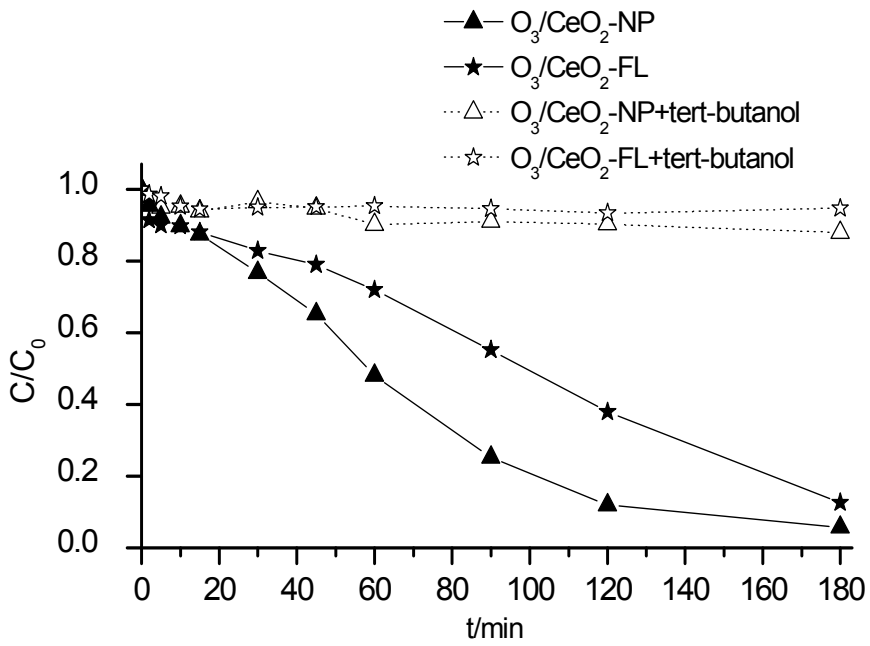

Figure 3.8: Evolution of dimensionless concentration of oxalic acid during catalytic ozonation and effect of *tert*-butanol ($C_{0,\ oxalic\ acid}$ = 1 mM, $m_{catalyst}$ = 350 mg, $C_{tert\text{-}butanol}$ = 10 mM).

3.3.2.2 Other organic compounds

3.3.2.2.1 Aniline

Aromatic amines, such as aniline, are common pollutants present in several industrial effluents, as is the case of textile processing industry wastewater. In this case, such compounds may arise from the biodegradation of dyes, especially from those containing azo chromophores (- *N* = *N* -). Generally, these pollutants are not susceptible to anaerobic or aerobic biodegradation, and their elimination cannot be accomplished by conventional biological treatments [12]. Figure 3.9 presents the kinetic results for aniline degradation and TOC removal during single ozonation and ozonation in the presence of the nanostructured cerium oxides.

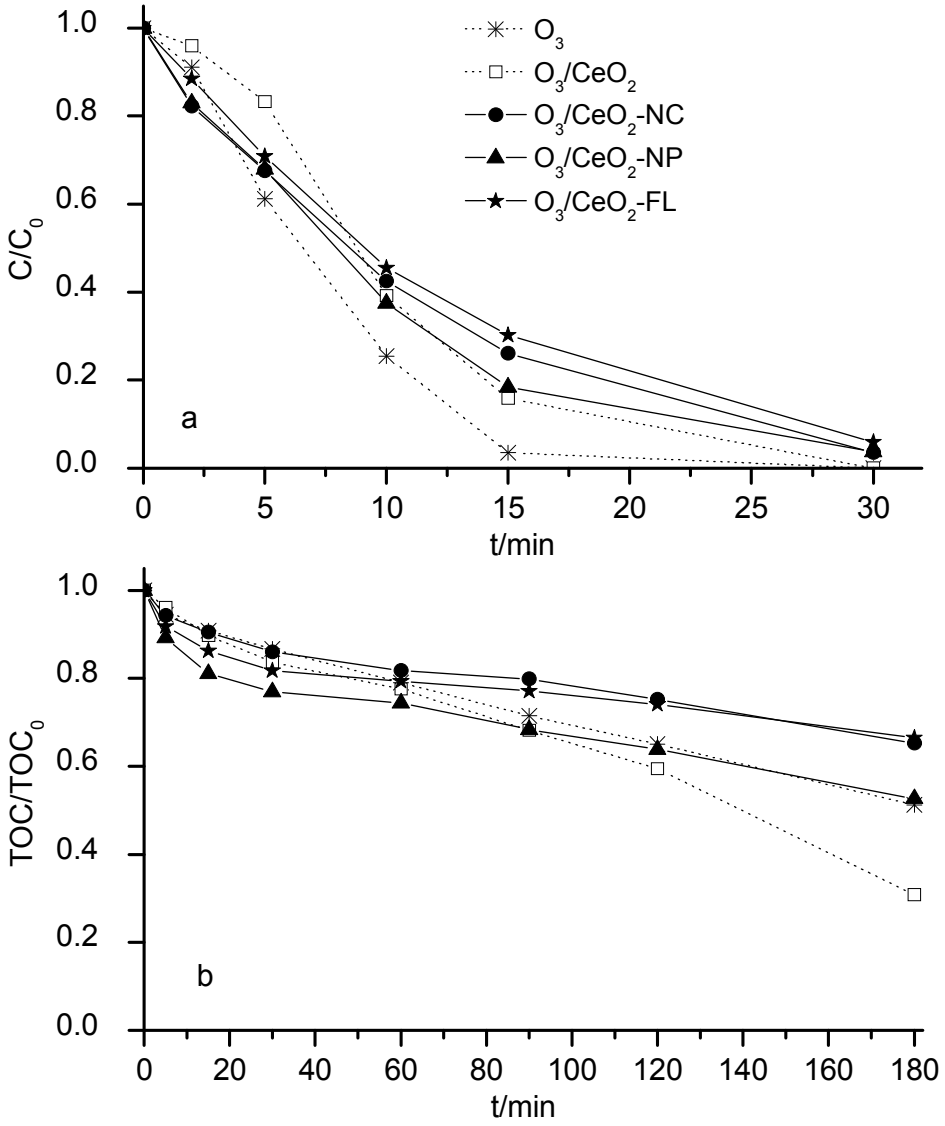

Figure 3.9: Aniline (a) and TOC (b) removal during single ozonation and ozonation catalysed by cerium oxides.

The complete conversion of aniline can be accomplished by single ozonation in a short reaction period, approximately 15 min. Ozone is an extremely powerful oxidant capable of reacting with a vast range of compounds, and it attacks selectively aromatic moieties and unsaturated bonds. Aromatic compounds possessing electron donor groups, such as $-NH_2$, have a high electronic density in *ortho*- and *para*- positions and react actively with ozone by electrophilic attack. This

results in the formation of several intermediates that are further transformed into saturated compounds, such as small chain carboxylic acids, which are not mineralised by direct ozone attack. Therefore, the degree of mineralisation attained in the single ozonation of aniline is not satisfactory. Under the experimental conditions used in this work, the TOC removal achieved after 3 h by single ozonation for the solution of aniline was ca. 50%.

It is observed that ozonation catalysed by cerium oxides leads to a slower removal of aniline compared to single ozonation (Figure 3.9a). When a catalyst is added, the formation of $HO^{\bullet}$ radicals is promoted, which are less selective species than ozone. Thus, the $HO^{\bullet}$ radicals attack aniline and by-products, while ozone is selective to aniline. However, after 30 min of reaction all materials also promote the total conversion of aniline.

In the case of TOC removal, it is verified that the cerium oxide prepared by the precipitation method allow a better degree of mineralisation than single ozonation or the catalytic ozonation in the presence of cerium oxides prepared by hydrothermal synthesis.

In these experiments, oxalic and oxamic acid concentrations were followed, since these are final oxidation products of aniline ozonation. Figure 3.10 shows the evolution of their concentration during aniline degradation.

It is observed that the concentration of both acids increases over time in all cases and the concentration of oxalic acid is greater than oxamic acid. Cerium oxides prepared by hydrothermal synthesis originate more oxalic acid than ceria prepared by the precipitation method, which is in accordance with the degree of mineralisation obtained, since the ozonation in the presence of these samples resulted in a lower TOC removal. From the values of TOC determined and the concentrations of oxalic and oxamic acids, it is possible to conclude that other non-detected by-products remain in solution. The percentage of TOC corresponding to other by-products is presented in Table 3.3.

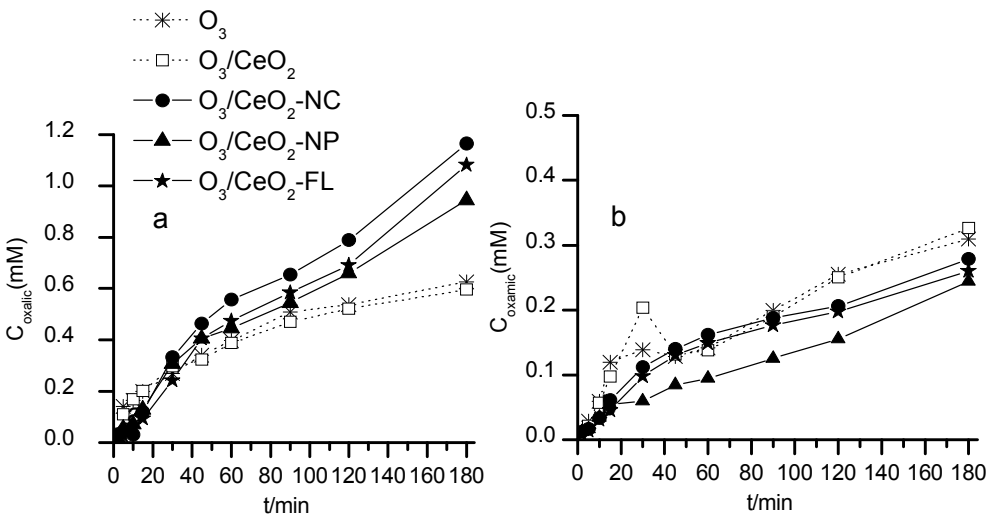

Figure 3.10: Evolution of oxalic (a) and oxamic (b) acid concentrations during aniline ozonation.

Table 3.3: % TOC of non-detected by-products.

	% TOC $_{\text{non-detected by-products}}$				
t (min)	O_3	O_3/CeO_2	O_3/ CeO_2-NC	O_3/ CeO_2-NP	O_3/ CeO_2-FL
5	54	49	38	44	62
15	87	84	69	76	80
30	86	82	80	81	89
60	80	79	71	74	85
90	71	69	67	65	81
120	64	59	58	57	78
180	46	6	31	25	62

Summarizing, it is possible to verify that the cerium oxide prepared by the precipitation method presents a different performance compared to the nanosized cerium oxides synthesized hydrothermally, which suggests that they promote the ozonation of aniline by different mechanisms. After 90 min of reaction, an increase in the TOC removal rate is observed for the catalytic ozonation in the presence of the cerium oxide sample prepared by the precipitation method, allowing a mineralisation degree of 70% after 180 min (see Figure 3.9b). In addition, this

sample originate less oxalic acid than the nanostructured cerium oxides, which may be justified by the fact that oxalic acid is already being consumed, while in the ozonation catalysed by cerium oxides synthesized hydrothermally the primary by-products are still being degraded. This suggestion is consistent with the amount of TOC of other intermediates (Table 3.3), since they represent approximately 10% of TOC after 180 min of reaction for the catalyst prepared by the precipitation method, while the other nanosized samples lead to a much higher percentage of non-detected by-products.

3.3.2.2.2 Dye C. I. Reactive Blue 5

Intense colour is one of the main characteristics of textile wastewater originated from spent dye baths and dye rinsing operations. Besides the undesirable aaesthetic impact caused by such effluents in receiving natural water courses, the persisting colour and the non-biodegradable nature of most of the textile dyes represent serious problems to the environment [49]. Owing to its extremely high redox potential (E_0 = 2.07 V), ozone is one of the most effective oxidant agents used for colour removal. It reacts selectively with aromatic and unsaturated moieties [50], such as the chromophore structures of dye molecules, leading to a fast decolourisation of the solutions. However, the oxidation of dyes and chemical auxiliaries present in textile effluents lead to the formation of intermediates that are frequently resistant to ozone attack. Such compounds of low reactivity towards ozone may be efficiently removed by oxidation via $HO^{\bullet}$ radicals [50]. Presently, advanced oxidation processes and catalytic oxidation are the main emerging routes for the removal of such compounds [10]. Ozonation of textile wastewater, spent and simulated dye baths has been focus of investigation [51-55].

Figure 3.11 presents the kinetic results of single ozonation and ozonation in the presence of the cerium oxides for the decolourisation and mineralisation of the reactive dye C. I. reactive blue 5. Figure 3.11a) shows that total decolourisation is observed after 30 minutes when ozone is applied, and this time is practically independent of the presence of the catalyst. Single ozonation also originates a decrease in the amount of TOC in solution. Nevertheless, this mineralisation rate is much lower than the colour removal rate (Figure 3.11b)), which is an indication that part of the dyes degradation products (colourless) remains in solution. The advantage of using the prepared materials as catalysts is clearly seen in TOC removals, which are higher than that obtained by single ozonation. After 90 min of

reaction, CeO_2-FL, the sample with the highest BET surface area, allowed a total TOC removal. In the case of the other catalysts, a complete mineralisation is obtained after about 120 min of reaction.

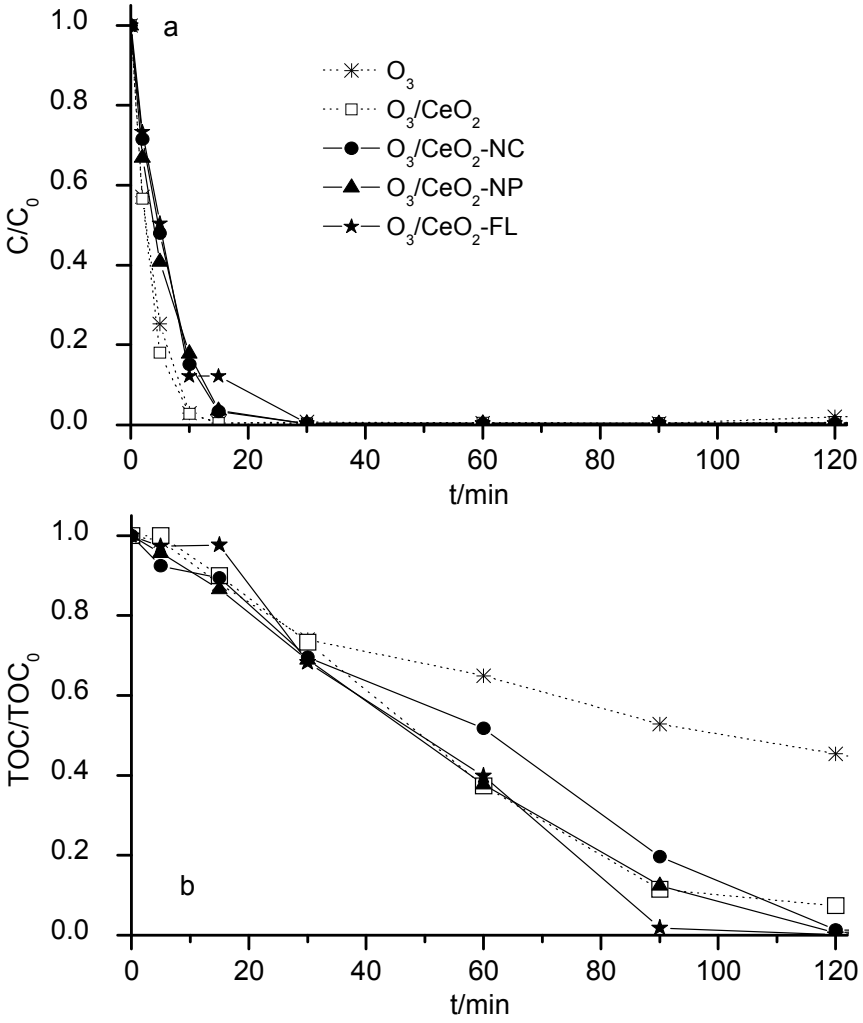

Figure 3.11: Colour (a) and TOC (b) removal for the reactive dye solution during catalytic and non-catalytic ozonation.

3.4 Conclusions

The present work reports the preparation of different nanostructured cerium oxide catalysts by the precipitation method and hydrothermal synthesis, with distinct

morphologies and particle sizes, which were used in the ozonation of organic compounds.

Cerium oxides were tested in the ozonation of oxalic acid, aniline and the textile dye C. I. reactive blue 5. The presence of surface Ce(IV)/Ce(III) redox couple was evidenced for all samples irrespective of their morphology and nanostructure, even though higher concentrations were clearly determined for the catalysts composed of nanoparticles and nanocubes. These samples presented the best performances for the ozonation of oxalic acid.

Aniline was easily removed after 30 min of reaction by single ozonation or catalytic ozonation. In the case of TOC removal, it is verified that the precipitated cerium oxide sample allowed the highest mineralisation degree. The presence of oxalic and oxamic acids as final oxidation products of aniline was evidenced by HPLC analyses.

The association of ozone and the nanomaterials prepared allowed a total TOC removal after 2 h in the ozonation of the dye solution tested.

Acknowledgements

This work was carried out with the financial support of Fundação para a Ciência e a Tecnologia – FCT (Portugal) and CNPq (Brazil). C.A.O. acknowledges the grant received from FCT (BD/45809/2008). The authors are indebted to FAPERJ (PADCT-Rio 2002) for the financial support for the acquisition of the Raman Horiba (Jobin Yvon) Spectrometer. They also acknowledge Ms. Nataly Amorim, Mr. Francisco Rangel and CETENE (Brazil) for the FE-SEM and TEM/HRTEM analyses.

References

[1] B. Kasprzyk-Hordern, M. Ziólek, J. Nawrocki, Catalytic ozonation and methods of enhancing molecular ozone reactions in water treatment, Appl. Catal. B: Environ. 46 (2003) 639-669.

[2] R. Andreozzi, A. Insola, V. Caprio, R. Marotta, V. Tufano, The use of manganese dioxide as a heterogeneous catalyst for oxalic acid ozonation in aqueous solution, Appl. Catal. A: Gen. 138 (1996) 75-81.

[3] F. J. Beltrán, Ozone reaction kinetics for water and wastewater systems. Lewis Publishers, Boca Raton, Florida (2004).

[4] D. S. Pines, D. A. Reckhow, Solid Phase Catalytic Ozonation Process for the Destruction of a Model Pollutant, Ozone-Sci. Eng. 25 (2003) 25-39.

[5] Y. Guan, E. Hensen, Y. Liu, H. Zhang, Z. Feng, C. Li, Template-Free Synthesis of Sphere, Rod and Prism Morphologies of CeO_2 Oxidation Catalysts, Catal. Lett. 137 (2010) 28-34.

[6] J. Kaspar, P. Fornasiero, M. Graziani, Use of CeO_2-based oxides in the three-way catalysis, Catal. Today 50 (1999) 285-298.

[7] A. M. Silva, A. M. Duarte de Farias, L. O. O. Costa, A. P. M. G. Barandas, L. V. Mattos, M. A. Fraga, F. B. Noronha, Partial oxidation and water–gas shift reaction in an integrated system for hydrogen production from ethanol, Appl. Catal. A: Gen. 334 (2008) 179-186.

[8] A. M. Duarte de Farias, D. Nguyen-Thanh, M. A. Fraga, Discussing the use of modified ceria as support for Pt catalysts on water-gas shift reaction, Appl. Catal. B: Environ. 93 (2010) 250-258.

[9] O. Pozdnyakova-Tellinger, D. Teschner, J. Kröhnert, F. C. Jentoft, A. Knop-Gericke, R. Schlögl, A. Wootsch, Surface Water-Assisted Preferential CO Oxidation on Pt/CeO_2 Catalyst, J. Phys. Chem. C 111 (2007) 5426-5431.

[10] P. C. C. Faria, J. J. M. Órfão, M. F. R. Pereira, Activated carbon and ceria catalysts applied to the catalytic ozonation of dyes and textile effluents, Appl. Catal. B: Environ. 88 (2009) 341-350.

[11] P. C. C. Faria, J. J. M. Órfão, M. F. R. Pereira, A novel ceria-activated carbon composite for the catalytic ozonation of carboxylic acids, Catal. Commun. 9 (2008) 2121-2126.

[12] P. C. C. Faria, D. C. M. Monteiro, J. J. M. Órfão, M. F. R. Pereira, Cerium, manganese and cobalt oxides as catalysts for the ozonation of selected organic compounds, Chemosphere 74 (2009) 818-824.

[13] C. T. Campbell, C. H. F. Peden, CHEMISTRY: Oxygen Vacancies and Catalysis on Ceria Surfaces, Science 309 (2005) 713-714.

[14] E. Aneggi, J. Llorca, M. Boaro, A. Trovarelli, Surface-structure sensitivity of CO oxidation over polycrystalline ceria powders, J. Catal. 234 (2005) 88-95.

[15] M. Nolan, J. E. Fearon, G. W. Watson, Oxygen vacancy formation and migration in ceria, Solid State Ionics 177 (2006) 3069-3074.

[16] H.-X. Mai, L.-D. Sun, Y.-W. Zhang, R. Si, W. Feng, H.-P. Zhang, H.-C. Liu, C.-H. Yan, Shape-Selective Synthesis and Oxygen Storage Behavior of Ceria Nanopolyhedra, Nanorods, and Nanocubes, J. Phys. Chem. B 109 (2005) 24380-24385.

[17] Tana, M. L. Zhang, J. Li, H. J. Li, Y. Li, W. J. Shen, Morphology-dependent redox and catalytic properties of CeO_2 nanostructures: Nanowires, nanorods and nanoparticles, Catal. Today 148 (2009) 179-183.

[18] B. M. Reddy, G. Thrimurthulu, L. Katta, Y. Yamada, S.-E. Park, Structural Characteristics and Catalytic Activity of Nanocrystalline Ceria−Praseodymia Solid Solutions, J. Phys. Chem. C 113 (2009) 15882-15890.

[19] W. Shan, X. Dong, N. Ma, S. Yao, Z. Feng, The Synthesis of Three-Dimensional CeO_2 and Their Catalytic Activities for CO Oxidation, Catal. Letters 131 (2009) 350-355.

[20] K. Niesz, D. E. Morse, Sonication-accelerated catalytic synthesis of oxide nanoparticles, Nano Today 5 (2010) 99-105.

[21] R. K. Hailstone, A. G. DiFrancesco, J. G. Leong, T. D. Allston, K. J. Reed, A Study of Lattice Expansion in CeO_2 Nanoparticles by Transmission Electron Microscopy, J. Phys. Chem. C 113 (2009) 15155-15159.

[22] X. h. Lu, X. Huang, S.-l. Xie, D.-z. Zheng, Z.-q. Liu, C.-l. Liang, Y.-X. Tong, Facile Electrochemical Synthesis of Single Crystalline CeO_2 Octahedrons and Their Optical Properties, Langmuir 26 (2010) 7569-7573.

[23] K. Zhou, Z. Yang, S. Yang, Highly Reducible CeO_2 Nanotubes, Chem. Mater. 19 (2007) 1215-1217.

[24] C. Sun, J. Sun, G. Xiao, H. Zhang, X. Qiu, H. Li, L. Chen, Mesoscale Organization of Nearly Monodisperse Flowerlike Ceria Microspheres, J. Phys. Chem. B 110 (2006) 13445-13452.

[25] S. Letichevsky, C. A. Tellez, R. R. Avillez, M. I. P. Silva, M. A. Fraga, L. G. Appel, Obtaining CeO_2-ZrO_2 mixed oxides by coprecipitation: role of preparation conditions, Appl. Catal. B: Environ. 58 (2005) 203-210.

[26] Z. Yang, K. Zhou, L. Liu, Q. Tian, D. Liu, S. Yang, Single-crystalline ceria nanocubes: size-controlled synthesis, characterization and redox property, Nanotechnology 18 (2007) 185606-185609.

[27] B. J. Reddy, R. L. Frost, W. N. Martens, Characterization of conichalcite by SEM, FTIR, Raman and electronic reflectance spectroscopy, Mineral. Mag. 69 (2005) 155-168.

[28] J. E. Spanier, R. D. Robinson, F. Zhang, S.-W. Chan, I. P. Herman, Size-dependent properties of CeO_{2-y} nanoparticles as studied by Raman scattering, Phys. Rev. B 64 (2001) 245407.

[29] V. Perrichon, A. Laachir, G. Begere, R. Fréty, L. Tournayan, O. Touret, Reduction of cerias with different textures by hydrogen and their reoxidation by oxygen, J. Chem. Soc., Faraday Trans. 90 (1994) 1.

[30] F. Larachi, J. Pierre, A. Adnot, A. Bernis, Ce 3d XPS study of composite $Ce_xMn_{1-x}O_{2-y}$ wet oxidation catalysts, Appl. Surf. Sci. 195 (2002) 236-250.

[31] E. Abi-aad, R. Bechara, J. Grimblot, A. Aboukais, Preparation and characterization of ceria under an oxidizing atmosphere. Thermal analysis, XPS, and EPR study, Chem. Mater. 5 (1993) 793-797.

[32] M. L. Trudeau, A. Tschöpe, J. Y. Ying, XPS investigation of surface oxidation and reduction in nanocrystalline CeO_2, Surf. Inter. Anal. 23 (1995) 219-226.

[33] A. Laachir, V. Perichon, A. Badri, J. Lamotte, E. Catherine, J.C. Lavalley, J. El-Fallah, L. Hilaire, F. Le Normand, E. Quéméré, G.N. Sauvion, O. Touret, Reduction of CeO_2 by hydrogen. Magnetic susceptibility and Fourier-transform infrared, ultraviolet and X-ray photoelectron spectroscopy measurements J. Chem. Soc., Faraday Trans. 97 (1991) 1601-1609.

[34] A. Fujimori, Mixed-valent ground state of CeO_2, Phys. Rev. B 28 (1983) 2281-2283.

[35] Y. A. Teterin, A. Y. Teterin, A. M. Lebedev, I. O. Utkin, The XPS spectra of cerium compounds containing oxygen, J. Elec. Spec. Rel. Phen. 88-91 (1998) 275-279.

[36] H. Y. Zhu, T. Hirata, Ce3d and Zr3d X-ray photoelectron spectroscopy spectra of ZrO_2-12 mol % CeO_2 after heat-treatments and Ar+ etching, J. Mater. Sci. Lett. 12 (1993) 749-751.

[37] E. Paparazzo, XPS studies of damage induced by X-ray irradiation on CeO_2 surfaces, Surf. Sci. Lett. 234 (1990) L253-L258.

[38] G. Praline, B. E. Koel, R. L. Hance, H. I. Lee, J. M. White, X-Ray photoelectron study of the reaction of oxygen with cerium, J. Elec. Spec. Rel. Phen. 21 (1980) 17-30.

[39] T. L. Barr, C. G. Fries, F. Cariati, J. J. Bart, N. Giordano, A spectroscopic investigation of cerium molybdenum oxides, J. Chem. Soc., Dalton Trans. 9 (1983) 1825-1829.

[40] J. Z. Shyu, K. Otto, W. L. H. Watkins, G. W. Graham, R. K. Belitz, H. S. Gandhi, Characterization of Pd/γ-alumina catalysts containing ceria, J. Catal. 114 (1988) 23-33.

[41] J. Z. Shyu, W. H. Weber, H. S. Gandhi, Surface characterization of alumina-supported ceria, J. Phys. Chem. 92 (1988) 4964-4970.

[42] F. B. Noronha, E. C. Fendley, R. R. Soares, W. E. Alvarez, D. E. Resasco, Correlation between catalytic activity and support reducibility in the CO_2 reforming of methane over $Pt/Ce_xZr_{1-x}O_2$ catalysts, Chem. Eng. J. 82 (2001) 21-31.

[43] M. S. P. Francisco, V. R. Mastelaro, P. A. P. Nascente, A. O. Florentino, Activity and Characterization by XPS, HR-TEM, Raman Spectroscopy, and BET Surface Area of CuO/CeO_2-TiO_2 Catalysts, J. Phys. Chem. B 105 (2001) 10515-10522.

[44] B. Ernst, L. Hilaire, A. Kiennemann, Effects of highly dispersed ceria addition on reducibility, activity and hydrocarbon chain growth of a Co/SiO_2 Fischer-Tropsch catalyst, Catal. Today 50 (1999) 413-427.

[45] J. Silvestre-Albero, F. Rodríguez-Reinoso, A. Sepúlveda-Escribano, Improved Metal-Support Interaction in $Pt/CeO_2/SiO_2$ Catalysts after Zinc Addition, J. Catal. 210 (2002) 127-136.

[46] F. P. Logemann, J. H. J. Année, Water treatment with a fixed bed catalytic ozonation process, Water Sci. Technol. 35 (1997) 353-360.

[47] B. Legube, N. K. V. Leitner, Catalytic ozonation: a promising advanced oxidation technology for water treatment, Catal. Today 53 (1999) 61-72.

[48] C. Cooper, R. Burch, An investigation of catalytic ozonation for the oxidation of halocarbons in drinking water preparation, Water Res. 33 (1999) 3695-3700.

[49] N. C. G. Tan (2001). Integrated and sequential anaerobic/aerobic biodegradationof azo dyes. Wageningen, The Netherlands, Wageningen University.

[50] J. Hoigné, H. Bader, Rate constants of reactions of ozone with organic and inorganic compounds in water--II: Dissociating organic compounds, Water. Res. 17 (1983) 185-194.

[51] O. S. G. P. Soares, J. J. M. Órfão, D. Portela, A. Vieira, M. F. R. Pereira, Ozonation of textile effluents and dye solutions under continuous operation: Influence of operating parameters, J. Hazard. Mat. 137 (2006) 1664-1673.

[52] Y.-C. Hsu, J.-T. Chen, H.-C. Yang, J.-H. Chen, Decolorization of dyes using ozone in gas-induced a reactor, AIChE J. 47 (2001) 169-176.

[53] A. Baban, A. Yediler, D. Lienert, N. Kemerdere, A. Kettrup, Ozonation of high strength segregated effluents from a woollen textile dyeing and finishing plant, Dyes Pigments 58 (2003) 93-98.

[54] M. F. Sevimli, H. Z. Sarikaya, Ozone treatment of textile effluents and dyes: effect of applied ozone dose, pH and dye concentration, J. Chem. Technol. Biotechnol. 77 (2002) 842-850.

[55] P. C. C. Faria, J. J. M. Órfão, M. F. R. Pereira, Adsorption of anionic and cationic dyes on activated carbons with different surface chemistries, Water Res. 38 (2004) 2043-2052.

Chapter 4

Ceria and cerium-based mixed oxides as ozonation catalysts[1]

Ceria (CeO_2) and cerium-based mixed oxides (Ce-Sm, Ce-La and Ce-Zr with different compositions) were prepared by the precipitation method from aqueous solutions of nitrate precursors. The materials synthesized were tested as catalysts in the ozonation of oxalic acid, aniline and the textile dye C. I. Reactive Blue 5.

Different performances were obtained depending on the type of organic compound and catalyst involved. In the case of oxalic acid, cerium – zirconium catalysts with more zirconium presented the best catalytic activities, allowing a total removal after 3 h of reaction. The good performance of these samples was justified by the increase of Ce(III) species on their surfaces. In the catalytic ozonation of aniline, the highest mineralisation degree was achieved with CeO_2 and $Ce_{0.75}Zr_{0.25}O_2$, the latter being the sample with the largest amount of oxygen vacancies on its structure. All the prepared catalysts significantly improved the mineralisation rate in the ozonation of the dye solution relatively to single ozonation (no catalyst). By itself, adsorption on the surface of catalysts is not relevant in the removal of organic compounds.

[1] C. A. Orge, J. J. M. Órfão, M. F. R. Pereira, A. M. Duarte de Farias, M. A. Fraga, Ceria and cerium-based mixed oxides as ozonation catalysts, Chem. Eng. J. 200–202 (2012) 499-505.

4 Ceria and cerium based mixed oxides as ozonation catalysts

4.1 Introduction

Ozonation processes are used in the decontamination of drinking water and wastewater, since they promote high COD (chemical oxygen demand) reduction, increase the biodegradability and, in general, the secondary products are not toxic for the environment. On the other hand, ozone alone presents limitations in the mineralisation of organic compounds and in the removal of refractory pollutants. The ozonation of several hazardous organic compounds such as pesticides, dyes and aromatic hydrocarbons originates significant amounts of saturated organic compounds such as aldehydes, ketones and carboxylic acids. Due to the low reactive nature towards ozone, these compounds tend to accumulate in solution. Hence, single ozonation is not sufficient to achieve a high mineralisation degree [1]. To overcome this drawback, ozonation processes are being modified in order to increase their oxidizing capability [2]. Some studies have shown that several metals in solution or in the solid phase under various forms (metal oxides, supported metals) may catalyse ozonation reactions, being able to destroy some very recalcitrant pollutants [3]. Heterogeneous catalytic ozonation, which is one of the most attractive alternatives, aims at enhance the removal of more refractory compounds by the transformation of ozone into more reactive species such as hydroxyl radicals and/or by adsorption and reaction of the pollutants on the surface of the catalyst [4]. The efficiency of the catalytic ozonation depends on the surface properties of the catalyst as well as on the solution pH and on the chemical nature of the reactants. Oxides of transition metals, such as manganese [5], titanium [6] or cobalt [7], are amongst the most frequently studied ozonation catalysts.

Ceria (CeO_2) is a cubic fluorite-type oxide, and is considered as the most important of rare-earth oxides, hence it has been extensively investigated and used in several industrial applications. However, the main applications of cerium oxide are as catalysts, catalyst promoters or catalyst supports. The importance of ceria in catalysis is related to its redox properties [8, 9]. Surface oxygen vacancies of ceria participate in the activation of oxygen and also stabilize metal nanoparticles dispersed on its surface [10]. In order to improve these properties, doping of ceria with trivalent or tetravalent cations has been undertaken [11, 12]. In the present work, the effect of using Zr^{4+}, La^{3+} and Sm^{3+} as dopants is assessed.

Oxalic acid is one of the most important final products of the oxidation processes, with a high refractory character relatively to single ozonation [2]. Therefore, it is a very good model compound to evaluate the activity of catalysts for ozonation.

Aromatic amines, such as aniline, are common pollutants present in several industrial effluents, as is the case of textile processing wastewater. Such compounds may arise from the biodegradation of dyes, especially from those containing azo chromophores (- *N* = *N* -). Generally, these pollutants are not susceptible to anaerobic or aerobic biodegradation, and their elimination cannot be accomplished by conventional biological treatments [13, 14].

Intense colour is one of the main characteristics of textile wastewater originated from spent dye baths and dye rinsing operations. Besides the undesirable aesthetic impact caused by such effluents in receiving natural water courses, the persisting colour and the non-biodegradable nature of most of the textile dyes represent serious problems to the environment [15]. The oxidation of dyes and chemical auxiliaries present in textile effluents lead to the formation of intermediates that are frequently resistant to ozone attack. Such compounds of low reactivity towards ozone may be efficiently removed by oxidation via HO• radicals [16]. Therefore, advanced oxidation processes and catalytic oxidation are the main emerging routes for the removal of those compounds [1].

In a previous study, cerium oxides prepared by the precipitation method and hydrothermal synthesis, with distinct morphologies and particle sizes were tested as catalysts in the ozonation of selected organic compounds [17]. In the case of oxalic acid, an increase in the catalytic activity with the increase of the percentage of Ce(III) on the catalyst surface was observed. Ce(III) species are effective in the decomposition of ozone in HO• radicals, which are the main oxidant species responsible for the oxidation of compounds in the liquid phase. In the catalytic ozonation of aniline, cerium oxide prepared by the precipitation method was the best catalyst, allowing a mineralisation degree of 70% after 180 min of reaction.

The main goal of this work is to study the ozonation of selected organic pollutants (oxalic acid, aniline and the dye C. I. Reactive Blue 5) in the presence of cerium oxide and cerium-based mixed oxides synthesized by the precipitation method.

4.2 Materials and methods

4.2.1 Materials

The preparation and characterization of ceria and the cerium-based mixed oxides used in this work were reported elsewhere [18]. Briefly, ceria was prepared by precipitation from a ammonium cerium (IV) nitrate solution using NH_4OH as precipitation agent [19]. The mixed metal oxides were prepared by co-precipitation also using NH_4OH. These catalysts were obtained by dissolution of metal nitrates in water; for the Ce-Zr samples $ZrO(NO_3)_2$ (35 wt.% in dilute nitric acid) was used as zirconium precursor. In all cases, the resultant precipitates were filtered, washed with deionized water and calcined at 500 °C in air for 4 h.

The concentrations of the solutions were previously calculated in order to obtain solids with 75 wt% of CeO_2 and 25 wt% of the doped metal oxide for the samples labelled as $Ce_{0.75}Sm_{0.25}O_2$, $Ce_{0.75}La_{0.25}O_2$, $Ce_{0.75}Zr_{0.25}O_2$. Other cerium and zirconium mixed oxides were also prepared containing 60 wt%, 50 wt% and 25 wt% of CeO_2 (samples named as $Ce_{0.60}Zr_{0.40}O_2$, $Ce_{0.50}Zr_{0.50}O_2$ and $Ce_{0.25}Zr_{0.75}O_2$).

Ceria and cerium-based materials were characterized by a wide range of techniques such as N_2 adsorption at -196 °C, X-ray diffraction, Raman spectroscopy and temperature programmed reduction. The conditions of these analyses were described in [18].

Ceria and cerium-based mixed oxides were additionally characterized by X-ray photoelectron spectroscopy (XPS) with a VG Scientific ESCALAB 200A spectrometer operating at 15 keV and 300 W. XPS data corresponding to Ce 3d spectra were fitted using the software XPSpeak. To minimize the number of degrees of freedom of the curve fitting procedure, constraints on the binding energy (BE), full width at half maximum (FWHM) and peak areas were applied to each doublet pair.

4.2.2 Experimental set-up and analytical methods

The removal of pollutants was investigated in a slurry lab-scale reactor equipped with agitation. In each experiment the reactor was filled with 700 mL of pollutant solution ($C_{0,oxalic\ acid}$ = $C_{0,aniline}$= 1 mM, $C_{0,\ dye}$= 50 mg L^{-1}; these are the concentrations used in a previous work [17], and were also used here to allow the comparison of results) at the natural pH ($pH_{0,\ oxalic\ acid}$ ≈ 3.0, $pH_{0,\ aniline}$ ≈ 6.5, $pH_{0,\ dye}$ ≈ 5.5). In the catalytic ozonation experiments, 100 mg of catalyst (d_p < 100 μm) was

introduced in the reactor. Ozone was produced from pure oxygen in a BMT 802X ozone generator. The experiments were performed at constant gas (oxygen + ozone) flow rate (150 cm^3 min^{-1}) and constant inlet ozone concentration (50 g m^{-3}). The concentration of ozone in the gas phase was monitored with a BMT 964 ozone analyzer. Ozone in the gas phase leaving the reactor was removed in a series of gas washing bottles filled with iodide potassium solution. The agitation was maintained constant in order to keep the reactor content perfectly mixed and the temperature was set to 25 °C. In adsorption experiments, the ozone-containing stream (mixture of ozone and oxygen) was replaced by an oxygen stream, in order to maintain the experimental conditions and to remove the effect of ozone. In the experiments carried out in the presence of *tert*-butanol, a concentration of 10 mM of this radical scavenger was used [20]. In the ozonation experiments of oxalic acid and aniline, liquid samples were taken regularly for quantification of dissolved ozone by the indigo method [21]. Successive oxalic acid ozonation experiments with samples $Ce_{0.75}Zr_{0.25}O_2$ and $Ce_{0.50}Zr_{0.50}O_2$ were carried out under the standard conditions. After each run, the solution was filtered and the catalyst dried in order to be used in the subsequent run. This procedure was repeated two times.

The concentrations of oxalic acid and aniline were followed by HPLC using a Hitachi Elite Lachrom HPLC equipped with a diode array detector. The stationary phase was an Aminex HPX-87H column (300 mm x 7.8 mm), working at room temperature under isocratic elution with H_2SO_4 4 mM [22-24]. The concentration of dye in the solutions was followed by UV-Vis spectrophotometry with a JASCO V-560 UV/Vis spectrophotometer. The degree of mineralisation was followed by TOC analysis in a Shimadzu TOC-5000A Analyzer.

4.3 Results and discussion

4.3.1 Catalysts characterization

The characterization of all catalysts used in this study is only briefly described in this section, since most of the results were presented and extensively discussed in a previous work [17]. BET surface areas are presented in Table 4.1. While adding Sm or La results in oxides that possess smaller surfaces areas than CeO2, the loading with Zr has the opposite effect and the surface area increases with the amount of zirconium.

Table 4.1: BET surface area [17] and relative amount of cerium as Ce(IV) on the surface of the catalysts.

Sample	S_{BET} ($m^2 g^{-1}$)	Ce (IV) %
CeO_2	98	12.4
$Ce_{0.75}Sm_{0.25}O_2$	64	11.8
$Ce_{0.75}La_{0.25}O_2$	66	11.1
$Ce_{0.75}Zr_{0.25}O_2$	112	11.9
$Ce_{0.60}Zr_{0.40}O_2$	134	9.7
$Ce_{0.50}Zr_{0.50}O_2$	157	9.4
$Ce_{0.25}Zr_{0.75}O_2$	219	7.5

Structural characteristics of the synthesized oxides were assessed by X-ray diffraction (XRD) and laser Raman spectroscopy (LRS) and revealed that all solids possess a face-centered cubic (fcc) fluorite structure. The formation of CeO_2-based solid solutions could also be confirmed for all samples doped with zirconium, lanthanum or samarium. It was made pretty evident by the shift of the diffraction angles as a consequence of the deformation and different organization of the CeO_2 lattice, which was seen to expand or retract according to the ionic radius of the doping element. Further experimental support was provided by the shift of the F_{2g} Raman active mode of the fluorite structure corresponding to the symmetric stretching of two O around Ce atoms. Additionally, the expected generation of structural defects, particularly oxygen vacancies, could be satisfactorily accomplished. Once again, their occurrence could be evidenced by distinct bands at high wavenumbers in Raman spectra. A quantitative evaluation of the concentration of bulk oxygen vacancies was indirectly performed by temperature-programmed reduction (TPR) analyses. Even though it is well known that oxygen vacancies are inherently present in the structure of bare CeO_2, TPR results allowed concluding that the amount of such vacancies is significantly higher for all solid solutions, particularly for those samples containing zirconium. Therefore it is feasible to assume the presence of Ce(III) at different concentrations, as such species are responsible for keeping the oxide electrically neutral, compensating the O vacancies.

The oxidation states of cerium species on the surface of the prepared samples were characterized by XPS analysis. According to the literature [25], the Ce 3d XPS spectra of Ce (IV) can be resolved into six features. If some Ce (III) species are

present, then two additional peaks and the corresponding satellites are necessary to describe spectra. Furthermore, Ce (IV) and Ce (III) always show peaks at ~882.5 and ~916.5 eV as well as at ~885.0 and ~903.7 eV, which are considered fingerprints characterizing Ce (IV) and Ce (III), respectively [26]. Although Ce 3d spectra of samples present the characteristic features of cerium (IV) oxide, the coexistence of both Ce (III) and Ce (IV) species must be considered in order to obtain a good fitting of the experimental data. Spectra were fitted with ten peaks [27, 28]. In the Ce $3d_{5/2}$ spin-orbit split doublet for Ce (IV), components v_0 and v_2 represent the intense peaks and v_1 a weak satellite (see Figure 4.1). Correspondingly, v'_0 and v'_2 components represent the Ce $3d_{3/2}$ doublet intense peaks, and v'_1 the associated weak satellite [27, 29-32]. For the oxidation state +3, the main components u_0 and u_1 characterize the Ce $3d_{5/2}$, and u'_0 and u'_1 the Ce $3d_{3/2}$ contribution [27, 33, 34]. The relative area of the Ce $3d_{3/2}$ peak at ca. 917 eV (v'_2), characteristic of Ce (IV) species (it is absent in pure Ce_2O_3) has been used for semiquantitative estimation of the relative amount of cerium present as Ce (IV) on the surface [2, 35]. As example, Figure 4.1 presents the experimental and fitted Ce 3d spectra of sample CeO_2. The percentages of Ce (IV) determined are reported in Table 4.1. The relative amount of Ce(IV) for sample CeO_2 was 12.4% and doping with other metal oxides decreases this value, especially when more than 25 wt% of Zr is introduced. According to the results, it is possible to conclude that the Ce(IV)/Ce(III) redox couple is present on the surface of ceria and cerium-based mixed oxides.

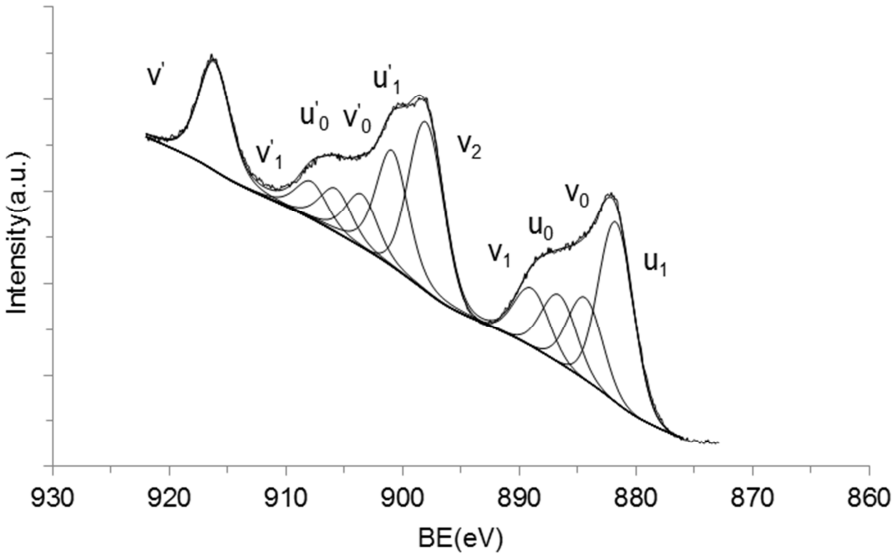

Figure 4.1: Experimental and fitted Ce 3d spectra of sample CeO_2.

4.3.2 Ozonation of selected organic compounds

4.3.2.1 Oxalic acid

The ozonation of oxalic acid was carried out at its natural solution pH, which was ca. 3. Figure 4.2 shows the results obtained by single ozonation and catalytic ozonation in the presence of cerium oxide and mixed oxides.

Comparing the mixed oxides containing 75 wt% of ceria, Figure 4.2 a), samples $Ce_{0.75}Zr_{0.25}O_2$ and $Ce_{0.75}Sm_{0.25}O_2$ have similar performances, removing about 70% of oxalic acid after 3 h of reaction, and no differences between these samples and ceria were observed. On the other hand, $Ce_{0.75}La_{0.25}O_2$ presents the worst catalytic efficiency. Therefore, the introduction of 25 wt% of zirconium, samarium or lanthanum oxides on ceria was not efficient, since the catalytic activity of cerium oxide is similar or superior. A different effect occurs when more than 40 wt% of zirconium oxide is introduced (Figure 4.2 b)). In fact, ozonation catalysed by $Ce_{0.25}Zr_{0.75}O_2$, $Ce_{0.50}Zr_{0.50}O_2$ and $Ce_{0.60}Zr_{0.40}O_2$ allowed a total oxalic acid removal after 3 h of reaction. The good performances obtained with these samples may be justified by the small percentage of Ce(IV) (high fraction of Ce(III)) present on the surface (cf. Table 4.1).

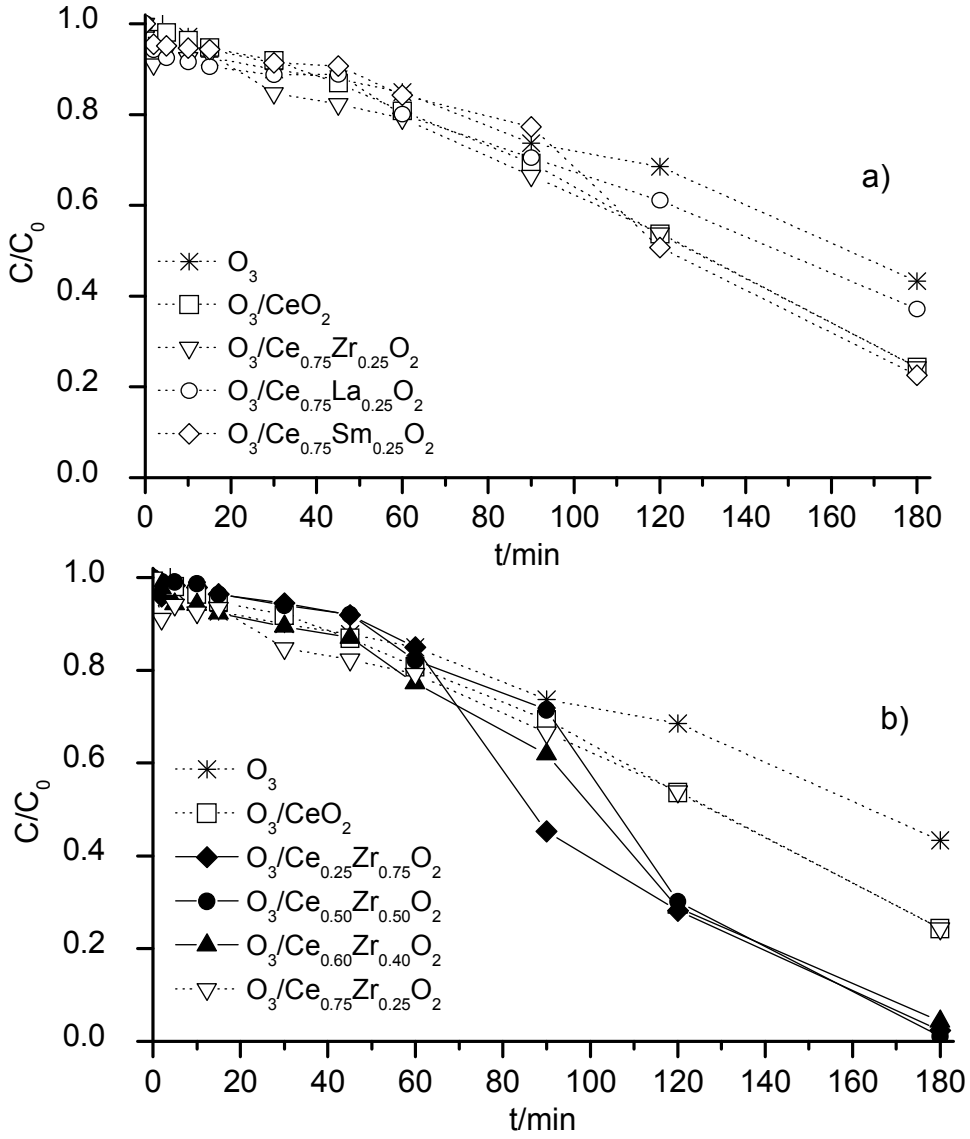

Figure 4.2: Evolution of the dimensionless concentration of oxalic acid during non-catalytic and catalytic ozonation with ceria and mixed oxides with 75 wt% of CeO_2 and 25 wt% of the doped metal oxide (a) and with ceria and cerium-zirconium oxides (b).

In accordance with the literature and our previous works, Ce(III) species are effective in the decomposition of ozone into $HO^{\bullet}$ radicals, which are the main oxidant species responsible for the oxidation of the compounds in the liquid phase [2, 17, 36]. In fact, Matheswaran et al. [37] found a significant synergic effect

between the cerium oxide redox pair Ce(IV)/Ce(III) and ozone towards phenol mineralisation. Faria et al. [2] and Orge et al. [19] showed that cerium oxide is an effective ozonation catalyst for the removal of carboxylic acids. It was suggested [3, 38] that cerium oxide promotes the decomposition of ozone into $HO^{\bullet}$ radicals. In a recent work, it was verified that the catalytic activity increased with the percentage of Ce(III) on the surface of nanostructured cerium oxides [17]. Total oxalic acid degradation was only achieved by the catalysts composed of nanoparticles and nanocubes, which were the samples with the highest concentration of Ce(III) species.

In order to verify if the ozonation of oxalic acid in the presence of cerium-based mixed oxides involves $HO^{\bullet}$ radicals in the liquid phase, some experiments in the presence of *tert*-butanol, a well-known $HO^{\bullet}$ radical scavenger, were carried out. An adsorption experiment of oxalic acid on $Ce_{0.75}Zr_{0.25}O_2$ was also included in the study. The results depicted in Figure 4.3 show that ozonation catalysed by $Ce_{0.75}Zr_{0.25}O_2$, $Ce_{0.75}La_{0.25}O_2$ and $Ce_{0.75}Sm_{0.25}O_2$ is strongly inhibited in the presence of *tert*-butanol. This experimental observation indicates that, under the current conditions, the oxidation mechanism of oxalic acid occurs predominantly via $HO^{\bullet}$ radicals in the liquid bulk. On the other hand, it is observed that oxalic acid is not removed by adsorption on $Ce_{0.75}Zr_{0.25}O_2$.

Analysing the aqueous ozone concentration (results not shown), an increase during the first 30 min from around 5 to 9 mg L^{-1} was observed, slightly decreasing thereafter.

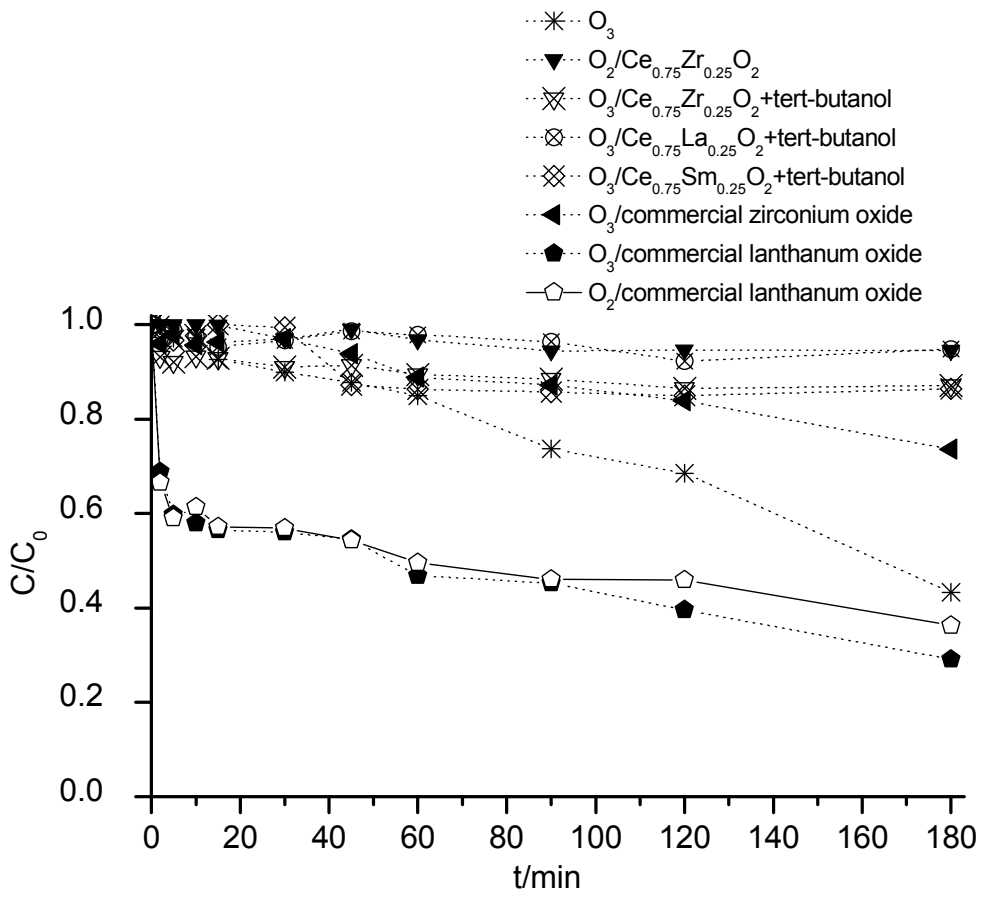

Figure 4.3: Evolution of the dimensionless concentration of oxalic acid during adsorption, catalytic ozonation and effect of *tert*-butanol ($C_{tert\text{-butanol}}$ = 10 mM).

Replicated experiments and successive runs of oxalic acid removal in the presence of $Ce_{0.75}Zr_{0.25}O_2$ and $Ce_{0.50}Zr_{0.50}O_2$ were carried out in order to evaluate the reproducibility of the results and the stability of the catalysts, since these are important factors, especially for practical industrial applications. The former type of experiments revealed relative differences lower than ± 2.5% around the average final conversion (data not shown). On the other hand, the results obtained in the cyclic experiments are presented in Figure 4.4 a) and b) for samples $Ce_{0.75}Zr_{0.25}O_2$ and $Ce_{0.50}Zr_{0.50}O_2$, respectively. It is possible to notice a complete loss of activity of the $Ce_{0.75}Zr_{0.25}O_2$ sample from the first to the second run, since the removal achieved is similar to single ozonation. On the other hand, the cyclic experiments in the presence of $Ce_{0.50}Zr_{0.50}O_2$ show that there is a decrease of the catalytic activity

from the first for the second run, but no significant differences were verified from the second to the third run, a 79% oxalic acid conversion being achieved after 3h of reaction.

The ozonation in the presence of cerium-based mixed oxides presented moderate or high catalytic activities, especially for most of the catalysts containing cerium and zirconium oxides. In order to better evaluate this performance, experiments using a commercial zirconium oxide (ZrO_2, powder, 99% purity, Aldrich; S_{BET} = 8 m^2 g^{-1}) and a commercial lanthanum oxide (La_2O_3, powder, 99.99% purity, Aldrich; S_{BET} = 11 m^2 g^{-1}) were carried out. The results obtained for these commercial samples are also presented in Figure 4.3. They show that ozonation of oxalic acid catalysed by the commercial zirconium oxide sample is not efficient, since only 26% removal was attained after 3 h of reaction. On the other hand, an unexpected 70% removal of oxalic acid after 3 h is achieved in the presence of lanthanum oxide. Then, in order to understand this result, the adsorption of oxalic acid on the commercial lanthanum oxide sample was evaluated (Figure 4.3), and no important differences were verified between ozonation and adsorption, showing that the relatively high removal efficiency results from the adsorption of oxalic acid. According to the literature lanthanum oxide has a high basicity and contains medium and strong basic sites, which contrasts with ZrO_2 that has only negligible amounts of weak basic sites [39]. Therefore, a high affinity due to electrostatic interactions of the anionic species in solution (oxalic acid has a pKa1 = 1.23 and a pKa2 = 4.19) to the positively charged surface of lanthanum oxide is expected, which justifies the high adsorption capacity observed. In conclusion, the presence of ceria in the mixed oxides is essential for the observation of catalytic activity.

Summarizing, it is assumed that the ozonation of oxalic acid catalysed by ceria and cerium-based mixed oxides mainly occurs in the liquid phase where the oxidant species are predominantly $HO^{\bullet}$ radicals, being the presence of Ce(III) species on the surface of samples the key parameter to obtain active catalysts. The most active catalysts tested were those containing 40 wt% or more of zirconium oxide (in these samples the relative amount of cerium as Ce(IV) on the surface was lower than 10%), the other catalysts present activities similar to ceria (in these samples the relative amount of cerium as Ce(IV) on the surface was higher than 11%). The worst catalyst was $Ce_{0.75}La_{0.25}O_2$, and its poor performance may be related to the high oxalic acid adsorption capacity of lanthanum oxide (see Figure 4.3) that may partially block the access of ozone to the catalyst active sites, decreasing the formation of $HO^{\bullet}$ radicals.

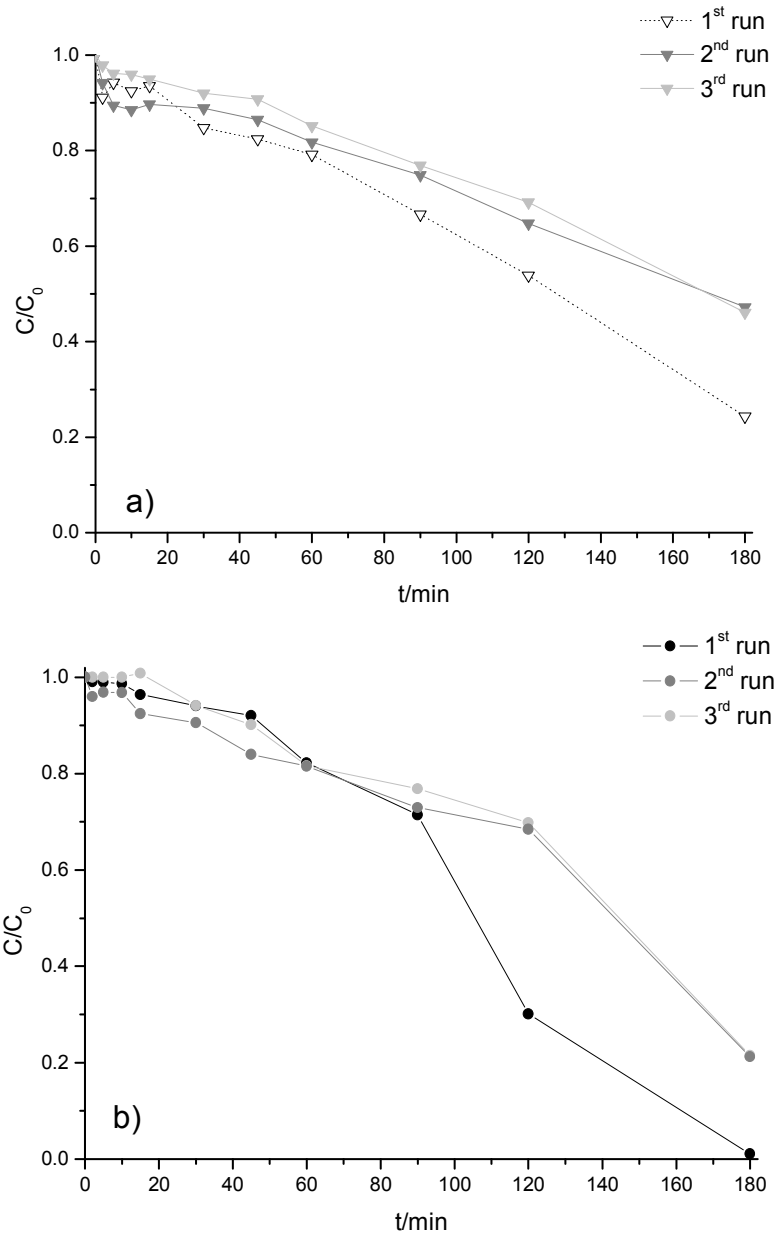

Figure 4.4: Evolution of the dimensionless concentration of oxalic acid during Successive catalytic ozonation experiments using a) $Ce_{0.75}Zr_{0.25}O_2$ and b) $Ce_{0.50}Zr_{0.50}O_2$.

4.3.2.2 Other organic compounds

The materials prepared were also tested in the ozonation of aniline and a textile dye (C. I. Reactive Blue 5).

Figure 4.5 shows the results of aniline degradation during single ozonation and ozonation in the presence of some of the mixed oxides considered in this study. The adsorption of aniline on sample $Ce_{0.75}Zr_{0.25}O_2$ was also included in Figure 4.5. Aniline is easily decomposed both by single ozonation and in the presence of the tested materials, being completed converted after 20-30 min of reaction. Moreover, it is observed that catalytic ozonation leads to a slightly slower aniline removal rate than single ozonation. Ozone is an extremely powerful oxidant capable of reacting with a vast range of compounds, and it attacks selectively aromatic moieties and unsaturated bonds. Aromatic compounds possessing electron donor groups, such as $-NH_2$, have a high electronic density in *ortho*- and *para*- positions and react actively with ozone by electrophilic attack. This results in the formation of several intermediates that are further transformed into saturated compounds, such as small chain carboxylic acids, which are not significantly mineralised by direct ozone attack. When a catalyst is added, the formation of $HO^{\bullet}$ radicals is promoted, but this strong oxidant is less selective than ozone. Thus, in the catalytic ozonation, the $HO^{\bullet}$ radicals formed attack both aniline and intermediates, while in single ozonation, ozone is selective to aniline, which originates a faster degradation. It is expected that the advantage of using a catalyst will be noticed in terms of TOC removal. However, the complete mineralisation of aniline solutions is difficult to achieve, since several refractory by-products are formed, such as oxalic and mainly oxamic acids [17].

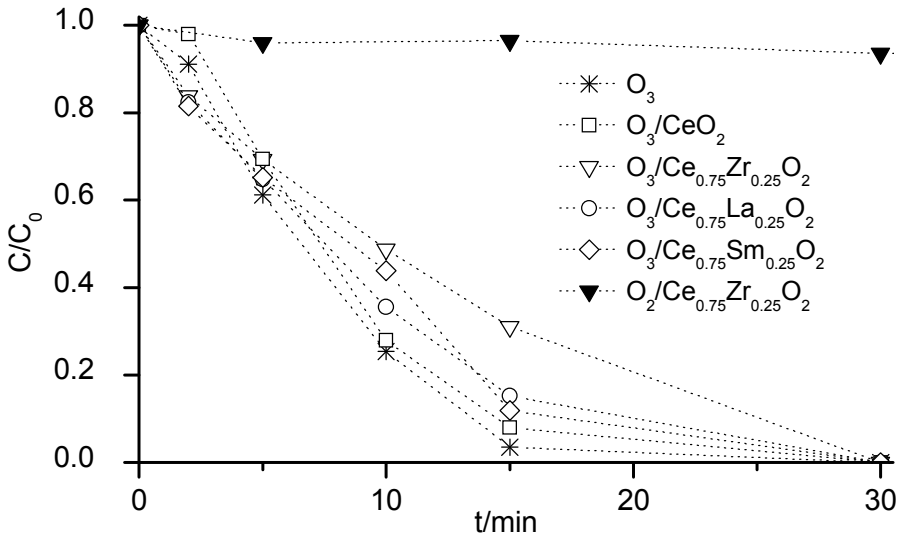

Figure 4.5: Evolution of the dimensionless concentration of aniline during adsorption, single ozonation and ozonation catalysed by ceria and some ceria-based mixed oxides.

The evolution of TOC during single ozonation and ozonation catalysed by cerium oxide and mixed oxides is presented in Figure 4.6. The addition of cerium oxide and all mixed oxides with 75 wt% of ceria slightly improves the mineralisation degree attained in comparison with single ozonation. Among these samples, CeO_2 and $Ce_{0.75}Zr_{0.25}O_2$ present the best performances, allowing about 70% mineralisation after 3 h of reaction. Within the cerium-zirconium oxides series, the catalyst with higher cerium loading leads to a higher mineralisation degree. This result may be explained by the higher concentration of vacancies in these structures, as assessed by laser Raman spectroscopy and temperature-programmed reduction analysis discussed in detail in [17]. Similarly to single ozonation, the other samples allow around 50% TOC removal after 3 h of reaction. It can be observed that aniline is only marginally adsorbed on $Ce_{0.75}Zr_{0.25}O_2$ (Figure 4.5) and, therefore, the TOC measured does not change during the corresponding experiment. It is possible to verify that the catalysts show different performances in aniline and oxalic acid removal. The most active samples in oxalic acid conversion have worse performance in aniline mineralisation. Oxalic acid is a small molecule that is mineralised directly, while the aniline degradation pathway is complex, several intermediates and by-products being formed. By comparing Figures 4.5 and 4.6, it may be concluded that the remaining TOC is mostly due to the formation of by-products of refractory nature, which is in agreement with the literature [13, 14]. The

main identified degradation by-products in the ozonation of aniline are oxalic and oxamic acids [14]. In previous studies, it was shown that oxamic acid is very difficult to mineralise and ceria was not an efficient catalyst for this process [2]. The present study confirms the difficulty of ceria in promoting the removal of oxamic acid and also indicates that the use of mixed oxides is not advantageous. The total mineralisation was also not achieved in the ozonation catalysed by nanostructured cerium oxides [17]. Moreover, the mixed oxides prepared in this work, especially those containing 75 wt% of ceria, present a higher mineralisation degree than the nanostructured cerium oxides.

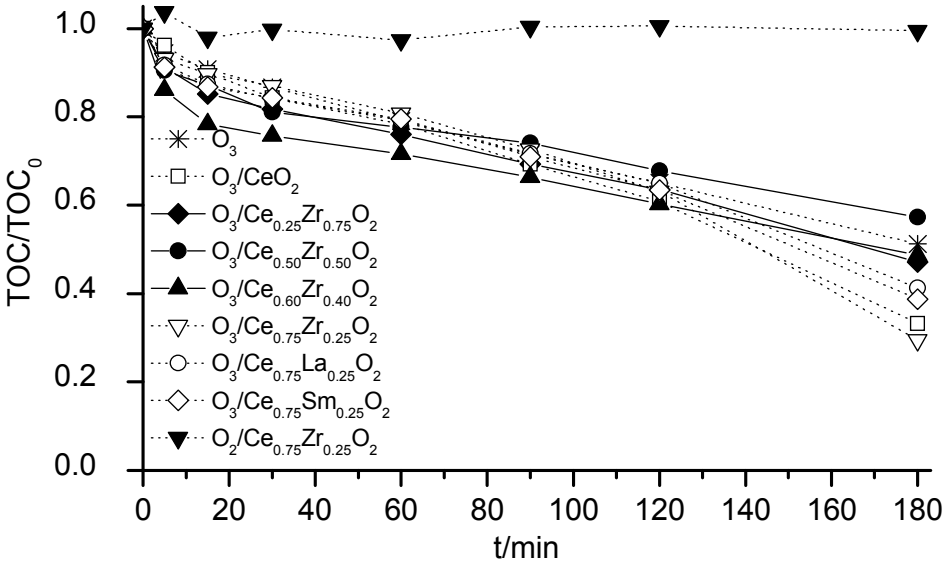

Figure 4.6: Evolution of the dimensionless TOC concentration in the aniline solution during adsorption, non-catalytic and catalytic ozonation in the presence of ceria and ceria-based mixed oxides.

Figure 4.7 depicts the evolution of the dimensionless dye concentration during single and catalysed ozonation of the reactive dye as well as an adsorption experiment performed on $Ce_{0.75}Zr_{0.25}O_2$. First of all, it should be mentioned that dye adsorption on $Ce_{0.75}Zr_{0.25}O_2$ is negligible (Figure 4.7). By applying ozone, total decolourisation is observed after about 15 min (Figure 4.7) independently of the presence or absence of catalysts. It is known that ozone is a strong oxidant that selectively attacks the chromophore groups of dye molecules, and then colour removal is easily attained by single ozonation. Nevertheless, mineralisation (Figure 4.8) is much more difficult to achieve than colour removal, which is a clear

indication that part of the dye degradation products (colourless) remains in solution. Single ozonation originated a decrease in the TOC concentration of only 55% after 2 h. The advantage of using the prepared materials as catalysts was clearly seen in the TOC removal curves, since mineralisation degrees close to 100% were obtained within the same reaction time with practically all catalysts tested. Moreover, it should be highlighted that no important difference could be observed in the present case with the catalysts studied herein. Similar performances were observed with cerium oxides prepared by different procedures [17], where TOC removals close to 100% were also obtained when nanostructured cerium oxides were used as catalysts.

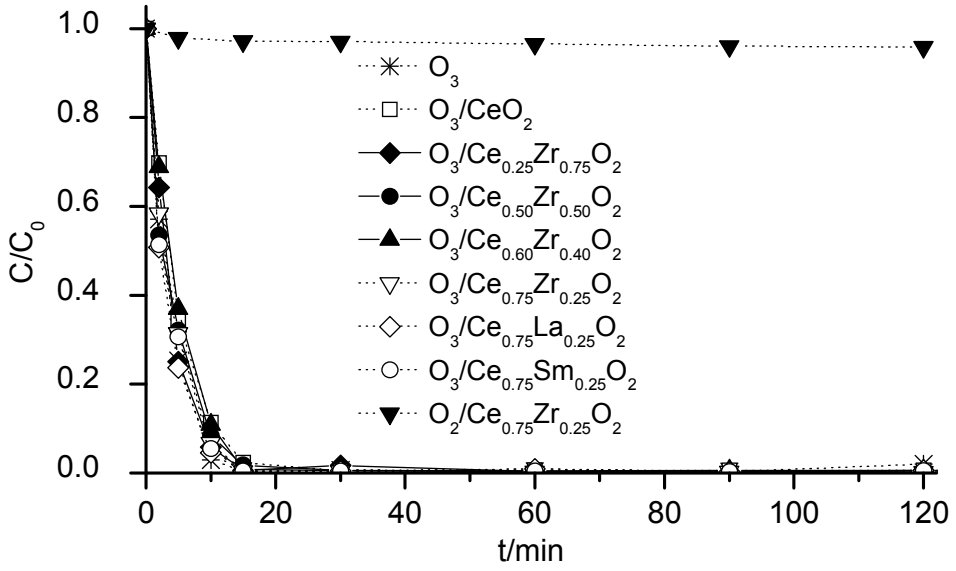

Figure 4.7: Evolution of the dimensionless dye concentration during non-catalytic, adsorption and catalytic ozonation in the presence of ceria and ceria-based mixed oxides.

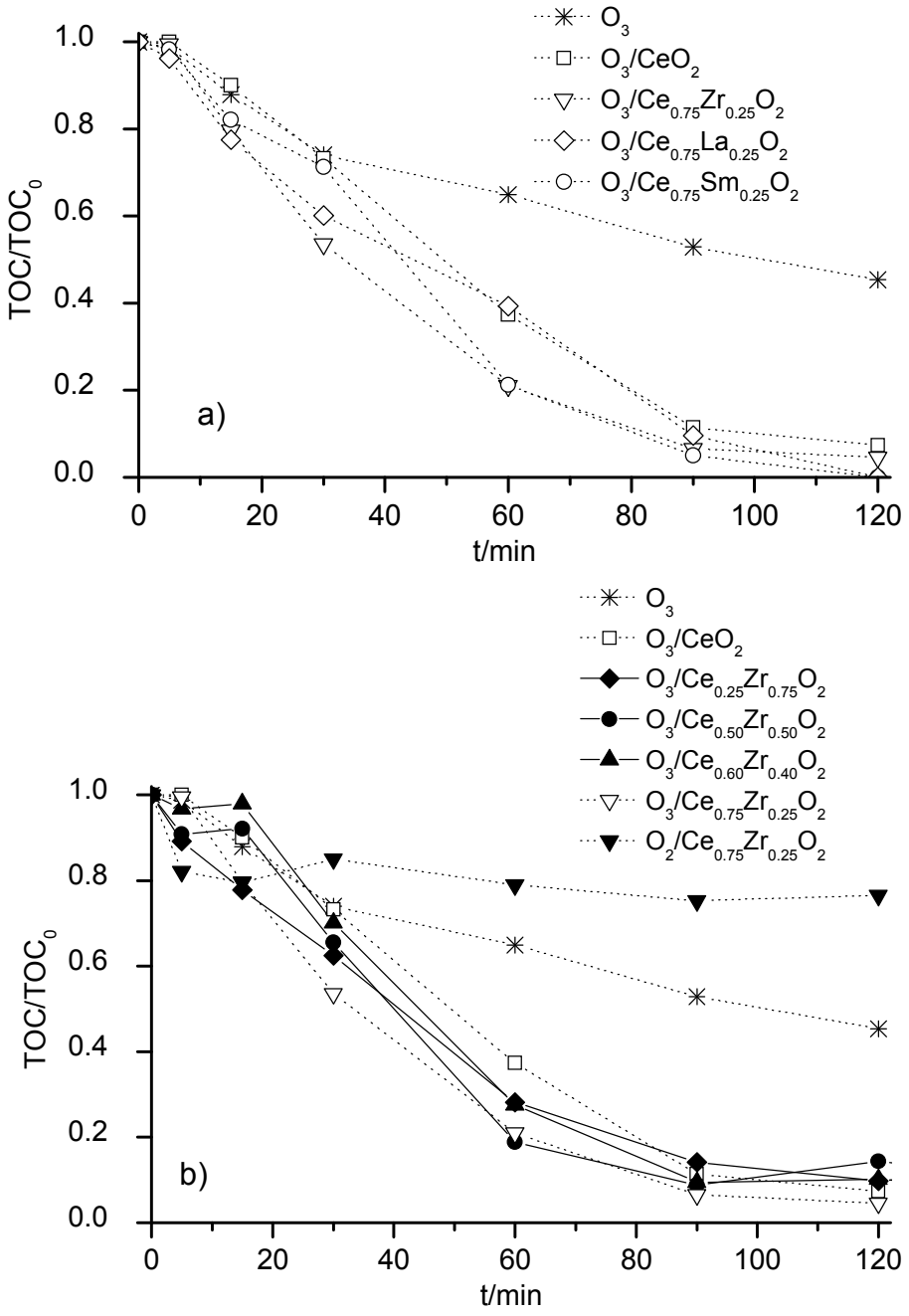

Figure 4.8: Evolution of the dimensionless TOC concentration during non-catalytic and catalytic ozonation in the presence of ceria and mixed oxides with 75 wt% of CeO_2 and 25 wt% of the doped metal oxide (a) and during non-catalytic, adsorption and catalytic ozonation in the presence of ceria and cerium-zirconium oxides (b).

4.4 Conclusions

Ceria and cerium-based mixed oxides were prepared by the precipitation method and tested in the ozonation of organic pollutants. In this study, different catalytic performances were obtained depending on the type of organic compound to be treated.

In the case of oxalic acid, catalysts based on CeO_2-ZrO_2 solid solutions exhibit an enhanced catalytic activity when the amount of zirconium oxide is higher than 25 wt%, which may be related to the larger percentage of the Ce(III) species on their surfaces. On the other hand, the combination of 25 wt% of zirconium, samarium or lanthanum oxides with cerium oxide was not particularly interesting, since the ozonation catalysed by these samples or by cerium oxide did not present significant differences. It is assumed that the ozonation of oxalic acid catalysed by the prepared materials mainly occurs in the liquid phase, where the oxidant species are predominantly $HO^{\bullet}$ radicals formed by the interaction between ozone and Ce(III) species on the catalyst surface.

The combination of ozone with cerium oxide or $Ce_{0.75}Zr_{0.25}O_2$ allowed the highest TOC removal after 180 min in the degradation of aniline (~ 70%).

The association of ozone and all mentioned catalysts leads to an improved TOC removal in the ozonation of the dye solution, allowing a complete or near complete mineralisation in all cases after about 2 h.

Adsorption experiments on catalysts showed that its contribution to pollutant removal during catalytic ozonation is negligible.

Acknowledgements

This work was partially supported by project PEst-C/EQB/LA0020/2011, financed by FEDER through COMPETE - Programa Operacional Factores de Competitividade and by FCT - Fundação para a Ciência e a Tecnologia (Portugal), and by CNPq (Brazil). C.A.O. thanks FCT for the research fellowship BD/45809/2008. The authors are indebted to Dr. Carlos M. Sá (CEMUP) for assistance with XPS analysis.

References

[1] P. C. C. Faria, J. J. M. Órfão, M. F. R. Pereira, Activated carbon catalytic ozonation of oxamic and oxalic acids, Appl. Catal. B: Environ. 79 (2008) 237-243.

[2] P. C. C. Faria, J. J. M. Órfão, M. F. R. Pereira, A novel ceria-activated carbon composite for the catalytic ozonation of carboxylic acids, Catal. Commun. 9 (2008) 2121-2126.

[3] B. Legube, N. K. V. Leitner, Catalytic ozonation: a promising advanced oxidation technology for water treatment, Catal. Today 53 (1999) 61-72.

[4] B. Kasprzyk-Hordern, M. Ziólek, J. Nawrocki, Catalytic ozonation and methods of enhancing molecular ozone reactions in water treatment, Appl. Catal. B: Environ. 46 (2003) 639-669.

[5] R. Andreozzi, A. Insola, V. Caprio, R. Marotta, V. Tufano, The use of manganese dioxide as a heterogeneous catalyst for oxalic acid ozonation in aqueous solution, Appl. Catal. A: Gen. 138 (1996) 75-81.

[6] F. J. Beltrán, Ozone reaction kinetics for water and wastewater systems. Lewis Publishers, Boca Raton, Florida, (2004).

[7] D. S. Pines, D. A. Reckhow, Solid Phase Catalytic Ozonation Process for the Destruction of a Model Pollutant, Ozone: Sci. Eng. 25 (2003) 25-39.

[8] F. Esch, S. Fabris, L. Zhou, T. Montini, C. Africh, P. Fornasiero, G. Comelli, R. Rosei, Electron Localization Determines Defect Formation on Ceria Substrates, Science 309 (2005) 752-755.

[9] Y. Guan, E. Hensen, Y. Liu, H. Zhang, Z. Feng, C. Li, Template-Free Synthesis of Sphere, Rod and Prism Morphologies of CeO_2 Oxidation Catalysts, Catal. Lett. 137 (2010) 28-34.

[10] C. T. Campbell, C. H. F. Peden, CHEMISTRY: Oxygen Vacancies and Catalysis on Ceria Surfaces, Science 309 (2005) 713-714.

[11] F. J. Perez-Alonso, I. Melián-Cabrera, M. López Granados, F. Kapteijn, J. L. G. Fierro, Synergy of $FexCe_{1-x}O_2$ mixed oxides for N_2O decomposition, J. Catal. 239 (2006) 340-346.

[12] A. Bueno-López, K. Krishna, M. Makkee, J. A. Moulijn, Enhanced soot oxidation by lattice oxygen via La^{3+}-doped CeO_2, J. Catal. 230 (2005) 237-248.

[13] P. C. C. Faria, D. C. M. Monteiro, J. J. M. Órfão, M. F. R. Pereira, Cerium, manganese and cobalt oxides as catalysts for the ozonation of selected organic compounds, Chemosphere 74 (2009) 818-824.

[14] P. C. C. Faria, J. J. M. Órfão, M. F. R. Pereira, Ozonation of aniline promoted by activated carbon, Chemosphere 67 (2007) 809-815.

[15] N. C. G. Tan, Integrated and sequential anaerobic/aerobic biodegradationof azo dyes. Wageningen University, Wageningen, The Netherlands (2001).

[16] J. Hoigné, H. Bader, Rate constants of reactions of ozone with organic and inorganic compounds in water--II: Dissociating organic compounds, Water Res. 17 (1983) 185-194.

[17] C. A. Orge, J. J. M. Órfão, M. F. R. Pereira, A. M. Duarte de Farias, R. C. R. Neto, M. A. Fraga, Ozonation of model organic compounds catalysed by nanostructured cerium oxides, Appl. Catal. B: Environ. 103 (2011) 190-199.

[18] A. M. D. Farias, D. Nguyen-Thanh, M. A. Fraga, Discussing the use of modified ceria as support for Pt catalysts on water–gas shift reaction, Appl. Catal. B: Environ. 93 (2010) 250-258.

[19] S. Letichevsky, C. A. Tellez, R. R. Avillez, M. I. P. Silva, M. A. Fraga, L. G. Appel, Obtaining CeO_2-ZrO_2 mixed oxides by coprecipitation: role of preparation conditions, Appl. Catal. B: Environ. 58 (2005) 203-210.

[20] F. J. Beltran, F. J. Rivas, L. A. Fernandez, P. M. Alvarez, R. Montero-de-Espinosa, Kinetics of Catalytic Ozonation of Oxalic Acid in Water with Activated Carbon, Ind. Eng. Chem. Res. 41 (2002) 6510-6517.

[21] H. Bader, J. Hoigne, Determination of ozone in water by the indigo method, Water Research 15 (1981) 449-456.

[22] B. R. Laboratories, Guide to Aminex® HPLC columns: for food and beverage, biotechnology, and bio-organic analysis (1994).

[23] M. Skoumal, P.-L. Cabot, F. Centellas, C. Arias, R. M. Rodríguez, J. A. Garrido, E. Brillas, Mineralization of paracetamol by ozonation catalyzed with Fe^{2+}, Cu^{2+} and UVA light, Appl. Catal. B: Environ 66 (2006) 228-240.

[24] E. Brillas, I. Sirés, C. Arias, P. L. Cabot, F. Centellas, R. M. Rodríguez, J. A. Garrido, Mineralization of paracetamol in aqueous medium by anodic oxidation with a boron-doped diamond electrode, Chemosphere 58 (2005) 399-406.

[25] F. Larachi, J. Pierre, A. Adnot, A. Bernis, Ce 3d XPS study of composite $Ce_xMn_{1-x}O_{2-y}$ wet oxidation catalysts, Appl. Surf. Sci. 195 (2002) 236-250.

[26] E. Abi-aad, R. Bechara, J. Grimblot, A. Aboukais, Preparation and characterization of ceria under an oxidizing atmosphere. Thermal analysis, XPS, and EPR study, Chem. Mater. 5 (1993) 793-797.

[27] M. L. Trudeau, A. Tschöpe, J. Y. Ying, XPS investigation of surface oxidation and reduction in nanocrystalline CeO_2, Surf. Inter. Anal. 23 (1995) 219-226.

[28] A. Laachir, V. Perichon, A. Badri, J. Lamotte, E. Catherine, J.C. Lavalley, J. El-Fallah, L. Hilaire, F. Le Normand, E. Quéméré, G.N. Sauvion, O. Touret, Reduction of CeO_2 by hydrogen. Magnetic susceptibility and Fourier-transform infrared, ultraviolet and X-ray photoelectron spectroscopy measurements J. Chem. Soc., Faraday Trans. 97 (1991) 1601-1609.

[29] A. Fujimori, Mixed-valent ground state of CeO_2, Phys. Rev. B 28 (1983) 2281.

[30] Y. A. Teterin, A. Y. Teterin, A. M. Lebedev, I. O. Utkin, The XPS spectra of cerium compounds containing oxygen, J. Elec. Spec. Rel. Phen. 88-91 (1998) 275-279.

[31] H. Y. Zhu, T. Hirata, Ce3d and Zr3d X-ray photoelectron spectroscopy spectra of ZrO_2-12 mol % CeO_2 after heat-treatments and Ar+ etching, J. Mater. Sci. Lett. 12 (1993) 749-751.

[32] E. Paparazzo, XPS studies of damage induced by X-ray irradiation on CeO_2 surfaces, Surf. Sci. Lett. 234 (1990) L253-L258.

[33] G. Praline, B. E. Koel, R. L. Hance, H. I. Lee, J. M. White, X-Ray photoelectron study of the reaction of oxygen with cerium, J. Elec. Spec. Rel. Phen. 21 (1980) 17-30.

[34] T. L. Barr, C. G. Fries, F. Cariati, J. J. Bart, N. Giordano, A spectroscopic investigation of cerium molybdenum oxides, J. Chem. Soc., Dalton Trans. 9 (1983) 1825-1829.

[35] J. Z. Shyu, K. Otto, W. L. H. Watkins, G. W. Graham, R. K. Belitz, H. S. Gandhi, Characterization of Pd/ɣ-alumina catalysts containing ceria, J. Catal. 114 (1988) 23-33.

[36] C. A. Orge, J. J. M. Órfão, M. F. R. Pereira, Catalytic ozonation of organic pollutants in the presence of cerium oxide-carbon composites, Appl. Catal. B: Environ. 102 (2011) 539-546.

[37] M. Matheswaran, S. Balaji, S. J. Chung, I. S. Moon, Studies on cerium oxidation in catalytic ozonation process: A novel approach for organic mineralization, Catal. Commun. 8 (2007) 1497-1501.

[38] C. Cooper, R. Burch, An investigation of catalytic ozonation for the oxidation of halocarbons in drinking water preparation, Water Res. 33 (1999) 3695-3700.

[39] S. Kus, M. Otremba, M. Taniewski, The catalytic performance in oxidative coupling of methane and the surface basicity of La_2O_3, Nd_2O_3, ZrO_2 and Nb_2O_5, Fuel 82 (2003) 1331-1338.

Chapter 5

Catalytic ozonation of organic pollutants in the presence of cerium oxide – carbon composites[1]

Cerium oxide-carbon composites were prepared and tested as ozonation catalysts for the removal of two selected carboxylic acids, oxalic and oxamic, and one textile dye (C. I. Reactive Blue 5). The results were compared with those obtained in non-catalytic ozonation and ozonation catalysed by cerium oxide and carbon materials (activated carbon, carbon xerogel). With the exception of cerium oxide, a total degradation of oxalic acid was obtained in approximately 90 min for all prepared catalysts and the catalytic activity increases with the amount of carbon present in the composites. Despite of oxamic acid be more refractory to ozonation than oxalic acid, 75% of oxamic acid removal was achieved after 10 h of reaction in the presence of the ceria-activated carbon composite with 90% of carbon material. In the mineralisation of the textile dye, the catalytic activity of the composites increases with the amount of activated carbon introduced.

[1] C. A. Orge, J. J. M. Órfão, M. F. R. Pereira, Catalytic ozonation of organic pollutants in the presence of cerium oxide-carbon composites, Appl. Catal. B: Environ. 102 (2011) 539-546.

5 Catalytic ozonation of organic pollutants in the presence of cerium oxide – carbon composites

5.1 Introduction

The ozone molecule has a high capacity to react with numerous compounds by means of redox reactions because ozone has a high standard redox potential. Some of these reactions take place by explicit electron transfer, while most of them occur by oxygen transfer from the ozone molecule to the other reactant. Addition reactions occur between a compound with available π electrons, such as unsaturated compounds, and a molecule with electrophilic character, such as ozone. Ozone molecule is selective and attacks, preferentially, aromatic structures and unsaturated bonds, such as those of the dye chromophores, leading to fast decolourisation. Ozonation alone has been shown to achieve a limited mineralisation level concerning either the removal of micropollutants in drinking water treatment or the removal of refractory chemical oxygen demand (COD) in industrial effluents. Consequently, various advanced oxidation processes (AOPs) resultant from the combination of ozone with H_2O_2, UV radiation or Fenton's reagent have been investigated as potential methods for the removal of organic compounds [1]. Such processes aim at the production of $HO^{\bullet}$ radicals, which are non-selective oxidant species and react with a vast number of compounds at very high rates, comparatively to those of direct ozone reactions [2, 3]. However, there are some disadvantages limiting their application. AOPs are characterized by a strong dependence on the pH of the solution. The presence of radical scavengers in the water or wastewater to be treated can result in a significant reduction of the efficiency of contaminants removal. Nevertheless, catalytic ozonation was found to be effective for the removal of several organic compounds from drinking water and wastewater, and intense research is being carried out on this subject.

Metal oxides represent one of the most important and widely employed classes of solid catalysts, either as active phases or supports [4]. Several reported studies have shown that metal oxides and supported metal oxides can be efficient for the catalytic ozonation of a vast range of organic contaminants. Supported and unsupported oxides of transition metals are frequently studied ozonation catalysts. Among them, cobalt [5] and manganese [6] oxides have proven to be efficient ozonation catalysts. Nevertheless, metal leaching and low stability are sometimes

associated to the use of such materials in ozonation reactions. Due to the importance of catalytic ozonation as a promising technology for the elimination of recalcitrant organic compounds from water and wastewater, the continuous search for more efficient catalysts is of great importance.

Heterogeneous catalytic ozonation aims to enhance the removal of highly refractory compounds by the transformation of ozone into more reactive species and/or by adsorption and reaction of the pollutants on the surface of the catalyst [4, 7, 8]. The efficiency of catalytic ozonation depends on the solution pH, the chemical nature of the reactants and the surface properties of the catalyst [4].

Faria et al. [9] verified that manganese, cobalt and cerium oxides catalyse the ozonation of sulfanilic acid and aniline, significantly increasing the mineralisation rate of the corresponding solutions, comparatively to single ozonation. The experimental results showed that intimate mixtures of metal oxides of cerium and manganese or cerium and cobalt, obtained by coprecipitation, are more efficient ozonation catalysts than the corresponding single metal oxides, which might be related both to their higher surface areas and enhanced redox properties. Composites of metal oxides and activated carbon have also been shown to be effective ozonation catalysts for the degradation of the mentioned aromatic compounds and an azo textile dye [7, 10]. The same group of authors showed excellent results in the catalytic ozonation of oxalic acid with a ceria-activated carbon composite, as a result of a strong synergic effect between activated carbon and cerium oxide [11].

This work reports the preparation of composites of cerium oxide with carbon materials with different compositions, aiming to evaluate their performances as ozonation catalysts for the mineralisation of organic pollutants in aqueous solution. For that purpose, oxalic acid, oxamic acid and the dye CI Reactive Blue 5 were selected.The carbon materials used were an activated carbon, a carbon xerogel and an oxidised activated carbon.

5.2 Experimental

5.2.1 Materials

Three organic molecules were selected for this study: oxalic acid (99%, Sigma-Aldrich), oxamic acid (96%, Sigma-Aldrich) and the textile dye CI Reactive blue 5

(commercial name Cibacron Blue BR with a purity of ~50%, according to the supplier).

A commercial activated carbon, Norit GAC 1240 Plus (supplied by Norit), was used as received (sample AC0). This sample was also submitted to a chemical treatment in order to obtain a sample with a different surface chemistry: oxidation with nitric acid 6 M at boiling temperature during 3 h in a Soxhlet (sample ACoxid).

The synthesis of the carbon xerogel (sample XC) consisted in the policondensation of resorcinol (99%, Aldrich) with formaldehyde (37%, Aldrich), at an initially controlled pH (pH = 6.0), in order to promote the mesoporosity [12]. Polymerisation was carried out at 85 °C during 3 days. Then, the gel was ground and dried in an oven during 4 days (first day at 60 °C, second day at 80 °C, third day at 100 °C and fourth day at 120 °C). Finally, the material was carbonised under nitrogen flow at 800 °C using the following temperature programme: from room temperature to 150 °C (hold 2 h) at 2 °C min^{-1}, 2 °C min^{-1} to 400 °C (hold 1h), 2 °C min^{-1} to 600 °C (hold 1 h), 2 °C min^{-1} to 800 °C (hold 6 h) and cooling down to room temperature.

Cerium oxide was prepared by precipitation, according to the procedure described by Imamura et al. [13], using an aqueous solution of $Ce(NO_3)_3.6H_2O$. In each batch, 200 mL of a sodium hydroxide 3 M solution was added drop wise to the metal salt solution (ca. 15 g/100 mL H_2O) under continuous stirring. The resultant precipitate was thoroughly washed with distilled water, dried at 100 °C for 24 h and calcinated in air (50 Ncm^3 min^{-1}) at 450 °C for 3 h. Composites of carbon materials and metal oxide were prepared by a similar procedure to that described for cerium oxide, where a given amount of carbon material was dispersed in the metal solution before addition of NaOH. After precipitation, the suspension was shacked for 5 h at room temperature. Then, it was filtered and thoroughly washed and dried in an oven for 24 h at 100 °C. This material was thermally treated at 450 °C for 3 h under a flow of N_2 (50 Ncm^3 min^{-1}). All catalysts were sieved to a particle size of 100 - 300 μm prior to reaction studies.

The textural characterization of the materials was based on the corresponding N_2 equilibrium adsorption isotherms, determined at -196 °C with a Quantachrome Instruments NOVA 4200e apparatus. BET surface areas (S_{BET}), mesoporous surface areas ($S_{\neq \mu pores}$) and micropore volumes ($V_{\mu pores}$) of the samples were calculated. The relative amount of metal oxide in the composite was determined by thermogravimetric analysis under air in a STA 409 PC/4/H Luxx Netzsch thermal

analyser. The morphology and semi-quantitative elemental analysis of the catalysts were obtained by SEM and energy dispersive X-ray spectroscopy (EDS) on a JEOL JSM 35C/Noran Voyager system. XRD spectra were recorded on a Philips X'Pert MPD diffractometer (Cu Kα = 0.15406 nm) and XPS was performed with a VG Scientific ESCALAB 200A spectrometer. XPS data corresponding to Ce 3d spectra were fitted using the software XPSpeak. To minimize the number of degrees of freedom of the curve fitting procedure, constraints on the binding energy (BE), full width at half maximum (FWHM) and peak areas were applied to each doublet pair.

5.2.2 Kinetic experiments

The removal of pollutants was investigated in a slurry lab-scale reactor equipped with agitation and recirculation jacket. In each experiment the reactor was filled with 700 cm^3 of pollutant solution ($C_{0,oxalic\ acid}$ = $C_{0,oxamic\ acid}$ = 1 mM, $C_{0,dye}$ =100 mg L^{-1}) at the natural pH ($pH_{0,oxalic\ acid}$ ≈ 3.0, $pH_{0,oxamic\ acid}$ ≈ 3.0, $pH_{0,dye}$ = 5.5). In the adsorption and catalytic ozonation experiments, 350 mg of catalyst (particle size = 100 - 300 μm) were introduced in the reactor. Ozone was produced from pure oxygen in a BMT 802X ozone generator. The experiments were performed at constant gas flow rate (150 $Ncm^3\ min^{-1}$) and constant inlet ozone concentration (50 g Nm^{-3}). The concentration of ozone in the gas phase was monitored with a BMT 964 ozone analyzer. Ozone in the gas phase leaving the reactor was removed in a series of gas washing bottles filled with potassium iodide solution. The agitation was maintained constant at 300 rpm in order to keep the reactor content perfectly mixed and the temperature was set to 25 °C. In the adsorption experiments, the ozone-containing stream was replaced by an oxygen stream. In the experiments carried out in the presence of *tert*-butanol, a concentration of 10 mM of this radical scavenger was used [14].

The concentration of both oxalic and oxamic acids was followed by HPLC using a Hitachi Elite Lachrom apparatus equipped with a diode array detector. The stationary phase was an Aminex HPX-87H column (300 mm x 7.8 mm) working at room temperature under isocratic elution with H_2SO_4 4 mM. Solution decolourisation was followed by UV-Vis spectrophotometry with a JASCO V-560 UV/Vis spectrophotometer at the maximum absorption wavelength (597 nm), previously determined. The degree of mineralisation was followed by total organic carbon (TOC) analysis in a Shimadzu TOC-5000A Analyzer.

5.3 Results and discussion

5.3.1 Characterization of the catalysts

Thermal analysis revealed the relative amounts of both materials in the composites (see Table 5.1). The textural characterization was based on the corresponding N_2 equilibrium adsorption isotherms determined at -196 °C. Table 5.1 presents the textural properties of the cerium oxide-carbon composites. Original activated carbon has the highest BET surface area, although the oxidized activated carbon does not present significant differences. In general, BET surface areas, mesoporous surface areas and micropore volumes increase with the amount of carbon material present in the composites. This was expected according to the contribution of the carbon introduced.

The X-ray diffraction patterns of selected catalysts are shown in Figure 5.1. For samples Ce-O, AC0-Ce-O_1 and XC-Ce-O_2 the dominant diffraction peaks are those characteristic of cerianite (CeO_2). Compared to Ce-O, in sample XC-Ce-O_2 an increase in the crystallite diameter (d) was observed, while for AC0-Ce-O_1 a small decrease was verified.

The oxidation states of surface cerium species on samples Ce-O, AC0-Ce-O_1, AC0-Ce-O_3, AC0-Ce-O_4, XC-Ce-O_2 and ACoxid-Ce-O_2 were characterized by XPS analysis. According to the literature [15], the Ce 3d XPS spectra of Ce (IV) can be resolved into six features. If some Ce (III) species are present, then two additional peaks and the corresponding satellites are necessary to describe spectra. Furthermore, Ce (IV) and Ce (III) always show peaks at ~882.5 and ~916.5 eV as well as at ~885.0 and ~903.7 eV, which are considered fingerprints characterising Ce (IV) and Ce (III), respectively [16]. Although Ce 3d spectra of samples present the characteristic features of cerium (IV) oxide, the coexistence of both Ce (III) and Ce (IV) species must be considered in order to obtain a good fitting of the experimental data. Spectra were fitted with ten peaks [17, 18]. In the Ce $3d_{5/2}$ spin-orbit split doublet for Ce (IV), v_0 and v_2 components represent the intense peaks and v_1 a weak satellite (see Figure 5.2). Correspondingly, v'_0 and v'_2 components represent the Ce $3d_{3/2}$ doublet intense peaks, and v'_1 the associated weak satellite [17, 19-22]. For the oxidation state +3, the main components u_0 and u_1 characterize the Ce $3d_{5/2}$, and u'_0 and u'_1 the Ce $3d_{3/2}$ contribution [17, 23, 24].The experimental and fitted Ce 3d spectra of samples CeO_2, AC0-Ce-O_1/3/4, ACoxid-Ce-O_2 and XC-Ce-O_2 are shown in Figure 5.2.

Table 5.1: Physical characterization of catalysts.

Samples	% carbon material	$S_{B.E.T.}$ ($m^2\ g^{-1}$)	$S_{\neq\mu pores}$ ($m^2\ g^{-1}$)	$V_{\mu pores}$ ($cm^3\ g^{-1}$)	d (nm)[a]
Ce-O	-	121	121	0	9.8
AC0	-	897	254	0.285	-
XC	-	603	238	0.191	-
ACoxid	-	843	245	0.313	-
AC0-Ce-O_1	10	272	157	0.058	9.4
AC0-Ce-O_2	40	240	156	0.042	-
AC0-Ce-O_3	60	751	233	0.269	-
AC0-Ce-O_4	90	773	247	0.270	-
XC-Ce-O_1	25	175	158	0.009	-
XC-Ce-O_2	50	184	156	0.014	10.7
XC-Ce-O_3	75	381	228	0.081	-
ACoxid-Ce-O_1	25	209	119	0.047	-
ACoxid-Ce-O_2	50	274	149	0.066	-
ACoxid-Ce-O_3	75	463	190	0.149	-

[a] crystallite diameters determined by XRD analyses .

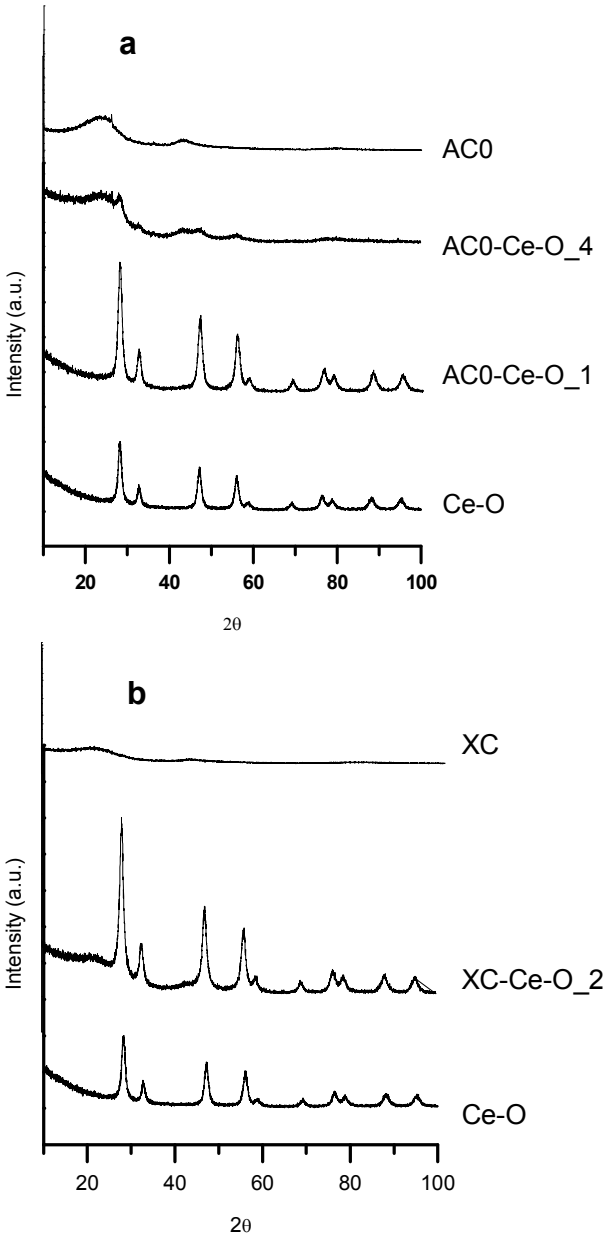

Figure 5.1: X-ray diffractograms of selected catalysts: (a) AC0, AC0-Ce-O_1, AC0-Ce-O_4 and Ce-O and (b) XC, XC-Ce-O_2 and Ce-O.

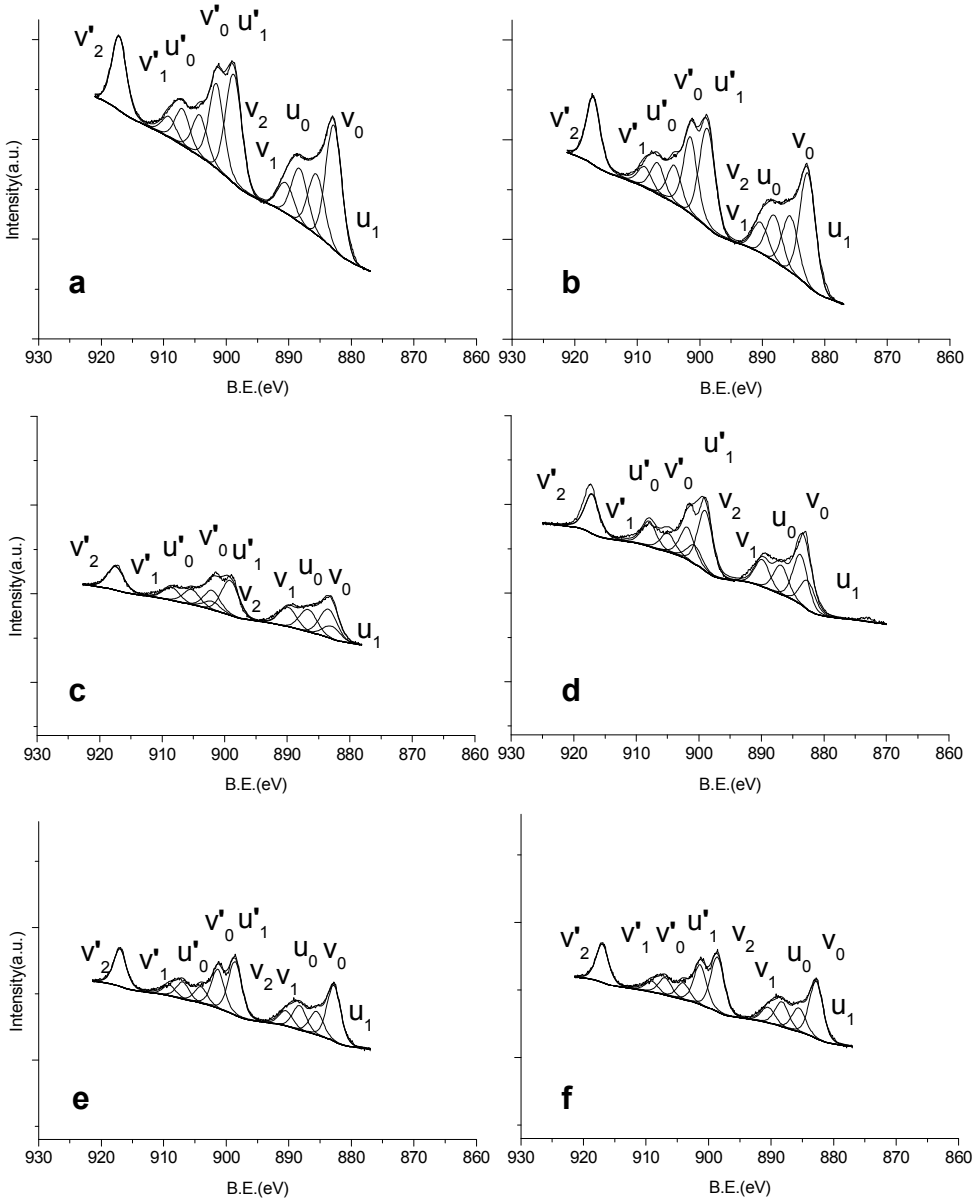

Figure 5.2: Experimental and fitted Ce 3d XPS spectra of samples (a) CeO_2, (b) AC0-Ce-O_1, (c) AC0-Ce-O_3, (d) AC0-Ce-O_4, (e) ACoxid-Ce-O_2 and (f) XC-Ce-O_2.

The relative area of the Ce $3d_{3/2}$ peak at ca. 917 eV (v'_2), characteristic of Ce (IV) species (it is absent in pure Ce_2O_3) has been used for semiquantitative estimation of the relative amount of cerium present as Ce (IV) on the surface [11, 25]. The

percentages of Ce (IV) determined are reported in Table 5.2. According to the XPS results it is possible to conclude that the Ce (IV)/Ce (III) redox couple exists on the surface of the prepared ceria containing catalysts. It is verified that no significant differences are observed in the relative amount of Ce (IV) on the surface of the different samples.

Table 5.2: Relative % of Ce (IV) on surface.

Sample	Ce (IV) (%)
Ce-O	11.8
AC0-Ce-O_1	11.8
AC0-Ce-O_3	12.1
AC0-Ce-O_4	12.4
XC-Ce-O_2	12.4
ACoxidado-Ce-O_2	12.7

SEM and EDS analyses of samples (Figure 5.3) revealed the morphology and the semi-quantitative elemental composition of the particles. In the same composite particle it is possible to identify carbon areas (dark areas, Z1) and Ce enriched zones (clear areas, Z2).

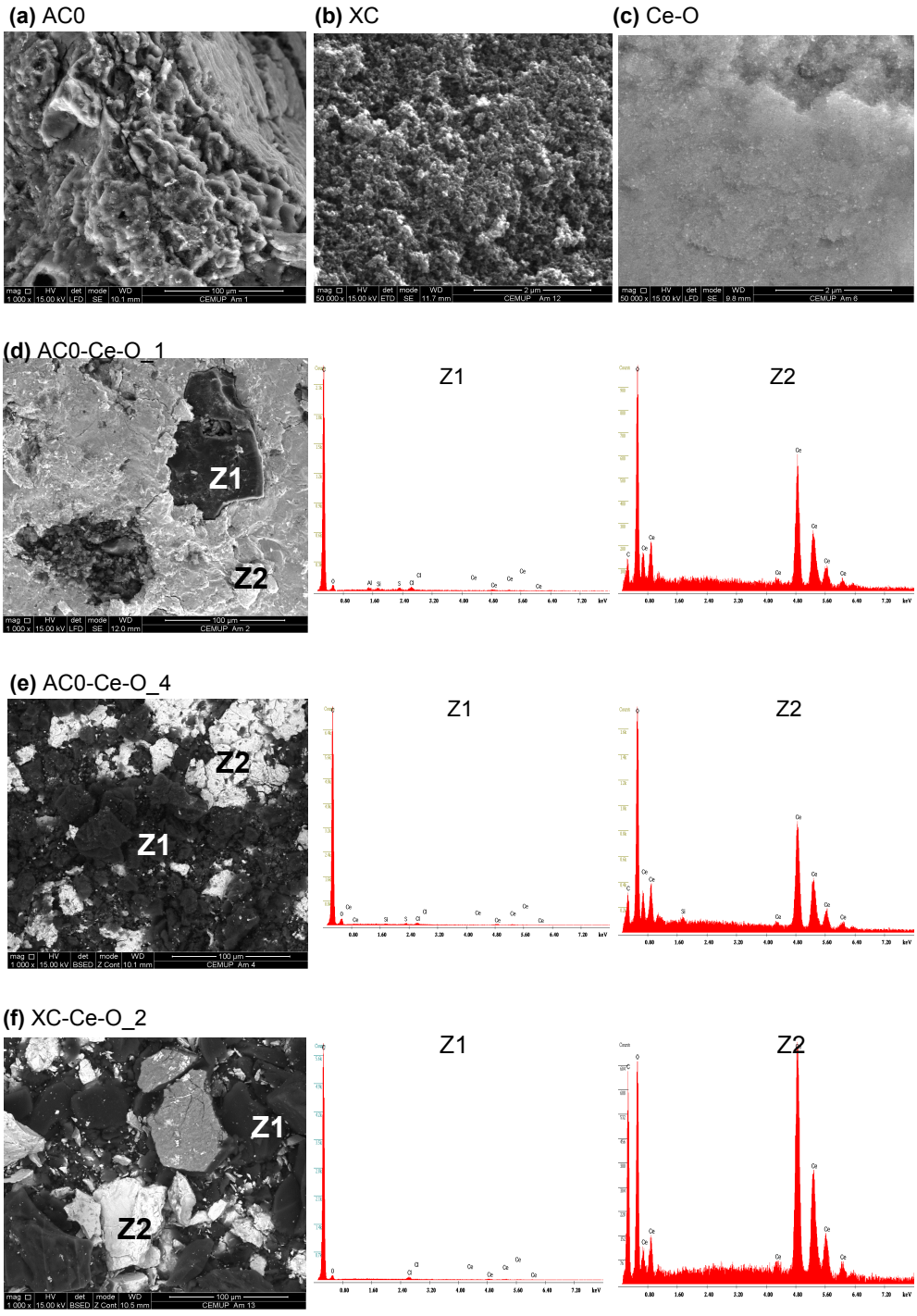

Figure 5.3: SEM images and EDS analyses of samples (a) AC0, (b) XC, (c) Ce-O, (d) AC0-Ce-O_1, (e) AC0-Ce-O_4, (f) XC-Ce-O_2.

5.3.2 Oxalic acid removal

Oxalic acid was selected for this study because it is one of the most important final products of non-catalytic oxidation processes, with a high refractory character relatively to single ozonation. The ozonation of oxalic acid was carried out at the natural pH of its solutions, which is ca. 3.0. Figure 5.4 presents the results obtained for its degradation by catalytic ozonation in the presence of cerium oxide – carbon composites. Data obtained with the activated carbon (AC0), carbon xerogel (XC), oxidised activated carbon (ACoxid) and cerium oxide (Ce-O) are also included, as well as single ozonation and adsorption in AC0 and XC. It can be observed, both for the activated carbon and the carbon xerogel, that single adsorption is not sufficient to remove oxalic acid, but adsorption on activated carbon is more significant, allowing a removal of 45% after 180 min of reaction. In acidic conditions, this carboxylic acid is also not effectively removed by single ozonation, but its mineralisation degree is enhanced by the addition of any of the materials tested. Cerium oxide is the worst catalyst, leading to an 83% conversion of oxalic acid after 180 min of reaction. The ozonation of oxalic acid in the presence of both composites and carbon materials showed excellent results, leading to nearly complete mineralisation in 90 min or less. Samples AC0-Ce-O_3 and AC0-Ce-O_4 have higher catalytic activity than activated carbon. All cerium oxide – carbon xerogel composites have better performance than carbon xerogel. ACoxid-Ce-O_3 also has better catalytic activity than the oxidised activated carbon. It is observed in all prepared composites that the catalytic activity increases with the amount of carbon material introduced. As expected, the final pH of the solutions increases with the oxalic acid conversion: 3.8 for single ozonation, 3.9 for Ce-O and about 5.5 for the other catalysts.

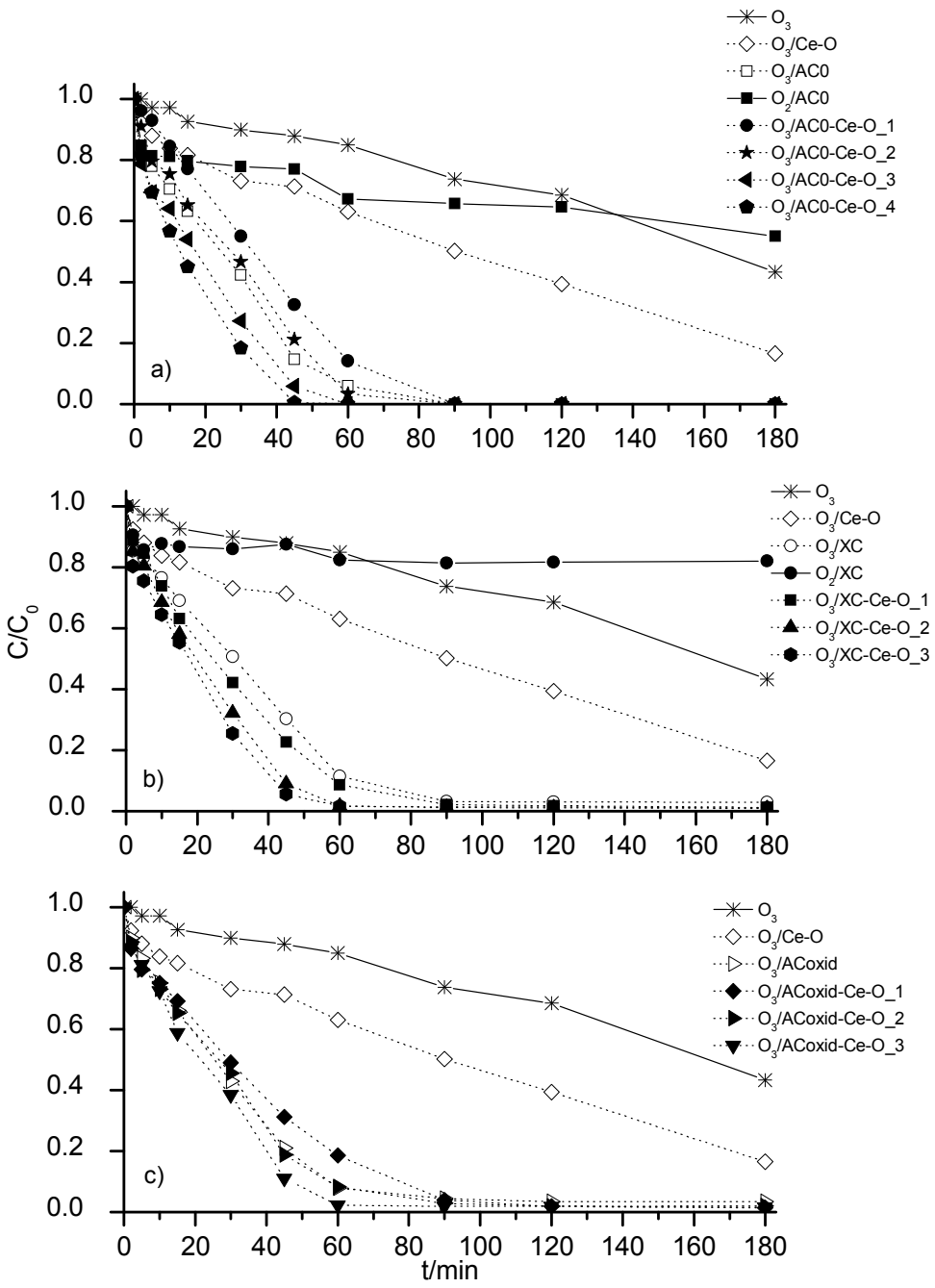

Figure 5.4: Oxalic acid removal by single ozonation and catalytic ozonation in the presence of: (a) AC0-Ce-O composites, (b) XC-Ce-O composites and (c) ACoxid-Ce-O composites.

5.3.3 Oxamic acid removal

The oxidation of organic compounds containing nitrogen functional groups can also result in the formation of oxamic acid [26, 27], which is more refractory to oxidation than oxalic acid. The results obtained for single ozonation and catalytic ozonation with cerium oxide-activated carbon composites are depicted in Figure 5.5. For comparative purposes experimental data of ozonation catalysed by activated carbon and cerium oxide are also presented. Single ozonation is practically inactive for oxamic acid degradation, but the addition of cerium oxide led to about 30% removal after 3 h. In the ozonation catalysed by composites an enhanced removal rate of oxamic acid was observed, especially with AC0-Ce-O_3 and AC0-Ce-O_4, catalysts with higher surface areas. These two materials, although having lower surface areas than activated carbon, present comparatively better performances, which shows the synergic effect of using these composites. In the case of sample AC0-Ce-O_4, the reaction time was extended to 10 h; after this period, 75% of oxamic acid removal was achieved. The final pH of the solutions increases with the oxamic acid conversion: from 3.2 for single ozonation to 3.7 for AC0-Ce-O_4.

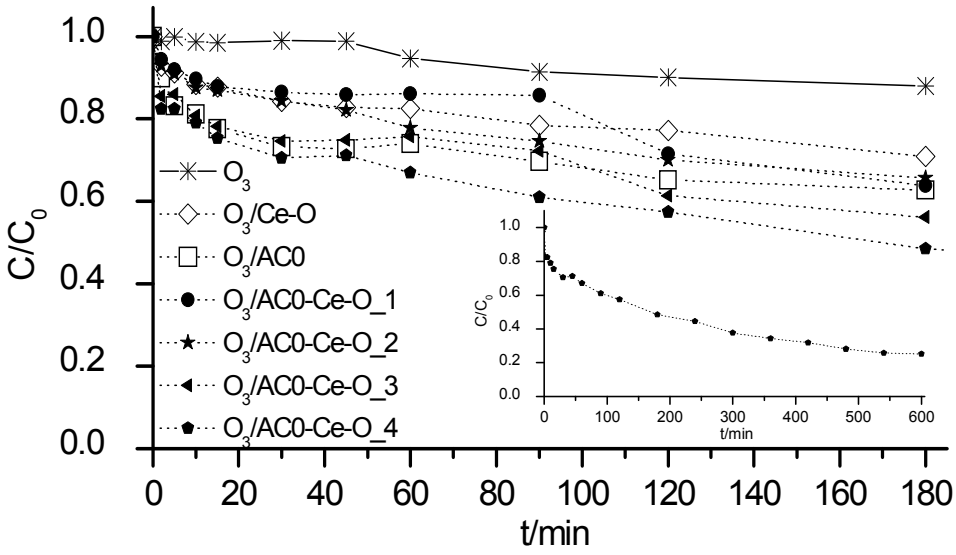

Figure 5.5: Oxamic acid removal by single ozonation and catalytic ozonation in the presence of cerium oxide, activated carbon or cerium oxide - activated carbon composites.

5.3.4 C. I. Reactive Blue 5 removal

Figure 5.6 presents the kinetic results of single ozonation and ozonation in the presence of cerium oxide-activated carbon composites for the selected dye. A total decolourisation is observed after 30 min when ozone is applied, and this time is practically independent of the presence of the catalyst. This is a clear indication that ozone by itself can easily decompose the chromophore groups of the dye molecule. Single ozonation also originates a decrease in the amount of TOC in solution. Nevertheless, this mineralisation level is much lower than colour removal, which is an indication that part of the dye degradation products (colourless) remains in solution. The advantage of using the prepared materials as catalyst is clearly seen in the TOC removal, which is higher than that obtained by single ozonation. Before 2h of reaction it is clear that the catalytic performance of the composites increases with the amount of carbon in its composition, and that samples AC0-CeO_3 and AC0-CeO_4 are clearly better than AC0, although presenting a lower surface area, which shows the synergic effect of the composites. After 2 h of reaction, the performance of the catalysts is not so different, showing that some refractory compounds are produced, such as oxamic acid [9]. Due to the formation of some acid compounds during ozonation, the final pH of the solutions decreases, being its lower value obtained for single ozonation (3.4) and a slightly higher value is observed (around 3.7) when a catalyst was used, which is an evidence that some of the acid compounds produced (such as oxalic acid) have already started to be decomposed.

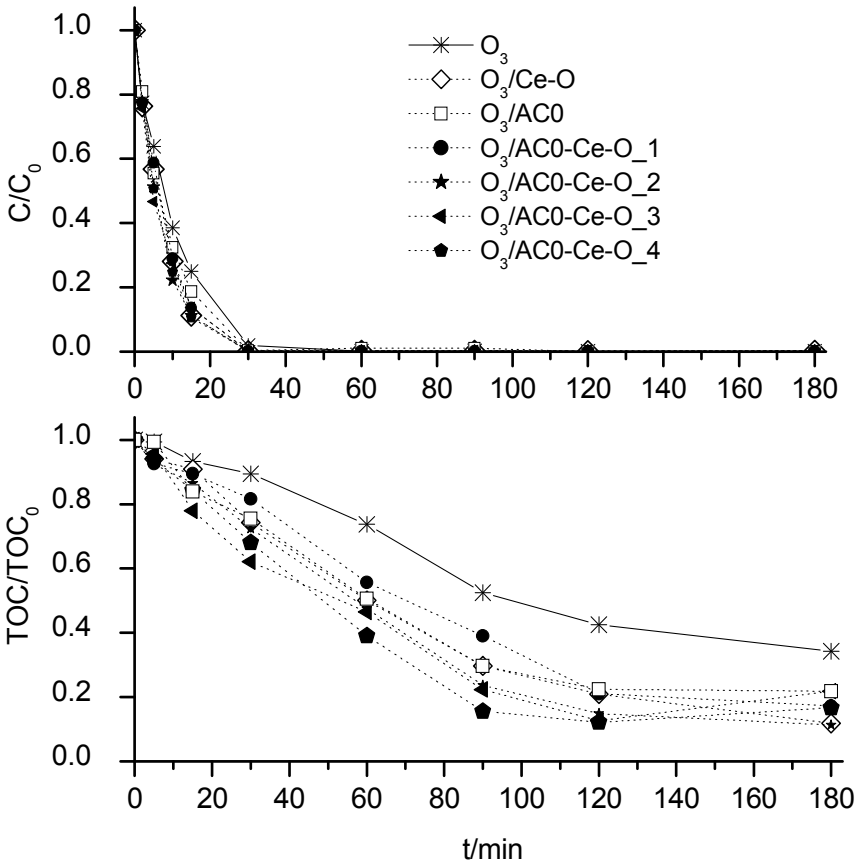

Figure 5.6: Colour and TOC removal for the reactive dye during single ozonation, and using cerium oxide, activated carbon or cerium oxide - activated carbon composites as catalysts.

5.3.5 Consideration on reaction mechanism

The ozonation of organic compounds involves a number of complex reactions and many mechanistic approaches have been presented in the literature. In general, the proposed mechanisms of ozonation catalysed by metal oxides assume that the adsorption of organic molecules and ozone takes place on the surface of the catalyst [28]. Ozone interaction with the metal oxide surface results in the formation of free radicals that can initiate a radical chain type reaction both on the surface of the catalyst and in the liquid phase, leading to the production of $HO^{\bullet}$ radicals [1, 29]. The ozonation in the presence of the prepared composites showed excellent results and in order to better understand this enhanced effect, experiments using a

physical mixture of activated carbon and cerium oxide (in the same proportion as in sample AC0-Ce-O_3), and carbon xerogel and cerium oxide (in the same proportion as in sample XC-Ce-O_2) were carried out. The results obtained for physical mixtures of carbon material and cerium oxide and the respectively composites are compared in Figure 5.7. They show that ozonation of oxalic acid catalysed by physical mixtures is less efficient than ozonation in the presence of the corresponding composites. This indicates that the intimate mixture between cerium oxide and carbon materials is necessary to explain the strong synergic effect observed in the catalytic ozonation.

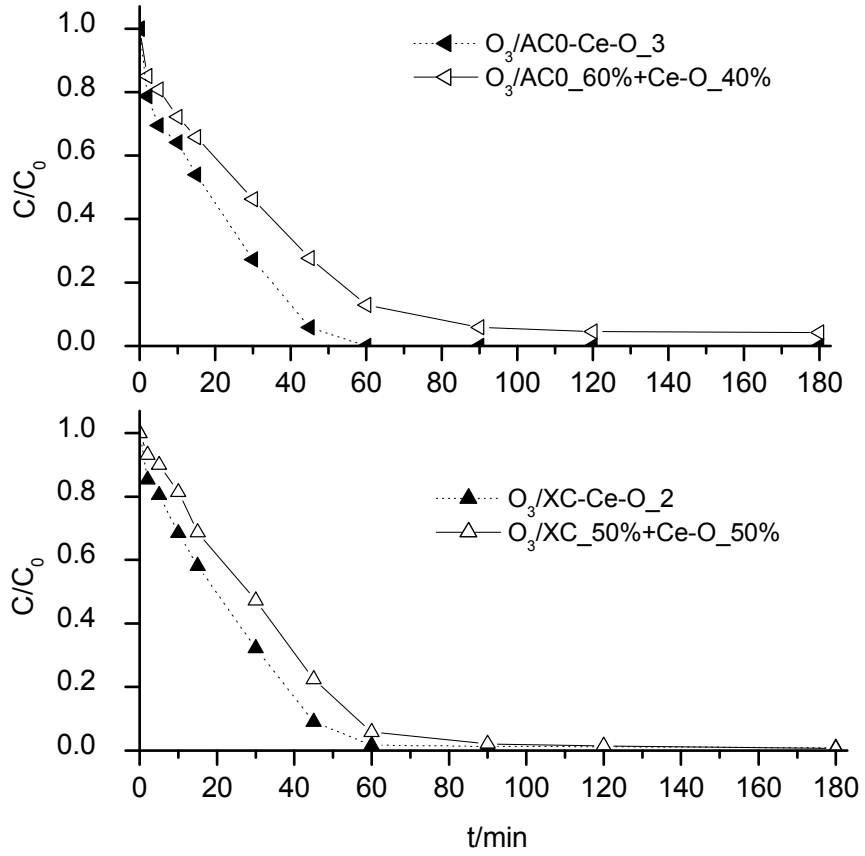

Figure 5.7: Evolution of the dimensionless concentration of oxalic acid during ozonation catalysed by AC0-Ce-O_3 or XC-Ce-O_2 composites and the corresponding physical mixtures of the same carbon materials with cerium oxide.

In order to study if the ozonation of oxalic acid in the presence of cerium oxide containing catalysts involves only $HO^{\bullet}$ radicals in the liquid phase, experiments with

Ce-O and AC0-Ce-O_4 were carried out in the presence of *tert*-butanol, a well known $HO^{\bullet}$ radical scavenger. The adsorption kinetics of oxalic acid on Ce-O has also been determined. The results obtained are presented in Figure 5.8. The results show that ozonation catalysed by cerium oxide is strongly inhibited in the presence of *tert*-butanol. This experimental observation indicates that, in these conditions, the oxidation mechanism of oxalic acid occurs predominantly via $HO^{\bullet}$ radicals in the liquid bulk. On the other hand, adsorption of oxalic acid on Ce-O was not very high (a maximum removal of 19% after 3 h). These results are different from those obtained with the activated carbon-cerium oxide composite. In the ozonation catalysed by AC0-Ce-O_4, the presence of *tert*-butanol practically does not modify the removal of oxalic acid. Thus, it can be concluded that oxalic acid is oxidised mainly on the surface of the composite, which is due to the contribution of activated carbon. According to the literature [11], in these ceria-carbon composites, the carbon material is supposed to play different roles. On one hand, it provides a high specific surface area where both organic compounds and ozone can adsorb and react. On the other hand, the availability of free electrons on the surface of the carbon material may contribute to formation of Ce (III) species, which are effective in the decomposition of ozone into $HO^{\bullet}$ radicals. Although the XPS results had shown similar compositions of Ce (III)/Ce (IV) in the prepared materials (see Table 3.2), it is expected that the in situ formation of Ce (III) during reaction would be enhanced by the increase of the carbon surface area. This explains the results obtained in Figure 5.4, where the activity of the composites increases with the percentage of carbon on its composition, and the performance for the same composition depends on the carbon used: AC0 > XC > ACoxid, which follows the amount of free electrons available on its surface. In particular, the oxidised sample has a large amount of oxygen-containing surface groups, with the capacity of attracting the π electrons, and carbon xerogels are expected to have a lower concentration of π electrons on the surface than activated carbon [30].

In these composites, a strong synergic effect between carbon materials and cerium oxide was observed, and therefore it is assumed that the mechanism responsible for the efficiency of the composites studied in the present work is that described by Faria et al. [11]. It is believed that the reaction mechanism comprises both surface reactions and liquid bulk reactions. On one hand, carbon material provides a high specific surface area where both organic compounds and ozone can adsorb and react. On the other hand, the availability of free electrons on the surface of carbon

may contribute to the formation of Ce (III) species, which are effective in the decomposition of ozone into HO• species.

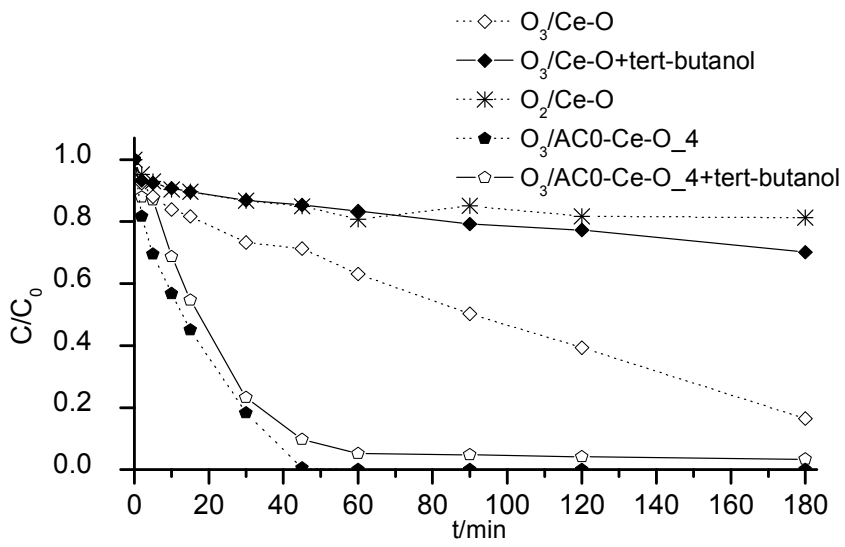

Figure 5.8: Evolution of the dimensionless concentration of oxalic acid during adsorption, catalytic ozonation and effect of *tert*-butanol ($C_{tert\text{-butanol}}$ = 10 mM).

5.4 Conclusions

Composites of cerium oxide with carbon materials in different compositions were evaluated as catalysts for the ozonation of organic pollutants.

The presence of the Ce (IV)/Ce (III) redox couple on the surface of the prepared ceria containing catalysts was evidenced by XPS analyses.

The results obtained in this study show that most of the composites have better performance than the parent carbon materials, i.e. a synergic effect clearly occurs. It is observed that the catalytic activity increases with the amount of carbon material present in the composites. In addition, there is a minimum amount of carbon material in the composite in order to have a synergic effect (approximately 50% for AC0 or ACoxid and 25% for XC). The catalytic performances for the same composition depend on the carbon used (AC0 > ACoxid and AC0 > XC), following the density of free electrons available on the surface.

The reaction mechanism is believed to comprise both surface reactions and also liquid bulk reactions involving $HO^{\bullet}$ radicals. It is assumed that the existence of delocalized electrons on the basal planes of carbon materials contributes to the

formation of Ce (III) species, which are active for the decomposition of O_3 into $HO^{\bullet}$ radicals.

Acknowledgments

This work was carried out with the support of Fundação para a Ciência e a Tecnologia (FCT) under programme POCTI/FEDER 2010 and research fellowship BD/45809/2008 (Portugal).

References

[1] B. Legube, N. K. V. Leitner, Catalytic ozonation: a promising advanced oxidation technology for water treatment, Catal. Today 53 (1999) 61-72.

[2] G. V. Buxton, C. L. Greenstock, W. P. Helman, A. B. Ross, Critical Review of rate constants for reactions of hydrated electrons, hydrogen atoms and hydroxyl radicals in Aqueous Solution, J. Phys. Chem. 17 (1988) 513-886.

[3] P. C. C. Faria, J. J. M. Órfão, M. F. R. Pereira, Ozonation of aniline promoted by activated carbon, Chemosphere 67 (2007) 809-815.

[4] B. Kasprzyk-Hordern, M. Ziólek, J. Nawrocki, Catalytic ozonation and methods of enhancing molecular ozone reactions in water treatment, Appl. Catal. B: Environ. 46 (2003) 639-669.

[5] D. S. Pines, D. A. Reckhow, Solid Phase Catalytic Ozonation Process for the Destruction of a Model Pollutant, Ozone-Sci. Eng. 25 (2003) 25-39.

[6] R. Andreozzi, A. Insola, V. Caprio, R. Marotta, V. Tufano, The use of manganese dioxide as a heterogeneous catalyst for oxalic acid ozonation in aqueous solution, Appl. Catal. A: Gen 138 (1996) 75-81.

[7] P. C. C. Faria, J. J. M. Órfão, M. F. R. Pereira, Activated carbon and ceria catalysts applied to the catalytic ozonation of dyes and textile effluents, Appl. Catal. B: Environ. 88 (2009) 341-350.

[8] P. C. C. Faria, J. J. M. Órfão, M. F. R. Pereira, Activated carbon catalytic ozonation of oxamic and oxalic acids, Appl. Catal. B: Environ. 79 (2008) 237-243.

[9] P. C. C. Faria, D. C. M. Monteiro, J. J. M. Órfão, M. F. R. Pereira, Cerium, manganese and cobalt oxides as catalysts for the ozonation of selected organic compounds, Chemosphere 74 (2009) 818-824.

[10] P. Faria, J. Órfão, M. Pereira, Mineralization of Substituted Aromatic Compounds by Ozonation Catalyzed by Cerium Oxide and a Cerium Oxide-activated Carbon Composite, Catal. Lett. 127 (2009) 195-203.

[11] P. C. C. Faria, J. J. M. Órfão, M. F. R. Pereira, A novel ceria-activated carbon composite for the catalytic ozonation of carboxylic acids, Catal. Commun. 9 (2008) 2121-2126.

[12] N. Job, A. Théry, R. Pirard, J. Marien, L. Kocon, J. N. Rouzaud, F. Béguin, J. P. Pirard, Carbon aerogels, cryogels and xerogels: Influence of the drying method on the textural properties of porous carbon materials, Carbon 43 (2005) 2481-2494.

[13] S. Imamura, A. Doi, S. Ishida, Wet oxidation of ammonia catalyzed by cerium-based composite oxides, Ind. Eng. Chem. Prod. Res. Dev. 24 (1985) 75-80.

[14] F. J. Beltran, F. J. Rivas, L. A. Fernandez, P. M. Alvarez, R. Montero-de-Espinosa, Kinetics of Catalytic Ozonation of Oxalic Acid in Water with Activated Carbon, Ind. Eng. Chem. Res. 41 (2002) 6510-6517.

[15] F. Larachi, J. Pierre, A. Adnot, A. Bernis, Ce 3d XPS study of composite $Ce_xMn_{1-x}O_{2-y}$ wet oxidation catalysts, Appl. Surf. Sci. 195 (2002) 236-250.

[16] E. Abi-aad, R. Bechara, J. Grimblot, A. Aboukais, Preparation and characterization of ceria under an oxidizing atmosphere. Thermal analysis, XPS, and EPR study, Chem. Mater. 5 (1993) 793-797.

[17] M. L. Trudeau, A. Tschöpe, J. Y. Ying, XPS investigation of surface oxidation and reduction in nanocrystalline CeO_2, Surf. Inter. Anal. 23 (1995) 219-226.

[18] A. Laachir, V. Perichon, A. Badri, J. Lamotte, E. Catherine, J.C. Lavalley, J. El-Fallah, L. Hilaire, F. Le Normand, E. Quéméré, G.N. Sauvion, O. Touret, Reduction of CeO_2 by hydrogen. Magnetic susceptibility and Fourier-transform infrared, ultraviolet and X-ray photoelectron spectroscopy measurements J. Chem. Soc., Faraday Trans. 97 (1991) 1601-1609.

[19] A. Fujimori, Mixed-valent ground state of CeO_2, Mixed-valent ground state of CeO_2 28 (1983) 2281-2283.

[20] Y. A. Teterin, A. Y. Teterin, A. M. Lebedev, I. O. Utkin, The XPS spectra of cerium compounds containing oxygen, J. Elec. Spec. Rel. Phen. 88-91 (1998) 275-279.

[21] H. Y. Zhu, T. Hirata, Ce3d and Zr3d X-ray photoelectron spectroscopy spectra of ZrO_2-12 mol % CeO_2 after heat-treatments and Ar+ etching, J. Mater. Sci. Lett. 12 (1993) 749-751.

[22] E. Paparazzo, XPS studies of damage induced by X-ray irradiation on CeO_2 surfaces, Surf. Sci. Lett. 234 (1990) L253-L258.

[23] G. Praline, B. E. Koel, R. L. Hance, H. I. Lee, J. M. White, X-Ray photoelectron study of the reaction of oxygen with cerium, J. Elec. Spec. Rel. Phen. 21 (1980) 17-30.

[24] T. L. Barr, C. G. Fries, F. Cariati, J. J. Bart, N. Giordano, A spectroscopic investigation of cerium molybdenum oxides, J. Chem. Soc., Dalton Trans. 9 (1983) 1825-1829.

[25] J. Z. Shyu, K. Otto, W. L. H. Watkins, G. W. Graham, R. K. Belitz, H. S. Gandhi, Characterization of Pd/γ-alumina catalysts containing ceria, J. Catal. 114 (1988) 23-33.

[26] M. Skoumal, P.-L. Cabot, F. Centellas, C. Arias, R. M. Rodríguez, J. A. Garrido, E. Brillas, Mineralization of paracetamol by ozonation catalyzed with Fe^{2+}, Cu^{2+} and UVA light, Appl. Catal. B: Environ 66 (2006) 228-240.

[27] N.K.V. Leitner, P. Berger, B. Legube, Environ. Sci. Technol. 36 (2002) 3083-3089.

[28] F. P. Logemann, J. H. J. Année, Water treatment with a fixed bed catalytic ozonation process, Water Sci. Technol. 35 (1997) 353-360.

[29] C. Cooper, R. Burch, An investigation of catalytic ozonation for the oxidation of halocarbons in drinking water preparation, Water Res. 33 (1999) 3695-3700.

[30] J. L. Figueiredo, J. P. S. Sousa, C. A. Orge, M. F. R. Pereira, J. J. M. Órfão, Adsorption of dyes on carbon xerogels and templated carbons: influence of surface chemistry, Adsorption 17 (2011) 431-441.

Chapter 6

Composites of manganese oxide with carbon materials as catalysts for the ozonation of oxalic acid[1]

Manganese oxide and manganese oxide-carbon composites were prepared and tested as catalysts for the removal of oxalic acid by ozonation. Their performances were compared with the parent carbon material (activated carbon or carbon xerogel) used to prepare the composites. Oxalic acid degradation by carbon materials is slower than that attained with manganese oxide or manganese oxide-carbon composites. A complete degradation after 90 and 45 min of reaction was obtained for carbon materials and for the catalysts containing manganese, respectively. The ozonation in the presence of the prepared composites are supposed to occur mainly by surface reactions, following a direct oxidation mechanism by molecular ozone and/or surface oxygenated radicals.

[1] C. A. Orge, J. J. M. Órfão, M. F. R. Pereira, Composites of manganese oxide with carbon materials as catalysts for the ozonation of oxalic acid, J. Hazard. Mater. 213–214 (2012) 133-139.

6 Composites of manganese oxide with carbon materials as catalysts for the ozonation of oxalic acid

6.1 Introduction

Metal oxides represent one of the most important and widely employed classes of solid catalysts, either as active phases or supports [1]. Several reported studies have shown that metal oxides and supported metal oxides can be efficient for the catalytic ozonation of a vast range of organic contaminants. Supported and unsupported oxides of transition metals are frequently studied ozonation catalysts [1].

Heterogeneous catalytic ozonation aims to enhance the removal of highly refractory compounds by the transformation of ozone into more reactive species and/or by adsorption and reaction of the pollutants on the surface of the catalyst [1-3]. The efficiency of catalytic ozonation depends on the solution pH, the chemical nature of the reactants and the surface properties of the catalyst.

Ozone, a powerful oxidizing agent ($E(O_3/O_2)$ = 2.07 V), is effective for the conversion of refractory organic compounds. However, generally it does not cause the complete mineralisation of solutions. In the presence of an appropriate catalyst or in combination with UV or H_2O_2, the ozonation process becomes more efficient in the degradation of organic compounds [4].

Magnesium oxides are the most widely studied metal oxides as ozonation catalyst, and they are reported to be the most efficient in ozone decomposition in gaseous medium. Manganese salts and oxides have been used as active catalysts in the homogeneous and heterogeneous catalytic ozonation systems and its efficiency has been proved for several organic compounds [1]. Nevertheless, there is a lack of understanding of the mechanisms governing their use in catalytic reactions [5].

Manganese, cobalt and cerium oxides were also tested as ozonation catalysts for aniline and sulfanilic acid removal. However, the highest efficiency was reported in the case of composites of metal oxides such as Ce–Mn and Co–Ce catalysts [6].

Faria et al. obtained excellent results in the catalytic ozonation of oxalic acid with a ceria-activated carbon composite, as a result of a strong synergic effect between activated carbon and cerium oxide [7]. In order to better understand this effect, composites of carbon materials and cerium oxide with different compositions (between 10 and 90 wt% of carbon) were prepared in a recent work, and it was

verified that most of the composites had better performances than the parent carbon materials, i.e. a synergic effect clearly occurs. The reaction mechanism was believed to comprise both surface reactions and also liquid bulk reactions involving $HO^{\bullet}$ radicals. It was assumed that the existence of delocalized electrons on the basal planes of carbon materials contributes to the formation of Ce (III) species, which are active for the decomposition of O_3 into $HO^{\bullet}$ radicals [8].

Considering the reported good catalytic performances of the cerium oxide-carbon materials composites in ozonation, there was a high expectation about the simultaneous used of carbon materials and manganese oxides. In the present work, the preparation of composites of manganese oxide-carbon materials with different compositions was carried out with the aim of evaluating their performance as ozonation catalysts for the mineralisation of oxalic acid and to investigate the reaction mechanism. The carbon materials used were an activated carbon, as received and oxidized with HNO_3, and a carbon xerogel. Then, the influence of composition, surface chemistry and textural properties of carbon materials in the composites was evaluated. The results obtained were compared to those previously obtained for composites of carbon materials and cerium oxide [8].

6.2 Experimental

6.2.1 Materials and their characterization

Oxalic acid (99%) was obtained by Sigma-Aldrich.

A commercial activated carbon, Norit GAC 1240 Plus (sample AC0), was used as received.

The synthesis of the carbon xerogel (sample XC) started by the policondensation of resorcinol (99%, Aldrich) with formaldehyde (37%, Aldrich), at an initially controlled pH (pH = 6.0), in order to promote the mesoporosity [9]. Polymerisation was carried out at 85 °C during 3 days. Then, the gel was ground and dried in an oven during 4 days at 120 °C. Finally, the material was carbonised under nitrogen flow (100 cm^3 min^{-1}) at 800 °C.

The activated carbon was submitted to a chemical treatment to obtain a material with a different surface chemistry: oxidation with nitric acid 6 M at boiling temperature during 3 h in a Soxhlet (sample ACoxid).

Manganese oxide (Mn-O) was prepared by precipitation, according to the procedure described by Imamura et al. [10], using an aqueous solution of $C_4H_6MnO_4.4H_2O$. In each batch, 200 mL of a sodium hydroxide 3 M solution was added drop wise to the metal salt solution (ca. 15 g/100 mL H_2O) under continuous stirring. The resultant precipitate was thoroughly washed with distilled water, dried at 100 °C for 24 h and calcinated in air (50 cm^3 min^{-1}) at 450 °C for 3 h. Composites of carbon materials and manganese oxide were prepared by a similar procedure to that described for the oxide, where a selected amount of carbon material was dispersed in the metal solution before addition of NaOH. After precipitation, the suspension was shaken for 5 h at room temperature. Then, it was filtered and thoroughly washed and dried in an oven for 24 h at 100 °C. This material was thermally treated at 450 °C for 3 h under a flow of N_2 (50 cm^3 min^{-1}). All catalysts were sieved to a particle size of 100-300 μm prior to reaction studies in order to minimize mass transfer effects.

The textural characterization of materials was based on the corresponding N_2 equilibrium adsorption isotherms, determined at -196 °C with a Quantachrome Instruments NOVA 4200e apparatus. The BET surface areas (S_{BET}), the mesopores surface areas ($S_{\neq \mu pore}$) and the micropore volumes ($V_{\mu pore}$) of the samples were calculated, using appropriate procedures (the *t*-method for the last two parameters). The relative amounts of manganese oxide in the composites were determined by thermogravimetric analysis under air in a STA 409 PC/4/H Luxx Netzsch thermal analyser. XRD spectra were recorded on a Philips X'Pert MPD diffractometer (Cu Kα = 0.15406 nm) and XPS analyses were performed with a VG Scientific ESCALAB 200A spectrometer. The morphology and semi-quantitative elemental analysis of the catalysts were determined by SEM and energy dispersive X-ray spectroscopy (EDS) on a JEOL JSM 35C/Noran Voyager system.

The amounts of manganese leached during reaction were measured in a GBC 932 Plus atomic absorption spectrometer (AAS), using the remaining solution after stopping the reaction.

6.2.2 Kinetic experiments

The removal of pollutants was investigated in a slurry lab-scale reactor equipped with stirring. In each experiment the reactor was filled with 700 cm^3 of solution of oxalic acid 1 mM at the natural pH ($pH_{oxaclic\ acid} \approx 3.0$) and 350 mg of catalyst (particle size = 100 - 300 μm). Ozone was produced from pure oxygen in a BMT 802X ozone generator. The experiments were performed at constant gas flow rate

(150 cm^3 min^{-1}) and constant inlet ozone concentration (50 g m^{-3}). The concentration of ozone in the gas phase was monitored with a BMT 964 ozone analyzer. Ozone in the gas phase leaving the reactor was removed in a series of gas washing bottles filled with potassium iodide solution. Ozone was introduced in the reactor by a diffuser with 1 cm of diameter and porosity #2 (pore size between 40 and 100 μm). In the experiments carried out in the presence of *tert*-butanol, a concentration of 10 mM of this radical scavenger was used [11]. The concentration of oxalic acid was followed by HPLC using a Hitachi Elite Lachrom apparatus equipped with a diode array detector. The stationary phase was an Aminex HPX-87H column (300 mm x 7.8 mm) working at room temperature, under isocratic elution with H_2SO_4 4 mM.

6.3 Results and discussion

6.3.1 Catalysts characterization

Three sets of composites of manganese oxide and carbon materials (activated carbon, oxidized activated carbon and carbon xerogel) with different compositions were prepared. The properties of the prepared materials are presented in Table 6.1. Thermal analysis revealed the relative amounts of both materials in the composites. BET surface areas, mesopore surface areas and micropore volumes of composites increase with the amount of carbon material present. This was expected and occurs due to the contribution of the carbon introduced.

SEM and EDS analyses of samples (Figure 6.1) revealed the morphology and the semi-quantitative elemental composition of the particles. It is possible to identify carbon areas (dark zones, Z1) and Mn enriched zones (clear zones, Z2) in the same composite particle.

Table 6.1: Properties of manganese oxide, carbon materials and composites.

Samples	% carbon material[a]	S_{BET} ($m^2\ g^{-1}$)	$S_{\neq\mu pore}$ ($m^2\ g^{-1}$)	$V_{\mu pore}$ ($cm^3\ g^{-1}$)	d[b] (nm)
Mn-O	-	44	44	0	55
AC0	-	897	254	0.285	-
XC	-	603	238	0.191	-
ACoxid	-	843	245	0.313	-
AC0-Mn-O_1	12	71	46	0.012	65
AC0-Mn-O_2	35	269	88	0.094	-
AC0-Mn-O_3	63	417	166	0.132	-
AC0-Mn-O_4	78	732	273	0.228	90
XC-Mn-O_1	25	96	60	0.018	-
XC-Mn-O_2	50	278	109	0.089	-
XC-Mn-O_3	75	495	102	0.201	-
ACoxid-Mn-O_1	25	81	58	0.012	-
ACoxid-Mn-O_2	50	254	109	0.077	-
ACoxid-Mn-O_3	75	564	207	0.187	-

[a] determined by thermogravimetry;

[b] crystallite diameters determined by XRD analyses.

In order to identify the phases of manganese oxide present in the composites and determine the crystallites diameters, selected samples were analysed by X -ray diffraction. The XRD patterns of Mn-O, AC0-Mn-O_1 and AC0-Mn-O_4 are shown in Figure 6.2. For selected catalysts the reflections are characteristic of hausmannite (Mn_3O_4). It is observed that the crystallite diameter (d) in the composites AC0-Mn-O_1 and AC0_Mn-O_4 are higher than that obtained in the single oxide (estimated values obtained by Scherrer equation are shown in Table 6.1).

With the aim of verifying the chemical states of the manganese species on the surface, selected samples were analysed by XPS (Figure 6.3). In the Mn $2p_{3/2}$ region two peaks were identified at 641.7 and 644.2 eV for sample Mn-O and at

642.7 and 645.5 eV for sample AC0-Mn-O_1. For sample AC0-Mn-O_2 three peaks were observed in the same region (643.1, 645.6 and 648.1 eV). Thus, according to the literature, Mn(II) and Mn(III) co-exist on the surface of samples Mn-O and AC0-Mn-O_1, but Mn(IV) is also present on the surface of AC0-Mn-O_2 [12].

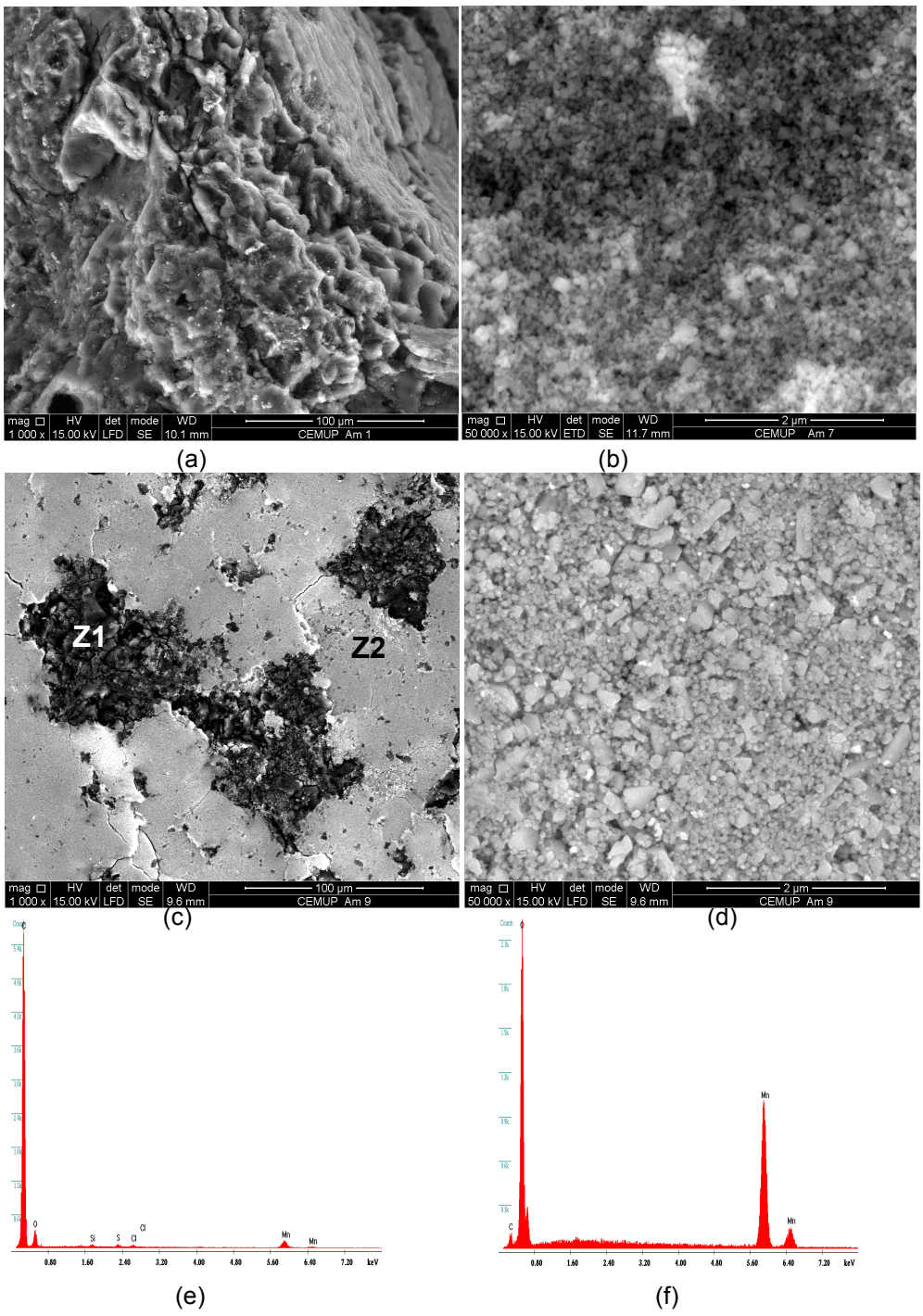

Figure 6.1: SEM micrograph of: (a) AC0, (b) Mn-O, (c) AC0-Mn-O_2 and (d) magnification of zone Z2; EDS analyses of zones Z1 (e) and Z2 (f).

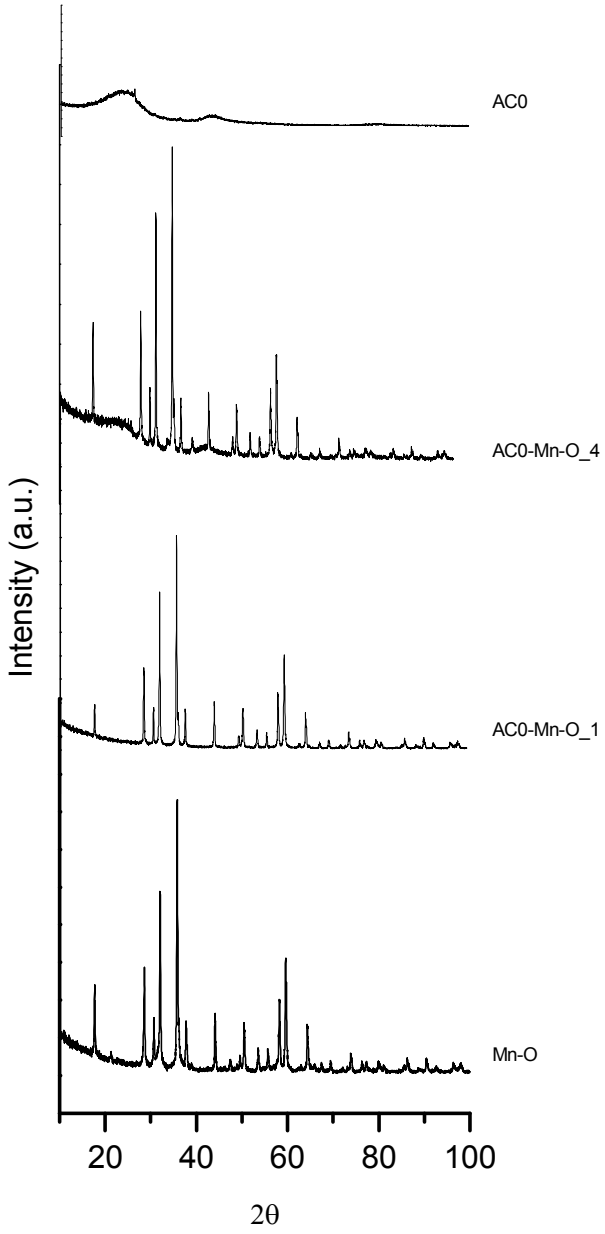

Figure 6.2: X-ray diffractograms of selected samples.

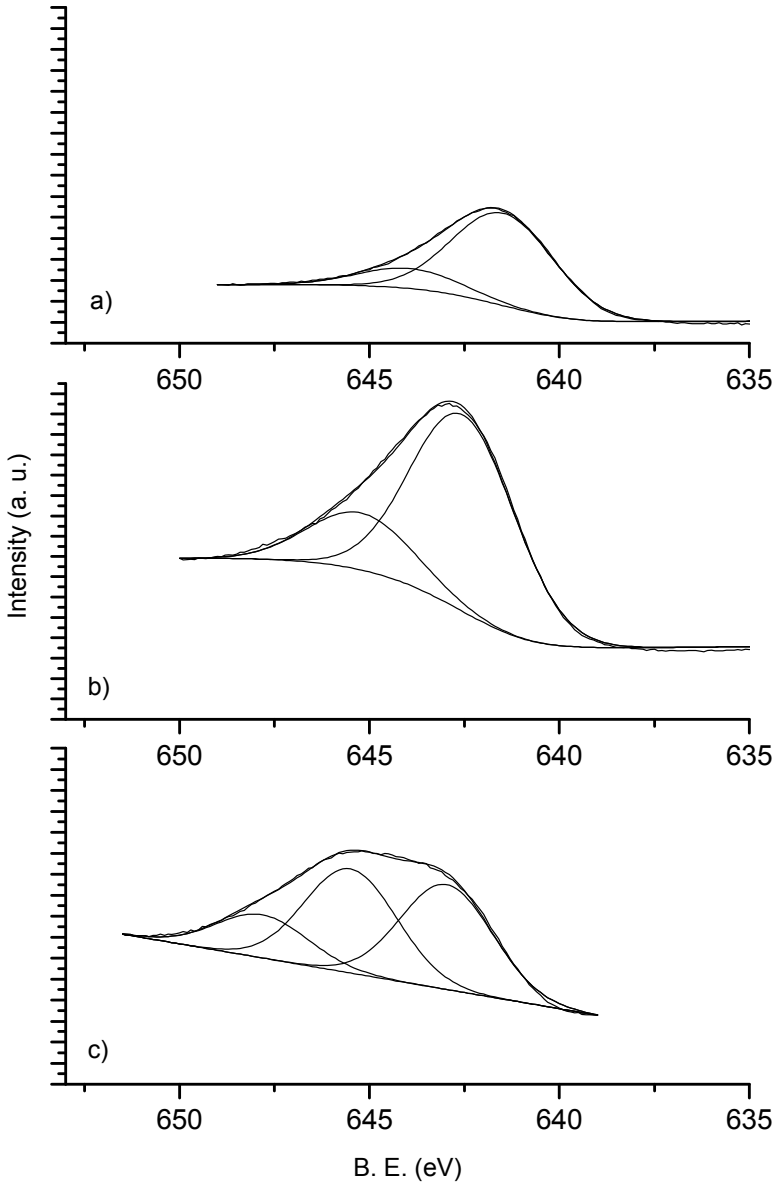

Figure 6.3: Experimental and fitted Mn 2p XPS spectra of samples (a) Mn-O, (b) AC0-Mn-O_1 and (c) AC0-Mn-O_2.

6.4 Ozonation of oxalic acid

Oxalic acid was selected for this study because it is one of the most important final products of oxidation processes, with a high refractory character relatively to single ozonation [7]. Figure 6.4 presents the results obtained for its degradation by catalytic ozonation in the presence of manganese oxide – carbon composites. Data obtained with AC0, XC, ACoxid and Mn-O are also included, as well as single ozonation. It is observed that in acidic conditions oxalic acid is not efficiently removed by single ozonation, but its mineralisation degree is enhanced by the addition of any of the catalysts tested. The ozonation of oxalic acid in the presence of carbon materials present worse results than ozonation catalysed by manganese oxide or by the prepared composites. The catalytic activity of manganese oxide-carbon composites practically does not change with the increase of the amount of carbon present. These results are significantly different from those obtained in a similar study using cerium oxide-carbon composites as catalysts [8], where it was observed that carbon materials performed better than cerium oxide, and the catalytic activity increased with the amount of carbon material present in the corresponding composites. The reasons for these different performances are discussed below.

Analyses of Mn by atomic absorption spectrometry in the remaining solutions after reaction in the presence of Mn-O and AC0-Mn-O_3 were carried out with the aim of determining the percentage of leached metal; values of 2.3% and 2.8% of the Mn initially present were detected, respectively. Summarizing, the prepared materials presented excellent results in the mineralisation of the selected pollutant, and only a small metal leaching was observed during the experiments.

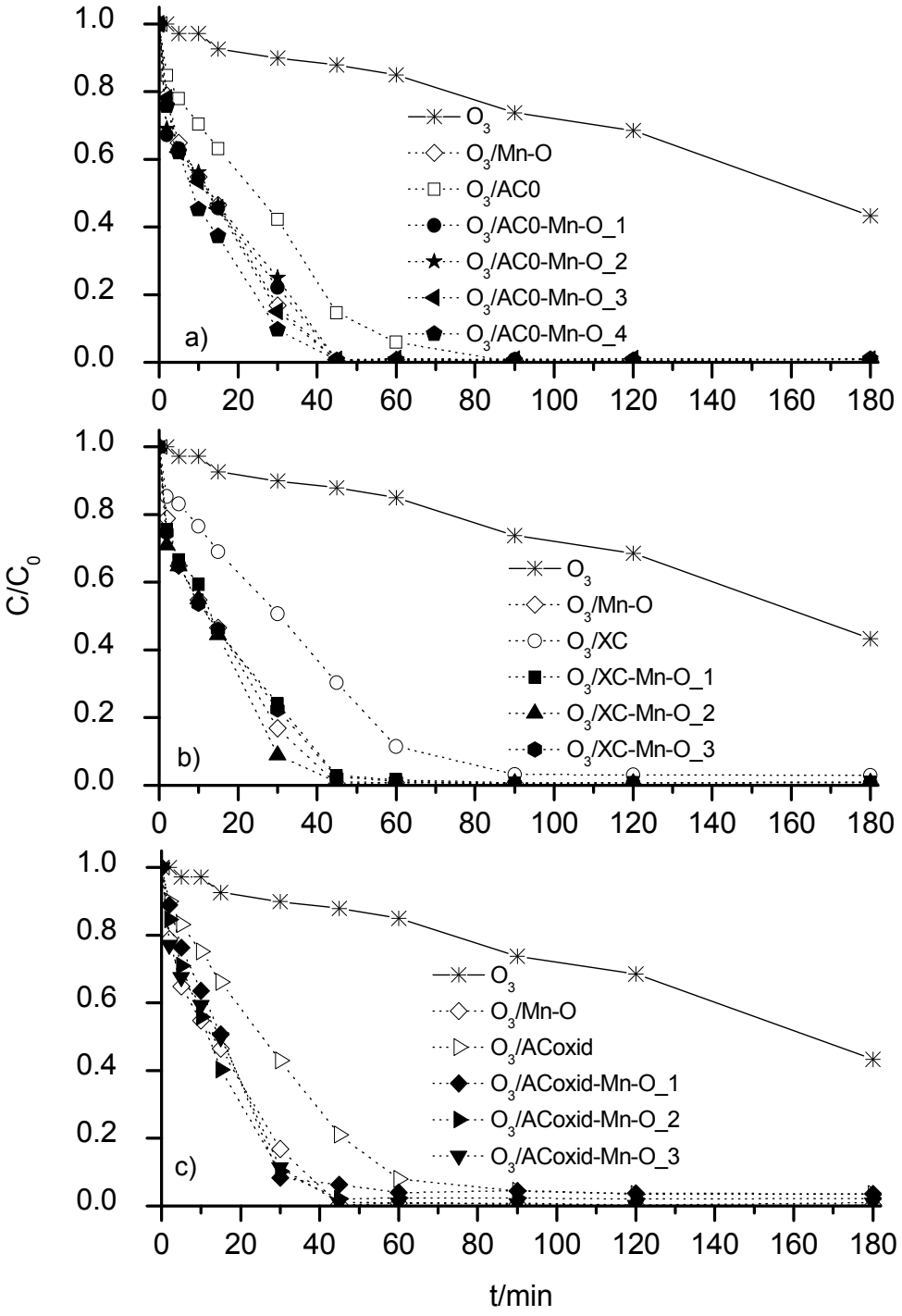

Figure 6.4: Oxalic acid removal by single ozonation and catalytic ozonation in the presence of: (a) AC0-Mn composites, (b) XC-Mn composites and (c) ACoxid-Mn composites (C_0 = 1 mM, m_{cat} = 350 mg, $V_{sol.}$ = 700 mL).

In order to improve the understanding of the reaction mechanism, experiments in the presence of *tert*-butanol, a well known $HO^{\bullet}$ radical scavenger, were carried out. This compound reacts very quickly with hydroxyl radicals ($k = 5 \times 10^8$ M^{-1} s^{-1}) and very slowly with ozone ($k = 0.03$ M^{-1} s^{-1}) [13]. The adsorption kinetic of oxalic acid on manganese oxide was also determined. The results obtained are presented in Figure 6.5. Adsorption of oxalic acid on Mn-O is very fast, allowing a maximum removal of about 25% after a few minutes. The results show that ozonation catalysed by Mn-O and AC0-Mn-O_3 in the presence of *tert*-butanol favoured the oxalic acid removal (see Figure 6.5). This is similar to what was reported for brucite as catalyst, where an increase of phenol [14] or azo dye [15] degradation rates were observed when *tert*-butanol was added. Therefore, it was proposed that catalytic ozonation with brucite probably proceeds according to direct oxidation by ozone, instead of the radical pathway by reactions with hydroxyl radicals generated in the ozone decomposition. Thus, it is suggested that catalytic ozonation in the presence of the materials prepared in this work does not follow the radical pathway by reactions with hydroxyl radicals in solution.

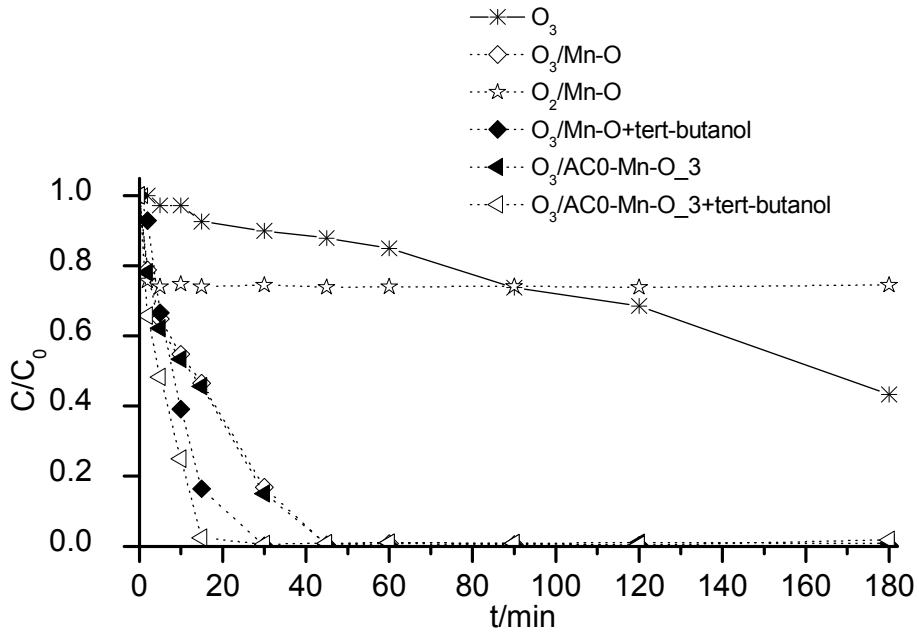

Figure 6.5: Evolution of dimensionless concentration of oxalic acid during adsorption on Mn-O, single ozonation and catalytic ozonation with Mn-O and AC0-Mn-O_3, and effect of *tert*-butanol (C_0 = 1 mM, m_{cat} = 350 mg, $V_{sol.}$ = 700 mL, $C_{tert\text{-}butanol}$ = 10 mM).

In order to evaluate the eventual deactivation of manganese oxide during the ozonation experiments, three consecutive runs were carried out with fresh oxalic acid solutions. The kinetic results presented in Figure 6.6 show that there is a slightly decrease in the catalytic activity, especially from the second for third run, but the total removal is still achieved after 45 min of reaction.

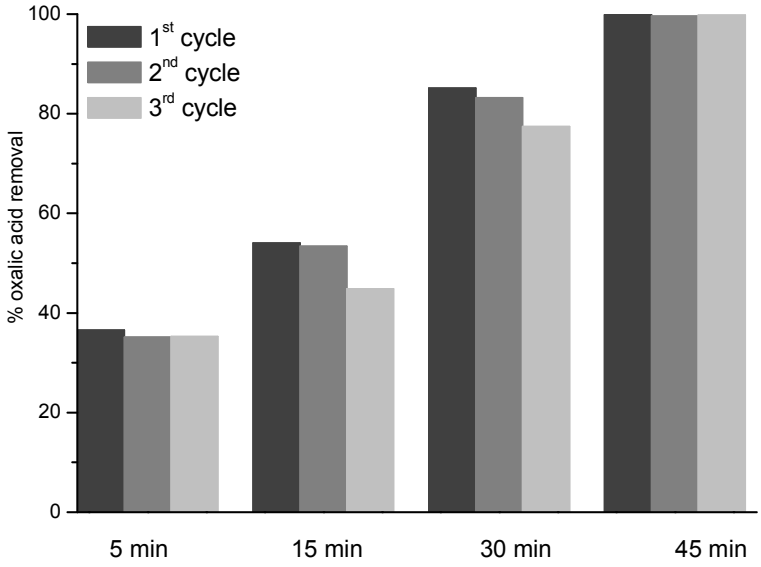

Figure 6.6: Evolution of oxalic acid removal during cyclic experiments (C_0 = 1 mM, m_{cat} = 350 mg, $V_{sol.}$ = 700 mL).

Experiments with an aqueous solution of manganese precursor with the equivalent amount of Mn leached during ozonation catalysed by manganese oxide, with or without *tert*-butanol, were carried out (Figure 6.7). A slower removal of oxalic acid in the ozonation with the solution of manganese precursor compared with the ozonation catalysed by Mn-O is observed, and after 3 h of reaction 11% of the pollutant still remains in solution. The results in the presence of *tert*-butanol show that the homogeneous catalysed ozonation of oxalic acid is strongly inhibited. This experimental observation indicates that, under these conditions, the oxidation mechanism of oxalic acid occurs predominantly via $HO^{\bullet}$ radicals in the liquid phase. In heterogeneous catalysed ozonation the effect of *tert*-butanol is completely different, since the presence of the radical scavenger enhances the oxalic acid

removal, as discussed before. Therefore, these results indicate that reactions in the liquid phase are not responsible for the performances observed with the catalysts containing manganese. Thus, it is proposed that surface reactions play an important role in catalytic ozonation in the presence of manganese catalysts, which is in accordance with the literature. Adsorption of organic molecules on the surface of oxide and subsequent attack of ozone was the mechanism initially proposed by Andreozzi et al. [16], and after defended by Tong et al. [17]. In general, the proposed mechanisms of metal oxides catalytic ozonation assume that the adsorption of organic molecules and ozone takes place on the surface of the catalyst [18].

An experiment using a physical mixture of activated carbon and manganese oxide (in the same proportion as in sample AC0-Mn-O_4) was carried out and the corresponding result is also presented in Figure 6.7. The physical mixture was prepared using activated carbon and manganese oxide, previously synthesised by the precipitation method, with particle size between 100 and 300 μm. No differences between ozonation catalysed by the physical mixture or the intimate mixture (composite) were observed, which confirms that in the manganese oxide-carbon composites there is no synergic effect for the ozonation reactions, contrarily to what was previously observed for ceria-carbon composites [8].

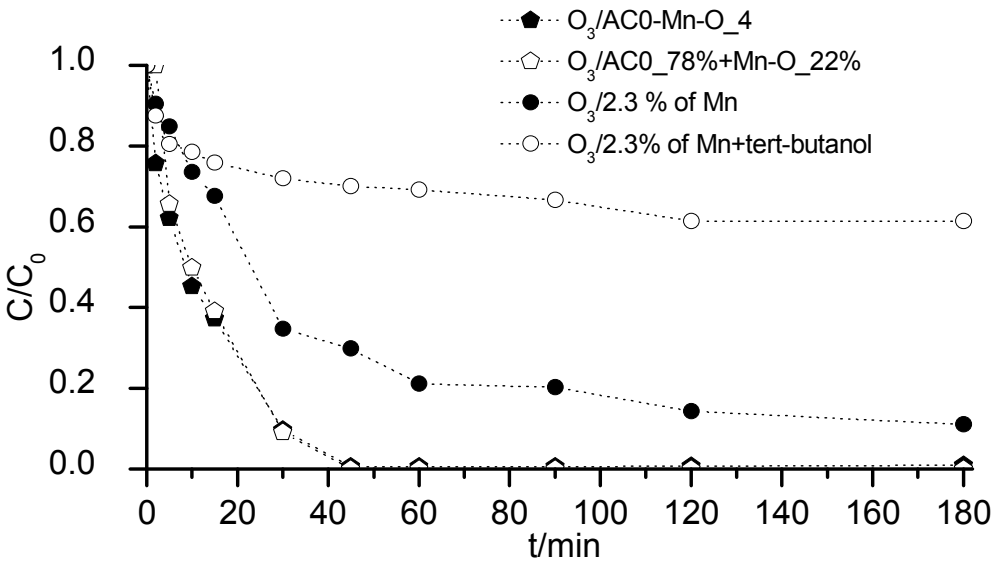

Figure 6.7: Evolution of dimensionless concentration of oxalic acid during ozonation catalysed by AC0-Mn-O_4 and the corresponding physical mixture of activated carbon and manganese oxide, and catalytic ozonation with a solution of the manganese precursor with or without *tert*-butanol (C_0 = 1 mM, m_{cat} = 350 mg, $V_{sol.}$ = 700 mL, percentage of Mn = 2.3%, $C_{tert\text{-butanol}}$ = 10 mM).

In fact, the obtained results with manganese oxide are very different from the results reported in that work with cerium oxide prepared by precipitation [8]. Contrary to manganese oxide, which has better performance than carbon materials, cerium oxide has lower catalytic activity, leading to an 83% conversion of oxalic acid after 180 min of reaction. Adsorption on manganese oxide allows a maximum removal of 25% in a few minutes. On the other hand, adsorption on cerium oxide was not so high and fast, leading to a maximum removal of 19% after 3 h under the conditions tested. The effect of *tert*-butanol is also completely different in ozonation catalysed by cerium oxide or manganese oxide. While the addition of *tert*-butanol in the catalytic ozonation in the presence of manganese oxide has a positive effect, since it favors the oxalic acid removal, in the ozonation catalysed by cerium oxide the influence of the radical scavenger is negative, decreasing the removal of oxalic acid. Therefore, in the case of cerium oxide the reaction mechanism of oxalic acid occurs predominantly via $HO^{\bullet}$ radicals in solution, since the presence of *tert*-butanol strongly inhibits the removal of oxalic acid. According to the results, the reaction mechanism in the presence of manganese oxide is different. The adsorption of

oxalic acid on the surface of Mn-O is relevant and ozone and/or surface oxygenated radicals react directly with adsorbed molecules of oxalic acid. Thus, $HO^{\bullet}$ radicals have a negative effect, since they decompose ozone producing new $HO^{\bullet}$ radicals and decreasing the amount of ozone available for surface reactions, which was demonstrated by the increase of oxalic acid removal when *tert*-butanol was added.
The results obtained for physical mixtures of carbon material and cerium oxide are also very different from the results observed with physical mixtures of activated carbon and manganese oxide. It was shown that ozonation of oxalic acid in the presence of physical mixtures was less efficient than ozonation in the presence of the corresponding composites of cerium oxide-carbon material [8]. This indicates that the intimate mixture between cerium oxide and carbon materials results in a strong synergic effect for ozonation reactions. In addition, it was observed that the catalytic activity increases with the amount of carbon material present in the composites, and there is a minimum amount of carbon material in the composite in order to have a synergic effect. Therefore, the reaction mechanism of cerium oxide-carbon composites is believed to comprise both surface reactions and also liquid bulk reactions involving $HO^{\bullet}$ radicals, while the proposed reaction mechanism of manganese oxide-carbon involves predominantly surface reactions, following a direct pathway through oxidation with molecular ozone and/or surface oxygenated radicals.

6.5 Conclusions

The results obtained in this study for the mineralisation of oxalic acid show that manganese oxide prepared is an effective ozonation catalyst and its catalytic activity is better than that of carbon materials. Synergic effects between manganese oxide and carbon materials in the prepared composites were not observed, contrarily to what was previously observed for ceria-carbon composites. The reaction mechanism is believed to occur mainly by surface reactions, following a direct oxidation of adsorbed molecules by molecular ozone and/or surface oxygenated radicals.

Acknowledgments

This work is supported by project PEst-C/EQB/LA0020/2011, financed by FEDER through COMPETE - Programa Operacional Factores de Competitividade and by FCT - Fundação para a Ciência e a Tecnologia. C.A.O. thanks FCT for the research

fellowship BD/45809/2008. The authors are indebted to Dr. Carlos M. Sá (CEMUP) for assistance with SEM and XPS analyses.

References

[1] B. Kasprzyk-Hordern, M. Ziólek, J. Nawrocki, Catalytic ozonation and methods of enhancing molecular ozone reactions in water treatment, Appl. Catal. B: Environ. 46 (2003) 639-669.

[2] P. C. C. Faria, J. J. M. Órfão, M. F. R. Pereira, Activated carbon catalytic ozonation of oxamic and oxalic acids, Appl. Catal. B: Environ. 79 (2008) 237-243.

[3] P. C. C. Faria, J. J. M. Órfão, M. F. R. Pereira, Activated carbon and ceria catalysts applied to the catalytic ozonation of dyes and textile effluents, Appl. Catal. B: Environ. 88 (2009) 341-350.

[4] L. F. Liotta, M. Gruttadauria, G. Di Carlo, G. Perrini, V. Librando, Heterogeneous catalytic degradation of phenolic substrates: Catalysts activity, J. Hazar. Mater. 162 (2009) 588-606.

[5] J. Nawrocki, B. Kasprzyk-Hordern, The efficiency and mechanisms of catalytic ozonation, Appl. Catal. B: Environ. 99 (2010) 27-42.

[6] P. C. C. Faria, D. C. M. Monteiro, J. J. M. Órfão, M. F. R. Pereira, Cerium, manganese and cobalt oxides as catalysts for the ozonation of selected organic compounds, Chemosphere 74 (2009) 818-824.

[7] P. C. C. Faria, J. J. M. Órfão, M. F. R. Pereira, A novel ceria-activated carbon composite for the catalytic ozonation of carboxylic acids, Catal. Commun. 9 (2008) 2121-2126.

[8] C. A. Orge, J. J. M. Órfão, M. F. R. Pereira, Catalytic ozonation of organic pollutants in the presence of cerium oxide-carbon composites, Appl. Catal. B: Environ. 102 (2011) 539-546.

[9] N. Job, A. Théry, R. Pirard, J. Marien, L. Kocon, J. N. Rouzaud, F. Béguin, J. P. Pirard, Carbon aerogels, cryogels and xerogels: Influence of the drying method on the textural properties of porous carbon materials, Carbon 43 (2005) 2481-2494.

[10] S. Imamura, A. Doi, S. Ishida, Wet oxidation of ammonia catalyzed by cerium-based composite oxides, Ind. Eng. Chem. Prod. Res. Dev. 24 (1985) 75-80.

[11] F. J. Beltran, F. J. Rivas, L. A. Fernandez, P. M. Alvarez, R. Montero-de-Espinosa, Kinetics of Catalytic Ozonation of Oxalic Acid in Water with Activated Carbon, Ind. Eng. Chem. Res. 41 (2002) 6510-6517.

[12] F. Li, L. Zhang, D. G. Evans, X. Duan, Structure and surface chemistry of manganese-doped copper-based mixed metal oxides derived from layered double hydroxides, Colloids Surf. A: Physicochem. Eng. Aspects 244 (2004) 169-177.

[13] J. Hoigné, H. Bader, Rate constants of reactions of ozone with organic and inorganic compounds in water--II: Dissociating organic compounds, Water. Res. 17 (1983) 185-194.

[14] K. He, Y. M. Dong, Z. Li, L. Yin, A. M. Zhang, Y. C. Zheng, Catalytic ozonation of phenol in water with natural brucite and magnesia, J. Hazar. Mater. 159 (2008) 587-592.

[15] Y. Dong, K. He, B. Zhao, Y. Yin, L. Yin, A. Zhang, Catalytic ozonation of azo dye active brilliant red X-3B in water with natural mineral brucite, Catal. Commun. 8 (2007) 1599-1603.

[16] R. Andreozzi, A. Insola, V. Caprio, R. Marotta, V. Tufano, The use of manganese dioxide as a heterogeneous catalyst for oxalic acid ozonation in aqueous solution, Appl. Catal. A: Gen 138 (1996) 75-81.

[17] S. Tong, W. Liu, W. Leng, Q. Zhang, Characteristics of MnO_2 catalytic ozonation of sulfosalicylic acid and propionic acid in water, Chemosphere 50 (2003) 1359-1364.

[18] F. P. Logemann, J. H. J. Année, Water treatment with a fixed bed catalytic ozonation process, Water Sci. Technol. 35 (1997) 353-360.

Chapter 7

Carbon xerogels and ceria-carbon xerogel materials as catalysts in the ozonation of organic pollutants[1]

Carbon xerogels prepared at different pH and ceria-carbon xerogel materials with different compositions and synthesized by different procedures were evaluated as catalysts in the ozonation of oxalic acid and the textile dye C. I. Reactive Blue 5. The prepared samples were characterized by N_2 adsorption at -196 °C, X-ray diffraction and scanning electronic microscopy. All the catalysts containing both cerium oxide and carbon xerogel removed all oxalic acid in solution after 1 h of reaction. Cerium oxide supported on carbon xerogel and carbon xerogel containing 1% of cerium oxide prepared by one-pot synthesis were the most active catalysts for the ozonation of the dye solution. Considering the catalytic activity and the steps involved in the preparation of materials, the carbon xerogel containing 1% of cerium oxide prepared by one-pot synthesis is the most promising catalyst.

[1] C. A. Orge, J. J. M. Órfão, M. F. R. Pereira, Carbon xerogels and ceria–carbon xerogel materials as catalysts in the ozonation of organic pollutants, Appl. Catal. B: Environ. 126 (2012) 22-28.

7 Carbon xerogels and ceria-carbon xerogel materials as catalysts in the ozonation of organic pollutants

7.1 Introduction

Ozone is widely used in water treatment as disinfectant and oxidant. Transformation of organic compounds occurs via direct reaction with ozone or indirectly with hydroxyl radicals ($HO^{\bullet}$), resulting from ozone decomposition in water [1]. Ozone reacts selectively with organic compounds attacking preferentially aromatic rings and unsaturated bonds, whereas $HO^{\bullet}$ is a less selective and more powerful oxidant. Despite several advantages of using ozone, there are a few disadvantages that limit its application in water treatment, such as the cost of generation and its highly selective oxidation power [2]. In order to overcome the latter problem, some ozone-based advanced oxidation processes have been developed; among them catalytic ozonation has received wide interest as a promising technology for removing refractory organic pollutants in water. Ozone combined with appropriate catalysts can improve the removal of taste, color and organic contaminants.

Porous carbon materials prepared by polycondensation of hydroxylated aromatics (phenol, catechol, resorcinol, hydroquinone or phloroglucinol) and aldehydes (formaldehyde or furfural) in a solvent followed by drying and pyrolysis have been extensively studied [3]. The nature of the precursors, the gelation conditions and the drying method determine the texture of the carbon material obtained. For the preparation of carbon xerogels the most common precursors are resorcinol and formaldehyde, and the polymer is usually synthesized using water as solvent and Na_2CO_3 as catalyst. Carbon xerogels present excellent properties, such as high specific surface area, porosity and conductivity, controllable average pore size and they can be prepared in the desired form (monolith, thin film and powder) [4].

An extended mineralisation was observed when Mn, Co or Ce oxides supported on activated carbon were used in the ozonation of sulfanilic acid, aniline and a reactive dye [5]. The association of ozone and carbon xerogels with different surface chemical properties was reported in a previous study [6], and an improvement of the TOC removal from dye solutions was observed, especially with the more basic material. In a recent work, the effect of the composition and the influence of the surface chemistry and textural properties of carbon materials in the catalytic activity of ceria-carbon composites were evaluated. It was concluded that ceria-carbon

xerogel composites presented better performance than carbon xerogel in the ozonation of oxalic acid [7].

The aim of this work is to study the ozonation of selected organic pollutants (oxalic acid and the textile dye CI Reactive Blue 5) in the presence of carbon xerogels with different properties, and ceria-carbon xerogel materials with different compositions and synthesized by different procedures (incipient wetness method, one-pot synthesis and precipitation method).

7.2 Experimental

7.2.1 Materials and characterization methods

Two organic molecules were selected for this study: oxalic acid (99%, Sigma-Aldrich) and a textile dye (CI Reactive Blue 5).

Different sets of catalysts were prepared. The first one consists of carbon xerogels prepared by the sol-gel process at different initial pH (identified as XC_pH=5.45, XC_pH=6.0 and XC_pH=6.25). The second set of catalysts correspond to cerium oxide supported by the incipient wetness method on the carbon xerogel synthesized at pH = 5.45, with 1, 5 and 10 wt% of CeO_2 (samples 1%Ce/XC_supported, 5%Ce/XC_supported and 10%Ce/XC_supported, respectively). In the scope of the present investigation, a novel catalyst with 1wt% of cerium oxide was also prepared by one-pot synthesis (1%Ce/XC_in situ). Finally, a composite with 10% of cerium oxide and 90% of the carbon xerogel prepared at pH=5.45 was synthesized by the precipitation method as described in a previous work [7] (sample 10%Ce/90%XC).

The synthesis of the carbon xerogel consisted in the policondensation of resorcinol (99%, Aldrich) with formaldehyde (37%, Aldrich), at an initially controlled pH [3, 4, 8]. Carbon xerogels prepared at pH = 5.45, pH = 6.0 and pH = 6.25 were synthesized in order to obtain materials with different textural properties. After setting the pH of the sol-gel process with NaOH solutions, polymerisation was carried out at 85 °C during 3 days. Then, the gel was ground and dried in an oven during 4 days (first day at 60 °C, second day at 80 °C, third day at 100 °C and fourth day at 120 °C). Finally, the material was carbonised under nitrogen flow at 800 °C using the following temperature program: from room temperature to 150 °C (hold 2 h) at 2 °C min^{-1}, 2 °C min^{-1} to 400 °C (hold 1 h), 2 °C min^{-1} to 600 °C (hold 1 h), 2 °C min^{-1} to 800 °C (hold 6 h) and cooling down to room temperature.

Ceria supported on carbon xerogel materials were prepared by the incipient wetness method from cerium nitrate solutions in order to obtain the contents of cerium oxide mentioned above. After drying at 100 ºC for 24 h, the samples were thermally treated in N_2 (50 cm^3 min^{-1}) at 400 ºC for 1 h.

The ceria - carbon xerogel prepared by one-pot synthesis was obtained by a procedure similar to that described for the carbon xerogel at pH=5.45, but resorcinol and formaldehyde were dissolved in water containing cerium nitrate ($Ce(NO_3)_3.6H_2O$), which concentration was calculated in order to obtain 1 wt% of cerium oxide in the prepared material. This synthesis was ceria – carbon xerogels with 5 and 10 wt% of cerium oxide were also prepared by one-pot synthesis. However, after characterization, it was possible to conclude that the introduction of large amounts of cerium nitrate before polymerisation destroys the carbon xerogel structure. Thus, these materials were not considered in this study.

The textural characterization of the materials was based on the corresponding N_2 equilibrium adsorption/desorption isotherms, determined at -196 °C with a Quantachrome Instruments NOVA 4200e apparatus. BET surface areas (S_{BET}), mesoporous surface areas ($S_{\neq \mu pores}$), micropore volumes ($V_{\mu pores}$) and average mesopore diameters obtained by the Barret, Joyner and Halenda (BJH) method were calculated. The relative amount of cerium oxide in the catalyst was determined by thermogravimetric analysis under air in a STA 409 PC/4/H Luxx Netzsch thermal analyser. The morphology and the semi-quantitative elemental analysis of the catalysts were obtained by scanning electron microscopy (SEM) and energy dispersive X-ray spectroscopy (EDS), respectively, in a JEOL JSM 35C/Noran Voyager system. XRD spectra were recorded on a Philips X'Pert MPD diffractometer (Cu Kα = 0.15406 nm).

7.2.2 Kinetic experiments

The removal of pollutants was investigated in a slurry lab-scale reactor equipped with agitation. In each experiment the reactor was filled with 700 cm^3 of pollutant solution ($C_{0,oxalic\ acid}$ = 1 mM, $C_{0,dye}$ =100 mg L^{-1}) at the natural pH ($pH_{0,oxalic\ acid} \approx 3.0$, $pH_{0,dye}$ = 5.5). Single ozonation and adsorption experiments were also carried out under similar conditions for comparison purposes. In adsorption and catalytic ozonation experiments, 350 mg of catalyst (particle size = 100 - 300 μm) were introduced in the reactor. Ozone was produced from pure oxygen in a BMT 802X ozone generator. The experiments were performed at constant total gas flow rate

(150 cm^3 min^{-1}) and constant inlet ozone concentration (50 g m^{-3}). The concentration of ozone in the gas phase was monitored with a BMT 964 ozone analyzer. Ozone in the gas phase leaving the reactor was removed in a series of gas washing bottles filled with potassium iodide solution. A stirring rate of 400 rpm was used in order to keep the reactor content perfectly mixed. In the adsorption tests, the ozone-containing stream was replaced by an oxygen stream. In the experiments carried out in the presence of *tert*-butanol, a concentration of 10 mM of this radical scavenger was used [9].

The concentration of oxalic acid was followed by HPLC using a Hitachi Elite Lachrom apparatus equipped with a diode array detector. The stationary phase was an Aminex HPX-87H column (300 mm x 7.8 mm) working at room temperature under isocratic elution with H_2SO_4 4 mM. Dye solution decolourisation was followed by UV-Vis spectrophotometry with a JASCO V-560 UV/Vis spectrophotometer at the maximum absorption wavelength (597 nm), previously determined. The degree of mineralisation was followed by total organic carbon (TOC) analysis in a Shimadzu TOC-5000A equipment.

7.3 Results and discussion

7.3.1 Characterization of the catalysts

The properties of the prepared materials are presented in Table 7.1.

The main differences among the carbon xerogels (XC) prepared at different initial pH are in the average mesopore diameter. The carbon xerogel prepared at pH = 5.45 has the largest mesopore sizes (d_{BJH} = 24.4 nm). The catalysts of cerium oxide supported on carbon xerogel and the composite present similar textural properties. The sample 1%Ce/XC_in situ has a specific surface area and an average mesopore diameter smaller than XC pH=5.45.

Table 7.1: Properties of the prepared samples.

Sample	S_{BET} ($m^2 g^{-1}$)	S_{meso} ($m^2 g^{-1}$)	V_{micro} ($cm^3 g^{-1}$)	d_{BJH}[a] (nm)	d_p (nm)
XC pH=6.25	540	168	0.192	3.2	-
XC pH=6.0	588	241	0.176	4.1	-
XC pH=5.45	566	233	0.165	24.4	-
1%Ce/XC_in situ	510	244	0.137	14.1	-
1%Ce/XC_supported	547	237	0.158	24.2	-
5%Ce/XC_supported	559	250	0.156	24.5	8.3[b]
10%Ce/XC_supported	558	249	0.159	25.9	9.2[b]
10%Ce/90%XC	573	228	0.174	24.3	3.6 (77.8%); 46 (22.2%)[c]

[a] average mesopore diameter obtained by the Barret, Joyner and Halenda (BJH) method applied to the desorption isotherm;

[b] crystallite diameters of CeO_2 determined by XRD analyses;

[c] crystallite diameters determined by XRD analyses using Rietveld refinement and the relative amount of each grain size.

Figure 7.1 shows the X-ray diffraction patterns of the prepared catalysts. According to the results, the dominant diffraction peaks are those characteristic of cerianite (CeO_2). The intensity of peaks in samples 1%Ce/XC_in situ and 1%Ce/XC_supported is low, since these catalysts only have 1 wt% of cerium oxide. Besides cerianite, the 10%Ce/90%XC composite also has secondary phases, which are identified by small peaks at 31.5º, 36º and 39º. Since this sample presents wide peaks, it is necessary to apply a model of two characteristic particle sizes (Rietveld refinement), instead of a model with a single particle size distribution. The values of crystallite diameters and the relative amount of each grain size are presented in Table 7.1. The 10%Ce/90%XC sample presents two different average sizes, i. e. particles with 3.6 and 46 nm, small particles being predominant. No significant differences between the crystallite diameters of the cerium oxide supported on carbon xerogel materials were observed (Table 7.1).

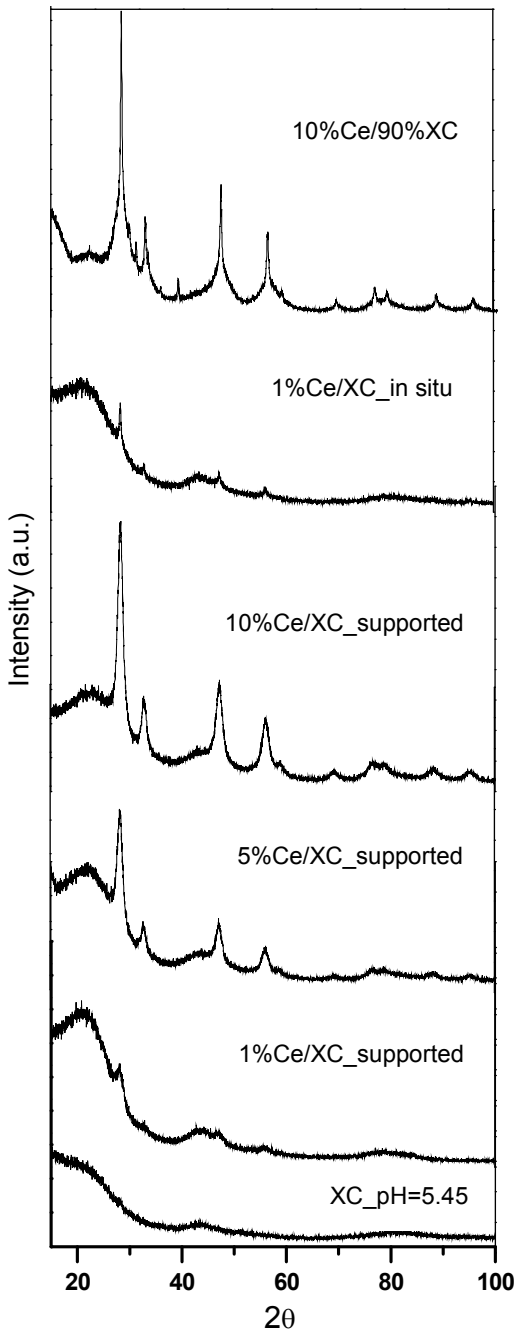

Figure 7.1: X-ray diffractograms of carbon xerogel XC_pH=5.45 and ceria – carbon xerogel materials.

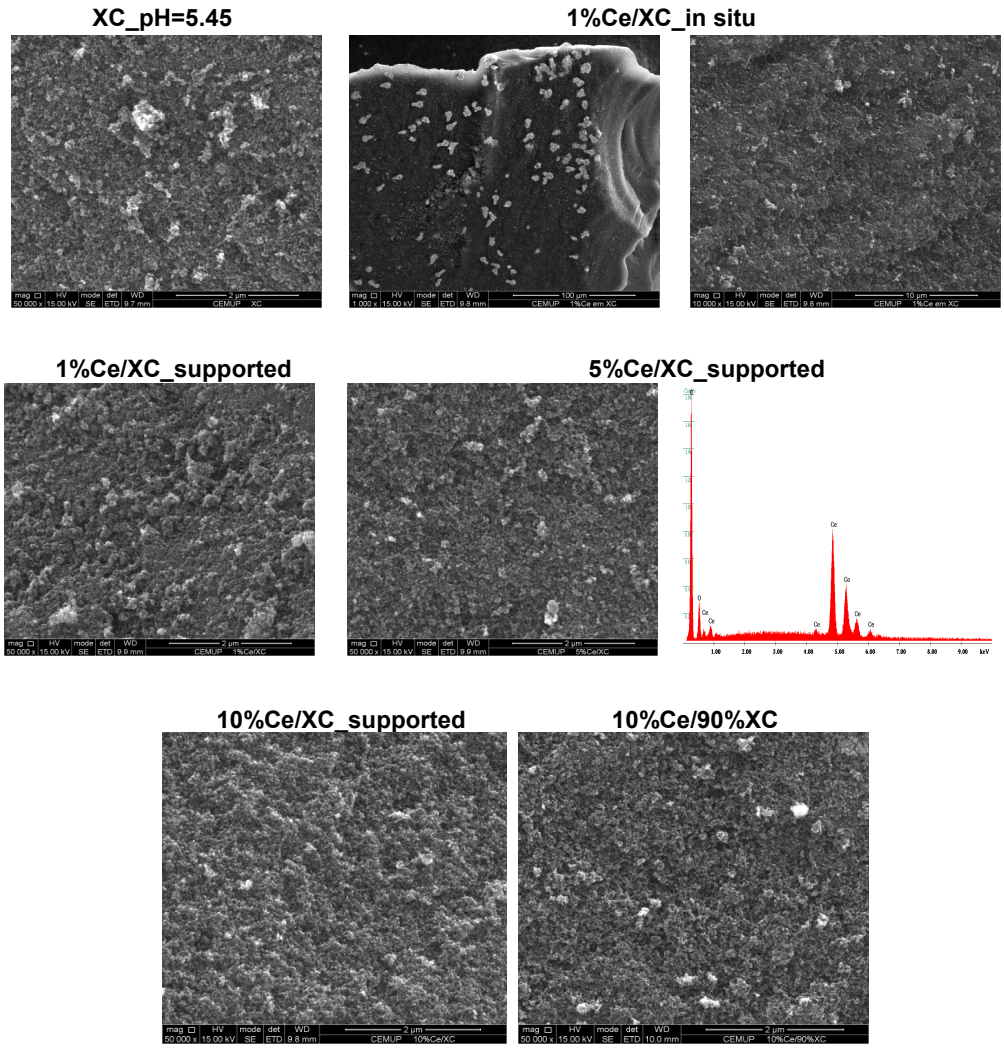

Figure 7.2: SEM images of the prepared materials and EDS analysis of the sample 5%Ce/XC_supported.

The morphology of the synthesized materials was examined by SEM and some representative images are depicted in Figure 7.2. Analyses of EDS were also performed (spectrum obtained with sample 5%Ce/XC_supported is included in Figure 7.2 as an example) with the aim of evaluating the presence of cerium in the prepared samples. Carbon xerogel and ceria – carbon xerogel materials present similar morphologies.

7.3.2 Kinetic results

7.3.2.1 Oxalic acid removal

Oxalic acid was selected for this study because it remains in solution after non-catalytic ozonation processes due to its high refractory character [10]. Figure 7.3 shows the results obtained for oxalic acid degradation by single ozonation and catalytic ozonation in the presence of the prepared materials. The kinetic results obtained with cerium oxide prepared by the precipitation method (Ce-O) were also included [7].

The addition of any of the prepared materials resulted in better performance than single ozonation and ozonation catalysed by cerium oxide, a total removal being achieved after 1 h of catalytic ozonation. The carbon xerogel prepared at pH = 6.25 showed a better performance than the other carbon xerogels, but no differences were observed between the carbon xerogels prepared at pH 6.0 and 5.45. The addition of cerium oxide to the carbon xerogel increased the catalytic activity, regardless of the preparation method. Ceria supported on carbon xerogel with more cerium oxide presented the best performance. No significant differences between catalysts with 1% of cerium oxide prepared by one-pot synthesis and prepared by the incipient wetness method were observed. The performance verified for the composite (10%Ce/90%XC) is slightly lower than that observed in the ozonation catalysed by 10% of cerium oxide supported on the carbon xerogel sample.

The absence of internal and external diffusional limitations was experimentally confirmed because there was no increase in the performance of the catalysts using smaller particles (dp < 50 μm) or higher stirring rates (700 rpm), respectively [11].

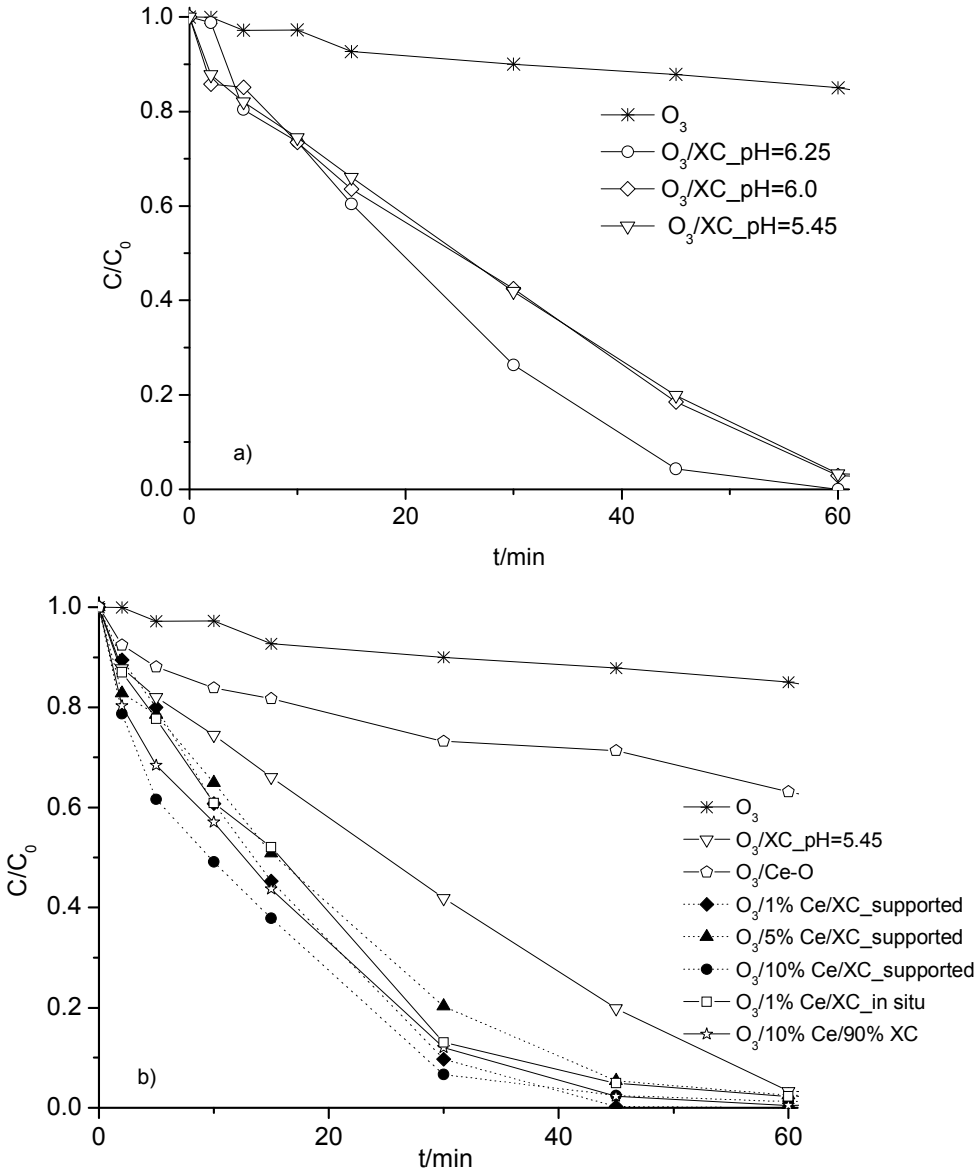

Figure 7.3: Evolution of the dimensionless concentration of oxalic acid during single ozonation and ozonation catalyzed by carbon xerogels prepared at different pH (a) and by cerium oxide and ceria – carbon xerogel materials (b).

7.3.2.2 Reactive dye removal

Textile industries are responsible for the discharge of large quantities of dyes into natural waterways due to inefficiencies in dyeing techniques [12]. Up to 50% of dyes are lost directly into watercourses when using reactive dyes [13]. The presence of dyes in the effluent, even at very low concentrations, could be highly visible and undesirable [14]. Coulored wastewater influences negatively the aesthetic nature of water and reduces light penetration through the water's surface, and also the photosynthetic activity of aquatic organisms. Moreover, textile wastewater contain toxic and potential carcinogenic substances and therefore they must be adequately treated [15]. There are several treatment methods that can be applied to textile effluents, involving biological, physical or chemical processes; however, conventional biological wastewater treatment methods are ineffective in removing the colour. On the contrary, ozone is frequently used for decolourising dye wastewater because it attacks, preferentially, aromatic structures and unsaturated bonds, such as dye chromophores, which are responsible for the colour.

Figure 7.4 presents the kinetic results of single and catalytic ozonation of the dye C. I. Reactive Blue 5. Total decolourisation is attained in less than 30 minutes when ozone is applied, and this time is practically independent of the presence of the catalysts. Single ozonation also originates a decrease in the concentration of TOC in solution; nevertheless, mineralisation occurs at a much lower rate than colour removal, which means that part of the dye degradation products (colourless) still remains in solution. The advantage of using a catalyst is clearly seen in the TOC removal, which is faster than that corresponding to single ozonation. In Figure 7.4 a) it is possible to verify that the catalytic activity of the carbon xerogels increases when the pH used in the preparation process decreases. This result may be explained by the larger mesopores obtained in the preparation at lower pH (see Table 7.1), which may allow an easier access of the dye, a bulky molecule, and primary degradation compounds to the interior of the pores.

With the exception of the composite prepared by the precipitation method, all catalyst containing cerium oxide and carbon xerogel showed better performances than the carbon xerogel prepared at pH = 5.45, and a complete mineralization was achieved after 2-3 h of reaction. The catalysts of cerium oxide supported on carbon xerogel had a similar performance, regardless of the amount of cerium oxide present. The catalysts prepared by one-pot synthesis (1%Ce/XC_in situ) led to total mineralization after 2 h of reaction. It is possible to conclude that the introduction of

cerium in the carbon xerogel, before or after polymerization, is very efficient for the complete mineralization of the reactive dye.

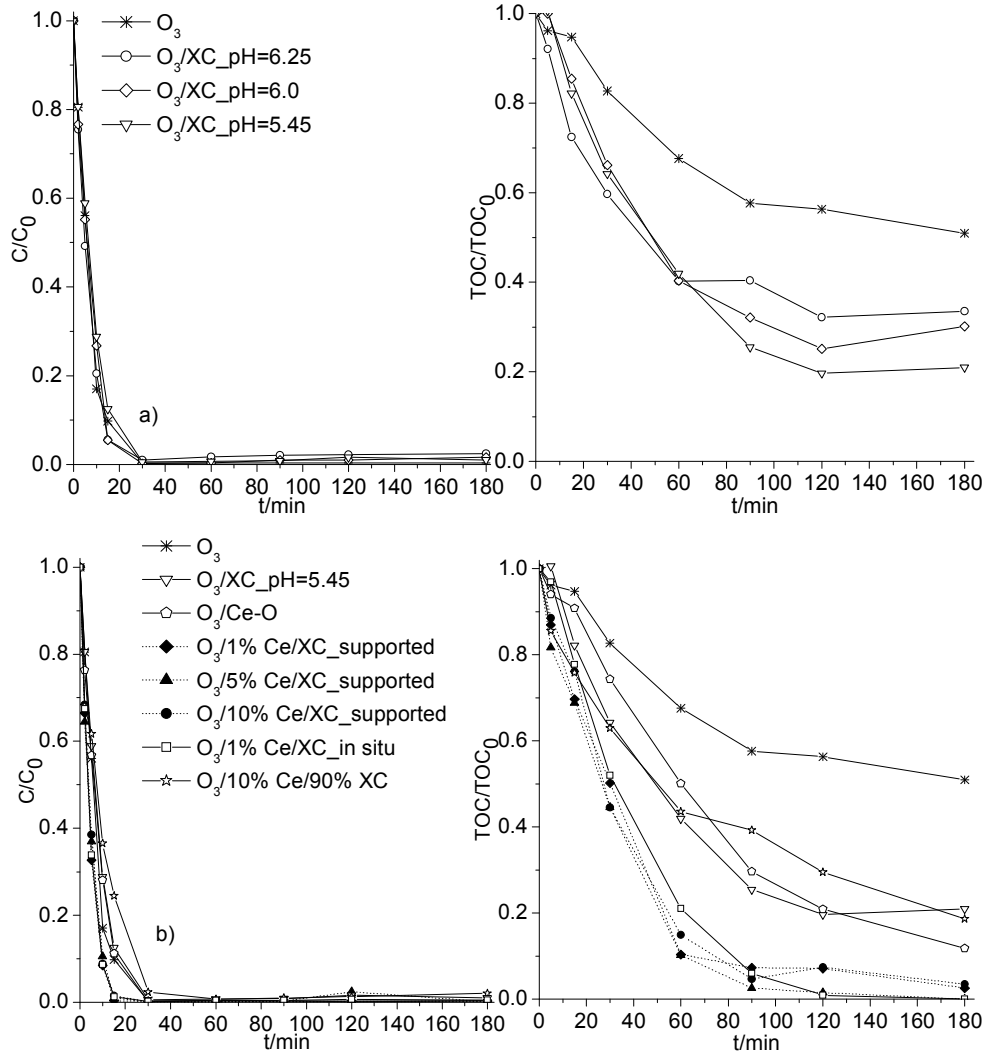

Figure 7.4: Colour and TOC removal for the reactive dye during single ozonation, and ozonation catalyzed by carbon xerogels prepared at different pH (a) and by cerium oxide and ceria - carbon xerogel materials (b).

7.3.3 Considerations on the reaction mechanism

In order to study if the ozonation of oxalic acid in the presence of the prepared catalysts involves $HO^{\bullet}$ radicals in the liquid phase, experiments of oxalic acid ozonation with 1%Ce_XC_supported, 1%Ce_XC_in situ and 10%Ce/90%XC were carried out in the presence of *tert*-butanol, a well known $HO^{\bullet}$ radical scavenger. Adsorption kinetics of oxalic acid were also determined on the same samples. The results obtained are presented in Figure 7.5.

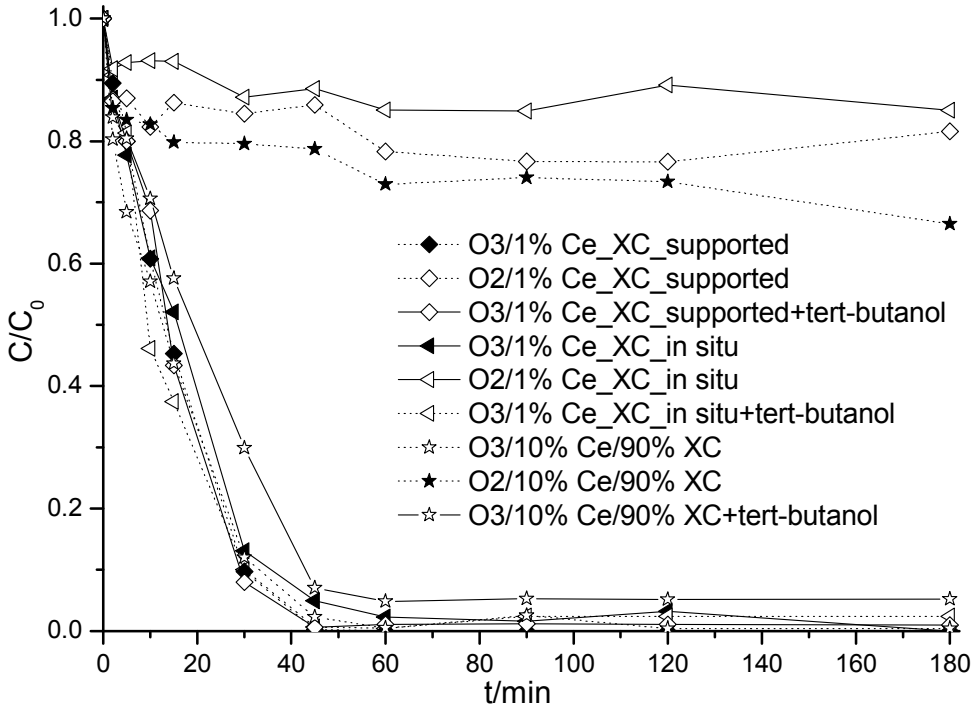

Figure 7.5: Evolution of the dimensionless concentration of oxalic acid during adsorption, catalytic ozonation and effect of *tert*-butanol ($C_{tert\text{-butanol}}$ = 10 mM).

The results show that ozonation catalysed by 1%Ce_XC_supported or by 1%Ce_XC_in situ is practically not affected by the presence of *tert*-butanol, which indicates that the oxidation of oxalic acid does not occur via $HO^{\bullet}$ radicals in the liquid bulk. On the other hand, a slightly decrease in the catalytic ozonation of oxalic acid in the presence of *tert*-butanol was observed when the ceria-activated carbon composite was used. In a previous work, where composites of cerium oxide and carbon materials were evaluated, a similar performance was observed, and it was

suggested that oxalic acid is oxidized mainly on the surface of the composite, which is due to the contribution of the carbon material [7]. Adsorption on 10%Ce/90%XC composite allowed an oxalic acid removal slightly higher than that verified with the other catalysts, the process being able to remove 34% after 3 h. Therefore, it is possible to conclude that organic compounds and ozone can adsorb and react on the surface of catalysts. Since the oxidation of oxalic acid in the presence of the prepared materials does not occur, at least significantly, by bulk reactions involving $HO^{\bullet}$ radicals, it is believed that the reaction mechanism comprises predominantly surface reactions.

With the aim of evaluating the eventual deactivation of the prepared materials during the ozonation experiments, five consecutive runs with sample 5%Ce/XC_supported were carried out with fresh oxalic acid solutions. The kinetic results presented in Figure 7.6 show that there is a significant decrease of the catalytic activity from the first to third run. After the fourth run no important differences were observed, and a complete oxalic acid mineralization was achieved after 90 min of reaction. According to the literature, the catalysts suffer a slight progressive oxidation by exposure to dissolved ozone and consequently the amount of oxygenated groups increases [16]. The amount of free electrons available on the catalyst surface decreases, since most of the oxygenated groups have the capacity of attracting them [17]. Then, the decrease observed in the activity of this sample in successive runs might be due to the introduction during reaction of electron-withdrawing oxygenated groups that reduce the electron density on the carbon basal planes. The role of the mentioned free electrons on the reaction mechanism was discussed elsewhere [7, 10, 18, 19] for different ceria and carbon containing catalysts.

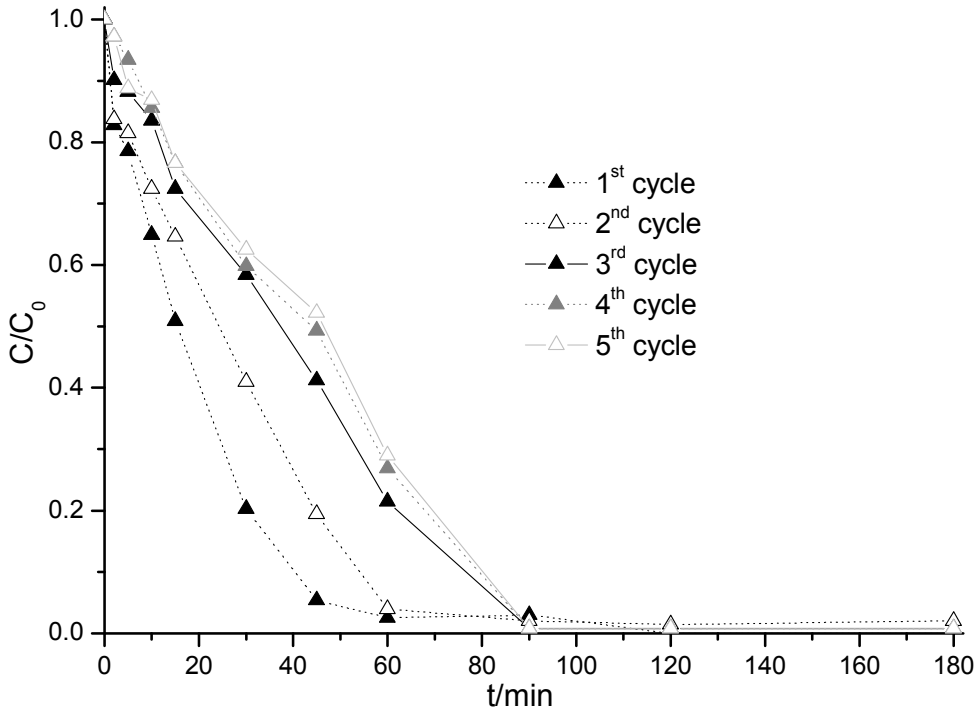

Figure 7.6: Evolution of the dimensionless concentration of oxalic acid in successive experiments with the 5 %Ce_XC_supported sample.

7.3.4 Selection of the best catalyst

In order to select the best catalyst it is necessary to evaluate several parameters. Considering the catalytic activity, as well as the time used in the preparation of the studied catalysts and the cost associated, the catalyst with 1 wt% of cerium oxide prepared by one-pot synthesis (1%Ce/XC_in situ) seems to be the best option. Although samples 1%Ce/XC_in situ and 1%Ce/XC_supported did not present different activities, the preparation of the catalyst of cerium oxide supported on carbon xerogel is longer and costly. Synthesis of ceria-supported on carbon xerogel requires two steps: preparation of carbon xerogel and ceria impregnation. Then, a carbonization of carbon xerogel and a final thermal treatment are necessary. On the other hand, 1%Ce/XC_in situ is prepared in one step, since the cerium precursor is introduced during the preparation of the carbon material, which requires less time and only one thermal treatment. Comparing with the composite, the sample prepared by one-pot synthesis remains the best material. In the case of oxalic acid, no significant differences were observed, but in the dye degradation the composite

had a worse performance. In addition to the synthesis of the composite being performed in two steps, which requires two thermal treatments, the amount of cerium precursor necessary to obtain the composite was larger, and therefore its preparation is more expensive.

7.4 Conclusions

Carbon xerogels with different textural properties and ceria-carbon xerogels materials with different compositions and synthesized by different routes were tested in the ozonation of oxalic acid and a reactive dye.

Pore sizes of carbon xerogels play a key role in the degradation of the selected pollutants: small pores are better for oxalic acid (small molecule) and the opposite is observed for the reactive dye (large molecule).

The catalyst prepared by one-pot synthesis and all materials of cerium oxide supported on carbon xerogel presented better performance than the carbon xerogel in the ozonation of oxalic acid and the reactive dye.

The reaction mechanism is expected to involve the oxidation of the organic compounds on the catalyst surface, since the presence of a radical scavenger did not change, at least significantly, the kinetic results.

Among the studied materials, the sample with 1 wt% of cerium oxide prepared by one-pot synthesis was considered the best catalyst: in addition to its high catalytic activity, the preparation method is easier and less expensive.

Acknowledgments

This work was supported by project PEst-C/EQB/LA0020/2011 financed by FEDER through COMPETE. C. A. O. acknowledges the grant received from FCT (BD/45809/2008). The authors are indebted to Dr. Pedro Tavares (UTAD) for assistance with XRD analysis.

References

[1] I. A. Katsoyiannis, S. Canonica, U. von Gunten, Efficiency and energy requirements for the transformation of organic micropollutants by ozone, O_3/H_2O_2 and UV/H_2O_2, Water Res. 45 (2011) 3811-3822.

[2] S. Tong, R. Shi, H. Zhang, C. Ma, Catalytic performance of Fe_3O_4-CoO/Al_2O_3 catalyst in ozonation of 2-(2,4-dichlorophenoxy)propionic acid, nitrobenzene and oxalic acid in water, J. Environ. Sci. 22 (2010) 1623-1628.

[3] N. Job, R. Pirard, J. Marien, J.-P. Pirard, Porous carbon xerogels with texture tailored by pH control during sol–gel process, Carbon 42 (2004) 619-628.

[4] N. Mahata, A. R. Silva, M. F. R. Pereira, C. Freire, B. de Castro, J. L. Figueiredo, Anchoring of a [Mn(salen)Cl] complex onto mesoporous carbon xerogels, J. Colloid Interface Sci. 311 (2007) 152-158.

[5] P. C. C. Faria, D. C. M. Monteiro, J. J. M. Órfão, M. F. R. Pereira, Cerium, manganese and cobalt oxides as catalysts for the ozonation of selected organic compounds, Chemosphere 74 (2009) 818-824.

[6] C. Orge, J. Sousa, F. Gonçalves, C. Freire, J. Órfão, M. Pereira, Development of Novel Mesoporous Carbon Materials for the Catalytic Ozonation of Organic Pollutants, Catal. Lett. 132 (2009) 1-9.

[7] C. A. Orge, J. J. M. Órfão, M. F. R. Pereira, Catalytic ozonation of organic pollutants in the presence of cerium oxide-carbon composites, Appl. Catal. B: Environ. 102 (2011) 539-546.

[8] N. Job, A. Théry, R. Pirard, J. Marien, L. Kocon, J. N. Rouzaud, F. Béguin, J. P. Pirard, Carbon aerogels, cryogels and xerogels: Influence of the drying method on the textural properties of porous carbon materials, Carbon 43 (2005) 2481-2494.

[9] F. J. Beltran, F. J. Rivas, L. A. Fernandez, P. M. Alvarez, R. Montero-de-Espinosa, Kinetics of Catalytic Ozonation of Oxalic Acid in Water with Activated Carbon, Ind. Eng. Chem. Res. 41 (2002) 6510-6517.

[10] P. C. C. Faria, J. J. M. Órfão, M. F. R. Pereira, A novel ceria-activated carbon composite for the catalytic ozonation of carboxylic acids, Catal. Commun. 9 (2008) 2121-2126.

[11] S. L. Pirard, C. Diverchy, S. Hermans, M. Devillers, J.-P. Pirard, N. Job, Kinetics and diffusional limitations in nanostructured heterogeneous catalyst with controlled pore texture, Catal. Commun. 12 (2011) 441-445.

[12] K. Turhan, I. Durukan, S. A. Ozturkcan, Z. Turgut, Decolorization of textile basic dye in aqueous solution by ozone, Dyes Pigments 92 (2012) 897-901.

[13] G. McMullan, C. Meehan, A. Conneely, N. Kirby, T. Robinson, P. Nigam, I. M. Banat, R. Marchant, W. F. Smyth, Microbial decolourisation and degradation of textile dyes, Appl. Micro. Biotech. 56 (2001) 81-87.

[14] P. Nigam, G. Armour, I. M. Banat, D. Singh, R. Marchant, Physical removal of textile dyes from effluents and solid-state fermentation of dye-adsorbed agricultural residues, Bioresource Technol. 72 (2000) 219-226.

[15] M. W. Chang, J. M. Chern, Decolorization of peach red azo dye, HF6 by Fenton reaction: Initial rate analysis, J. Taiwan Inst. Chem. Eng. 41 (2010) 221-228.

[16] P. C. C. Faria, J. J. M. Orfao, M. F. R. Pereira, Ozone Decomposition in Water Catalyzed by Activated Carbon: Influence of Chemical and Textural Properties, Ind. Eng. Chem. Res. 45 (2006) 2715-2721.

[17] J. L. Figueiredo, J. P. S. Sousa, C. A. Orge, M. F. R. Pereira, J. J. M. Órfão, Adsorption of dyes on carbon xerogels and templated carbons: influence of surface chemistry, Adsorption 17 (2011) 431-441.

[18] P. Faria, J. Órfão, M. Pereira, Mineralization of Substituted Aromatic Compounds by Ozonation Catalyzed by Cerium Oxide and a Cerium Oxide-activated Carbon Composite, Catal. Lett. 127 (2009) 195-203.

[19] P. C. C. Faria, J. J. M. Órfão, M. F. R. Pereira, Activated carbon and ceria catalysts applied to the catalytic ozonation of dyes and textile effluents, Appl. Catal. B: Environ. 88 (2009) 341-350.

Chapter 8

Perovskites as catalysts for the ozonation of selected organic compounds[1]

The ozonation of two model compounds (oxalic acid and dye C. I. Reactive Blue 5) was carried out in the presence of La containing perovskites prepared by the citrate method. With the exception of $LaFe_{0.9}Cu_{0.1}O_3$, ozonation catalysed by perovskites presented better performance than single ozonation in the case of oxalic acid, allowing a total degradation with some of the catalysts. In oxalic acid removal, the presence of lattice oxygen species on the perovskites surface plays an important role, while the introduction of Cu has a negative effect. $LaCoO_3$ was considered the best catalyst in oxalic acid degradation; in addition to its high activity, no metal leaching was observed. Regarding colour removal of dye solution, single ozonation was slightly more efficient than catalytic ozonation in the presence of $LaCoO_3$. On the other hand, ozonation catalysed by $LaCoO_3$ improved the TOC removal, allowing almost complete mineralisation of dye solution after 3 h of reaction.

[1] C. A. Orge, J. J. M. Órfão, M. F. R. Pereira, B. P. Barbero, L. E. Cadús, Perovskites as catalysts for the ozonation of selected organic pollutants, to be submitted (2012).

8 Perovskites as catalysts for the ozonation of selected organic compounds

8.1 Introduction

Perovskite have a general formula ABO_3, where A is usually a rare earth cation and B a transition metal cation [1]. This kind of material can tolerate substitutions at both cation sites with the crystal structure remaining unaltered. The substitution at A site with ions having lower valence can allow the formation of structural defects such as anionic or cationic vacancies and/or a change in the oxidation state of the transition metal cation to maintain the electroneutrality of the compound. When the oxidation state of B cation increases, the redox process generates larger amounts of available oxygen at low temperature and the overall oxidation activity is enhanced. Moreover, the oxygen vacancies favour the catalytic activity in oxidation reaction because they increase the lattice oxygen mobility [2]. The preparation method of perovskites is important both in defining suitable textural characteristics for catalysis and in achieving phases of great purity. The literature describes numerous synthesis methods, most of which involve synthesizing materials for applications other than catalysis and allow incorporation of cations into the functional perovskite structure due to the high calcination temperatures used. The most commonly technique used to overcome the problem of purity is the sol-gel citrate method. This method allows to obtain catalysts with high surface areas, but it has the drawback of sintering, which depends on the temperature [3]. Metal oxides with a perovskite structure have been consistently proposed during the last two decades as alternative catalysts for the total oxidation of methane and volatile organic compounds. The use of these materials has been especially promoted in applications involving high temperatures and oxygen steam-rich atmospheres, where their thermal stability comes into play [4].

Heterogeneous catalytic ozonation is gaining an increasing interest in the drinking water and wastewater treatment field [5]. The main advantages of this technique are the ability to enhance the rate of oxidation of organic compounds and especially to improve the mineralisation degree achieved at the end of the process [6]. Carbon materials, metal oxides and supported metal oxides have been proposed as effective ozonation catalysts, but only a few studies addressed the catalytic activity of perovskites on ozonation processes. Perovskite $LaTi_{0.15}Cu_{0.85}O_3$ was successfully used in the ozonation of pyruvic acid, a refractory substance typically generated

after oxidation of phenol-like compounds [7], and in the ozonation of gallic acid [8]. The same perovskite was evaluated in the ozonation of different phenolic wastewaters and the catalytic activity and stability were confirmed by consecutive experiments [9]. More recently, a perovskite containing copper was appointed as a very efficient catalysts to improve TOC removal in the ozonation of sulfamethoxazole, a sulfonamide type synthetic antibiotic [10].

In this work, a wide range of La-containing perovskites prepared by the citrate method and characterized by different techniques were used to investigate the catalytic ozonation of oxalic acid and the reactive dye C. I. Reactive Blue 5.

8.2 Experimental

8.2.1 Catalysts preparation and characterization

Perovskites were prepared by the citrate method as described by Merino et al. [1]. Summarizing, aqueous solutions of the metal nitrates were added to the solution of citric acid, and then stirred for 15 min. The resulting solution was concentrated by slowly evaporating water under vacuum in a rotavapor at 75 °C until a gel was obtained. The gel was dried in an oven, slowly increasing the temperature to 200 °C and maintaining this temperature overnight, to produce a solid amorphous citrate precursor, which was then milled and calcined in air at 700 °C for 2 h.

Perovskites were characterized by a wide range of techniques as reported elsewhere [1]. Briefly, BET specific surface areas were calculated from N_2 adsorption isotherms at -196 °C obtained in a Micromeritics Accusorb 2100E apparatus. The elemental composition was determined by inductively coupled plasma-optical emission spectroscopy (ICP-OES). XRD patterns were recorded at room temperature with a Rigaku diffractometer operated at 30 kV and 20 mA and Ni-filtered Cu-Kα radiation (λ = 0.15418 nm). Temperature-programmed reduction (TPR) experiments were performed in a quartz reactor with a TCD detector; samples were pretreated in helium and the temperature was increased from room temperature to 700 °C under a reducing atmosphere of 5% H_2/N_2. XPS spectra were recorded on a VG Scientific ESCALAB 200A spectrometer and XPS data were fitted using the software XPSpeak.

8.2.2 Kinetics experiments

Two organic molecules were selected for this study: a carboxylic acid (oxalic acid, 99%, Sigma-Aldrich) and a textile dye (CI Reactive blue 5). Their main characteristics are shown in Table 8.1.

Table 8.1: Main characteristics of selected pollutants.

Compound		M (g mol^{-1})	pKa	$\lambda_{max.}$(nm)
Oxalic acid ($C_2H_2O_4$)	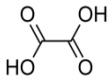	90.04	1.23, 4.19	-
Dye Cibacron Blue BR ($C_{29}H_{20}ClN_7O_{11}S_3$)	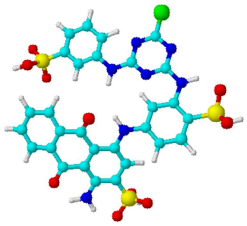	74.16	-	597

Ozonation of pollutants was investigated in a slurry lab-scale reactor equipped with agitation. In each experiment the reactor was filled with 700 cm^3 of pollutant solution ($C_{0,oxalic\ acid}$ = 1 mM, $C_{0,\ dye}$ = 50 mg L^{-1}) at the natural pH ($pH_{0,\ oxalic\ acid}$ = 3.0, $pH_{0,\ dye}$ = 5.5). In the catalytic ozonation experiments, 100 mg of catalyst (dp < 100 µm) were introduced in the reactor. Ozone was produced from pure oxygen in a BMT 802X ozone generator. The experiments were performed at constant gas flow rate (150 cm^3 min^{-1}) and constant inlet ozone concentration (50 g m^{-3}). The concentration of ozone in the gas phase was monitored with a BMT 964 ozone analyzer. Ozone in the gas phase leaving the reactor was removed in a series of gas washing bottles filled with iodide potassium solution. The agitation was maintained constant in order to keep the reactor content perfectly mixed. In the experiments carried out in the presence of *tert*-butanol, a concentration of 10 mM of this radical scavenger was used [11].

The concentration of oxalic acid was followed by HPLC using a Hitachi Elite Lachrom HPLC equipped with a diode array detector. The stationary phases was an Aminex HPX-87H column (300 mm x 7.8 mm), working at room temperature under isocratic elution with H_2SO_4 4 mM. The concentration of dye in the solution was

followed by UV-Vis spectrophotometry with a JASCO V-560 UV/Vis spectrophotometer. The degree of mineralisation was determined by total organic carbon (TOC) analysis in a Shimadzu TOC-5000A Analyser.

8.3 Results

8.3.1 Catalysts characterization

Perovskites were characterized by several techniques. Table 8.2 presents the BET surface area and the percentage of lattice oxygen species (O^{2-}) on the surface of the prepared perovskites. La-containing perovskites have BET surface areas between 7 and 15 $m^2\ g^{-1}$. $LaFeO_3$ presents the highest BET surface area and the introduction of Cu decreases this value. The study of the catalysts surface by XPS was carried out as described in [12]. XPS analyses of selected samples allow to conclude that oxygen vacancies exist on perovskite surface, except on $LaFeO_3$. $LaAl_{0.9}Cu_{0.1}O_3$ has the largest amount of lattice oxygen species on surface; however no important differences between the samples were observed.

Figure 8.1 shows the TPR profiles of La-containing perovskites. $LaMnO_3$ has a splitted signal with a maximum at around 400 °C. $LaCoO_3$ has two reduction stages, one between 350 and 450 °C and the other at around 600 °C [1]. Sample $LaNiO_3$ presents two peaks, the first corresponds to the reduction of Ni^{3+} ions in $LaNiO_3$ to yield the $La_2Ni_2O_5$ phase, with a loss of oxygen from the structure, and the second peak with a maximum consumption of H_2 between 500 and 600 °C leads to nickel deposited on lanthanum oxide [13]. $LaFeO_3$ does not show any reduction peak in this temperature range. Samples $LaFe_xCu_{1-x}O_3$ and $LaAl_xCu_{1-x}O_3$ present a signal at approximately 300 °C, which corresponds to the Cu reduction.

Table 8.2: BET surface areas and percentage of lattice oxygen species of La-containing perovskites.

Perovskite	S_{BET} ($m^2\ g^{-1}$)	% O^{2-} (lattice)[a]
$LaFeO_3$	15.2	0
$LaNiO_3$	9.8	N. D.
$LaCoO_3$	7.4	39.4*
$LaMnO_3$	14.6	N. D.
$LaFe_{0.9}Cu_{0.1}O_3$	10.5	46.3
$LaFe_{0.7}Cu_{0.3}O_3$	11.5	41.8
$LaAl_{0.9}Cu_{0.1}O_3$	6.9	57.4
$LaAl_{0.7}Cu_{0.3}O_3$	8.4	48.1
$La_{0.8}Ce_{0.2}Al_{0.7}Cu_{0.3}O_3$	N. D.	-

[a] determined by O 1s XPS peak deconvolution.

* value from [12].

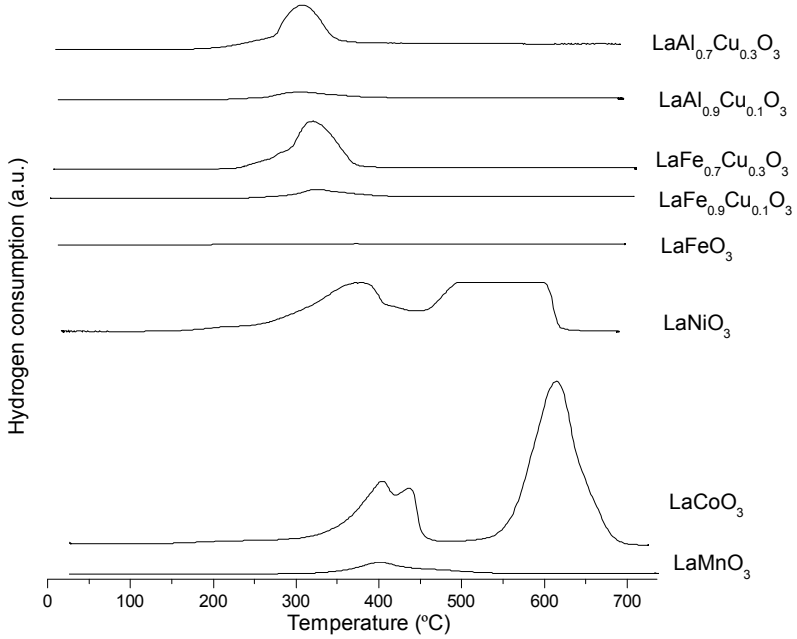

Figure 8.1: Temperature programmed reduction profiles of La-containing perovskites.

The XRD diffractograms of the prepared catalysts are depicted in Figure 8.2. $LaFe_xCu_{1-x}O_3$ samples present the same diffraction peaks as $LaFeO_3$, but a shift to higher angles is observed. This displacement suggest that Cu may be present as Cu^{3+}, since the diameter of Fe^{3+} is bigger than Cu^{3+}. As the diameter of Fe^{3+} is smaller than Cu^{2+}, the shift would be to lower angles in this case. $LaAl_xCu_{1-x}O_3$ samples have a diffractogram similar to $LaAlO_3$ [14], but displacement to lower angles is verified, which suggests that Cu is present as Cu^{2+}, whose diameter is bigger than Al^{3+}. The catalyst $La_{0.8}Ce_{0.2}Al_{0.7}Cu_{0.3}O_3$ is amorphous.

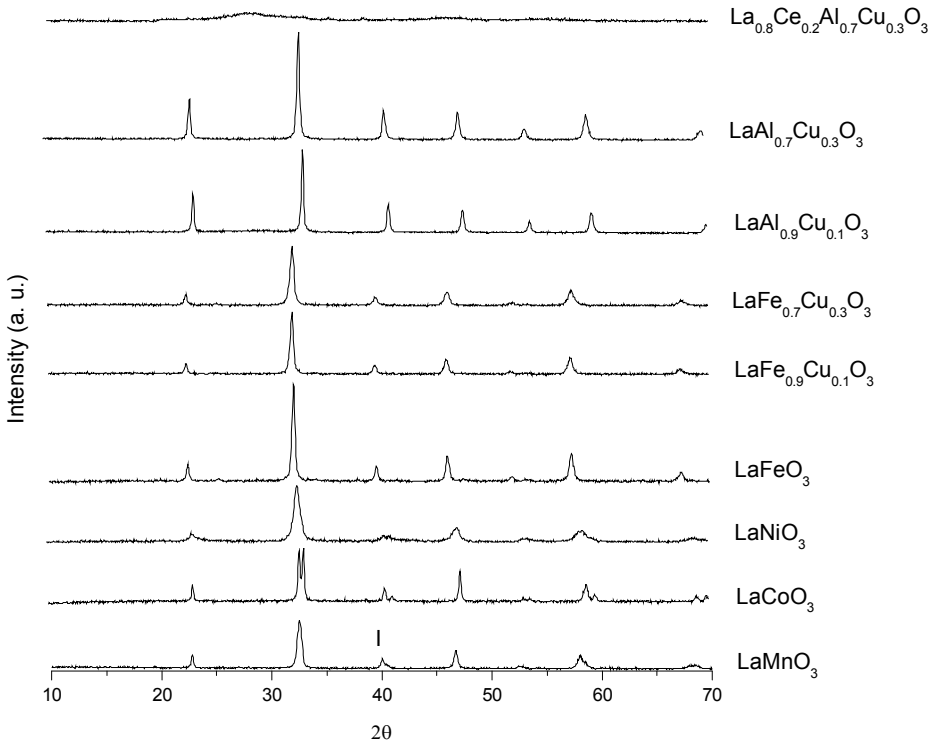

Figure 8.2: X-ray diffractograms of samples.

8.3.2 Oxalic acid removal

Oxalic acid was selected for this study because it is one of the most important final products of non-catalytic oxidation processes, with a high refractory character relatively to single ozonation [15]. The ozonation of oxalic acid was carried out at the natural pH of solutions, which is ca. 3. Figure 8.3 presents the results obtained

for its degradation by single ozonation and catalytic ozonation in the presence of perovskites.

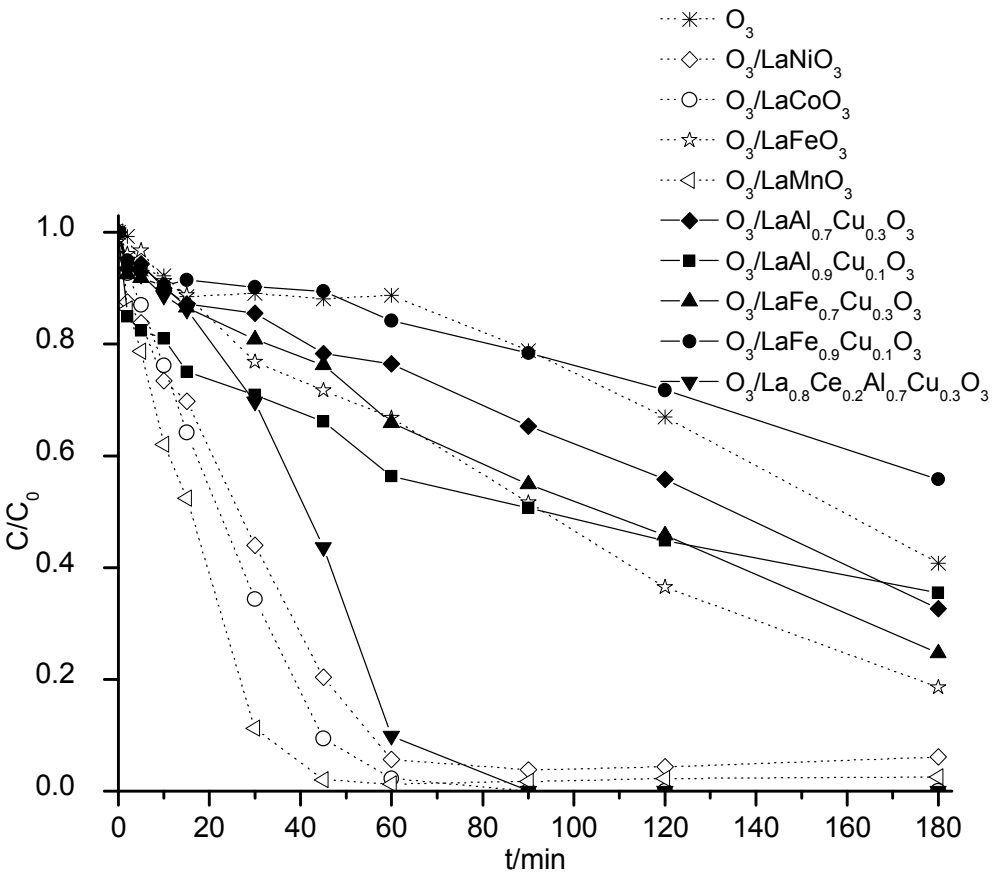

Figure 8.3: Oxalic acid removal by single ozonation and catalytic ozonation in the presence of perovskites (C_0 = 1mM, $m_{catalyst}$ = 100 mg).

With the exception of $LaFe_{0.9}Cu_{0.1}O_3$ all catalysts allow better performances than single ozonation, and complete removal was achieved in the presence of $LaMnO_3$, $LaCoO_3$, $LaNiO_3$ and $La_{0.8}Ce_{0.2}Al_{0.7}Cu_{0.3}O_3$. Perovskites formed by La and a transition metal (open symbols) show higher catalytic activities than the other samples, except $LaFeO_3$ which is the only sample without lattice oxygen species on the surface. $LaMnO_3$ presents the best performance; however, a small amount of metal leaching during the reaction was observed. In spite of the low BET surface area, $LaCoO_3$ presents a high performance, since it has oxygen vacancies on its

surface. Comparing samples $LaAl_{0.7}Cu_{0.3}O_3$ and $La_{0.8}Ce_{0.2}Al_{0.7}Cu_{0.3}O_3$, it is verified that the catalytic activity increases when part of lanthanum is exchanged with cerium. The higher performance verified in $La_{0.8}Ce_{0.2}Al_{0.7}Cu_{0.3}O_3$ may be explained by the presence of different amorphous phases in its structure. Although $LaAl_{0.9}Cu_{0.1}O_3$ presents better catalytic activity than $LaAl_{0.7}Cu_{0.3}O_3$, no differences were observed after 3 h of reaction. $LaFe_xCu_{1-x}O_3$ perovskites show a worse performance than $LaFeO_3$, which means that the introduction of Cu has a negative effect in the catalytic activity.

The ozonation of organic compounds involves a number of complex reactions and many mechanistic approaches have been presented in the literature. In general, the proposed mechanisms of ozonation catalysed by metal oxides assume that the adsorption of organic molecules and ozone takes place on the surface of the catalyst [16]. Ozone interaction with the metal oxide surface results in the formation of free radicals that can initiate a radical chain type reaction, both on the surface of the catalyst and in the liquid phase, leading to the production of $HO^{\bullet}$ radicals [5, 17]. There is few reported information about catalytic activity of perovskite type catalysts on ozonation processes. Rivas et al. observed a positive effect in pyruvic acid removal when *tert*-butanol was added in the ozonation catalysed by $LaTi_{0.15}Cu_{0.85}O_3$ and then, they suggested that the reaction took place on the solid surface [7]. This was experimentally confirmed by direct measurements of dissolved ozone in the presence and absence of the scavenger. Addition of *tert*-butanol had no effect in gallic acid removal in ozonation catalysed by the same perovskite, although its presence decreases the mineralisation degree achieved [8]. Thus, it was suggested that free radicals play an important role in the mineralisation process and/or the scavenger adsorbs onto the solid avoiding the adsorption of gallic acid and intermediates. Beltrán et al. considered a possible mechanism to explain the TOC removal of sulfamethoxazole solutions observed in the ozonation catalysed by $LaTi_{0.15}Cu_{0.85}O_3$ and $LaTi_{0.15}Co_{0.85}O_3$ [10]. Ozone adsorption on the catalyst surface to yield superoxide ion species (by metal-ozone electron transfer), which eventually lead to hydrogen peroxide or react with ozone to generate hydroxyl radicals [18], was considered in the kinetic study.

Additional experiments were performed in order to investigate the catalytic activity and the mechanism of oxalic acid ozonation in the presence of perovskites. $LaMnO_3$ was chosen for supplementary reactions, since it allowed complete oxalic acid degradation. With the aim of evaluating the eventual deactivation of the sample

during the ozonation experiments, three consecutive runs were carried out with fresh oxalic acid solutions.

The kinetic results presented in Figure 8.4 show that a slightly decrease in the catalytic activity of $LaMnO_3$ from the first to the second run was observed, while no differences were noticed between the second and third cycles (total removal was achieved after 2 h of reaction). Concluding, sample $LaMnO_3$ remained highly active after 3 runs.

Replicated experiments of oxalic acid removal in the presence of $LaMnO_3$ were carried out in order to evaluate the reproducibility of the results. The corresponding curves in Figure 8.4 confirm the reproducibility of the results, since no differences were observed.

Since a small metal leaching was observed during ozonation catalysed by $LaMnO_3$, an experiment using the aqueous solution obtained after the catalytic reaction was carried out with the aim of evaluating the contribution of the leached metal in oxalic acid removal. Similar oxalic acid removal was observed with this solution and single ozonation, which suggests that the Mn leached is not the principal responsible for the catalytic activity observed with sample $LaMnO_3$.

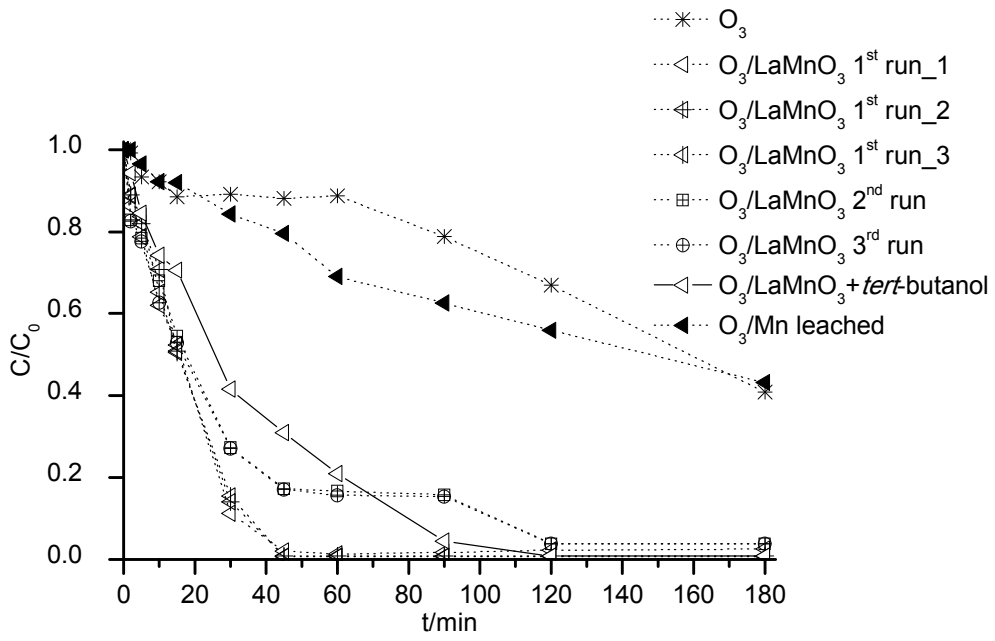

Figure 8.4: Evolution of dimensionless concentration of oxalic acid during catalytic ozonation, effect of *tert*-butanol, cyclic experiments and reproducibility tests using $LaMnO_3$ (C_0 = 1mM, $m_{catalyst}$ = 100 mg, $C_{tert\text{-butanol}}$ = 10 mM).

In order to study if the ozonation of oxalic acid in the presence of perovskites involves only $HO^{\bullet}$ radicals in the liquid phase, one experiment with $LaMnO_3$ was carried out in the presence of *tert*-butanol, a well known $HO^{\bullet}$ radical scavenger. The results show that ozonation catalysed by $LaMnO_3$ is slightly inhibited in the presence of *tert*-butanol; nevertheless, the catalyst still has significant activity, leading to complete mineralisation after 2 h of reaction. These experimental observations indicate that, in these conditions, oxidation via $HO^{\bullet}$ radicals in the liquid bulk occurs, but it is expected that surface reactions play also an important role in catalytic ozonation. Therefore, it is believed that the reaction mechanism comprises both surface reactions and liquid bulk reactions involving $HO^{\bullet}$ radicals.

8.3.3 Reactive dye ozonation

Research on the decolourisation of textile effluents has been often focused on reactive dyes for three reasons. First, reactive dyes represent an increasing market share; second, a large fraction of the applied reactive dyes is wasted because of dye hydrolysis in the alkaline dyebaths; and third, conventional wastewater

treatment plants have a low removal efficiency for reactive and other anionic soluble dyes, which leads to coloured waterways, and public complaints [19]. Therefore, there is a demand for the development of practical and highly efficient technologies for treatment of dye-containing wastewater [20]. The use of ozone in textile effluent treatment appears as a very attractive alternative with considerable application potential. Ozone is a powerful oxidizing agent ($E°$ = 2.08 V), and can react with several classes of compounds by direct or indirect reactions. Chromophore groups generally correspond to conjugated double bonds that can be broken by ozone (directly or indirectly) forming smaller molecules, which decreases the colour intensity of the effluent [21]. Non-catalytic ozonation is a powerful process for the degradation of dyes since ozone has the ability to selectively react with chromophores, leading to high and fast colour removal [22].

As reported in the previous section, oxalic acid is a small molecule and it has been identified as one of the most common final oxidation products refractory to single ozonation. In order to evaluate the catalytic activity of perovskites with bulky molecules, the dye C. I. Reactive Blue 5 was selected as model compound. For that study, the best catalyst in oxalic acid degradation was chosen. According to the data depicted in Figure 8.3, $LaMnO_3$ presented the best performance; however, small metal leaching was observed during catalytic ozonation. Therefore, $LaCoO_3$ was selected for this study, since it shown high catalytic activity (total removal was attained after 2 h of reaction) and no leaching of metal was observed during oxalic acid removal. Figure 8.5 shows the kinetic results of single ozonation and catalytic ozonation in the presence of $LaCoO_3$ for the decolourisation and mineralisation of the reactive dye C. I. Reactive Blue 5.

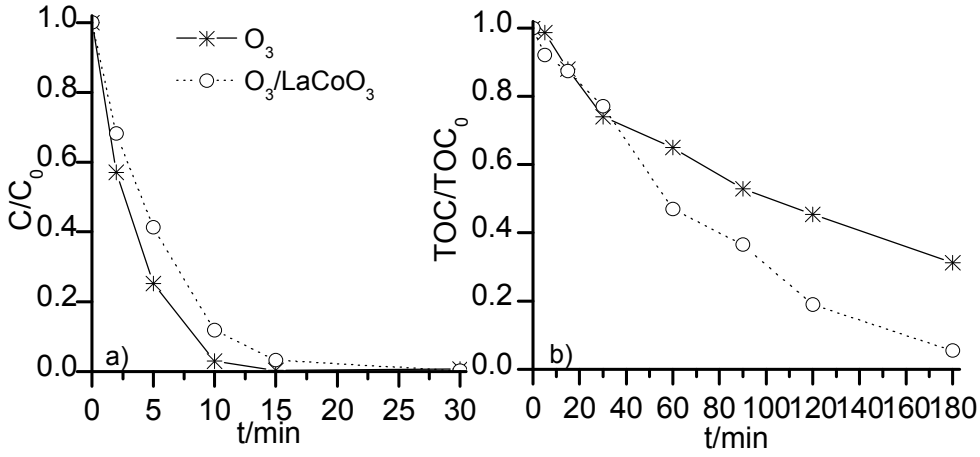

Figure 8.5: Colour degradation (a) and dimensionless TOC (b) for the reactive dye during single ozonation and using $LaCoO_3$ as catalyst.

The complete decolourisation of solution can be accomplished by single ozonation in a short reaction period (approximately 10 min). Ozonation catalysed by $LaCoO_3$ presented a slightly slower decolourisation rate, but complete colour removal was achieved after ca. 15 min of reaction. Ozone is a strong oxidant that selectively attacks the chromophore groups of dye molecules, and colour removal is easily attained by single ozonation [23]. However, the mineralisation rate of solutions of this type of compounds is generally low [24]. When a catalysts is added, the formation of $HO^{\bullet}$ radicals is promoted, but this strong oxidant is less selective than ozone. Thus, in the catalytic ozonation, the $HO^{\bullet}$ radicals formed attack both dye and intermediates, while in single ozonation, ozone is selective to chromophore groups, which originates a faster decolourization. Single ozonation also originates a decrease in the amount of TOC in solution, leading to a mineralisation degree close to 70% after 3 h of reaction. Nevertheless, this mineralisation is lower than colour removal, which is an indication that some of the dyes degradation products (colourless) still remain in solution. The advantage of using a catalyst is seen in the TOC removal, which is faster than that obtained by non-catalytic ozonation. Catalytic ozonation in the presence of $LaCoO_3$ allowed an almost complete mineralisation after 3 h of reaction.

8.4 Conclusions

In this study, the use of lanthanum containing perovskites synthesised by the citrate method as ozonation catalysts was reported.

With the exception of $LaFe_{0.9}Cu_{0.1}O_3$, the perovskites tested as catalyst in oxalic acid ozonation showed better performances than single ozonation. Perovskites formed by La and a transition metal presented higher catalytic activities than the other perovskites, with the exception of $LaFeO_3$. The presence of lattice oxygen vacancies plays an important role in the degradation rate, while the introduction of copper in perovskites has a negative effect. It is suggested that reactions in the liquid phase and surface reactions are responsible for the catalytic activity observed. $LaCoO_3$ was considered the best catalyst, since it allowed fast oxalic acid degradation and no leaching of metal was observed, contrarily to sample $LaMnO_3$, which also presents a good performance.

Single ozonation allowed a complete colour removal of the reactive dye in a few minutes. Catalytic ozonation in the presence of $LaCoO_3$ enhanced the mineralisation of the dye solution, leading a TOC removal close to 100% after 3 h. However, no improvement was observed in the rate of colour removal

Acknowledgements

This work was supported by project PEst-C/EQB/LA0020/2011, financed by FEDER through COMPETE. C. A. O. acknowledges the grant received from FCT (BD/45809/2008).

References

[1] N. A. Merino, B. P. Barbero, P. Grange, L. E. Cadús, $La_{1-x}Ca_xCoO_3$ perovskite-type oxides: preparation, characterisation, stability, and catalytic potentiality for the total oxidation of propane, J. Catal. 231 (2005) 232-244.

[2] B. P. Barbero, J. A. Gamboa, L. E. Cadús, Synthesis and characterisation of $La_{1-x}Ca_xFeO_3$ perovskite-type oxide catalysts for total oxidation of volatile organic compounds, Appl. Catal. B: Environ. 65 (2006) 21-30.

[3] N. A. Merino, B. P. Barbero, P. Ruiz, L. E. Cadús, Synthesis, characterisation, catalytic activity and structural stability of LaCo1−yFeyO3±λ perovskite catalysts for combustion of ethanol and propane, J. Catal. 240 (2006) 245-257.

[4] G. Pecchi, P. Reyes, R. Zamora, C. Campos, L. E. Cadús, B. P. Barbero, Effect of the preparation method on the catalytic activity of La1−xCaxFeO3 perovskite-type oxides, Catal. Today 133-135 420-427.

[5] B. Legube, N. K. V. Leitner, Catalytic ozonation: a promising advanced oxidation technology for water treatment, Catal. Today 53 (1999) 61-72.

[6] F. J. Beltrán, Ozone reaction kinetics for water and wastewater systems Lewis Publishers, Boca Raton, Florida (2004).

[7] F. J. Rivas, M. Carbajo, F. J. Beltrán, B. Acedo, O. Gimeno, Perovskite catalytic ozonation of pyruvic acid in water: Operating conditions influence and kinetics, Appl. Catal. B: Environ. 62 (2006) 93-103.

[8] M. Carbajo, F. J. Beltrán, F. Medina, O. Gimeno, F. J. Rivas, Catalytic ozonation of phenolic compounds: The case of gallic acid, Appl. Catal. B: Environ. 67 (2006) 177-186.

[9] M. Carbajo, F. J. Beltrán, O. Gimeno, B. Acedo, F. J. Rivas, Ozonation of phenolic wastewaters in the presence of a perovskite type catalyst, Appl. Catal. B: Environ. 74 (2007) 203-210.

[10] F. J. Beltrán, P. Pocostales, P. M. Álvarez, F. López-Piñeiro, Catalysts to improve the abatement of sulfamethoxazole and the resulting organic carbon in water during ozonation, Appl. Catal. B: Environ. 92 (2009) 262-270.

[11] F. J. Beltran, F. J. Rivas, L. A. Fernandez, P. M. Alvarez, R. Montero-de-Espinosa, Kinetics of Catalytic Ozonation of Oxalic Acid in Water with Activated Carbon, Ind. Eng. Chem. Res. 41 (2002) 6510-6517.

[12] N. A. Merino, B. P. Barbero, P. Eloy, L. E. Cadús, $La_{1-x}Ca_xCoO_3$ perovskite-type oxides: Identification of the surface oxygen species by XPS, Appl. Surf. Sci. 253 (2006) 1489-1493.

[13] G. Pecchi, M. G. Jiliberto, E. J. Delgado, L. E. Cadús, J. L. G. Fierro, Effect of B-site cation on the catalytic activity of La1−xCaxBO3 (B = Fe, Ni) perovskite-type oxides for toluene combustion, J. Chem. Technol. Biotechnol. 86 (2011) 1067-1073.

[14] L. E. Cadús, personal communication.

[15] P. C. C. Faria, J. J. M. Órfão, M. F. R. Pereira, Activated carbon catalytic ozonation of oxamic and oxalic acids, Appl. Catal. B: Environ. 79 (2008) 237-243.

[16] F. P. Logemann, J. H. J. Année, Water treatment with a fixed bed catalytic ozonation process, Water Sci. Technol. 35 (1997) 353-360.

[17] C. Cooper, R. Burch, An investigation of catalytic ozonation for the oxidation of halocarbons in drinking water preparation, Water Res. 33 (1999) 3695-3700.

[18] K.M. Bulanin, J.C. Lavalley, A. A. Tsyganenko, Infrared Study of Ozone Adsorption on TiO_2 (Anatase), J. Phys. Chem. 99 (1994) 10294–10299.

[19] P. C. Vandevivere, R. Bianchi, W. Verstraete, Treatment and reuse of wastewater from the textile wet-processing industry: Review of emerging technologies, J. Chem. Technol. Biotechnol. 72 (1998) 289-302.

[20] Y. Peng, D. Fu, R. Liu, F. Zhang, X. Xue, Q. Xu, X. Liang, NaNO2/FeCl3 dioxygen recyclable activator: An efficient approach to active oxygen species for degradation of a broad range of organic dye pollutants in water, Appl. Catal. B: Environ. 79 (2008) 163-170.

[21] E. Oguz, B. Keskinler, Z. Çelik, Ozonation of aqueous Bomaplex Red CR-L dye in a semi-batch reactor, Dyes Pigments 64 (2005) 101-108.

[22] P. C. C. Faria, J. J. M. Órfão, M. F. R. Pereira, Activated carbon and ceria catalysts applied to the catalytic ozonation of dyes and textile effluents, Appl. Catal. B: Environ. 88 (2009) 341-350.

[23] P. C. C. Faria, D. C. M. Monteiro, J. J. M. Órfão, M. F. R. Pereira, Cerium, manganese and cobalt oxides as catalysts for the ozonation of selected organic compounds, Chemosphere 74 (2009) 818-824.

[24] P. C. C. Faria, J. J. M. Órfão, M. F. R. Pereira, Mineralisation of coloured aqueous solutions by ozonation in the presence of activated carbon, Water Res. 39 (2005) 1461-1470.

Chapter 9

Benchmarking of selected catalysts in the catalytic ozonation of oxalic acid, dye C. I. Reactive Blue 5 and textile effluents[1]

The aim of this part of the work was to evaluate the efficiency of selected catalysts in the ozonation of real wastewater samples. For that purpose, a raw textile wastewater and a textile effluent collected after biological treatment were assessed. In order to select the catalysts to be used in the treatment of these effluents, ozonation of oxalic acid and dye C. I. Reactive Blue 5 were performed, under identical experimental conditions, with the samples that presented the best performances during this thesis. The composite with 10% of ceria and 90% of activated carbon and the mixed oxide $Ce_{0.75}Zr_{0.25}O_2$ had the best catalytic activity in the oxalic acid and dye removals, respectively. Complete decolourisation of real effluents was achieved by all ozonation systems. Although the activity of the catalysts was affected by the presence of inorganic carbon due to its scavenging effect towards hydroxyl radicals, a significant decrease in organic carbon was observed during ozonation experiments, especially in the catalytic ozonation of the bio-treated effluent. Catalytic ozonation was found to be a promising technology for the treatment of textile effluents.

[1] C. A. Orge, J. J. M. Órfão, M. F. R. Pereira, Benchmarking of selected catalysts in the catalytic ozonation of oxalic acid, dye C. I. Reactive Blue 5 and textile effluents, to be submitted (2012).

9 Benchmarking of selected catalysts in the catalytic ozonation of oxalic acid, dye C. I. Reactive Blue 5 and textile effluents

9.1 Introduction

The chemical industry has an important impact on the environment. The industrial effluents are generally highly polluted with organic and inorganic compounds and many of them are toxic, mutagenic, carcinogenic or simply almost non-biodegradable. Then, these compounds lead to pollution of the soil and groundwater and cause perturbations in the ecosystem as well as serious health problems [1]. Due to their toxicity and biorefractory nature, conventional biotreatment technologies are often ineffective to deal with this type of wastewater.

In particular, textile wastewaters are highly coloured and have low metal and suspended solid contents, high temperature, alkaline pH in most situations, high chemical oxygen demand (COD), and contain chlorinated organic compounds and surfactants [2]. Textile effluents are toxic and mostly not biodegradable and also resistant to physico-chemical treatment methods. The non-biodegradability of textile effluents is due to a high content of dyestuffs, surfactants and additives which generally are organic compounds of complex structures.

Ozone as oxidation agent can improve the conversion of organic pollutants into easily biodegradable compounds, but its performance is often not strong enough to remove the organic matter by direct mineralisation in a reasonable time and cost. In such cases, the efficiency of the oxidation process can be improved by using advanced oxidation processes (AOPs) [3]. For example, a combination of ozone with H_2O_2 and/or UV radiation, as well as the simultaneous application of ozone and solid catalysts to generate reactive hydroxyl radicals with high oxidation potential are promising AOPs [4]. Therefore, catalytic ozonation is a potential technology for the treatment of wastewaters from several industries.

The aim of this part of the thesis was to evaluate the catalytic activity of selected catalysts with real textile effluents. In this context, a raw wastewater and an effluent collected after a biological treatment were used as case studies. For that purpose the most promising catalysts reported in this study were tested, in the same conditions, in the ozonation of oxalic acid and a selected reactive dye, and the best catalysts were then evaluated with real wastewater samples.

9.2 Experimental

Oxalic acid and the dye C. I. Reactive Blue 5 were chosen as model organic compounds. Their properties are presented in Table 9.1. Real wastewater samples originated from a textile plant were also used as case studies.

Table 9.1: Properties of selected compounds.

Compound	M (g mol^{-1})	pKa	λ_{max} (nm)
Oxalic acid 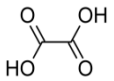	90.04	1.23, 4.19	-
C.I. Reactive Blue 5 (Cibacron Blue BR) 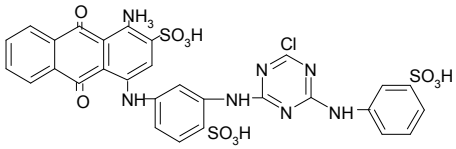	774.16	-	597

The real textile effluents were characterized by different parameters: pH, total organic carbon (TOC), conductivity, chemical oxygen demand (COD), five day biochemical oxygen demand (BOD_5), total phosphorus, total suspended solids, ionic compounds and absorbance in the UV/Vis spectrum. pH was determined using a Hanna pH 211 pH meter. TOC analysis was performed in a Shimadzu TOC-5000A analyzer. Conductivity was evaluated using a WTW LF538 conductivity instrument. COD was determined according to the Open Reflux Method (method 5220 B. of Standard Methods [5]). BOD_5 was calculated by the dilution method as described in Standard Methods 5210 B. [5]. Digestion followed by ascorbic acid method (method 4500 B. and 4500 E. [5]) was used to determine the total phosphorus present in the effluents. Total suspended solids were measured according to the total solids dried at 103 - 105 °C (method 2540 B. [5]). Ionic compounds were quantified using a HPLC system equipped with a conductivity detector. The separation was achieved using a Dionex ICS-2100 Ion Chromatography System with a Dionex IonPac AS11-HC column (250 mm × 4 mm), under isocratic elution with a solution of NaOH 30 mM at a flow rate of 1.5

mL/min, and a Dionex DX-120 Ion Chromatography System using an IonPac CS12A column (250 mm × 4 mm) working with a solution of methane sulfonic acid 20 mM as the mobile phase at a flow rate of 1.0 mL min^{-1}, for anions and cations, respectively. The system was equipped with a conductivity detector, which performance was improved by electrolyte suppression using ASRS 300 or CSRS ULTRA II self-regeneration suppressors for anions and cations, respectively.

For this study, the catalysts that had better performances in the previous chapters were selected. The preparation and characterization of the catalysts used in this part of the thesis were presented and discussed in detail in the previous chapters (see chapters 3 to 8).

The removal of oxalic acid, reactive dye and textile effluents was performed in a slurry lab-scale reactor equipped with agitation (see Appendix A). Oxalic acid and dye experiments were carried out with 100 mg of catalyst (dp < 100 μm) and 700 mL of pollutant solutions (C_0, oxalic acid = 1 mM, C_0, dye = 50 mg L^{-1}) in order to compare the catalytic activity of different samples under the same conditions, which correspond to a catalyst amount lower than that used in some previous chapters. The experiments were performed at ambient temperature and with an inlet concentration of ozone of 50 g m^{-3}. The concentration of ozone in the gas phase was monitored with a BMT 964 ozone analyser and the total gas flow rate was 150 cm^3 min^{-1}. Textile effluents were submitted to non-catalytic and catalytic ozonation, as well as adsorption experiments. Since the raw wastewater has a high organic load and the bio-treated effluent presents considerable concentration of inorganic carbon, 350 mg of catalyst were used in the respective reaction tests, but the remaining conditions were identical.

HPLC analyses were performed using a Hitachi Elite Lachrom apparatus equipped with a diode array detector, in order to follow the oxalic acid concentration. The stationary phase was an Aminex-87H column (300 mm × 7.8 mm) working under isocratic elution with H_2SO_4 4 mM at room temperature. For the reactive dye, solution decolourisation was followed by UV/Vis spectrophotometry at the maximum absorption wavelength, previously determined. The degree of mineralisation was followed by total organic carbon (TOC) analysis. For non-catalytic and catalytic ozonation experiments, COD and BOD_5 of the remaining solutions were also determined.

9.3 Oxalic acid removal

With the aim of evaluating the most promising catalysts prepared within this work, oxalic acid degradation was carried out with the best samples presented in each chapter of this thesis. AC0, XC_pH=6.00 and XC_pH=6.25 were chosen among carbon materials; Mn-O, $Ce_{0.25}Zr_{0.75}O_2$, CeO_2-NP and $LaMnO_3$ were the metal oxides selected; and amongst samples of metal oxide/carbon materials, AC0-Ce-O_4, XC-Ce-O_3, ACoxid-Ce-O_3, AC0-Mn-O_4, XC-Mn-O_2, ACoxid-Mn-O_2 and 1%Ce/XC_in situ were tested. The obtained results are depicted in Figure 9.1.

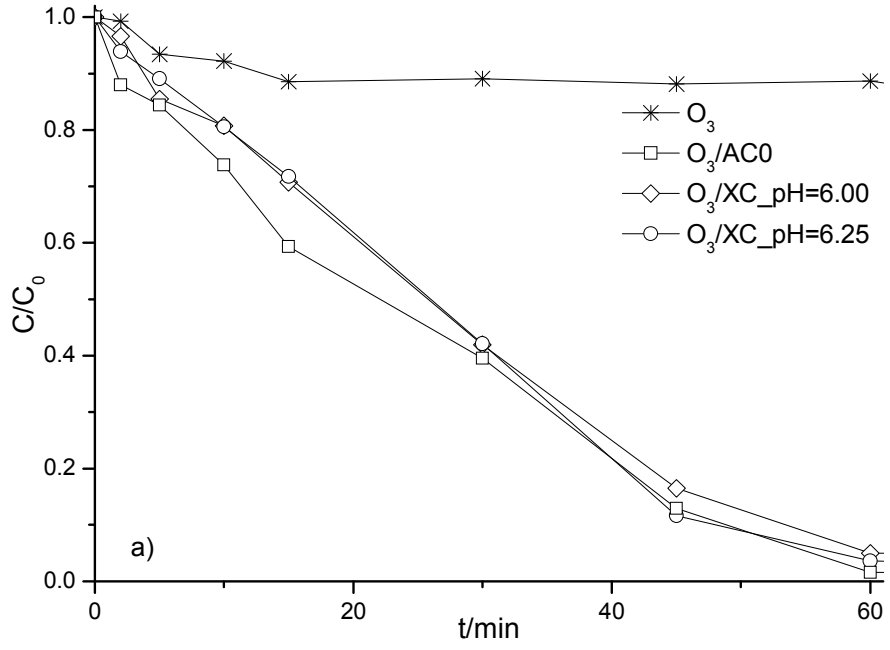

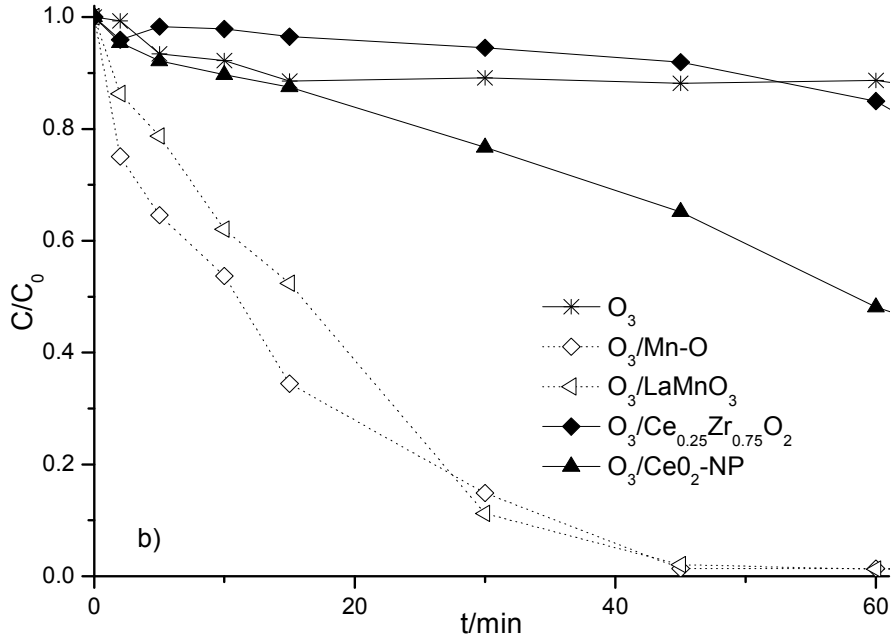
1.0
0.8
0.6
0.4
0.2
0.0
C/C0
0
20
40
60
t/min
b)
O3
O3/Mn-O
O3/LaMnO3
O3/Ce0.25Zr0.75O2
O3/Ce02-NP

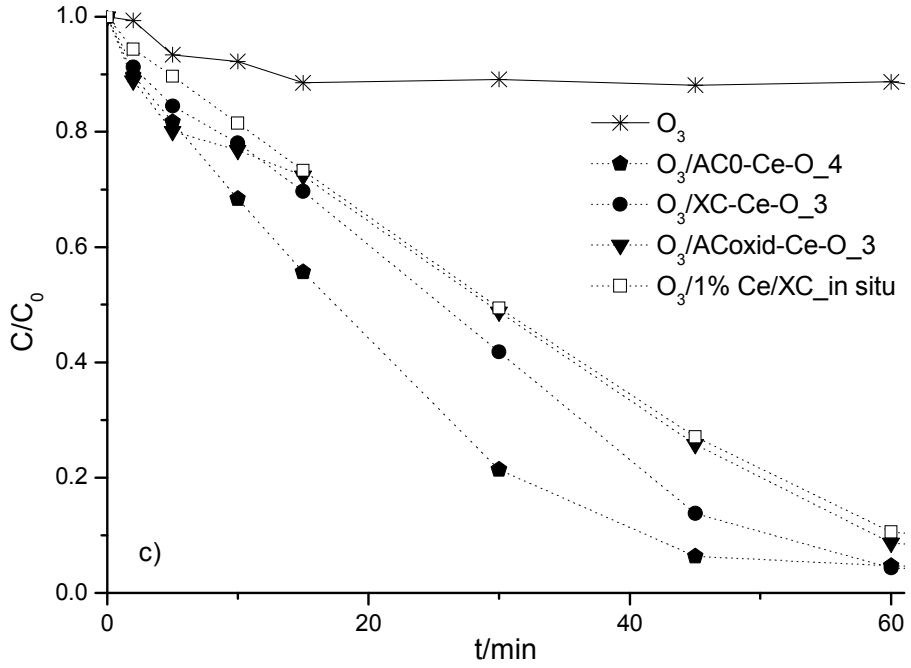
1.0
0.8
0.6
0.4
0.2
0.0
C/C0
0
20
40
60
t/min
c)
O3
O3/AC0-Ce-O_4
O3/XC-Ce-O_3
O3/ACoxid-Ce-O_3
O3/1% Ce/XC_in situ

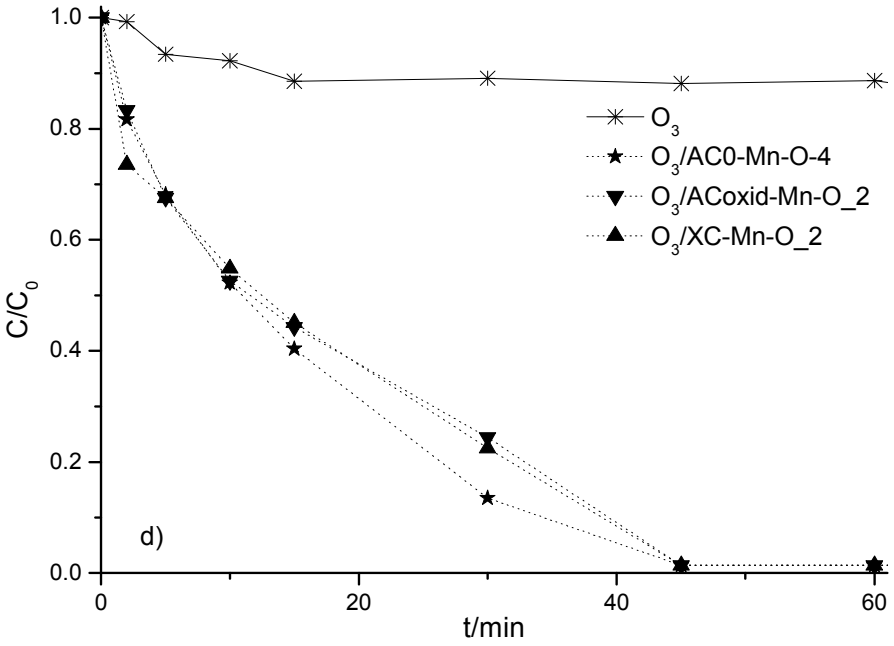

Figure 9.1: Evolution of the dimensionless concentration of oxalic acid during non-catalytic and catalytic ozonation with carbon materials (a), metal oxides (b), ceria-carbon materials (c) and manganese-carbon materials (d).

According to the results, activated carbon presented a slightly better catalytic activity than carbon xerogels, but after 30 min of reaction no differences were observed and a complete degradation was achieved at 60 min. Among metals oxides, ceria containing catalysts did not present a remarkable performance until 1 h of test under these experimental conditions, while manganese samples had high catalytic activity. Ceria-carbon materials allowed a total oxalic acid removal after 1 h of reaction; however, the composite with 10% of ceria and 90% of activated carbon prepared by the precipitation method (AC0-Ce-O_4) presented the best performance during all reaction time. Similar results were observed with samples of manganese oxide and carbon material. The composite with 22% of manganese oxide and 78% of activated carbon synthesized by the precipitation method (AC0-Mn-O_4) had better catalytic activity, but the differences among the manganese-carbon materials were not significant.

Excluding $Ce_{0.25}Zr_{0.75}O_2$ and CeO_2-NP, since these samples did not allow total oxalic acid degradation after 1 h of reaction, and manganese catalysts, because some leaching of metal was observed during the experiments, the catalytic results of the remaining materials were compared in Figure 9.2.

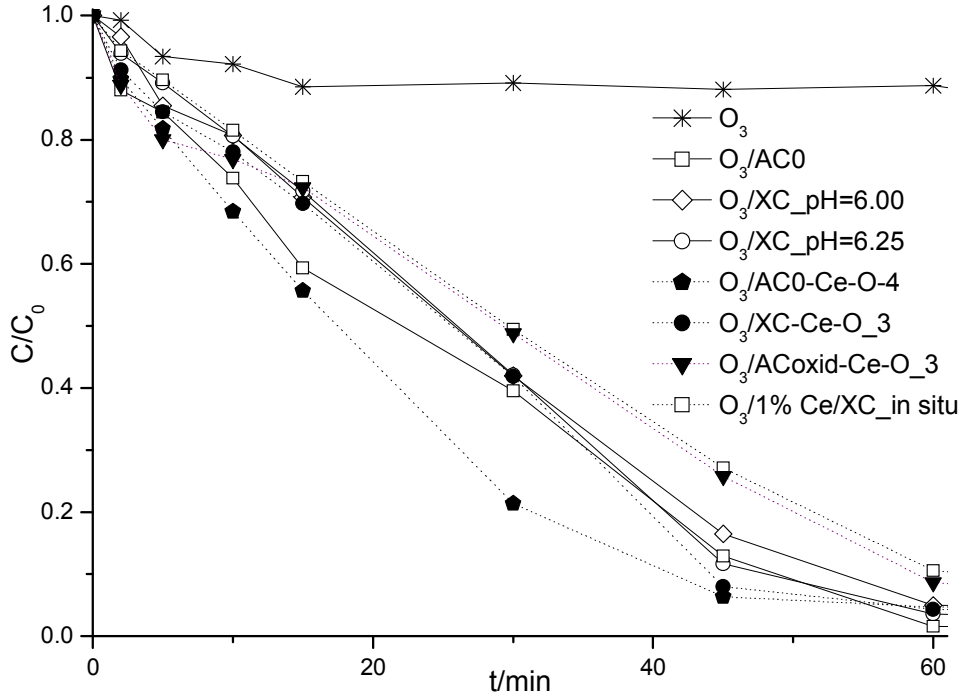

Figure 9.2: Evolution of the dimensionless concentration of oxalic acid during non-catalytic and catalytic ozonation with carbon materials and ceria-carbon materials.

Therefore, the composite AC0-Ce-O_4 showed to be the best catalyst in the removal of oxalic acid under these experimental conditions.

9.4 Reactive dye removal

For the study of reactive dye degradation, the composite AC0-Ce-O_4 was selected among samples containing carbon. According to the results in the previous section, this catalyst is highly active in oxalic acid ozonation under the experimental conditions used in this work. Moreover, it also presented high activity in the reactive dye removal (see chapter 5). Samples CeO_2-FL, $Ce_{0.75}Zr_{0.25}O_2$ and $LaCoO_3$ were selected amongst metal oxides. Figure 9.3 shows the kinetic results of single and catalytic ozonation of the reactive dye. As expected, single and catalytic ozonation in the presence of the selected catalysts allowed attaining total decolourisation in a short reaction time, confirming the strong potential of ozone to remove colour. Regarding the evolution of TOC along time, sample $Ce_{0.75}Zr_{0.25}O_2$ presented the

best performance under the experimental conditions used, allowing nearly total mineralisation after 2 h of reaction.

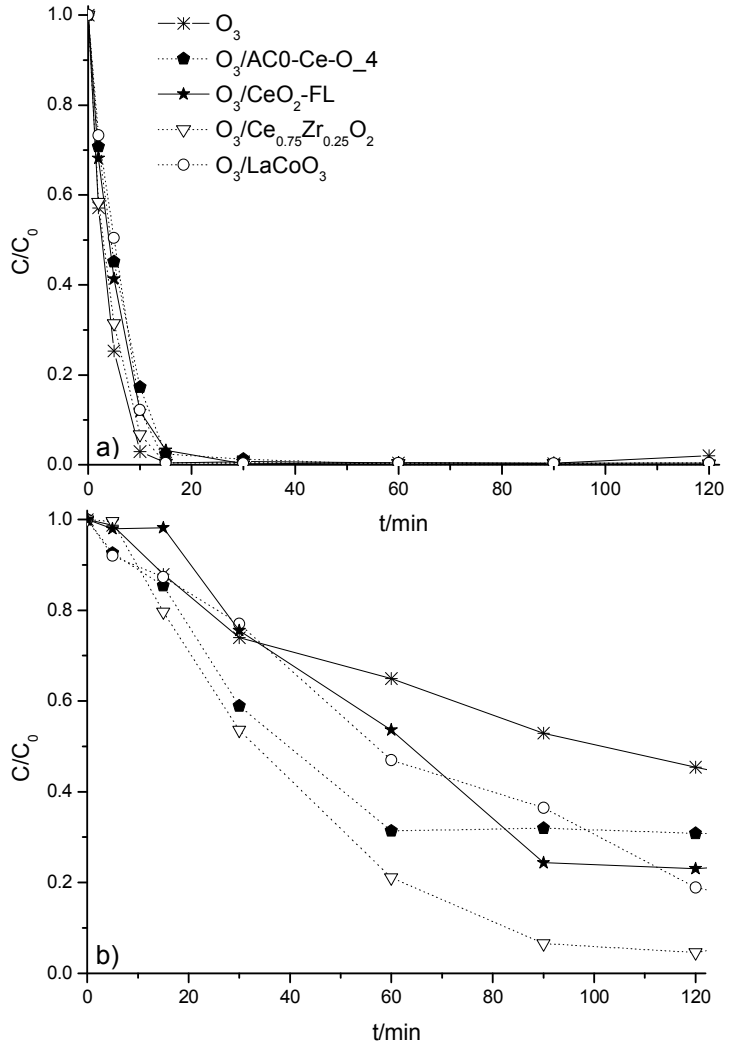

Figure 9.3: Colour (a) and TOC (b) removal for the reactive dye during single and catalytic ozonation in the presence of the best prepared catalysts.

9.5 Treatment of real effluents

In order to evaluate the efficiency of the prepared catalysts in the ozonation of real wastewater samples, two textile effluents were tested. Raw liquid effluent originated

in a textile plant (effluent A) and a textile effluent collected after a conventional biological treatment and before the physicochemical step (effluent B) were evaluated. The samples chosen for this study were AC0-Ce-O_4 and $Ce_{0.75}Zr_{0.25}O_2$, since they presented the best catalytic activities in oxalic acid and dye degradation, respectively. In this context, textile wastewaters were used as case studies. Textile wastewater A presents a reddish-brown colour and effluent B has a pinkish colour. Some characterization parameters are listed in Table 9.2.

Table 9.2: Parameters of the industrial effluents selected.

Parameters	Effluent A	Effluent B
pH	9.3	7.1
TOC (mg L^{-1})	210	42
Inorganic carbon (mg L^{-1})	111	148
Conductivity (mS cm^{-1})	11.78	11.69
COD (mg O_2 L^{-1})	437	112
BOD_5 (mg O_2 L^{-1})	118	5
Total Phosphorus (mg L^{-1})	1.0	1.6
Total suspended solids (mg L^{-1})	30	25
F^- (mg L^{-1})	0.45	0.77
Cl^- (mg L^{-1})	950	2.5
NO_2^- (mg L^{-1})	2.6	<LOQ[a]
SO_4^{2-} (mg L^{-1})	46.5	1.67
Br^- (mg L^{-1})	7.6	5.8
NH^{4+} (mg L^{-1})	0.02	0.19
Li^+ (mg L^{-1})	0.05	<LOQ[a]
NO_3^- (mg L^{-1})	0.92	0.11
Ca^{2+} (mg L^{-1})	<LOQ[a]	0.98
Abs (λ = 620 nm[b])	0.384	0.044
Abs (λ = 525 nm[b])	0.516	0.085
Abs (λ = 436 nm[b])	0.502	0.112

[a] below the limit of quantification;

[b] wavelength defined by ISO7887:2011 for the examination and determination of colour.

The UV-Vis spectra of the effluents are depicted in Figure 9.4. In real wastewaters, the examination and determination of the colour should be done at three different

wavelengths (436, 525 and 620 nm), according to what is established by ISO7887:2011. Effluent A presents a stronger colour than effluent B, but the textile effluent collected after conventional treatment still has an intense colouration. The large concentrations of TOC, COD and BOD_5 confirm the high organic load of textile wastewater A (see Table 9.2). Although textile effluent B presents a lower concentration of TOC than effluent A, it has a high content of inorganic carbon (HCO_3^-, CO_3^{2-}). Effluent B exhibits a small BOD_5, since the biodegradable organic compounds were removed by biological treatment.

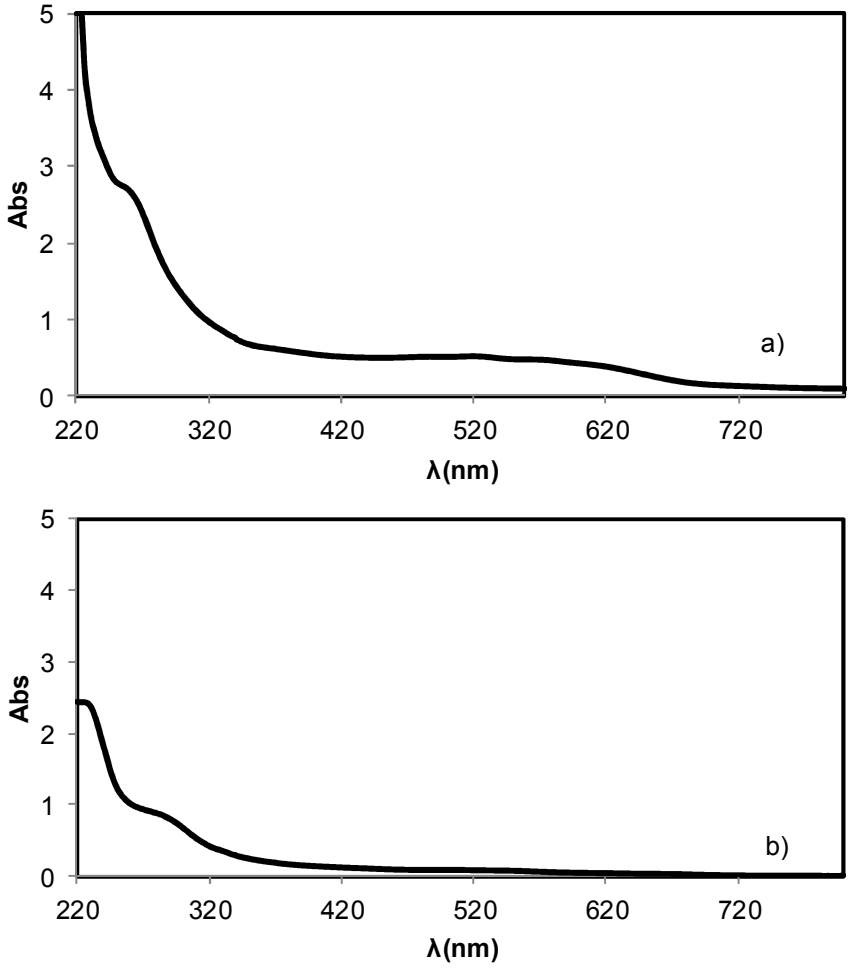

Figure 9.4: UV-Vis spectra of effluents A (a) and B (b).

Figure 9.5 depicts the evolution of UV/Vis spectrum of effluent A during single ozonation, ozonation catalysed by AC0-Ce-O_4 and $Ce_{0.75}Zr_{0.25}O_2$ and adsorption on AC0-Ce-O_4 and $Ce_{0.75}Zr_{0.25}O_2$. The percentage of colour removal at wavelength equal to 620, 525 and 436 nm after 3 h of reaction is presented in Table 9.3. Complete decolourisation was achieved by single ozonation, confirming the strong potential of ozone to attack dye chromophores. Analyzing the absorbance values obtained during non-catalytic and catalytic ozonation systems after 3 h of reaction, the decolourisation of the effluent was slightly enhanced by the presence of catalyst. On the other hand, adsorption on AC0-Ce-O_4 and $Ce_{0.75}Zr_{0.25}O_2$ were not enough for the decolourisation of textile wastewater.

Table 9.3: Characterization of the remaining solution after non-catalytic, catalytic and adsorption experiments with effluent A after 3 h.

	% Removal				
	O_3	O_3/ AC0-Ce-O_4	O_3/ $Ce_{0.75}Zr_{0.25}O_2$	O_2/ AC0-Ce-O_4	O_2/ $Ce_{0.75}Zr_{0.25}O_2$
colour λ=620nm	75	94	91	66	53
colour λ=525nm	78	94	92	55	34
colour λ=436nm	70	91	88	59	38
COD	26	35	21	-	-
BOD_5	12	33	21	-	-

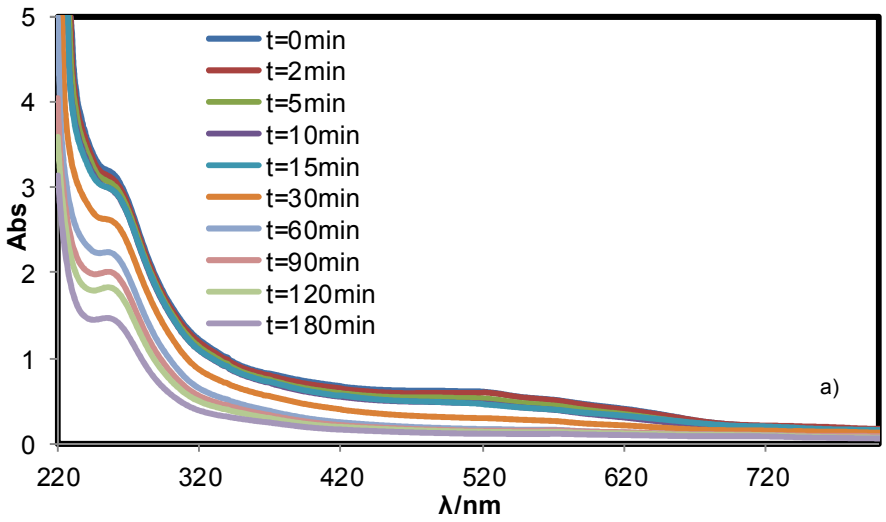

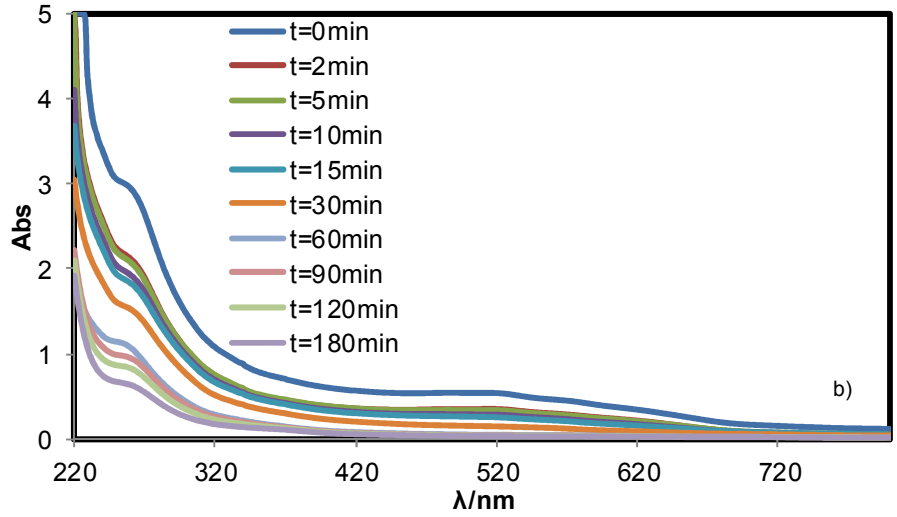
t=0min
t=2min
t=5min
t=10min
t=15min
t=30min
t=60min
t=90min
t=120min
t=180min
Abs
λ/nm
b)

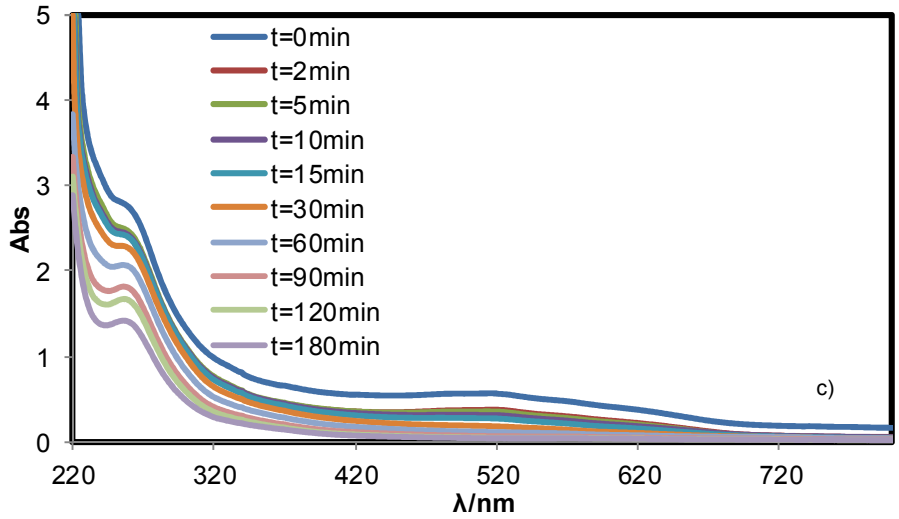
t=0min
t=2min
t=5min
t=10min
t=15min
t=30min
t=60min
t=90min
t=120min
t=180min
Abs
λ/nm
c)

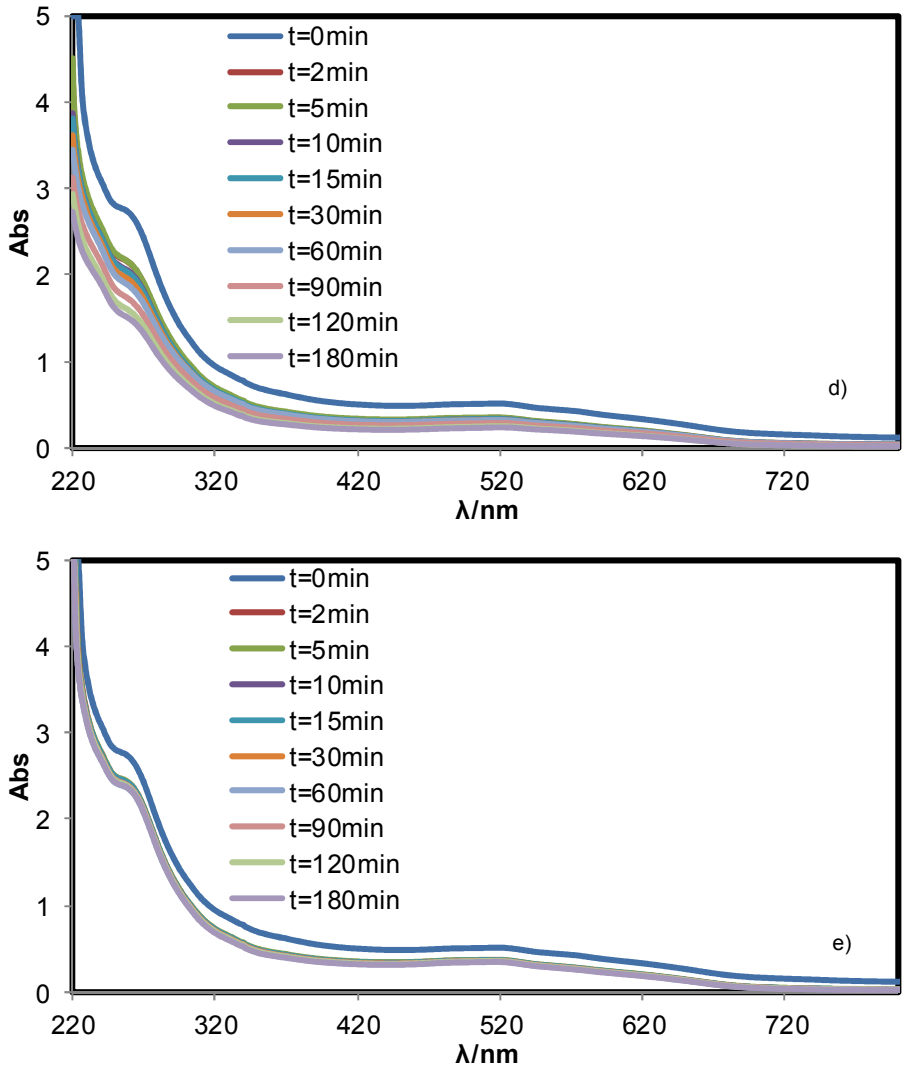

Figure 9.5: Evolution of UV-Vis spectrum of real effluent A during non-catalytic ozonation (a), catalytic ozonation in the presence of AC0-Ce-O_4 (b) and $Ce_{0.75}Zr_{0.25}O_2$ (c), and adsorption on AC0-Ce-O_4 (d) and $Ce_{0.75}Zr_{0.25}O_2$ (e).

The evolution in the mineralisation degree of the effluent achieved by non-catalytic ozonation and catalytic ozonation is shown in Figure 9.6. Adsorption on AC0-Ce-O_4 and $Ce_{0.75}Zr_{0.25}O_2$ is also presented in order to better understand the results. Although single ozonation allowed a complete decolourisation of textile effluent A, the degree of mineralisation achieved was around of 10% after 3 h of reaction. The introduction of the selected catalysts increased the mineralisation rate. Composite AC0-Ce-O_4 presented better catalytic activity than sample $Ce_{0.75}Zr_{0.25}O_2$, removing

44% of the organic content after 3 h of reaction. Adsorption on AC0-Ce-O_4 was more relevant than adsorption on $Ce_{0.75}Zr_{0.25}O_2$, allowing a TOC removal of 35%.

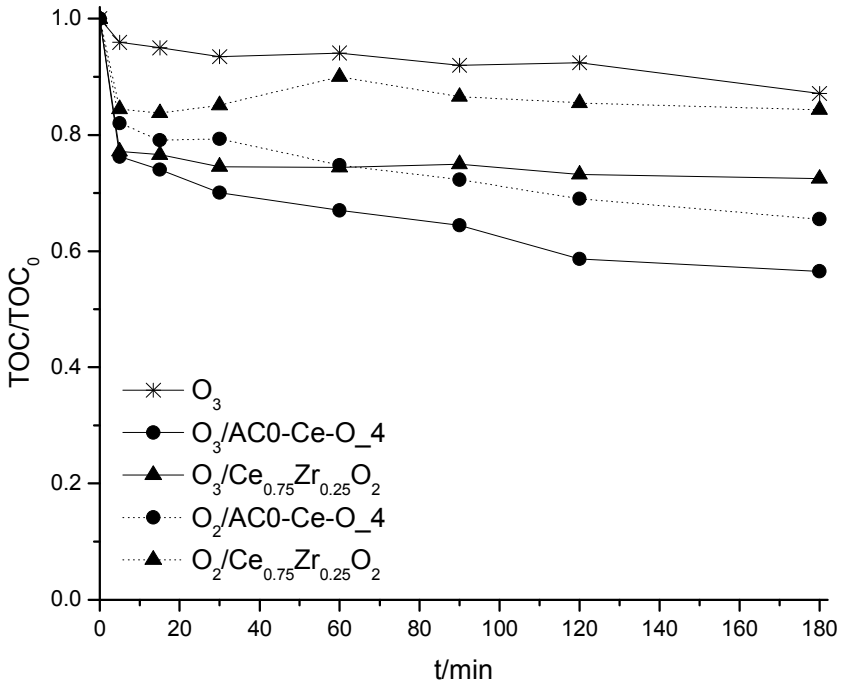

Figure 9.6: Evolution of dimensionless TOC during single ozonation, catalytic ozonation and adsorption experiments of the real textile effluent A.

COD and BOD_5 were determined after the ozonation reactions (see Table 9.3). Similar to what occurs with TOC removal, the best results of COD and BOD_5 removal were obtained with the composite, leading to a reduction of 35 and 33%, respectively. Ozonation catalysed by $Ce_{0.75}Zr_{0.25}O_2$ allowed better BOD_5 removal than non-catalytic ozonation, but COD decrease is lower. The ratio BOD_5/COD is usually used to measure the biodegradability. The biodegradability of effluent A is 0.27 and this value remained after catalytic ozonation both in the presence of AC0-Ce-O_4 and $Ce_{0.75}Zr_{0.25}O_2$, since the catalytic systems had similar performances in terms of BOD_5 and COD removal. On the other hand, a slightly increase in biodegradability was observed after single ozonation (BOD_5/COD = 0.32).

A similar study was performed with effluent B. Considering the low adsorption capacity of $Ce_{0.75}Zr_{0.25}O_2$ for the previously effluent and for the organic compounds

tested during this work, adsorption on $Ce_{0.75}Zr_{0.25}O_2$ was not carried out with effluent B.

Figure 9.6 shows the evolution of the UV/Vis spectrum of effluent B during non-catalytic ozonation, ozonation catalysed by AC0-Ce-O_4 and $Ce_{0.75}Zr_{0.25}O_2$ and adsorption on AC0-Ce-O_4. The percentages of colour removal at wavelengths equal to 620, 525 and 436 nm after 3 h of reaction are presented in Table 9.4.

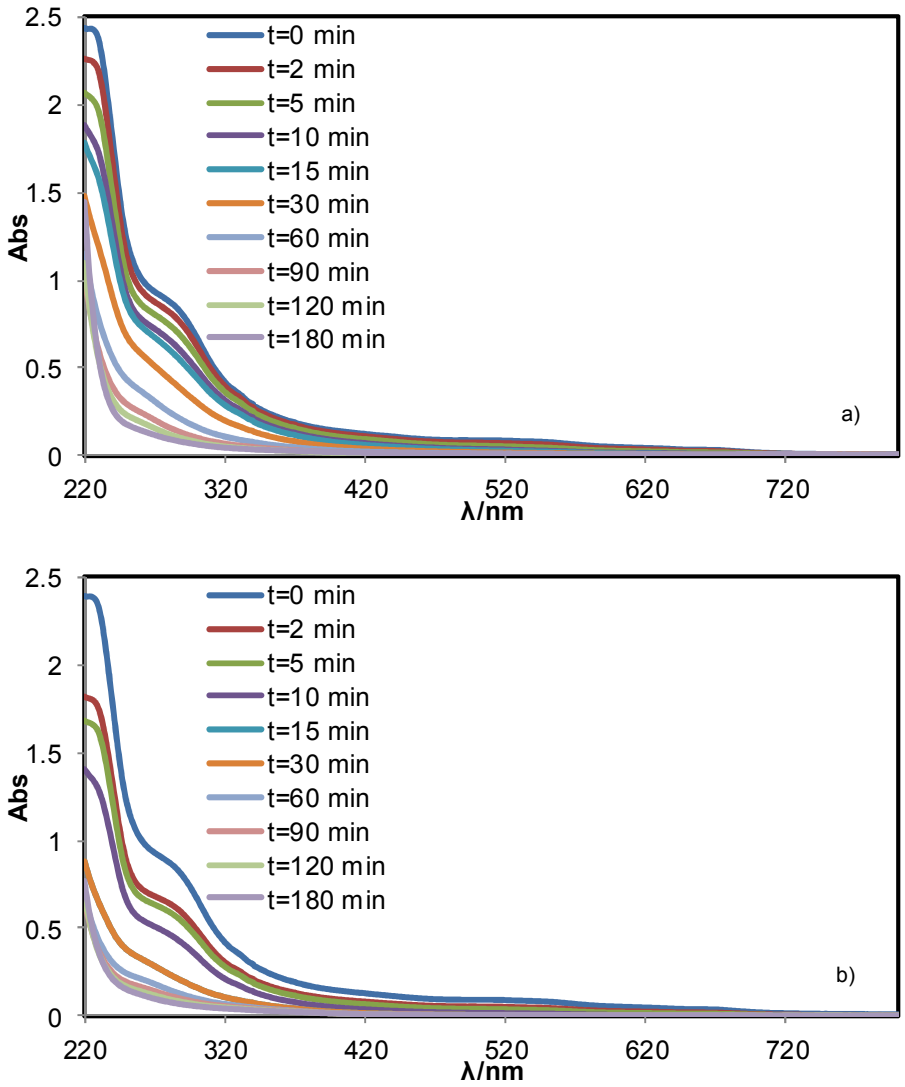

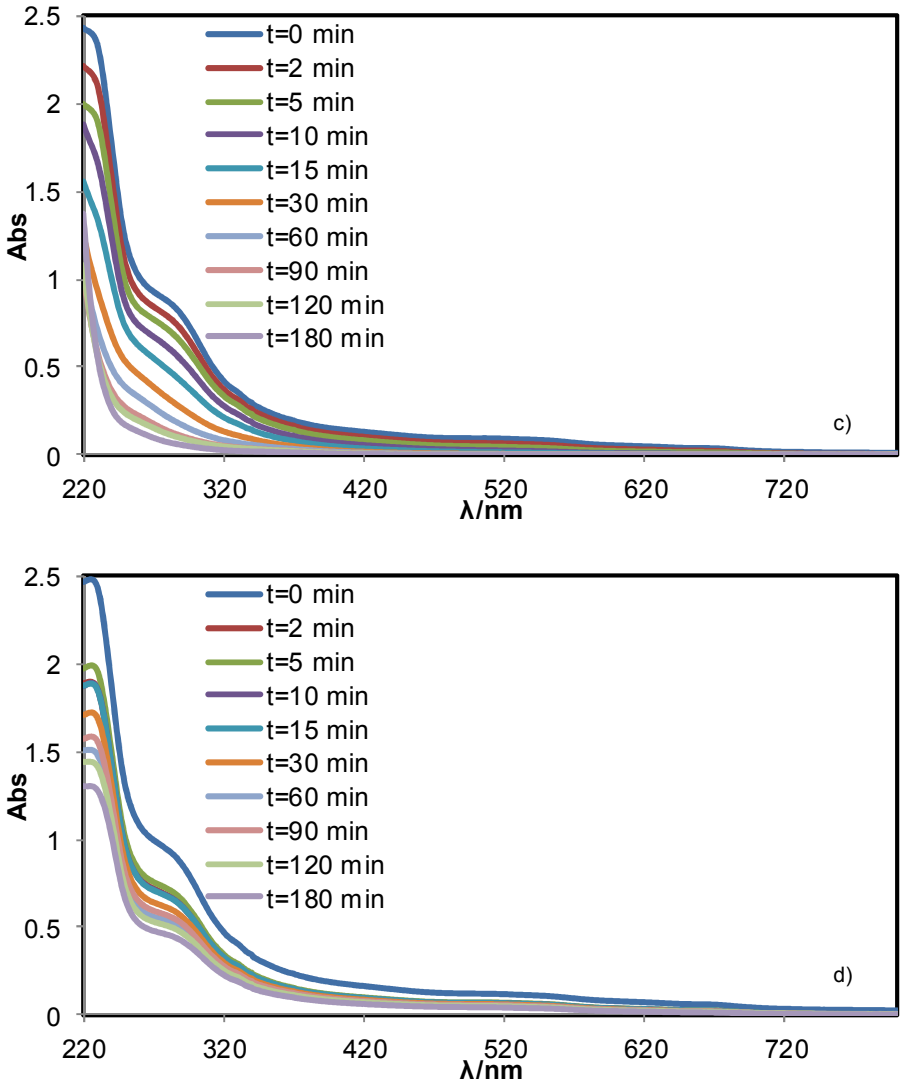

Figure 9.7: Evolution of the UV-Vis spectrum of the real effluent B during non-catalytic ozonation (a), catalytic ozonation in the presence of AC0-Ce-O_4 (b) and $Ce_{0.75}Zr_{0.25}O_2$ (c), and adsorption on AC0-Ce-O_4 (d).

Similarly to what occurred with effluent A, ozonation catalysed by the selected materials allowed a slightly higher decolourisation than single ozonation. Adsorption on composite did not lead to total decolourisation. The kinetic data corresponding to the evolution of TOC during single and catalytic ozonation, as well as adsorption on the composite are depicted in Figure 9.8. Non-catalytic ozonation allowed a TOC removal of 34% within 180 min of reaction. The mineralisation of the effluent was

enhanced by all the catalytic ozonation systems. Although AC0-Ce-O_4 presented better performance than $Ce_{0.75}Zr_{0.25}O_2$ during the first 90 min of reaction, a removal of around 50% of TOC was achieved by both catalysts after 3 h of reaction. Adsorption on AC0-Ce-O_4 allowed a removal of 25% of TOC after 1 h of reaction and this value is practically unchanged during the remaining contact time.

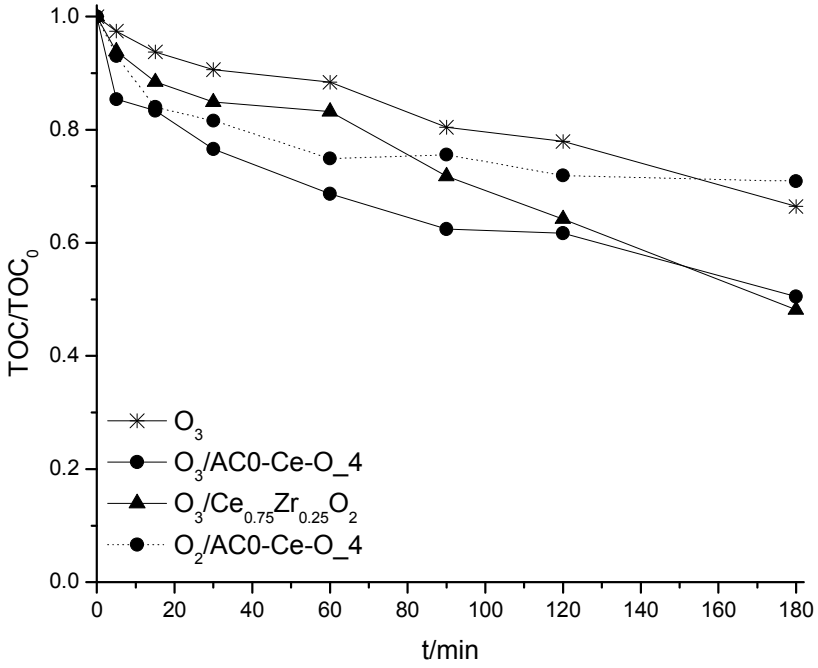

Figure 9.8: Evolution of dimensionless TOC during single ozonation, catalytic ozonation and adsorption of the real textile effluent B.

Table 9.4: Characterization of the remaining solution after non-catalytic, catalytic and adsorption experiments with effluent B after 3 h.

	% Removal			
	O_3	O_3/ AC0-Ce-O_4	O_3/ $Ce_{0.75}Zr_{0.25}O_2$	O_2/ AC0-Ce-O_4
colour at λ = 620 nm	82	92	97	58
colour at λ = 525 nm	87	94	98	52
colour at λ = 436 nm	87	93	98	51
COD	77	71	71	-

COD and BOD_5 analyses in the remaining solutions of single and catalytic ozonation in the presence of the selected materials were carried out. The values of COD removal (in percentage) by ozonation are presented in Table 9.4. Although non-catalytic ozonation allowed the best COD removal (77% after 3 h of reaction) no important differences were observed between experiments. Similar to what occurred with TOC removal, AC0-Ce-O_4 and $Ce_{0.75}Zr_{0.25}O_2$ did not present differences in terms of COD removal, leading to 71% after 3 h of reaction. Contrarily to what was observed with effluent A, ozonation reactions increased the BOD_5 of effluent B. Single ozonation enhanced the BOD_5 to 11 mg O_2 L^{-1} and catalytic ozonation in the presence of AC0-Ce-O_4 and $Ce_{0.75}Zr_{0.25}O_2$ increased it to 14 and 13 mg O_2 L^{-1}, respectively. The enhancement of BOD_5 after ozonation reactions was explained by the conversion of recalcitrant molecules into biodegradable organic compounds.

Comparing the results of real effluents A and B, non-catalytic ozonation and catalytic ozonation, specially in the presence of $Ce_{0.75}Zr_{0.25}O_2$, were more efficient in the treatment of effluent B, leading to higher mineralisation degrees. The results presented are in accordance with the literature. Ozonation is more appropriate to be used as a final wastewater treatment than as a main process. However, a complete mineralisation of effluents was not achieved by catalytic ozonation, as expected. Although the bio-treated effluent has a low organic load, it presents a high concentration of inorganic carbon. The presence of inorganic ions, such as carbonates (CO_3^{2-}) and bicarbonates (HCO_3^-), may affect the destruction of organic compounds in water and wastewater by advanced oxidation processes [6]. CO_3^{2-} and HCO_3^- are well known as hydroxyl radical scavengers. Both species react with hydroxyl radicals to produce carbonate radical ions via the following reactions [7], respectively at moderate and high pH levels:

$$HCO_3^- + HO^{\cdot} \rightarrow CO_3^{-\cdot} + H_2O \qquad k = 8.5 \times 10^6\ M^{-1}\ s^{-1} \qquad 9.1$$

$$CO_3^{2-} + HO^{\cdot} \rightarrow CO_3^{-\cdot} + HO^- \qquad k = 3.9 \times 10^8\ M^{-1}\ s^{-1} \qquad 9.2$$

The mineralisation of organic compounds, achieved by ozonation, is usually favoured at higher pH values, due to the participation of $HO^{\bullet}$ radicals in the reaction mechanism. However, the scavenging effect of both CO_3^{2-} and HCO_3^- species decreases the amount of $HO^{\bullet}$ radicals available for reaction with the organic compounds, in this way inhibiting the mineralisation process. In chapters 3, 4 and 5 cerium oxide catalysts were shown to react via $HO^{\bullet}$ oxidation. According to chapter 5, the reaction mechanism of cerium oxide – carbon composites is believed to comprise both surface reactions and also liquid bulk reactions involving $HO^{\bullet}$ radicals. Then, the presence of CO_3^{2-} and HCO_3^- species in effluents reduces the amount of $HO^{\bullet}$ radicals, partially inhibiting the mineralisation process. Nevertheless, AC0-Ce-O_4 and $Ce_{0.75}Zr_{0.25}O_2$ samples had catalytic activities in the tested effluents, leading to higher mineralisation degrees when compared to single ozonation.

Concluding, catalytic ozonation processes are a feasibly alternative to treat textile effluents, since they allow a complete decolourisation and successfully enhanced the mineralisation of textile wastewaters.

9.6 Conclusions

The present study reports experimental kinetic data for the ozonation of oxalic acid, the dye C. I. Reactive Blue 5 and real textile effluents (raw textile wastewater and a bio-treated effluent). Oxalic acid and reactive dye removal tests were carried out under identical experimental conditions with the samples that presented higher catalytic activities in the previous chapters. After analysing the results, the best catalysts were chosen and tested with real wastewaters.

In the case of oxalic acid, the composite with 10% of cerium oxide and 90% of activated carbon prepared by the precipitation method, sample AC0-Ce-O_4, presented the best performance under these experimental conditions, allowing a faster removal rate.

For dye degradation, the oxide $Ce_{0.75}Zr_{0.25}O_2$ synthesized by the co-precipitation method had the best catalytic activity under the selected experimental conditions, leading to nearly complete mineralisation after 2 h of reaction.

Non-catalytic and catalytic ozonation in the presence of the selected materials were proven to be efficient in the removal of colour of real wastewaters, which confirms the high potential of ozone to decolourise solutions. Although processes involving ozone are generally used as final treatment, ozonation catalysed by composite AC0-Ce-O_4 still allowed a TOC removal of 45% in the raw textile effluent. When using catalysts in the experiments with the bio-treated effluent, a 1.5 increase in TOC removal was achieved after 3 h of reaction, relatively to single ozonation. In terms of COD, both single and catalytic ozonation in the presence of the tested materials allowed removals above 70% in the effluent collected after biological treatment. The presence of high concentrations of inorganic ions with scavenging properties may restrain the results obtained with real wastewaters, preventing higher mineralisation levels.

References

[1] B. Li, X. Xu, L. Zhu, W. Ding, Q. Mahmood, Catalytic ozonation of industrial wastewater containing chloro and nitro aromatics using modified diatomaceous porous filling, Desalination 254 (2010) 90-98.

[2] U. Rott, R. Minke, Overview of wastewater treatment and recycling in the textile processing industry, Water Sci. Technol. 40 (1999) 137-144.

[3] M. Ernst, F. Lurot, J.-C. Schrotter, Catalytic ozonation of refractory organic model compounds in aqueous solution by aluminum oxide, Appl. Catal. B: Environ. 47 (2004) 15-25.

[4] S. T. Oyama, Chemical and catalytic properties of ozone, Catal. Rev. - Sci. Eng. 42 (2000) 279-322.

[5] L. S. Clesceri, A. E. Greenberg, A. D. Eaton, Standard Methods for the Examination of Water and Wastewater. American Public Health Association, Washington, DC (1998).

[6] P. C. C. Faria, J. J. M. Órfão, M. F. R. Pereira, Activated carbon and ceria catalysts applied to the catalytic ozonation of dyes and textile effluents, Appl. Catal. B: Environ. 88 (2009) 341-350.

[7] G. V. Buxton, C. L. Greenstock, W. P. Helman, A. B. Ross, Critical Review of rate constants for reactions of hydrated electrons, hydrogen atoms and hydroxyl radicals in Aqueous Solution, J. Phys. Chem. Ref. Data 17 (1988) 513-886.

Chapter 10

Conclusions and future work

In this last chapter, a general overview of the most important results and the main relevant conclusions are presented. Finally, some suggestions for future work are provided.

10 Conclusions and future work

10.1 Motivation

Earth's freshwater resources are limited and many governments have been more stringent with environmental regulations. Therefore, all industries need to implement efficient solutions for the treatment of their effluents. Ozone, due to its high oxidation and disinfection potential, has received much attention in water treatment technology. Despite several advantages of using ozone, it has a few disadvantages, which limit its application in water treatment. Ozone has relatively low solubility and stability in water and reacts slowly with some organic compounds; in addition its production is expensive. Consequently, ozonation becomes an option that may be not economical feasible.

Advanced oxidation processes (AOPs) are effective for the treatment of several contaminants by the generation of hydroxyl radicals at ambient conditions. Among AOPs, ozone-based processes, such as O_3/H_2O_2, UV/O_3 and catalytic ozonation, are becoming increasingly important as final treatment to improve removal of persistent pollutants present in bio-treated effluents. Catalytic ozonation is a promising technology for the removal of recalcitrant organic compounds from drinking water and wastewater. Catalytic ozonation can be considered homogeneous, which is based on ozone activation by metal ions present in aqueous solution, or heterogeneous, where ozone decomposition is carried out by solid materials. In spite of the good results reported in the literature for homogeneous catalytic ozonation, it presents some drawbacks and it is not as popular as heterogeneous catalytic ozonation.

Metal oxides represent one of the most important and widely employed classes of solid catalysts, either as active phases or supports. Manganese oxide is the metal oxide mostly studied in catalytic ozonation. Minerals are also used as catalysts in heterogeneous ozonation. Among the carbon materials, ozonation catalysed by activated carbon has been reported in several researches. Carbons materials were also used as supports for metals and metal oxides. In recent years, heterogeneous catalytic ozonation in the presence of carbon nanotubes has been widely investigated.

The main goal of this PhD thesis was the evaluation of catalytic ozonation processes as tertiary treatment for industrial effluents, in order to improve mineralisation rates. In accordance with the results obtained in previous studies,

this thesis was essentially centred on the development of mesoporous carbon materials, metal oxides and metal oxide-carbon materials as catalysts for the ozonation of selected organic pollutants, including real textile effluents. The performances of mesoporous carbon materials prepared by the templating route and carbon xerogels were addressed. Among metal oxides, cerium and manganese oxides and the respective composites with carbon materials had special attention. The influence of the surface chemical and textural properties of carbon materials were studied, as well as the effect of composition and preparation method of metal oxide/carbon composites.

10.2 Main conclusions

Carbon materials have been applied in several areas due to their unique properties; however, most of them, namely activated carbons, are microporous and therefore cannot be efficiently used in applications involving bulky molecules, such as dyestuffs. Significant developments have been achieved in the synthesis of mesoporous carbon materials during the last decade. Therefore, in the first part of this study, the preparation, functionalization and characterization of templated carbons via SBA-15 and carbon xerogels are described. Two different classes of dyes were tested, reactive and acid dyes. Independently of the carbon material used and the dye studied, adsorption was not sufficient to remove the colour and TOC from the solutions. Total decolourisation of dye solutions was observed in less than 15 minutes when ozone is applied, and this time was practically independent of the presence of carbon materials. Single ozonation also originated a decrease in the amount of TOC in solution; nevertheless, this mineralisation was much lower than colour removal. The association of ozone and the mentioned mesoporous materials led to an improved TOC removal from the dye solutions and the catalytic effect increases with the carbon basicity. The results suggested that the ozone molecules have a higher affinity for basic carbons, which are known to have a high density of delocalized π electrons on the basal planes. Mesopore size diameter and mesopore surface area are key textural parameters in the ozonation of reactive and acid dyes, respectively. Finally, the successfully use of mesoporous carbons in the removal of oxalic acid was also demonstrated.

Cerium oxides prepared by different routes (precipitation method and hydrothermal synthesis) with distinct morphologies and particle sizes and cerium-based mixed oxides prepared by the precipitation method were tested in the ozonation of oxalic

acid, aniline and the textile dye C. I. Reactive Blue 5. In the case of oxalic acid, the catalytic effect increases with the concentration of Ce(III) species on the catalysts surface. Cerium oxides synthesized by the precipitation method and $Ce_{0.75}Zr_{0.25}O_2$ (the sample with the largest amount of oxygen vacancies on its structure) presented the best mineralisation results in aniline degradation. In these experiments, oxalic and oxamic acids concentrations were confirmed as final oxidation products of aniline ozonation. Cerium oxide prepared by the precipitation method presents a different performance compared to the nanosized cerium oxides synthesized hydrothermally, which suggests that they promote the ozonation of aniline by different mechanisms. All ceria containing catalysts significantly improved the mineralisation rate in the ozonation of the dye solution, leading to TOC removals close to 100% after 2 h of reaction, under the conditions studied. The ozonation catalysed by cerium oxides and ceria-based mixed oxides is strongly inhibited in the presence of *tert*-butanol. This experimental observation indicates that, in these conditions, the oxidation mechanism of oxalic acid occurs predominantly via $HO^{\bullet}$ radicals in the liquid bulk. In addition, it is believed that the presence of the Ce(IV)/Ce(III) redox pair on the surface of cerium containing catalysts enhances the decomposition of ozone into highly reactive species in solution, such as $HO^{\bullet}$ radicals.

The next part of this thesis was dedicated to the study of ozonation catalysed by composites of metal oxides and carbon materials with different compositions. For that purpose, cerium and manganese oxides were selected and the carbon materials used were an activated carbon, a carbon xerogel and an oxidised activated carbon. The results were compared with those obtained in single ozonation and ozonation catalysed by the parent carbon materials or the metal oxides used to prepare the composites. Experiments using a physical mixture of carbon materials and metal oxides, reactions in the presence of a radical scavenger (*tert*-butanol) and adsorption experiments were carried out with the aim of clarifying the reaction mechanism. Contrary to manganese oxide, which has better performance than carbon materials, cerium oxide presents lower catalytic activity. The presence of the Ce (IV)/Ce (III) redox couple on the surface of the prepared ceria containing catalysts was evidenced by XPS analyses. There is a minimum amount of carbon material in the composites with ceria in order to have a synergic effect and the catalytic performances for the same composition depend on the carbon used, increasing with the density of free electrons available on the surface. The reaction mechanism of ceria-carbon materials composites is believed to

comprise both surface reactions and liquid bulk reactions involving $HO^{\bullet}$ radicals. It is assumed that the presence of delocalized electrons on the basal planes of carbon materials contributes to the formation of Ce (III) species, which are active for the decomposition of O_3 into $HO^{\bullet}$ radicals. Synergic effect was not observed between manganese oxide and carbon materials in the prepared composites, and in this case the reaction mechanism is believed to occur mainly by surface reactions, following a direct oxidation of adsorbed molecules by molecular ozone and/or surface oxygenated species.

With the aim of evaluating the influence of the properties of carbon xerogels and the importance of the ceria-carbon xerogel materials preparation method in the catalytic activity**,** carbon xerogels prepared by the sol-gel process at different initial pHs and ceria-carbon xerogel materials with different compositions and synthesized by different procedures were tested as ozonation catalysts. Pore sizes of carbon xerogels were found to play a key role in the degradation of the selected pollutants, since carbon xerogels with small pores are better for oxalic acid (small molecule) and the opposite is observed for a reactive dye (large molecule). The novel catalyst prepared by one-pot synthesis and all materials of cerium oxide supported on carbon xerogel presented better performances than the carbon xerogel in the ozonation of oxalic acid and the reactive dye. The results showed that catalytic ozonation in the presence of 1 wt% Ce supported on the carbon xerogel or in the presence of the sample prepared by one-pot synthesis is practically not affected by the presence of *tert*-butanol, which indicates that the oxidation of oxalic acid does not occur via $HO^{\bullet}$ radicals in the liquid bulk. Therefore, the reaction mechanism over these catalysts is expected to involve the oxidation of organic compounds on the catalyst surface. The stability of the prepared catalysts was confirmed after five consecutive runs with fresh oxalic acid solutions. Considering the high catalytic activity, as well as the easier and less expensive preparation method, the catalyst prepared by one-pot synthesis seems to be the best option.

Lanthanum containing perovskites prepared by the citrate method and characterized by different techniques were tested as ozonation catalysts. The ozonation of oxalic acid in the presence of perovskites, especially with samples formed by La and a transition metal, showed excellent results, leading to complete degradation in some cases. The presence of lattice oxygen species on the perovskites surface plays an important role, while the introduction of Cu has a negative effect. Additional experiments with $LaMnO_3$ were performed in order to investigate the catalytic activity and the mechanism of oxalic acid ozonation in the

presence of perovskites. $LaMnO_3$ remained highly active after 3 runs and the reproducibility of the results was confirmed with replicated experiments. The results carried out with *tert*-butanol indicate that oxidation via $HO^{\bullet}$ radicals in the liquid bulk occurs, but it is expected that surface reactions play also an important role in catalytic ozonation. Although $LaMnO_3$ had the best catalytic activity, some metal leaching was observed. Therefore, $LaCoO_3$ was considered the best sample, and therefore was tested as catalysts in the reactive dye ozonation. Complete decolourisation was achieved by single ozonation and the presence of catalyst did not improve the colour removal. On the other hand, the TOC removal was enhanced by the presence of catalyst, leading to nearly complete mineralisation after 3 h, under the experimental conditions used.

The last part of this work was dedicated to assess the suitability of selected catalytic ozonation systems for the treatment of textile effluents. For that purpose two real effluents, collected before and after biological treatment, were evaluated. In order to select the catalysts to be used in the treatment of textile effluents, ozonation of oxalic acid and the dye C. I. Reactive Blue 5 was carried out, under identical experimental conditions, with the samples that presented the best performances along the present work. Therefore, the composite with 10% of ceria and 90% of activated carbon and the mixed oxide $Ce_{0.75}Zr_{0.25}O_2$ were chosen for the experiments with real effluents. Single and catalytic ozonation in the presence of the tested materials were proven to be efficient in the colour removal of real wastewaters, confirming the strong potential of ozone to decolourise solutions. Ozonation catalysed by the composite allowed the best TOC removal in the raw wastewater, 45% after 3 h of reaction. Both COD and BOD_5 also decreased after all ozonation processes tested. When using catalysts in the experiments with the bio-treated effluent, a 1.5 increase in TOC removal was achieved, relatively to single ozonation. In terms of COD, all ozonation systems allowed removals above 70%.

10.3 Suggestions for future work

Recently, several studies have documented a great variety of micropollutants including endocrine disrupting compounds (EDCs) and pharmaceuticals and personal care products (PPCPs) in surface water and groundwater. Concerns about their effects on the environment and human health are increasing, and advanced oxidation processes (AOPs) have been studied as potential techniques for removing those micropollutants from water. In particular, catalytic ozonation is an

innovative technology on the removal of persistent and recalcitrant water pollutants. Therefore, elimination of emergent organic pollutants by catalytic ozonation in the presence of the most promising catalysts prepared in this work could be an interesting option.

Since catalytic ozonation is a promising technology for the elimination of a wide range of compounds from water and wastewater, the continuous search for more efficient catalysts is of great importance. Nevertheless, metal leaching and low stability are sometimes associated to the use of supported and unsupported oxides of transition metals in ozonation reactions. Another obstacle to its practical application is the separation of these materials from the treated water. Magnetite nanoparticles are easy to be separated from aqueous media due to their magnetic properties. Over the years, spinel-type ferrite nanoparticles have been extensively studied in different areas, including catalysis, because of their exceptional properties and several synthesis methods have been developed. However, only few studies reported the use of magnetic oxides as ozonation catalysts. Magnetic nanoparticles and respective composites with carbon materials are also potential catalysts to be tested in ozonation reactions.

A detailed kinetic study using the most promising catalytic systems should be carried out.

The last part of this work was dedicated to real effluents from textile industry. Nevertheless, catalytic ozonation is a promising technique for treatment of wastewaters from several industries. Other effluents from various industries are possible alternatives to be studied with the prepared catalysts.

Appendices

Appendix A. Schematic representation of the experimental set-up

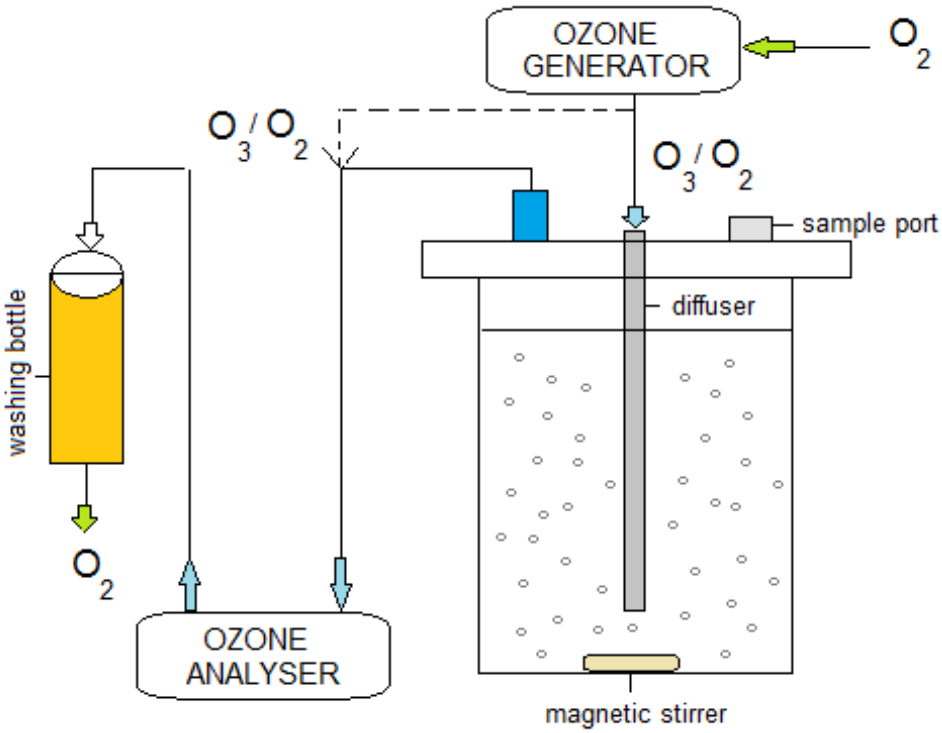

Figure A.1: Representation of the experimental set-up for adsorption and ozonation studies.

Appendix B. Screening of commercial metal oxides

The main goal of this section is to carry out a screening of commercial catalysts. Oxalic acid was used as model organic compound. Different commercial metal oxides were chosen for this screening: titanium dioxide (P25 Degussa) (sample TiO_2), cobalt (II, III) oxide (Sigma-Aldrich) (sample Co_3O_4), copper (II) oxide (Riedel-de Haën) (sample CuO), nickel oxide black (Aldrich) (sample NiO), ɣ-alumina (Degussa) (sample Al_2O_3), silica (Sigma-Aldrich) (sample SiO_2), zinc oxide (VP AdNano) (sample ZnO), iron(III) oxide (Sigma-Aldrich) (sample Fe_2O_3), lanthanum(III) oxide (Sigma-Aldrich) (sample La_2O_3), cerium(IV) oxide (Fluka) (sample CeO_2) and manganese(IV) oxide (Sigma-Aldrich) (sample MnO_2).

The textural characterization of materials was based on the corresponding N_2 equilibrium adsorption/desorption isotherms, determined at -196 °C with a Quantachrome Instruments NOVA 4200e apparatus. The degradation of oxalic acid was investigated in a slurry lab-scale reactor equipped with agitation. In each experiment the reactor was filled with 700 cm^3 of oxalic acid 1 mM at the natural pH ($pH_{0,\ oxalic\ acid}$ = 3.0). In the catalytic ozonation experiments, 100 mg of catalyst were introduced in the reactor. Ozone was produced from pure oxygen in a BMT 802X ozone generator. The experiments were performed at constant gas flow rate (150 $cm^3\ min^{-1}$) and constant inlet ozone concentration (50 g m^{-3}). The concentration of ozone in the gas phase was monitored with a BMT 964 ozone analyzer. Ozone in the gas phase leaving the reactor was removed in a series of gas washing bottles filled with iodide potassium solution. The agitation was maintained constant in order to keep the reactor content perfectly mixed and the temperature was set to 25 °C. The concentration of oxalic acid was followed by HPLC using a Hitachi Elite Lachrom HPLC equipped with a diode array detector and the stationary phases was an Aminex HPX-87H column (300 mm x 7.8 mm), working at room temperature under isocratic elution with H_2SO_4 4 mM.

Table B.1 presents BET surface areas of the commercial metal oxides. Samples NiO, Al_2O_3 and SiO_2 have the highest BET surface areas. On the other hand, samples Fe_2O_3 and MnO_2 present the lowest values, 6 and 7 $m^2\ g^{-1}$, respectively.

Table B.1: BET surface areas of commercial metal oxides.

Commercial sample	S_{BET} (m^2 g^{-1})
TiO_2	46
Co_3O_4	48
CuO	14
NiO	74
Al_2O_3	81
SiO_2	93
Zn-O	28
Fe_2O_3	6
La_2O_3	11
CeO_2	14
MnO_2	7

Figure B.1 shows the kinetic results of ozonation in the presence of commercial metal oxides. Cobalt oxide presented the best catalytic activity, allowing a total removal after 45 min of reaction. Nickel and copper oxides also showed had also a high performance, leading to a complete conversion degradation after 90 and 120 min of reaction, respectively. Iron, manganese, lanthanum and cerium oxides removed more than 50% of oxalic acid after 3 h of reaction. The other commercial oxides were not efficient in the reaction. A direct relationship between BET surface area and catalytic activity was not verified. Concluding, among the commercial oxides tested, cobalt, nickel and copper oxides were the most promising catalysts.

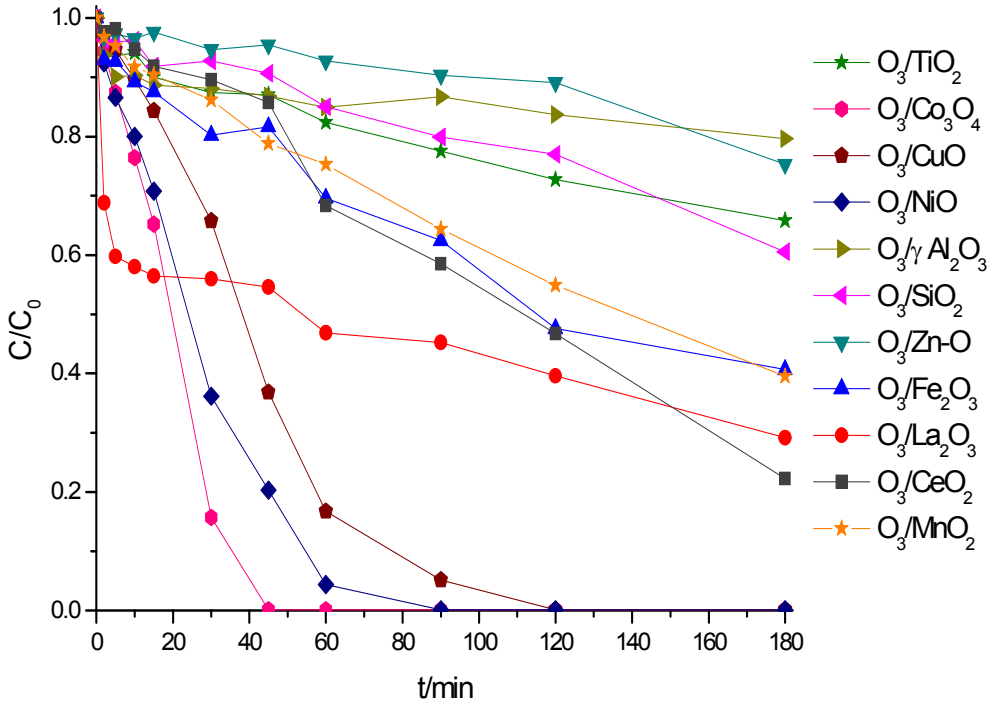

Figure B.1: Evolution of the dimensionless concentration of oxalic acid during catalytic ozonation with commercial samples.

Appendix C. Preparation and evaluation of manganese oxides synthesized by different procedures as ozonation catalysts

This section reports the preparation of manganese oxides synthesised by different procedures, including the use of mesoporous silica SBA-15 as template. The prepared samples were evaluated as catalysts in the ozonation of a model organic compound, oxalic acid (99%, Sigma-Aldrich). Firstly, manganese oxide was prepared by the precipitation method and evaluated as ozonation catalyst (chapter 6). This material showed high performance in oxalic acid removal, but a small amount of leached metal was observed in the remaining solution. Then, manganese oxides were prepared by diverse procedures, including the template synthesis. Additionally, manganese oxides prepared by the reflux method were also tested. After analysing the kinetic results of catalytic ozonation in the presence of the different manganese oxides for oxalic acid removal, no significant differences were observed between the catalysts. These materials presented excellent kinetic results, but a small amount of metal leaching in solution was always observed during the experiments.

C.1 Catalysts preparation

Different manganese oxides were prepared. In some procedures, mesostructured silica SBA-15 was used. Two cryptomelane-type manganese oxides prepared by Santos et al. [1] were also tested.

The synthesis of the SBA-15 consisted in the addition of a silicon source, tetraethylortosilicate (TEOS, 99%, Fluka), to an aqueous solution of hydrochloric acid (37%, Riedel-deHaën), containing an adequate surfactant (Pluronic P123, Aldrich), with molar ratios TEOS/P123/HCl/H_2O = 1.0/0.017/5.7/193. Then, a heat treatment at 100 °C during one day was carried out. The obtained product was dried and then calcined in air during 4 h at 600 °C using a heating rate of 2 °C min^{-1} [2, 3].

Mn-O_1 was synthesized using the SBA-15 as the hard template and manganese nitrate solution as the manganese source [4]. In this procedure, 2 g of SBA-15 powder were dispersed in 10 mL of water;, then 20 mL of $Mn(NO_3)_2.6H_2O$ (50 wt%) was added with continuous stirring at room temperature for 4 h. Afterwards, the

resulting solid material was filtered and dried at 100 °C for at least 3 h. The silica template in the manganese-silica composite was carefully removed by washing with NaOH 3 M solution for 30 min. The material was filtered, washed with water until the pH value of the filtrate was close to 7 and dried at 100 °C.

Sample Mn-O_2 was prepared using manganese (II) acetate tetrahydrate ($C_4H_{16}MnO_4.4H_2O$) as manganese precursor. In this procedure, manganese acetate (2.5 mmol/g of SBA-15) was dissolved in acetone at room temperature [5]. The SBA-15 powder was then placed into the solution. After the complete dissolution of manganese acetate, SBA-15 powder was added and the solution was maintained under continuous stirring until the solvent had evaporated completely. The material was washed with acetone several times to remove SBA-15. In order to compare the catalytic activity, sample Mn-O_2/SBA-15 was prepared by a similar procedure, but it was not washed with acetone.

Mn-O_3 catalyst was synthesized under ultrasonic irradiation [6]. In this synthesis 4 g of SBA-15 were dissolved in 60 mL of $Mn(NO_3)_2$ aqueous solution (0.4 M). The mixture was ultrasonically irradiated (24 kHz ultrasonic waves produced by UP400S equipment) at room temperature. After 60 min, the Mn-containing SBA-15 was filtered, washed with deionized water and dried at 60 °C for 24 h. The solid was calcined in air (50 cm^3 min^{-1}) with a heating rate of 1 °C min^{-1} from room temperature to 450 °C, and then this temperature was maintained for 2.5 h. The silica template was removed under ultrasonic irradiation at room temperature for 1 h using a NaOH aqueous solution (2 M). Finally the material was washed with deionized water and dried at 60 °C for 24 h. For comparative purposes, cobalt oxide (sample Co-O) was synthetized by a similar procedure, using $Co(NO_3)_2$ as cobalt precursor.

The Mn-O_4/SBA-15 was prepared by impregnation of silica SBA-15 [7]. In this procedure 1.2 g of $Mn(NO_3)_2$.4H2O were dissolved in 18 mL of water and 3 g of SBA-15 was slowly added under continuous stirring for 10 h and then dried out at 100 °C overnight. The catalyst was calcined at 500 °C for 12 h, with a heating rate of 1 °C min^{-1}.

Carbon nanotubes with manganese oxide were also synthesized. Sample Mn-O/MWCNT was prepared by a simple in-situ hydrothermal method [8]. This synthesis consisted in the addition of 0.5 g of dodecyl benzene sulphonic acid sodium (SDBS, $C_{18}H_{29}SO_3Na$) and 0.3001 g of MWCNT to 40 mL aqueous solution containing 0.005 M $MnSO_4.H_2O$ and 0.0005 M $KMnO_4$. The mixture was stirred for

2 h and then loaded into a Teflon-lined stainless-steel autoclave for 10 h at 160 °C. The black precipitate was washed with water and ethanol and dried at 60 °C overnight.

Samples KMn_8O_{16} and KMn_8O_{16}+Mn_3O_4 were prepared by Santos et al. as described in [1]. Briefly, these samples were obtained by the reflux method using an aqueous solution of $Mn(CH_3COO)_2.4H_2O$. The pH of this solution was maintained equal to 4.5 using a buffer solution of KCH_3COO/CH_3COOH. $KMnO_4$ or $NaMnO_4$ was dissolved in water and slowly added to the previous solution, in order to obtain cryptomelane (sample KMn_8O_{16}) and a catalyst containing cryptomelane and Mn_3O_4 (sample KMn_8O_{16}+Mn_3O_4). The precipitate formed was stirred and refluxed at 100 °C for 24 h. The solid was filtered and washed with distilled water and finally dried and calcined in air at 450 °C for 4.5 h.

C.2 Catalysts characterization

The textural properties of the different materials are presented in Table C.1. Figure C.1 shows the N_2 adsorption - desorption isotherms determined at -196 °C. The prepared nanostructured silica presents an isotherm of type IV with a H1 hysteresis, which is typical of materials with open-ended cylindrical mesopores. The prepared manganese oxides by template synthesis have BET surface areas and micropore volume lower than SBA-15. However, the prepared catalysts presented high BET surface areas, regardless of the preparation method.

Table C.1: Textural properties of the prepared samples.

Sample	S_{BET}(m^2 g^{-1})	S_{meso}(m^2 g^{-1})	V_{micro}(cm^3 g^{-1})	d^a(nm)
SBA-15	756	551	0.093	5.67
Mn-O_1	332	302	0.013	6.70
Mn-O_2	498	455	0.017	5.65
Mn-O_3	380	364	0.006	6.70
Mn-O_4/SBA-15	532	440	0.044	-
Mn-O_2/SBA-15	436	380	0.025	-
Mn-O/MWCNT	218	218	-	-
Co-O	278	267	0.004	6.69
KMn_8O_{16} [b]	45	-	-	-
KMn_8O_{16}+Mn_3O_4 [b]	84	-	-	-

[a] average mesopore diameter (d) obtained from the desorption isotherm using the Barrett, Joyner and Halenda (BJH) method;

[b] value from [1].

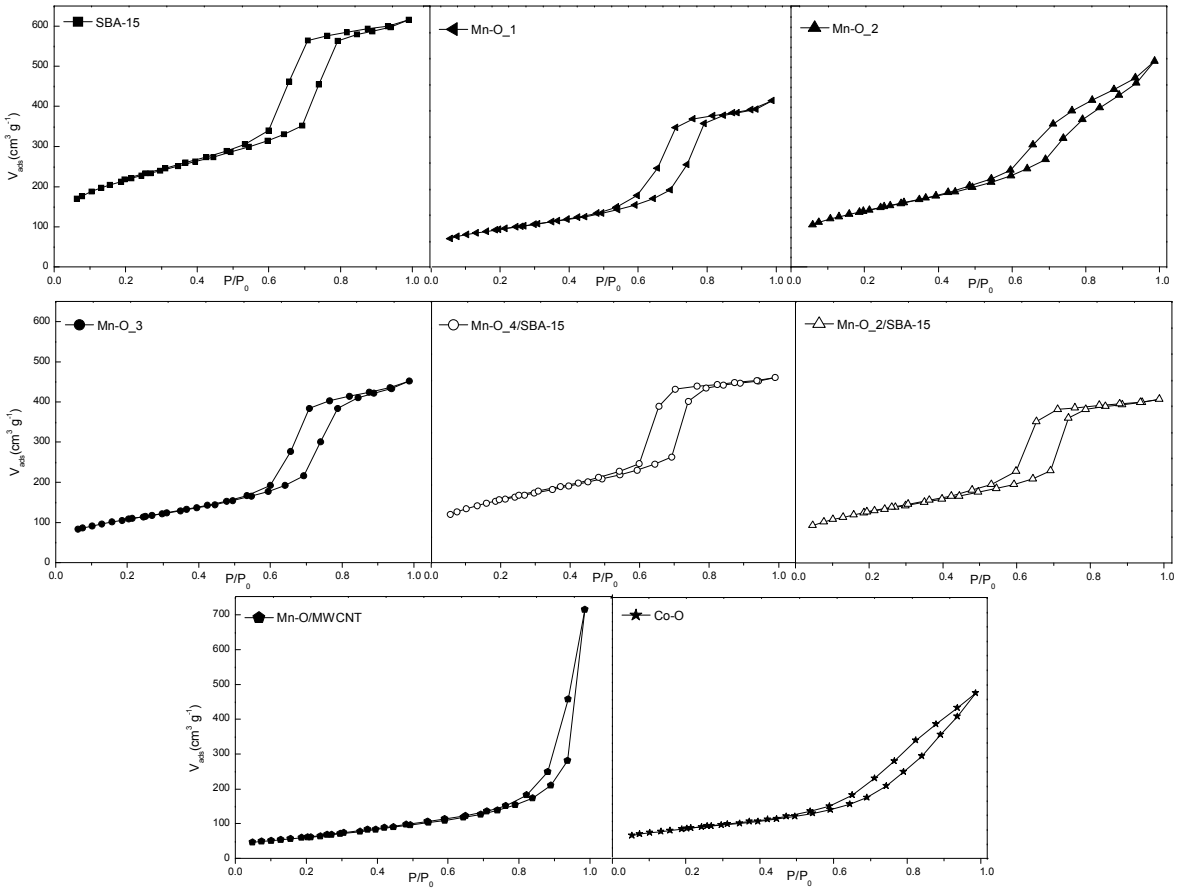

Figure C.1: N_2 adsorption-desorption isotherms determined at -196 °C.

C.3 Catalytic activity

The catalytic activity was evaluated in a slurry lab-scale reactor equipped with stirring. In each experiment the reactor was filled with 700 cm^3 of solution of oxalic acid and 350 mg of catalyst. The experiments were performed at constant gas flow rate (150 cm^3 min^{-1}) and constant inlet ozone concentration (50 g m^{-3}). The concentration of oxalic acid was followed by HPLC using a Hitachi Elite Lachrom apparatus equipped with a diode array detector. The stationary phase was an Aminex HPX-87H column (300 mm x 7.8 mm) working at room temperature, under isocratic elution with H_2SO_4 4 mM.

Figure C.2 shows the kinetics results of single ozonation and ozonation in the presence of the tested materials. Catalytic ozonation in the presence of manganese oxides synthesized by the reflux method removed all oxalic acid after 30 min of reaction, and no differences were observed between the two samples. SBA-15 is not active for the ozonation of oxalic acid. On the other hand, all manganese oxides prepared by template synthesis presented better performance than single ozonation. Mn-O_1 and Mn-O_3 samples did not lead to complete oxalic acid degradation, removing 85% and 75% after 1 h of reaction. Cobalt oxide did not remove all oxalic acid, in spite of having a slightly better performance than the manganese oxide prepared by the similar procedure (sample Mn-O_3). Mn-O_1, Mn_O/SBA-15 materials and Mn-O/MWCNT allowed total oxalic acid conversion after 45 min of reaction.

After these experiments, it is possible to conclude that no important differences were observed between manganese containing catalysts. In general, manganese oxides presented excellent catalytic activities, removing all oxalic acid after 30-45 min of reaction, but unfortunately small metal leaching was always observed during the experiments.

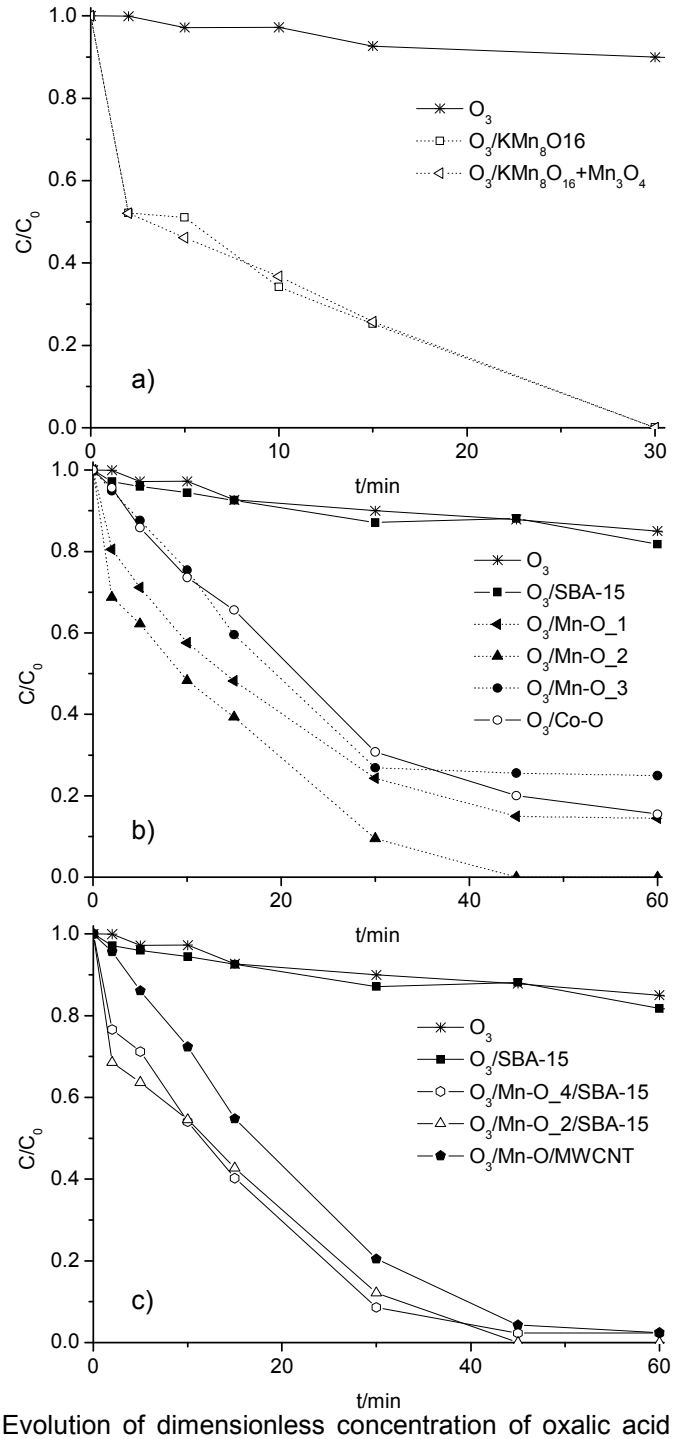

Figure C.2: Evolution of dimensionless concentration of oxalic acid (C_0 = 1 mM) during single ozonation and ozonation catalyzed by manganese oxides synthesized by the reflux method (a), manganese oxides and cobalt oxide prepared by template synthesis (b), and Mn-O/SBA-15 materials and Mn-O/MWCNT (c).

References

[1] V. Santos, M. Pereira, J. Órfão, J. Figueiredo, Synthesis and Characterization of Manganese Oxide Catalysts for the Total Oxidation of Ethyl Acetate, Top. Catal. 52 (2009) 470-481.

[2] D. Zhao, Q. Huo, J. Feng, B. F. Chmelka, G. D. Stucky, Nonionic Triblock and Star Diblock Copolymer and Oligomeric Surfactant Syntheses of Highly Ordered, Hydrothermally Stable, Mesoporous Silica Structures, J. Am. Chem. Soc. 120 (1998) 6024-6036.

[3] A. B. Fuertes, Synthesis of ordered nanoporous carbons of tunable mesopore size by templating SBA-15 silica materials, Microporous Mesoporous Mater. 67 (2004) 273-281.

[4] H. Chen, X. Dong, J. Shi, J. Zhao, Z. Hua, J. Gao, M. Ruan, D. Yan, Templated synthesis of hierarchically porous manganese oxide with a crystalline nanorod framework and its high electrochemical performance, J. Mat. Chem. 17 (2007) 855-860.

[5] Y. F. Han, F. Chen, Z. Zhong, K. Ramesh, L. Chen, E. Widjaja, Controlled Synthesis, Characterization, and Catalytic Properties of Mn_2O_3 and Mn_3O_4 Nanoparticles Supported on Mesoporous Silica SBA-15, J. Phys. Chem. B 110 (2006) 24450-24456.

[6] J. Deng, L. Zhang, H. Dai, Y. Xia, H. Jiang, H. Zhang, H. He, Ultrasound-Assisted Nanocasting Fabrication of Ordered Mesoporous MnO_2 and Co_3O_4 with High Surface Areas and Polycrystalline Walls, J. Phys. Chem.C 114 (2010) 2694-2700.

[7] R. Rosal, M. S. Gonzalo, A. Rodríguez, J. A. Perdigón-Melón, E. García-Calvo, Catalytic ozonation of atrazine and linuron on MnO_x/Al_2O_3 and MnO_x/SBA-15 in a fixed bed reactor, Chem. Eng. J. 165 (2010) 806-812.

[8] F. Teng, S. Santhanagopalan, D. D. Meng, Microstructure control of MnO_2/CNT hybrids under in-situ hydrothermal conditions, Solid State Sci. 12 (2010) 1677-1682.

Appendix D. Composites of manganese oxide with activated carbon as catalysts for the ozonation of a reactive dye

The manganese oxide sample and activated carbon - manganese oxide composites reported in chapter 6 were also evaluated as ozonation catalysts for the mineralisation of the dye C. I. Reactive Blue 5. The experimental reactions were carried out at the conditions described in chapter 6. The kinetic results of single and catalytic ozonation are presented in Figure D.1.

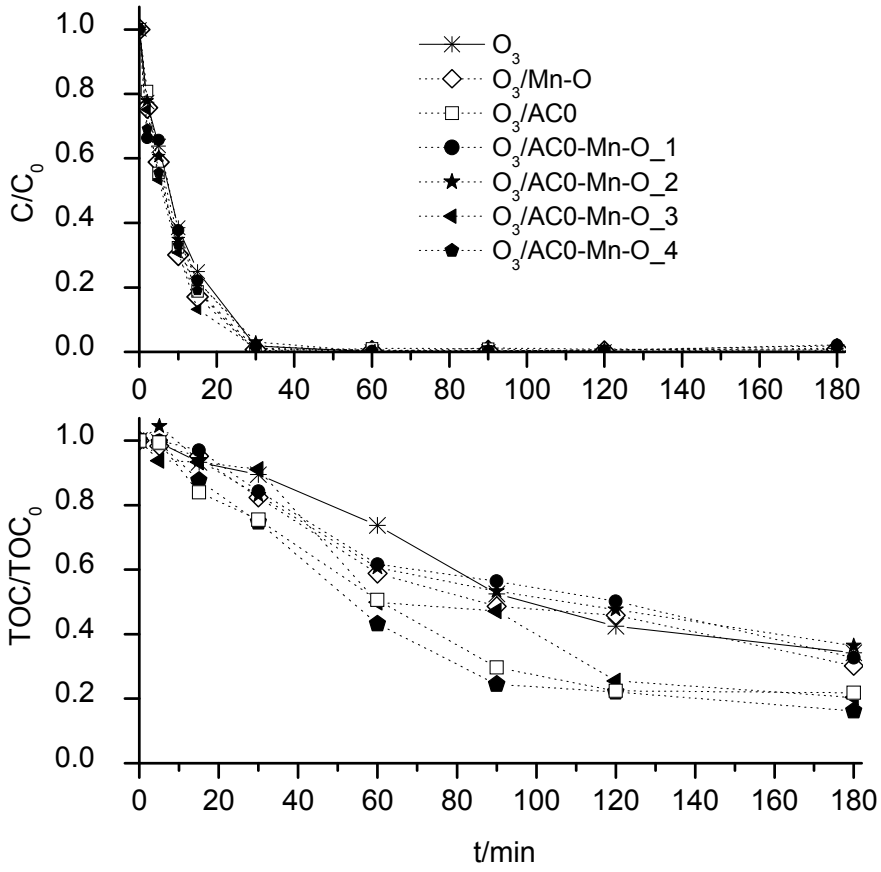

Figure D.1: Colour and TOC removal for the reactive dye using activated carbon, manganese oxide and composites.

A total decolourisation is observed after 30 minutes, and this time is practically independent of the presence of catalyst. Single and catalytic ozonation in the

presence of Mn-O, AC0-Mn-O_1 and AC0-Mn-O_2 allowed the removal of no more than about 65% of TOC after 3 h, which is an indication that part of the dyes degradation products (colourless) still remains in solution. AC0-Mn-O_4 had the best performance, allowing 84% TOC removal after 3 h of reaction. The high activity of this composite may be related both to its high surface area and to the presence of the Mn(III)/Mn(II) redox couple on its surface.